Vol. 199, August 15, 1987
Complete in one issue

ISSN 0003-2670

ANALYTICA CHIMICA ACTA

International journal devoted to all branches of analytical chemistry

ELSEVIER

ANALYTICA CHIMICA ACTA

International journal devoted to all branches of analytical chemistry
Revue internationale consacrée à tous les domaines de la chimie analytique
Internationale Zeitschrift für alle Gebiete der analytischen Chemie

PUBLICATION SCHEDULE FOR 1987

	J	F	M	A	M	J	J	A	S	O	N	D
Analytica Chimica Acta	192	193	194	195	196	197	198	199	200/1 200/2	201	202	203/1 203/2

Scope. *Analytica Chimica Acta* publishes original papers, short communications, and reviews dealing with every aspect of modern chemical analysis both fundamental and applied.

Submission of Papers. Manuscripts (three copies) should be submitted as designated below for rapid and efficient handling:

Papers from the Americas to: Professor Harry L. Pardue, Department of Chemistry, Purdue University, West Lafayette, IN 47907, U.S.A.

Papers from all other countries to: Dr. A. M. G. Macdonald, Department of Chemistry, The University, P.O. Box 363, Birmingham B15 2TT, England. Papers dealing particularly with computer techniques to: Professor J. T. Clerc, Universität Bern, Pharmazeutisches Institut, Baltzerstrasse 5, CH-3012 Bern, Switzerland.

Submission of an article is understood to imply that the article is original and unpublished and is not being considered for publication elsewhere. Papers in English, French and German are published. There are no page charges. Manuscripts should conform in layout and style to the papers published in this Volume. See inside back cover for "Information for Authors".

Reprints. Fifty reprints will be supplied free of charge. Additional reprints (minimum 100) can be ordered. An order form containing price quotations will be sent to the authors together with the proofs of their article.

Publication. *Analytica Chimica Acta* appears in 12 volumes in 1987. The subscription for 1987 (Vols. 192–203) is Dfl. 2700.00 plus Dfl. 300.00 (p.p.h.) (total approx. US $1463.40). All earlier volumes (Vols. 1–191) except Vols 23 and 28 are available at Dfl. 243.00 (US $118.50), plus Dfl. 18.00 (US $8.80) p.p.h., per volume.

Our p.p.h. (postage, packing and handling) charge includes surface delivery of all issues, except to subscribers in the U.S.A., Canada, Australia, New Zealand, P.R. China, India, Israel, South Africa, Malaysia, Thailand, Singapore, South Korea, Taiwan, Pakistan, Hong Kong, Brazil, Argentina and Mexico, who receive all issues by air delivery (S.A.L. — Surface Air Lifted) at no extra cost. For Japan, air delivery requires 50% additional charge; for all other countries airmail and S.A.L. charges are available upon request.

Subscription. Subscription should be sent to: Elsevier Science Publishers B.V., Journals Department, P.O. Box 211, 1000 AE Amsterdam, The Netherlands. Tel: 5803 911, Telex: 18582, to which requests for sample copies can also be sent. Claims for issues not received should be made within three months of publication of the issues. If not, they cannot be honoured free of charge. Readers in the U.S.A. and Canada can contact the following address: Elsevier Science Publishing Co. Inc., Journal Information Center, 52 Vanderbilt Avenue, New York, NY 10017, U.S.A., Tel: (212) 916-1250, for further information, or a free sample copy of this or any other Elsevier Science Publishers journal.

Advertisements. Advertisement rates are available from the publisher on request.

0003-2670/87/$03.5

Printed in The Netherlands

ANALYTICA CHIMICA ACTA

International journal devoted to all branches of analytical chemistry

(Abstracted, Indexed in: Anal. Abstr.; Biol. Abstr.; Chem. Abstr.; Curr. Contents Phys. Chem. Earth Sci.; Life Sci.; Index Med.; Mass Spectrom. Bull.; Sci. Citation Index; Excerpta Med.)

OL. 199 **CONTENTS** **AUGUST 15, 1987**

eview

:at methods in analytical chemistry. Kinetic techniques for catalyzed and uncatalyzed reactions
S. Pantel (Freiburg, F.R.G.) 1

eneral Analytical Chemistry

ultidetection flow-injection techniques for manipulation of sensitivity. Amplification and dilution methods
A. Ríos, F. Lázaro, M. D. Luque de Castro and M. Valcárcel (Córdoba, Spain) 15

ersatile automatic stopped-flow system for routine analysis
A. Loriguillo, M. Silva and D. Pérez-Bendito (Córdoba, Spain) 29

ptimization of single-column anion chromatography with indirect ultraviolet photometric and fluorimetric detection
S. Rapsomanikis and R. M. Harrison (Colchester, Gt. Britain). 41

ıe effect of substituents on the extraction behavior of hydroxamic acids
M. Hojjatie, T. Cecconie and H. Freiser (Tucson, AZ, U.S.A.). 49

'ectrometric Methods

etermination of nickel, cobalt, copper and uranium in water by cathodic stripping chronopotentiometry with continuous flow
M. P. Newton and C. M. G. van den Berg (Liverpool, Gt. Britain). 59

etermination of caprolactam by adsorptive voltammetry after separation by thin-layer chromatography
Z. Tocksteinová and M. Kopanica (Prague, Czechoslovakia). 77

ı amperometric sensor for carbon dioxide based on immobilized bacteria utilizing carbon dioxide
H. Suzuki (Atsugi, Japan), E. Tamiya and I. Karube (Yokohama, Japan) 85

icrobial electrode sensor for vitamin B_{12}
I. Karube, Y. Wang, E. Tamiya and M. Kawarai (Yokohama, Japan) 93

ɔmputer Methods and Applications

escriptions of molecular shape applied in studies of structure/activity and structure/property relationships
R. H. Rohrbaugh and P. C. Jurs (University Park, PA, U.S.A.) 99

ıectrometric Methods

ıser-excited ionic fluorescence spectrometry of rare-earth elements in the inductively-coupled plasma
M. E. Tremblay, B. W. Smith and J. D. Winefordner (Gainesville, FL, U.S.A.) 111

ductively-coupled plasma/atomic emission spectrometry of sulfur with a vacuum scanning spectrometer and its application to the analysis of coal liquefaction catalysts
M. Kubota, R. A. Reimer, K. Terajima, Y. Yoshimura and A. Nishijima (Ibaraki, Japan) 119

ifferential determination of antimony(III) and antimony(V) by indirect spectrophotometry with chromium(VI) and diphenylcarbazide, after reduction of antimony(V)
N. Yonehara, T. Fuji, H. Sakmoto and M. Kamada (Kagoshima, Japan) 129

simple stopped-flow method with continuous pumping for the spectrophotometric flow-injection determination of boron in plants
M. A. Z. Arruda and E. A. G. Zagatto (Piracicaba, Brazil) 137

ıe S_2 emission characteristics of several organic sulfur compounds obtained by molecular emission cavity analysis and pyrolysis
K. Nakajima and T. Takada (Tokyo, Japan) 147

ıort Communications

ıe pH-static enzyme sensor. An ISFET-based enzyme sensor, insensitive to the buffer capacity of the sample
B. H. van der Schoot and P. Bergveld (Enschede, The Netherlands) 157

(Continued overleaf)

(*Contents continued*)

Anodic response to oxygen of an electrochemical detector in high-performance liquid chromatography and flow-injection analysis
J. B. F. Lloyd (Birmingham, Gt. Britain) . . .
Determination of mercury traces by differential-pulse stripping voltammetry after sorption of mercury vapour on a gold-plated electrode
F. Scholz, L. Nitschke and G. Henrion (Berlin, G.D.R.) . . .
Determination of cyanuric acid in swimming pool water by differential pulse polarography
J. Struys and P. M. Wolfs (Bilthoven, The Netherlands) . . .
Determination of surface-active compounds in precipitation studies by a.c. polarography
N. Batina, B. Ćosović and Dj. Težak (Zagreb, Yugoslavia) . . .
Simultaneous determination of lead, copper, cadmium and zinc in pure zirconium metal by differential-pulse anodic stripping voltammetry
S. S. Dhaktode (Bombay, India) . . .
Determination of traces of palladium by adsorptive stripping voltammetry of the dimethylglyoxime complex
J. Wang and K. Varughese (Las Cruces, NM, U.S.A.) . . .
Sandwich techniques in flow injection analysis. Part 1. Continuous recalibration techniques for process control
J. Alonso, J. Bartrolí, M. del Valle, M. Escalada and R. Barber (Barcelona, Spain) . . .
Correlation steam/solid chromatography of trace organic compounds in water
M. Koel, M. Kaljurand and E. Küllik (Tallinn, U.S.S.R.) . . .
Determination of paraquat by flow-injection spectrophotometry
E. Chico Guijarro, P. Yáñez-Sedeño and L. M. Polo Díez (Madrid, Spain) . . .
Preconcentration of copper with the ion-pair of 1,10-phenanthroline and tetraphenylborate on naphthalene
M. Satake, G. Kano (Fukui, Japan), B. K. Puri (New Delhi, India) and S. Usami (Toyama, Japan) . . .
Spectrofluorimetric determination of proguanil in biological fluids
O. R. Idowu (Ibadan, Nigeria) . . .
Continuous-flow determination of manganese in natural waters containing iron
D. J. Hydes (Goldalming, Gt. Britain) . . .
Spectrofluorimetric determination of 1,4-thienodiazepines
F. U. Sanchez, J. R. Procopio and L. H. Hernandez-Hernandez (Madrid, Spain) . . .
Detection of nitrobenzene and related aromatics by reduction and indophenol formation
K. K. Verma and D. Gupta (Jabalpur, India) . . .
Spectrophotometric determination of perchlorate after extraction of its Brilliant Green ion-pair with microcrystalline benzophenone
D. Thorburn Burns and N. Tungkananuruk (Belfast, Northern Ireland) . . .
Spectrophotometric determination of manganese(VII) after extraction with the ethylene-bis(triphenylphosphonium) cation
D. Thorburn Burns and D. Chimpalee (Belfast, Northern Ireland) . . .
Determination of traces of boron in semiconductor amorphous silicon film by filament-vaporization inductively-coupled plasma/atomic emission spectrometry
E. Kitazume (Iwate, Japan), S. Ishioka and E. Mitani (Tokyo, Japan) . . .
The effect of the ordered phase CuAu on the accuracy of emission analysis of gold alloys
R. de Marco, D. J. Kew (Melbourne, Australia) and J. V. Sullivan (Clayton, Vic., Australia) . . .
Echelle-spectrometer/image-dissector system for elemental quantitation by continuous-source atomic absorption spectrometry
R. Masters, C. Hsiech and H. L. Pardue (West Lafayette, IN, U.S.A.) . . .
The coprecipitation of an organophosphate fraction from harbour water for x-ray fluorescence spectrometry
F. Ahern, J. M. Eckert, S. F. Hain, K. E. A. Leggett, N. C. Payne and K. L. Williams (Sydney, Australia) . . .
Long-term stability of a gas chromatography/mass spectrometry system in quantitative gas analysis
H. Egsgaard and E. Larsen (Roskilde, Denmark) . . .

Book Reviews . . .

Software Reviews . . .

Author Index . . .

ANALYTICA CHIMICA ACTA
VOL. 199 (1987)

ANALYTICA CHIMICA ACTA

International journal devoted to all branches of analytical chemistry

ELSEVIER Amsterdam–Oxford–New York–Tokyo

Analytica Chimica Acta, 199 (1987) 1—14
Elsevier Science Publishers B.V., Amsterdam — Printed in The Netherlands

Review

STAT METHODS IN ANALYTICAL CHEMISTRY
Kinetic Techniques for Catalyzed and Uncatalyzed Reactions

SIEGBERT PANTEL

Institut für Anorganische und Analytische Chemie der Universität, D-7800 Freiburg i.Br. (Federal Republic of Germany)

(Received 3rd October 1986)

SUMMARY

An important group of (catalytic-) kinetic methods uses "open systems", in which, during the course of the reaction, a reactant is added or a product is removed, or even both. The "Stat methods" belong to this group. In the Stat methods, a preset stationary state within a catalyzed or uncatalyzed system is kept constant by stepwise addition of a suitable reagent, so that any change in a concentration is just compensated. Methods based on electrochemical techniques (pH-stat, potentiostat, amperostat and biamperostat) and on spectrophotometric and luminescence techniques (absorptiostat, fluorostat and luminostat) are described and their applications are summarized.

Chemical methods of analysis can be divided into two main groups: (a) methods based on thermodynamic equilibrium (gravimetry, titrimetry, photometry, etc.), and (b) kinetic methods. In the former, measurements are made in a system which is in a stable (equilibrium) state and time is not a variable; in the latter, it is the temporal course of the chemical reaction which is observed, i.e., the characteristic quantity measured varies with time.

Kinetic methods themselves can be divided into two groups: those based on uncatalyzed reactions and those on catalyzed reactions. Both types can be used for the determination of reactants in the milligram to microgram range. Catalyzed reactions also allow the determination of catalysts and substances reacting with them (activators, inhibitors, re-activators) at great dilutions (microgram to picogram range); they are therefore especially useful in trace analysis. Although all analytical methods based on reactions in thermodynamic equilibrium involve kinetic laws, and although kinetic methods have been applied in analytical chemistry for over a hundred years, chemical methods in equilibrium have predominated in analytical practice.

In 1885, Witz and Osmond [1] described a method for the semiquantitative determination of vanadium based on the vanadium-catalyzed oxidation of aniline by chlorate with formation of aniline black, which was first reported by Guyard in 1876 [2]. About fifty years later, Sandell and Kolthoff [3, 4] used the iodide-catalyzed oxidation of arsenic(III) by cerium(IV), which had been used in titrimetry by Willard and Young [5], for the determination

0003-2670/87/$03.50

of iodide. Shortly afterwards, Szebelledy and Ajtai [6, 7] reported the determination of vanadium based on the vanadium-catalyzed oxidation of *p*-phenetidine with chlorate or bromate. Numerous other analytical applications of catalyzed reactions were then described (many of them by Szebelledy and co-workers) and in 1966, the first monograph on this subject was published by Yatsimirskii [8].

In biochemistry, enzyme-catalyzed reactions have been used for analytical purposes for much longer than in chemistry. For example, Osann [9] used peroxidase for an assay of peroxide in 1845; enzymatic methods were accepted for the determination of carbohydrates in the 19th century [10]. The first practical application of kinetic methods in routine analysis seems to have been in clinical chemistry [10, 11], but such methods were adopted increasingly in general analytical chemistry. This was certainly favoured by the rapid development of electronics, which simplified the construction of suitable measuring devices for this type of analytical chemistry; cheap microcomputers now simplify the evaluation of data sets from complicated reaction mechanisms [12].

Kinetic methods are now an important alternative to classical methods for trace analysis. Their sensitivity is comparable to that of activation, fluorescence and luminescence methods. Their practical application is limited by their relatively low selectivity (except for enzymatic methods) but in recent years appreciable improvements have been made by separation or masking. It is also possible to determine two or more catalytically active substances in the same solution without previous separation by using different temperatures [13] or different reactant concentrations [14]. A great advantage is that measurements of reaction rates can easily be automated, which is an important requirement for routine work. A useful feature of kinetic methods is that closely related substances (isomers, homologues) often react at different rates with the same reagent, although they cannot be differentiated under thermodynamic equilibrium conditions; kinetic methods often allow prior separation to be avoided. One of the first examples of such a "differential reaction rate method" allowed distinction between exogenic and endogenic double bonds with perbenzoic acid [15, 16]. Earlier, Clarens [17] reported the determination of different fractions of tannins by their different reaction rates with oxygen. Kinetic methods also enlarge the number of analytically useful reactions because reactions which take a long time to reach thermodynamic equilibrium or are affected by side-reactions or secondary reactions can often be utilized.

Kinetic methods of analysis are divided into two groups, namely open and closed systems. In closed systems, after the start of the reaction no further operations are needed, whilst in open systems, a reactant is added or a product is removed or even both during the course of the reaction. The "Stat" methods to be discussed here belong to the open category, as do most of the routine methods now used (e.g., the flow-through, steady-state and flow-injection techniques).

The history of the Stat methods began in 1951 with a paper by Jacobson and Leonis [18] who described an apparatus for keeping a preset pH value constant during a chemical reaction. Møller [19] described the first application of this apparatus for the determination of an enzyme (pH-stat). Later, this method was used by Weisz et al. [20] for the determination of inorganic catalysts with potentiometric monitoring of the indicator reaction, and by Klockow et al. [21] and Weisz and Rothmaier [22] with photometric monitoring. Since then, it has been shown that Stat methods are very widely applicable with different types of indication and are important in the examination of catalyzed and uncatalyzed reactions. Stat methods can be used for determinations of reactants, catalysts and substances reacting with them, and for the examination of substituent effects on the catalytic activity of organic substances such as thioureas [23, 24] or iodine-containing organic compounds [25].

THEORETICAL BASIS FOR KINETIC METHODS OF ANALYSIS

For catalyzed and uncatalyzed reactions in homogeneous solution, the same theoretical considerations are valid, except that in the latter case the order of reaction is one magnitude lower. Therefore the basic aspects are treated here for catalyzed reactions.

For a catalyzed reaction of the general type

$$A + B \overset{\text{catalyst}}{\rightleftharpoons} X + Y$$

the rate v is given by

$$v = dc_X/dt = kC_AC_BC_K$$

with $C_A = (C_A^\circ - C_X)$ and $C_B = (C_B^\circ - C_X)$, where C_A, C_B and C_X are the concentrations of reactants A and B and reaction product X at time t, respectively; C_A° and C_B° are the concentrations at the start of the reaction ($t = 0$). The concentration of the catalyst can be regarded as constant during the whole reaction time ($C_{cat} = C_{cat}^\circ$). The equation for the reaction rate of this model reaction is therefore second order, providing a complicated logarithmic correlation between measured value and time. For optimal evaluations, a linear relationship is desirable, but is obtained only in reactions of quasi-zero order. In closed systems, this is achieved by using a large excess of the reactant B (C_{cat} can be regarded as constant for every batch) and observing only a short time ("initial state"). In the Stat methods, a preset value of the concentration of one of the reactants is kept constant by stepwise addition of A at the same rate as it is consumed by the reaction with the second reactant B present in a comparatively large excess; or a reaction product X is removed at the same rate as it is formed by the reaction. This is done by stepwise addition of a reagent R, which reacts very quickly with product X. In those cases where A is added or re-formed by the reaction with R, the initial state can be maintained over a considerably longer time

than in closed systems. In enzymatic analysis, it is of great advantage that the substrate concentration A (usually an oxidant) can be kept very low over a long period of time, thus providing an extremely mild environment for the enzyme [26].

It is also possible to keep constant the concentration of the reaction product X by the addition of R without re-formation of A:

$$A + B \rightleftharpoons X + Y; X + R \rightarrow Z$$

In this case, however, the initial state cannot be drawn beyond that found in closed systems. Therefore, this variant is of advantage only in cases in which the reaction product X displaces the equilibrium of the indicator reaction in the direction of the back-reaction (enzymatic analysis).

Stat methods have the special advantage of giving easily evaluated addition plots when the uncatalyzed reaction proceeds with considerable velocity (Fig. 1), thus offering the possibility of determining very low catalyst concentrations [27]. When the blank value of the uncatalyzed reaction is taken into account, interferences from impurities in the system can be eliminated. It is therefore desirable in Stat methods that the uncatalyzed reaction proceeds with measurable velocity, as has been shown in several examples [23–29]. Alternatively, a small, constant amount of the catalyst can be added to each batch.

With regard to nomenclature, the reaction which is monitored instrumentally, is called the indicator reaction, and the substance, the concentration of which is actually measured, is termed the indicator substance. Activators enhance catalytic activity, inhibitors diminish catalytic activity, and the products which release a catalyst from its inhibited forms are called re-activators.

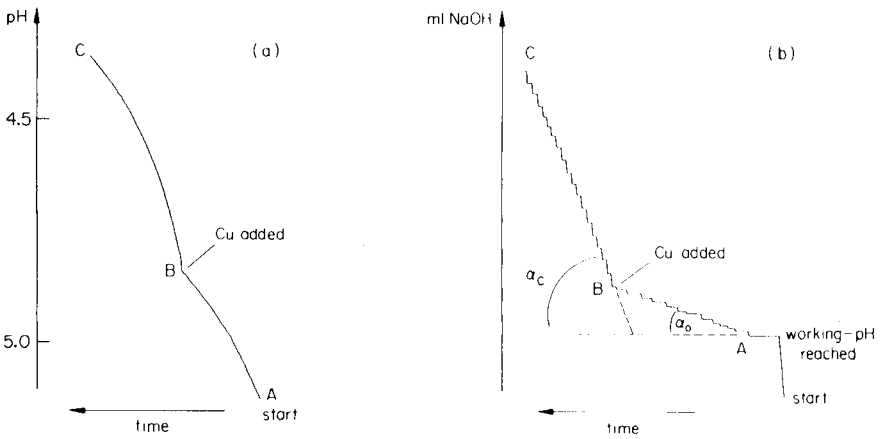

Fig. 1. Copper(II)-catalyzed oxidation of ascorbic acid with peroxodisulphate. The pH is followed (a) in a closed system and (b) with the pH-stat method under the same conditions. AB, uncatalyzed reaction; BC, catalyzed reaction. (Reproduced from [27].)

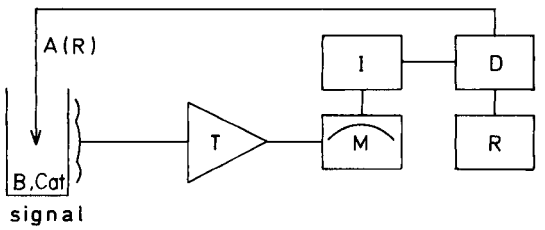

Fig. 2. Schematic representation of a Stat apparatus. Indicator reaction: A + B$\rightleftharpoons$X + Y. T, signal/voltage transducer; M, voltmeter; I, comparator; D, automatic burette; R, strip-chart recorder.

EXPERIMENTAL

Measuring device

The apparatus used in Stat methods is shown schematically in Fig. 2. The reaction vessel (in photometric procedures, this is a cuvette in a suitable spectrophotometer) is thermostatted to ±0.2°C or better. An appropriate sensor is placed in the vessel for electrochemical or thermometric procedures; this sensor and the capillary end of a burette are fitted through a teflon lid on the vessel; a hole (5-mm diameter) in the lid is used to insert the tip of an Eppendorf pipette to start the indicator reaction. The reaction mixture is stirred magnetically at constant speed.

The rate of addition of a suitable substance (A or R) is controlled by following some physical property of the indicator substance, proportional to its concentration (potential, absorbance, current, etc.). The signal obtained, converted if necessary by the transducer (T), must be in the millivolt range and is applied to the input of voltmeter, M. This signal is proportional to the concentration of the indicator substance and is compared in comparator I, with a preset working potential which corresponds to the concentration of the indicator substance that must be kept constant. Any difference between the actual potential and the preset working potential starts or stops the mechanism of the automatic burette, D, depending on the required direction. The stepwise addition of reagent from the burette is monitored by recorder, R, which is connected to the burette.

The measuring and regulating unit described is commercially available, e.g., the Metrohm Combititrator 3D, or the Radiometer automatic titrator TTT-2, or can be constructed in the laboratory from commercially available parts [30—35]. The reagent used can be delivered in the microlitre range from a burette or by electrostatic deflection of charged droplets [34], or generated coulometrically [35, 36]. When a burette is used, the concentration of the solution added must be such that 1/200 (or less) of the burette volume suffices to provide a response; the preset concentration in the reaction vessel must be maintained by $\leqslant$50% of the burette volume. The total volume added should not exceed 5—10% of the working volume in the reaction vessel, in order to keep the change in concentration minimal.

Procedure for the controlled addition of reactant A in catalyzed reactions

The reaction vessel is charged with a suitable amount of buffer solution, a neutral salt solution for definite ionic strength (if necessary), a solution of reactant B and enough water to give the required volume. After thermostatting for about 5 min, the voltmeter is set to zero and a known volume of reactant A, corresponding to the concentration to be kept constant in the reaction mixture during the measuring time (the preset concentration) is added manually from the burette of the Stat apparatus; the corresponding mV value at the voltmeter is set on the comparator as the preset working potential and the regulated addition of reactant A from the burette is started, producing an addition plot for the uncatalyzed reaction (AB in Fig. 1b). At point B, an appropriate volume of the catalyst solution is added from an Eppendorf pipette and the addition plot for the catalyzed reaction is then monitored (BC in Fig. 1b).

Procedure for the controlled addition of reagent R in catalyzed reactions (re-formation of A)

When the concentration of reactant A has to be kept constant by controlled addition of a suitable reagent R (e.g., the concentration of iodide through the reduction of iodine by controlled addition of ascorbic acid or thiosulphate), the reaction vessel is charged with buffer solution, neutral salt solution (if necessary), reactant B (oxidant) and water to give the required volume. After thermostatting for about 5 min, the uncatalyzed reaction is started by addition of reactant A from an Eppendorf pipette. The preset working potential is set to the value corresponding to the preset concentration of the reaction product X (e.g., iodine). The Stat apparatus is started, and the controlled addition of R begins as soon as the actual potential equals the preset working potential. The addition plots for the uncatalyzed and catalyzed reaction are monitored as described above.

The procedures for uncatalyzed reactions and titrations are similar, as are the determinations in which Z is formed instead of A, as well as the determinations of inhibitors or re-activators.

Evaluation of the recorder traces

The recorder traces in Stat methods are usually linear or almost linear because the reaction is of quasi-zero order during the measuring time. For evaluation (see Fig. 1b), the angles α_0 and α_C (where C represents the catalyst) are measured and the difference $\Delta \tan \alpha = \tan \alpha_C - \tan \alpha_0$ is calculated. Plotting $\Delta \tan \alpha$ against the catalyst concentration produces (in most cases) linear calibration graphs which can be used for the determination of unknown sample solutions. This mode of operation has the advantage that all interfering effects in the reaction mixture (impurities) are enclosed in α_0 and so can be eliminated in the evaluation.

When uncatalyzed reactions are used for the determination of reactants or the apparatus is applied as a titrator, this mode of evaluation via α_0 is of course impossible and only α is evaluated.

If non-linear recorder traces are obtained, evaluation should be done by using fixed-time or fixed-concentration techniques.

THERMAL METHODS

The heat of reaction is the most general measurable effect of chemical reactions. It can be used for the regulation of a Stat apparatus by adding or withdrawing just as much heat as is used (endothermic reactions) or formed (exothermic reactions) within the time unit. In the commoner case of exothermic reactions, this could be done by incremental addition of ice water at the same speed as heat is evolved. Another possibility is to heat the reaction mixture electrically to a temperature somewhat higher than the temperature of the thermostat [37]. The current in the heater is decreased in accord with the increase in heat production of the indicator reaction within the time unit. The time of heating or not heating serves as a measure of the reaction rate.

In this way, copper(II) can be determined in the 0.1—0.5 $\mu g\ ml^{-1}$ range by its catalytic action on the hydrogen peroxide/hydrazine indicator reaction, and molybdenum(VI) (5—50 $\mu g\ ml^{-1}$) can be determined by its catalysis of the bromate/iodide/ascorbic acid reaction [37].

ELECTROCHEMICAL METHODS

Potentiometric methods

Another widely applicable method for the regulation of a Stat apparatus is potentiometric indication. With reference to the Nernst equation, controlled addition can be used to keep constant either the ratio of the activities of two oxidation states of the same species or the activity of one oxidation state whilst the other one can be regarded as constant (e.g., in pH measurements).

An example of the first type is the molybdenum(VI)-catalyzed oxidation of iodide with hydrogen peroxide and controlled addition of iodide from the burette to keep the potential constant [20, 21]. In this case, more iodide is necessary than is consumed by the oxidation, because the iodine formed in the reaction must also be compensated; this is a potentiostat, but not a concentrostat. An example of the second type is the molybdenum(VI)-catalyzed oxidation of iodide with hydrogen peroxide, when the iodine formed is reduced by controlled addition of ascorbic acid or thiosulphate from the burette; in this case, both the potential and the concentration of iodide (and consequently of iodine) are kept constant during the measuring time. This is a potentiostat and real concentrostat too.

Indication of redox systems (potentiostat). A potentiostat apparatus with an inert platinum electrode was used to determine molybdenum(VI) (10–200 $ng\ ml^{-1}$) [20, 21] and thorium(IV) (1—5 $\mu g\ ml^{-1}$) with the iodide/hydrogen peroxide reaction and addition of iodide from the burette [38]. Iodide (6—60 $ng\ ml^{-1}$) was determined with the arsenic(III)/cerium(IV)

reaction [38] (cerium(IV) added from the burette) and vanadium(V) (20—200 ng ml^{-1}) with the iodide/bromate indicator reaction [38] (iodide added from the burette). Peroxidase (EC 1.11.1.7) was determined in the range 1—5 IU ml^{-1} with the iodide/hydrogen peroxide reaction (thiosulphate added from the burette) [39] and fluoride (0.38—3.8 ng ml^{-1}) as inhibitor for zirconium in the zirconium(IV)-catalyzed oxidation of iodide with perborate [40] (iodide added from the burette).

Indication with glass pH electrodes (pH-stat). The glass electrode is the most selective electrode known; it was the first electrode used with a Stat apparatus [18, 19]. Examples of the application of the pH-state method are mainly in the field of enzymatic analysis and general biochemistry [10, 31, 34, 36, 41—50]. In organic chemistry, the pH-stat is used for kinetic measurements and preparative purposes. There are also some examples of the application of the pH-stat in inorganic analytical chemistry using indicator reactions with production or consumption of protons. Of course, in pH-stat methods, buffers cannot be used, but several catalyzable redox systems have a more or less marked buffering action [27]; the sensitivity of the method is highest when the maximum pH change caused by acid or base addition and the optimal pH for the catalyzed reaction are in the same region.

Peroxodisulphate is a typical dehydrogenating oxidant in acidic, neutral and alkaline solution. The sodium salt is the more soluble, the potassium salt crystallizes with greater purity, and the ammonium salt is unstable; in oxidations with peroxodisulphate, therefore, the potassium salt is mostly used. These reactions are strongly catalyzed by silver and copper(II); the catalytic activity of osmium(VIII), nickel, vanadium(II) and gold(III) is lower. The applicability of this system was shown for the determination of copper(II) (0.5—5 ng ml^{-1}) serving as catalyst for the oxidation of ascorbic acid (sodium hydroxide added from the burette) [27].

Hydrogen peroxide is a less selective oxidizing reagent than peroxodisulphate, but can also be used for Stat purposes. One example may be mentioned because of its rather unusual mechanism: the oxidation of thiosulphate, which is catalyzed by many metal ions, among them molybdenum(VI). In the absence of the catalyst, this reaction at pH 3.5—4.5 shows a slow, steady increase in alkalinity, expressed by the equation:

$$2S_2O_3^{2-} + H_2O_2 \rightarrow S_4O_6^{2-} + 2OH^-$$

In the presence of molybdenum(VI), the reaction mixture becomes more acidic:

$$S_2O_3^{2-} + 4H_2O_2 \rightarrow 2SO_4^{2-} + 2H^+ + 3H_2O$$

Therefore, beneath a certain minimum concentration of the catalyst, no addition plot is observed with sodium hydroxide. This indicator reaction was used to determine molybdenum(VI) (0.25—2.5 μg ml^{-1}) by addition of sodium hydroxide from the burette [27]. With the zirconium(IV)-

catalyzed oxidation of iodide with consumption of protons, Zr(IV) was determined (0.15—1.5 μg ml^{-1}) with addition of sulphuric acid from the burette [27].

Another example of proton consumption is the vanadium(V)-catalyzed oxidation of iodide with bromate to form iodine, which is removed by an excess of thiosulphate added previously. Vanadium(V) can be determined in the range 0.16—1.6 μg ml^{-1} with addition of sulphuric acid from the burette [27].

Indication with other ion-selective electrodes. Similarly to the glass electrode, other ion-selective electrodes can also be used in the Stat apparatus. An iodide-selective electrode and a cyanide-selective electrode have been applied [51] for the determination of tungsten (0.2—4 μg ml^{-1}) based on the iodide/hydrogen peroxide indicator reaction in glycine buffer solution at pH 2.0 (addition of ascorbic acid from the burette) and for copper(II) (0.6—6 μg ml^{-1}) with the cyanide/hexacyanoferrate(III) indicator reaction in sodium hydroxide solution of pH 11 (addition of sodium cyanide from the burette). A linear calibration graph was obtained by plotting Δ tan α vs. the square of copper concentration. It was shown, however, that the results were better when the data were evaluated from the non-linear calibration graph Δ tan α vs. $[Cu^{2+}]$. Of course, many points are necessary to draw the non-linear graph whilst the linear plot can be defined by only two points. Therefore, it is simplest to draw the linear plot for Δ tan α vs. $[Cu^{2+}]^2$ with a few points, evaluate the slope and construct the non-linear plot using a calculator and plotter.

Amperometric methods

In this group, the amperometric and biamperometric techniques are most useful for application in Stat methods (amperostat and biamperostat). The difference between the methods is that amperometric indication requires only one polarized electrode, i.e., the current is proportional to the concentration of only one electroactive species, whereas biamperometric indication requires two polarized electrodes so that, when both the oxidizable and the reducible forms of a species are electroactive (e.g., Fe(II)/Fe(III), $[Fe(CN)_6]^{4-}/[Fe(CN)_6]^{3-}$), the current flowing at steady state will depend on the species present at lower concentration. For example, in determinations with hexacyanoferrate(III), where hexacyanoferrate(II) is a reaction product, the latter must be present in excess to reach a constant current during the observation time. This is sometimes inconvenient, especially in enzymatic reactions which are often easily reversible. In such cases, amperometric indication may be preferred.

Both amperometric and biamperometric measurements are very sensitive, and so are advantageous if only small changes in the concentration of the indicator substance are observed, e.g., in the determination of catalysts with weak activity. This has been used for the determination of iodine-containing organic compounds [25, 52] and substituted thioureas [23] with biampero-

metric indication, as well as for enzyme determinations [29] with amperometric indication.

Numerous redox systems can be followed biamperometrically. The polarization voltage applied depends on the reversibility of the redox pair, e.g., voltages are 10 mV for iodide/iodine, 50 mV for bromide/bromine or hydrogen peroxide, 100 mV for cerium(III)/cerium(IV) and 300 mV for copper(I)/copper(II). If the applied voltage is >1000 mV, a current flows in most cases, but this is due to electrolysis rather than to a biamperometric reaction. Biamperometry has the advantage that the electrode can be made very small (about 2-mm diameter), so that Stat measurements are possible in as little as 3 ml of solution.

Indication with hexacyanoferrate(II, III). An amperostat based on this general redox couple has been used to determine diaphorase (EC 1.6.4.3) with the NADH/hexacyanoferrate(III) indicator reaction (0.005—0.050 IU ml^{-1}), L-lactate dehydrogenase (EC 1.1.2.3 from bakers yeast) with L-lactate/hexacyanoferrate(III) (0.003—0.050 IU ml^{-1}), xanthine oxidase (EC 1.2.3.2 from buttermilk) with xanthine/hexacyanoferrate(III) (0.0005—0.005 IU ml^{-1}), and peroxidase (EC 1.11.1.7 from horseradish) with hydrogen peroxide/hexacyanoferrate(II) (0.0007—0.007 IU ml^{-1}) [29]. Molybdenum(VI) has been determined with hydrogen peroxide/hexacyanoferrate(II) in the range 23—230 ng ml^{-1} [29]. In all cases, hexacyanoferrate was added from the burette.

With the apparatus used in Stat methods, uncatalyzed kinetic methods can be utilized to determine substances which react only sluggishly with the reagent added from the burette. This was demonstrated for the determination of hydrogen peroxide (7—70 $\mu g\ ml^{-1}$) with hexacyanoferrate(II) (added from the burette to a preset concentration) and amperometric indication [29].

The Stat apparatus can also be used for titrimetric determinations with slowly reacting reagents. Such "kinetic titrations" have the advantage that a preset titrant concentration is kept constant and so the reaction is faster than in the classical titration because of the excess of titrant. This was demonstrated for the determination of cysteine (7—70 $\mu g\ ml^{-1}$) with hexacyanoferrate(III) added from the burette to maintain the preset concentration [29].

Indication with hydrogen peroxide (biamperostat). The hydrogen peroxide redox system can be used for the determination of substances which catalyze the autodecomposition of H_2O_2, added from the burette as it is consumed. In this way, catalase (EC 1.11.1.6) can be determined (0.020—0.200 IU ml^{-1}) and azide (10—100 ng ml^{-1}) can be determined via its inhibition of catalase [26]. Copper(II) (80—800 ng ml^{-1}) and 1,10-phenanthroline as an inhibitor for copper (0.25—2.5 $\mu g\ ml^{-1}$) can be determined with the same reaction [52].

Indication with iodide/iodine (biamperostat). The iodide/iodine system is best indicated biamperometrically because of its low polarization voltage; interferences by electrochemical oxidation are thus almost excluded. The oxidation of iodide by different oxidizing reagents is catalyzed by many metal ions such as Cr(VI), Mo(VI), W(VI), Zr(IV), Hf(IV), Th(IV), Nb(IV)

or Ta(IV), all of which are of interest in industry. In the metal ion-catalyzed oxidation of iodide with hydrogen peroxide, the iodine formed is reduced by controlled addition of ascorbic acid or thiosulphate from the burette, so that a preset concentration of iodide is maintained as well as a small concentration of the iodine formed in the indicator reaction.

Another interesting reaction, which can be monitored with the Stat method, is the iodine/azide system. Here it is especially advantageous that the concentration of iodine can be kept very small during the measuring time by addition from the burette as it is consumed, thus avoiding deactivation of the catalyst (e.g., organic sulfur(II) compounds). This is also possible by using competitive reactions [53, 54], but there the two reactions proceed simultaneously with unpredictable effects on each other.

The iodide/hydrogen peroxide indicator reaction has been used for the determination of molybdenum(VI) (0.15—1.5 $\mu g\ ml^{-1}$) with thiosulphate added from the burette [26] and for glucose oxidase (EC 1.1.3.4) (0.0012—0.012 IU ml^{-1}) [52] as well as for the determination of peroxidase (EC 1.11.1.7; 0.0012—0.018 IU ml^{-1}) [52]. With the copper(II)-catalyzed iodide/peroxodisulphate reaction, copper can be determined in the range 0.33—3.3 $\mu g\ ml^{-1}$ [26].

The iodine/azide reaction was used for systematic investigations of substituent effects in thiourea in aqueous and 20% (v/v) ethanolic solutions, and for the determination of thiourea (0.52—5.2 nmol ml^{-1}), phenylthiourea (0.5—5 nmol ml^{-1}), benzoylthiourea (1.2—12 nmol ml^{-1}) and tetramethylthiuram sulphide (0.12—1.2 nmol ml^{-1}) [23].

Indication with cerium(III)/cerium(IV) (biamperostat). The cerium(III)/cerium(IV) system can be followed biamperometrically. The oxidation of arsenic(III) by cerium(IV) is useful as the indicator reaction because it is catalyzed very sensitively not only by iodide but also by iodine-containing organic compounds such as thyroxine, proteins, hormones and drugs, and by monosubstituted iodobenzenes. Biamperometric indication is very useful for testing the catalytic activities of such iodine-containing organic compounds, because it is not only sensitive but unaffected by side-reactions; spectrophotometric methods cannot be used for many of these compounds because of the yellow iodo complexes formed in solution with cerium(IV). In the Stat method, the concentration of the oxidant, added from the burette, can be kept very low, thus avoiding oxidation of the catalyst, which was observed for the iodoanilines, for example.

The biamperometrically controlled arsenic(III)/cerium(IV) indicator reaction has been used for the systematic investigation of substituent effects in monosubstituted iodobenzenes [25] in aqueous and 20% (v/v) ethanolic solutions. The catalytic activities strongly depended on the nature of the second substituent and on the relative positions of the substituents in the benzene ring, and it was possible to distinguish between *ortho*-, *meta*- and *para*-substitution.

This biamperometric system has been used to determine 4-iodophenol (0.16—1.6 nmol ml^{-1}), 2-iodophenol (0.8—8 nmol ml^{-1}) and 4-iodo-*N*,*N*-

dimethylaniline (0.12—1.2 nmol ml^{-1}) [25] as well as L-thyroxine (13—130 ng ml^{-1}), 5-chloro-7-iodoquinolin-8-ol (13—130 ng ml^{-1}) [52] and iodide (80—800 ng ml^{-1}) [26].

SPECTROPHOTOMETRIC AND LUMINESCENCE METHODS

Any change in absorbance produced by an indicator reaction can be used to regulate the Stat apparatus, as can fluorescence or chemiluminescence reactions.

In decolorization reactions, the range for the determination of a catalyst depends essentially on the absorptivity of the substance measured. From the instrumental point of view, the concentration of the reactant to be kept constant should be such that it causes ca. 10% decrease in the transmittance.

Indication in the ultraviolet-visible range (absorptiostat)

The iodide-catalyzed reaction of arsenic(III) with cerium(IV) can be monitored spectrophotometrically and used for the determination of iodide (10—100 ng ml^{-1}) [21, 22]. Manganese(II) (20—200 ng ml^{-1}) can be determined through the malachite green/periodate reaction and molybdenum(VI) (0.25—2.5 μg ml^{-1}) through the iodide/hydrogen peroxide reaction (iodine measured) [22]. The indigo carmine/hydrogen peroxide reaction can be used [28] to determine sulphide (20—200 nmol ml^{-1}), thioacetamide (40—400 nmol ml^{-1}), thiourea (0.2—2 μmol ml^{-1}) and thiosulphate (0.1—1 μmol ml^{-1}), all of which act as catalysts. Iron(III) (0.65—6.5 ng ml^{-1}) and aluminium(III) (0.4—4 μg ml^{-1}) can be determined because they are activators for thiosulphate as catalyst; fluoride (0.6—6 μg ml^{-1}) can be determined via its deactivating action on aluminium(III) [28].

The oxidation of bromopyrogallol red with hydrogen peroxide is catalyzed by thiourea and some substituted thioureas. This has been used in mechanistic studies of these compounds and for the determination of thiourea, N-methylthiourea, N-allylthiourea or thioacetamide in the range 60—600 nmol ml^{-1} [24].

The application of the absorptiostat technique in the ultraviolet range is especially useful for enzyme-catalyzed reactions [33]. This has been utilized for the determination of 0.2—2 IU ml^{-1} catalase (EC 1.11.1.6) with hydrogen peroxide added from the burette, 0.0004—0.004 IU ml^{-1} ascorbate oxidase (EC 1.10.3.3) with ascorbic acid/atmospheric oxygen as indicator reaction and ascorbic acid added from the burette, and 4—40 μg ml^{-1} cytochrome c via the ascorbic acid/hydrogen peroxide reaction with addition of ascorbic acid from the burette. Copper(II) (0.1—1 μg ml^{-1}) can also be quantified on the basis of the ascorbic acid/hydrogen peroxide reaction. Peroxidase (0.05—0.50 IU ml^{-1}) has been determined by means of its catalysis of the dihydroxyfumaric acid/hydrogen peroxide reaction, 0.002—0.020 IU ml^{-1} sorbitol dehydrogenase (EC 1.1.1.14) by means of the D-fructose/NADH reaction, and 0.002—0.020 IU ml^{-1} lactate dehydrogenase (EC 1.1.1.27) by

the pyruvate/NADH reaction; in the latter two cases, NADH was added from the burette [33].

Indication by fluorescence or luminescence

Fluorimetry can be up to several orders of magnitude more sensitive than molecular absorption spectrophotometry. With the fluoristat technique [55], it is possible to quantify inorganic catalysts and enzymes which react with a fluorescent substrate to form non-fluorescent products. This is done by controlled addition of the fluorescent substrate at a speed such that the fluorescence remains constant during the reaction time observed. The Stat technique can also be used to follow reactions that produce fluorescent products from non-fluorescent substrates; in this case, the increasing fluorescence is quenched by controlled addition of a suitable substance to keep the fluorescence constant during the measuring time.

Alkaline phosphatase (EC 3.1.3.1) has been determined over the 0.04—0.8 IU ml^{-1} range with 1-naphthyl phosphate; 0.002—0.025 IU ml^{-1} sorbitol dehydrogenase can be quantified via the D-fructose/NADH reaction, and 0.03—0.30 IU ml^{-1} peroxidase via the scopoletin/hydrogen peroxide reaction. These three procedures involve a fluorescence decrease. Increases in fluorescence are utilized in the determination of 1.25—12.5 IU ml^{-1} pseudocholinesterase (EC 3.1.1.8) with 1-naphthyl acetate; erythrosine is added from the burette as quencher [55].

Various metal ions (e.g., Co, Mn, Cu, Pb) catalyze the chemiluminescent reaction between luminol (5-amino-2,3-dihydro-1,4-phthalazinedione) and hydrogen peroxide. In the Stat method [56], a preset level of radiation is kept constant in a catalyzed chemiluminescent reaction by regulated addition of the oxidant. To achieve this, the radiation intensity is measured with a photomultiplier and the current obtained is converted to an equivalent voltage in the millivolt range with a current/voltage transducer. In this way, copper(II) has been determined in the range 0.5—5 $\mu g\ ml^{-1}$ and L-histidine (2—20 $\mu g\ ml^{-1}$) by its inhibiting action on copper(II). Analogously, cobalt(II), manganese(II) and lead(II) can be determined in the range 0.5—2.5 $\mu g\ ml^{-1}$, 0.5—5 $\mu g\ ml^{-1}$ and 1.25—6 $\mu g\ ml^{-1}$, respectively [56].

REFERENCES

1 G. Witz and F. Osmond, Bull. Soc. Chim. Fr., 45 (1885) 309.
2 A. Guyard, Bull. Soc. Chim. Fr., 25 (1876) 58.
3 E. B. Sandell and I. M. Kolthoff, J. Am. Chem. Soc., 56 (1934) 1426.
4 E. B. Sandell and I. M. Kolthoff, Mikrochim. Acta (Wien), (1937) 9.
5 H. H. Willard and P. Young, J. Am. Chem. Soc., 50 (1928) 1372.
6 L. Szebelledy and M. Ajtai, Mikrochemie, 25 (1938) 258.
7 L. Szebelledy and M. Ajtai, Mikrochemie, 26 (1939) 87.
8 K. B. Yatsimirskii, Kinetic Methods of Analysis, Pergamon, Oxford, 1966.
9 G. Osann, Poggendorfs Ann., 67 (1845) 372.
10 G. G. Guilbault, Enzymatic Methods of Analysis, Pergamon, Oxford, 1970.
11 T. S. Lee and I. M. Kolthoff, Ann. N.Y. Acad. Sci., 67 (1951) 1484.

12 A. M. Albrecht-Gary, J.-P. Collin, P. Jost, P. Lagrange and J.-P. Schwing, Analyst, 103 (1978) 227.
13 Ch.-M. Wolff and J.-P. Schwing, Bull. Soc. Chim. Fr., (1976) 679.
14 H. Müller, M. Otto and G. Werner, Katalytische Methoden in der Spurenanalyse, Akadem. Verlagsgesellschaft Geest und Portig, Leipzig, 1980, p. 94 ff.
15 I. M. Kolthoff and T. S. Lee, J. Polym. Sci., 2 (1947) 200.
16 I. M. Kolthoff, T. S. Lee and M. A. Mairs, J. Polym. Sci., 2 (1947) 220.
17 J. Clarens, Bull. Soc. Chim. Fr., 29 (1921) 837.
18 C. F. Jacobson and J. Leonis, C. R. Trav. Lab. Carlsberg, Ser. Chim., 27 (1951) 333.
19 K. M. Møller, Biochim. Biophys. Acta, 16 (1955) 162.
20 H. Weisz, D. Klockow and H. Ludwig, Talanta, 16 (1969) 921.
21 D. Klockow, H. Weisz and K. Rothmaier, Fresenius' Z. Anal. Chem., 264 (1973) 385.
22 H. Weisz and K. Rothmaier, Anal. Chim. Acta, 75 (1975) 119.
23 S. Pantel, Anal. Chim. Acta, 152 (1983) 215.
24 S. Pantel, Anal. Chim. Acta, 158 (1984) 85.
25 S. Pantel, Anal. Chim. Acta, 141 (1982) 353.
26 S. Pantel and H. Weisz, Anal. Chim. Acta, 70 (1974) 391.
27 S. Pantel, Anal. Chim. Acta, 104 (1979) 205.
28 H. Weisz, S. Pantel and G. Marquardt, Anal. Chim. Acta, 143 (1982) 177.
29 S. Pantel, Anal. Chim. Acta, 167 (1985) 343.
30 K. J. Wood, Anal. Chem., 32 (1960) 537.
31 H. V. Malmstadt and E. H. Piepmeier, Anal. Chem., 37 (1965) 34.
32 R. Job and S. Freeland, Anal. Biochem., 79 (1977) 575.
33 S. Pantel and H. Weisz, Anal. Chim. Acta, 109 (1979) 351.
34 R. E. Lemke and G. M. Hieftje, Anal. Chim. Acta, 141 (1982) 173.
35 P. Bergveld, B. H. Van der Schoot and J. K. L. Onokiewicz, Anal. Chim. Acta, 151 (1983) 143.
36 R. E. Karcher and H. L. Pardue, Clin. Chem., 17 (1971) 214.
37 D. Klockow, G. Karenovics and W. Meiners, Anal. Chim. Acta, 100 (1978) 485.
38 H. Weisz, K. Rothmaier and H. Ludwig, Anal. Chim. Acta, 73 (1974) 224.
39 J. K. Grime and K. R. Lockhart, Anal. Chim. Acta, 106 (1979) 251.
40 D. Klockow, H. Ludwig and M. A. Giraudo, Anal. Chem., 42 (1970) 1682.
41 C. F. Jacobson, J. Leonis, K. Linderstrom-Lang and M. Ottesen, in D. Glick (Ed.), Methods of Biochemical Analysis, Vol. IV, Interscience, New York, 1957, p. 171.
42 E. C. Toren Jr. and F. J. Burger, Mikrochim. Acta (Wien), (1968) 1049.
43 H. J. Schneider, H. Schneider-Bernlöhr and M. Hanack, Justus Liebigs Ann. Chem., 722 (1969) 234.
44 W. Rick, Z. Klin. Chem. Klin. Biochem., 7 (1969) 530.
45 K. Tsuji, Microchem. J., 18 (1973) 163.
46 F. Malis and P. Fric, Arzneim.-Forsch., 24 (1974) 499.
47 A. Le Berre and A. Delacroix, Bull. Soc. Chim. Fr., 11 (1974) 2639.
48 S. Dupre, A. Antonucci, P. Piergrossi and M. Aureli, Ital. J. Biochem., 25 (1976) 229.
49 B. Tan and J. K. Grime, Anal. Lett., 12 (1979) 1551.
50 H. Garth and E. Zoch, J. Clin. Chem. Clin. Biochem., 22 (1984) 769.
51 A. Sardemann, Diploma Thesis, Freiburg i. Br., 1984.
52 S. Pantel and H. Weisz, Anal. Chim. Acta, 89 (1977) 47.
53 H. Müller, L. Beyer, Ch. Müller and Ch. Schröter, Z. Anorg. Allg. Chem., 446 (1978) 226.
54 D. Klockow, J. Auffarth and G. F. Graf, Fresenius' Z. Anal. Chem., 311 (1982) 244.
55 S. Pantel, Anal. Chim. Acta, 129 (1981) 231.
56 S. Pantel and H. Weisz, Anal. Chim. Acta, 74 (1975) 275.

Analytica Chimica Acta, 199 (1987) 15—27
Elsevier Science Publishers B.V., Amsterdam — Printed in The Netherlands

MULTIDETECTION FLOW-INJECTION TECHNIQUES FOR MANIPULATION OF SENSITIVITY
Amplification and Dilution Methods

A. RÍOS, F. LÁZARO, M. D. LUQUE DE CASTRO and M. VALCÁRCEL*

Department of Analytical Chemistry, Faculty of Sciences, University of Córdoba, Córdoba (Spain)

(Received 13th October 1986)

SUMMARY

Different multidetection flow-injection techniques are considered for the manipulation of analytical sensitivity and for broadening the determination range of an analyte with maximum accuracy. Conventional spectrophotometric detection in linear or cyclic flow systems and a diode-array detector for monitoring several wavelengths simultaneously are used. The formaldehyde/pararosaniline/sulfite system is used for studying these techniques.

The term multidetection is related to obtaining two or more values of the measured signal per analyzed sample. In static systems, this term usually refers to the use of detectors of different nature (e.g., spectroelectrometry [1]) or, recently, to the use of array detectors [2]. Flow systems involve a new aspect of multidetection because of the dynamic situation in which measurements are made [3]. Flow injection analysis (FIA) introduces a new, double kinetic aspect (physical and chemical) arising from one of its fundamental characteristics, the absence of physical homogenization or chemical equilibria. This dynamic character allows certain types of detection to be used. In this context, there are three types of multidetection. The first uses a single conventional detector, which either gives one peak per sample with measurements made at different times along the peak response [4], or gives more than one peak per sample [5]. Another uses an array detector (e.g., a diode-array spectrophotometer) which monitors the instrumental variable simultaneously at several values of time, wavelength, etc. [6]. A third possibility is the use of several detectors of the same [7] or different [8] nature, located in series [9] or in parallel [10], or of a double-beam spectrophotometer [11]. Usually, the information obtained is used for the determination of several components in a single sample, although it can also be used to manipulate sensitivity in determining a single analyte over a wide concentration range.

In this paper, the different methods of FIA available for multidetection with a single diode-array spectrophotometric detector are compared for the determination of a species (formaldehyde) in water by reaction with *para*-

0003-2670/87/$03.50

rosaniline/sulfite [12]. The sample is directly inserted into the system with no prior dilution or concentration, and the data provided by the detector are treated by amplification or dilution methods if the analyte concentration in the sample is below or above, respectively, the lower and the upper limit of the confidence range of the conventional calibration graph. This provides an excellent alternative to the customary manipulation of the sample prior to its injection as the manipulation of the data provided by the detector, in addition to making any prior operation unnecessary, eliminates the errors inherent in such treatments. Another dilution method not considered here is the peak-width method, which is related to the log of the analyte concentration [13].

PRINCIPLES

The application of the amplification and dilution methods described below are based on the following three principles.

First, when the analytical reaction provides a single peak at a given wavelength (Fig. 1a), the conventional flow-injection method involves measurement of the maximum height of the peak. The dilution method entails measurement of the signal at several locations on the peak other than at the maximum, in much the same way as Růžička and Hansen's "electronic dilution" [4]. The amplification method is based on the sum of several absorbance signals measured around the peak maximum.

Secondly, when several peaks are obtained at a given wavelength, as in a cyclic system [5] (Fig. 1b), the highest peak is normally measured. Here the dilution method involves measurement at a minimum, while the amplification method relies on the sum of several maxima (ΣS_m). In both these cases, the measurements can be made with a conventional spectrophotometer.

Thirdly, when peaks are obtained as a result of monitoring the reaction at several wavelengths (Fig. 1c) (e.g., the use of a diode-array spectrophotometer which allows simultaneous monitoring at several wavelengths), the conventional method uses the maximum of the peak obtained at the wavelength of maximum absorption. The dilution method uses a peak away from the maximum absorption wavelength, whilst the amplification method uses the sum of the peak heights obtained at several wavelengths around the wavelength of maximum absorption.

EXPERIMENTAL

Reagents and equipment

Solutions of 4 g l^{-1} *para*rosaniline (Fluka) in 0.252 M sulfuric acid/10% (v/v) ethanol, 0.5 g l^{-1} sodium sulfite (Merck) in water, and 37% (w/v) formaldehyde in water were prepared. The sulfite solution was prepared daily. The formaldehyde solution was standardized [14]. It was stable for several months.

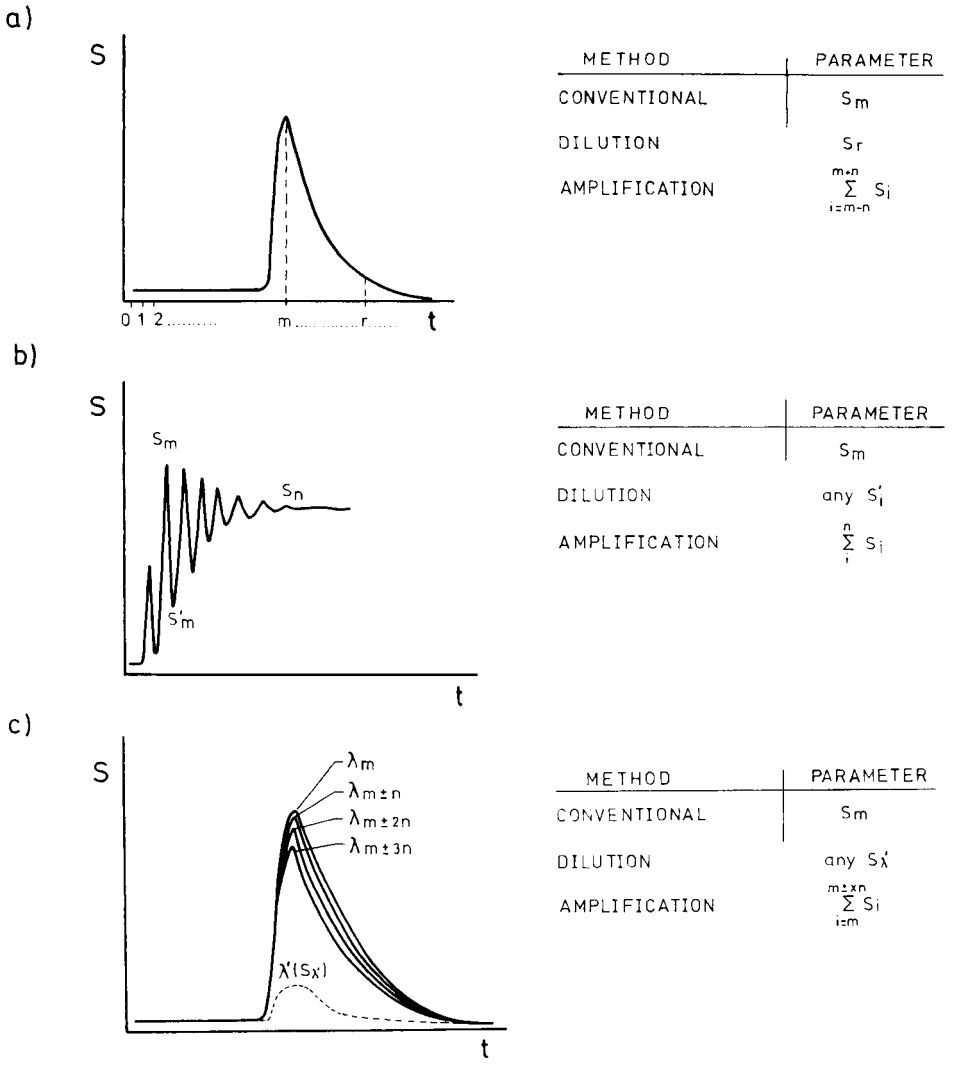

Fig. 1. Principles of the different types of dilution and amplification methods. (a) Single peak and measurement of the analytical signal at different times; S_i are signals measured at different times (between $m - n$ and $m + n$) around the maximum m of the signal. (b) Several peaks per injected sample obtained in a cyclic system and measurement of one or several maxima or minima; S_i are signals corresponding to the maxima of the different peaks. (c) Simultaneous production of several (n) peaks at n different wavelengths and measurement of the maximum absorbance of one or several of them; S_i, signals measured at the maximum (m) and at wavelengths around m.

A Hewlett-Packard 8451A diode-array spectrophotometer was used with an HP-9121 floppy disk unit, HP-98155A keyboard and HP-7470A plotter. Other equipment included a Gilson Minipuls-2 peristaltic pump, a Hellma 178.12QS flow cell (inner volume 18 μl), two Tecator L-100-1 injection

valves and a Tecator TM-II Chemifold.

The manifolds used are shown in Fig. 2. Multidetection in flow-through systems (a and c, Fig. 1) was implemented with configuration (a). Multidetection in a cyclic system (b, Fig. 1) was achieved with the aid of configuration (b). The sulfite and *para*rosaniline streams merge prior to valve S. In one position of this valve, the stream flowing through channel 1 flows through the detector and back to the valve S (channel 2 flows to waste, W_2). In the other position, valve S allows the contents of channel 2 to pass through the detector again, whilst the contents of channel 1 go to waste, W_1. In this system, the sample is injected through the valve located in the closed circuit, in which the flow is propelled by pump P′ (which can be a channel of pump P). The total length of the cycling circuit is 215 cm. The number of peaks obtained coincides with the number of cycles of the reacting sample through the detector before equilibrium is attained (Fig. 1b). By switching valve S to the first position, the system is flushed with fresh carrier solution and prepared for a new injection.

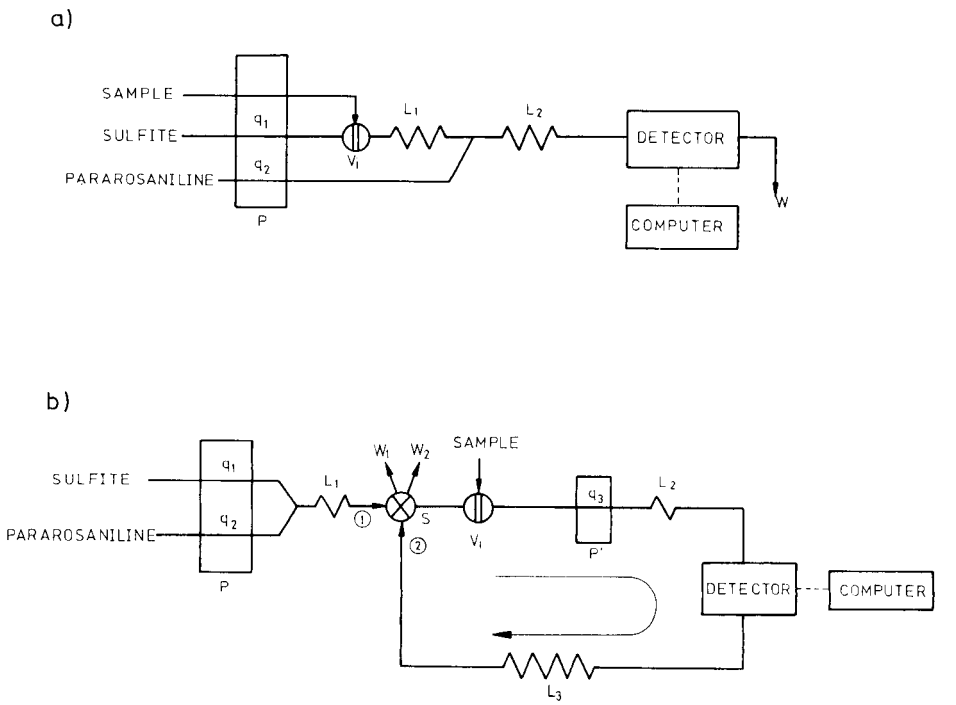

Fig. 2. Flow-injection configurations used to implement dilution and amplification methods by multidetection with a single detector. (a) Methods based on measurements on the peak at different times (conventional spectrophotometric detector) or at several wavelengths (diode array spectrophotometer). (b) Methods based on obtaining several peaks per injected sample (conventional spectrophotometric detector). P, pump; q, flow rate; L, reactor length; W, waste.

Programs for data treatment

Data were processed with the aid of a program suited to each multidetection technique and operating according to the flow diagram in Fig. 3. First, seven calibration graphs were obtained with formaldehyde standards: a conventional graph, three amplification graphs and three dilution graphs, to give a very wide determination range for the analyte. The following nomenclature is used: conventional calibration graph, N; dilution calibration graph, D_1 (first), D_2 (second), D_3 (third); amplification calibration graph, AM_1 (first), AM_2 (second), AM_3 (third). (L_l and L_u are the lower and upper limits, respectively, of the calibration graph.) When the sample is injected, the program selects the most suitable calibration graph (and hence the most suitable method) by gradually comparing the absorbance (A) with the corresponding limits (A_l, A_u) as shown in Fig. 3. After selection of the most suitable method and calibration graph, the analyte concentration is calculated by using the corresponding equation.

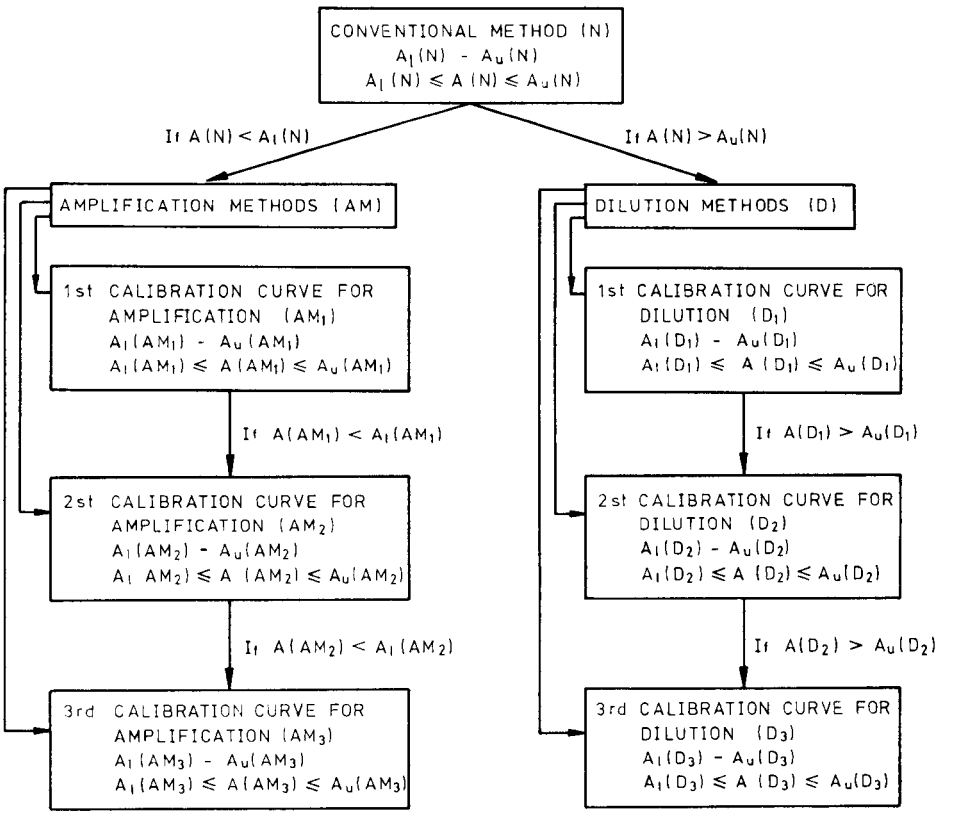

Fig. 3. Flow chart of the programs for developing the proposed amplification and dilution methods by multidetection (see text). A is an experimental parameter referred to each method, $A(X)$.

RESULTS AND DISCUSSION

A distinction is made between linear (Figs. 1a, 1c and 2a) and cyclic flow systems (Figs. 1b and 2b). After each linear calibration range had been established, the three manipulation methods were compared in terms of accuracy and precision.

Linear systems

The optimization of manifold 2(a) yielded the following values: flow rates $q_1 = q_2 = 0.42$ ml min^{-1}; injected volume $V_i = 200$ µl; reactor lengths $L_1 =$ 10 cm, $L_2 = 725$ cm (0.5-mm inner diameter in both cases). The values of the chemical variables yielding the greatest analytical signal with minimum baseline absorbance are given in the Experimental section.

Monitoring at a single wavelength (M_t methods). The conventional amplification and dilution methods were applied at different times along the single response peak obtained at the wavelength of maximum absorbance (Fig. 1a). Table 1 shows the linear ranges and slopes of the calibration graphs obtained for these methods, which provide a wide determination range for formaldehyde (0.1—240 µg ml^{-1}). The sensitivity over each range and the "manipulation factor" for sensitivity, defined as the ratio between the sensitivity (slope) of the calibration graph and the sensitivity of the conventional calibration graph are also given. This factor (chosen by the operator according to the number of measurements made and the location on the peak at which they are made) ranges between 23 and 0.04. As the ranges covered by the methods overlap, the range over which each method was applied appears in Table 1 under "programmed concentration range".

When a sample is injected, the calculation program selects the most suitable calibration graph for the particular determination, depending on the value of the absorbance considered (see Fig. 3). Tables 2 and 3 show the accuracy and precision provided by this multidetection technique for different formaldehyde concentrations. The smallest average errors were obtained in the range of the conventional calibration graph and increased as the calibration used shifted from this range. The relative standard deviation (RSD), calculated for eleven determinations, was lowest for concentrations in the range of N, AM_1, D_1 and D_2, increasing at the extremities (AM_3, AM_2 and D_3).

Monitoring at several wavelengths (M_λ methods). The detector (diode-array spectrophotometer) provides a flow-injection peak for each wavelength monitored, and measures only the absorbances at the maxima of these peaks, which are stored in the microprocessor. Therefore, this multidetection technique is based on simultaneous measurement at several wavelengths (Fig. 1c). Table 4 summarizes the features of the seven calibration graphs obtained by use of the various data-manipulation methods. Up to 25 wavelengths can be monitored simultaneously, which gives the maximum amplification. The overall range for determination of formaldehyde is

TABLE 1

Features of the calibration graphs obtained in the method of sensitivity manipulation by multidetection based on the measurement of the signal at different times on the peaks

Calibration	Measured parameter[a]	Determination range[b] (μg ml^{-1})	Programmed conc. range[c] (μg ml^{-1})	Sensitivity[d] (μg^{-1})	Manipulation factor[c]
AM_3	Sum of absorbances obtained at 23 times between 138.9 and 141.1 s	0.1—0.4	[HCHO] $\leqslant$ 0.32	2.059	23.0
AM_2	As above, at 9 intervals (139.6—140.4 s)	0.25—1.0	0.32 < [HCHO] $\leqslant$ 0.85	0.803	9.0
AM_1	As above, at 3 intervals (139.9—140.1 s)	0.7—3.0	0.85 < [HCHO] $\leqslant$ 2.5	0.268	3.0
N	Absorbance at 140.0 s	2.0—8.0	2.5 < [HCHO] $\leqslant$ 6.5	0.089	1.0
D_1	Absorbance at 162.0 s	5.0—20.0	6.5 < [HCHO] $\leqslant$ 18.5	0.039	0.44
D_2	Absorbance at 186.0 s	17.0—62.0	18.5 < [HCHO] $\leqslant$ 61.0	0.013	0.15
D_3	Absorbance at 205.0 s	60—240	[HCHO] > 61.0	0.0034	0.04

[a]Data acquisition every 0.1 s. [b]Giving absorbances of 0.2—0.8. [c]See text. [d]Slope of calibration graph.

TABLE 2

Accuracy of the methods for sensitivity manipulation by multidetection

Method	HCHO added ($\mu g\ ml^{-1}$)[a]	Error (%)	HCHO added ($\mu g\ ml^{-1}$)[b]	Error (%)	HCHO added ($\mu g\ ml^{-1}$)[c]	Error (%)
AM_3	0.09	+3.3	0.12	−5.3	0.11	−14.5
	0.17	−5.5	0.22	−3.4	0.25	−4.0
	0.23	+3.5	0.26	+3.6	0.50	−6.0
	0.32	−0.5	0.32	−1.2	0.77	+2.6
AM_2	0.35	+2.4	0.40	−2.1	0.96	−2.1
	0.52	−3.4	0.52	+1.5	1.00	+6.0
	0.69	+1.6	0.69	+0.9	1.10	+2.7
	0.84	−0.2	0.89	−0.6	1.35	+3.7
AM_1	0.92	+0.2	1.01	+1.9	1.50	−2.0
	1.35	−1.9	1.44	−1.4	2.15	−1.9
	1.87	+2.6	1.87	−0.9	2.30	−2.6
	2.30	−1.1	2.30	+0.8	2.50	−3.6
N	2.59	+0.9	3.17	+1.1	2.88	+2.1
	3.74	−1.2	4.03	−0.6	3.15	−1.9
	4.61	+0.3	5.18	−0.2	4.00	−0.5
	5.76	+0.1	6.91	+1.4	4.80	+1.7
D_1	7.20	−1.9	8.64	−0.5	5.50	+2.0
	10.37	+1.2	14.40	+1.4	6.00	−1.2
	13.8	+1.0	20.2	−1.3	7.50	+1.1
	17.3	−0.8	25.9	+0.5	9.25	+1.2
D_2	23.0	+1.5	34.6	−1.0	10.30	−2.0
	34.6	+0.7	66.2	+1.4	15.00	−1.5
	46.1	−3.3	72.0	−1.4	25.00	−1.3
	57.6	+1.6	83.5	−0.8	33.50	+0.8
D_3	86.4	+6.2	158	−0.3	40.50	+2.8
	144	−5.8	216	−0.4	75.00	−1.1
	202	+0.4	230	+8.2	115.0	+2.5
	271	+0.7	279	−0.3	148	+3.0

[a]Measurement of the absorbance at different times on the FIA peak. [b]Simultaneous monitoring at several wavelengths. [c]Monitoring of several peaks obtained in a cyclic system.

between 0.1 and 300 $\mu g\ ml^{-1}$, with manipulation factors from 24 to 0.03. The calibration ranges provided by the calculation program are also shown in Table 4.

Tables 2 and 3 show the accuracy and precision achieved by this multidetection technique by use of the calibration features described in Table 4 over the ranges indicated therein. The smallest average errors are again obtained for concentrations in the range of the conventional calibration graph, whilst the largest errors correspond to the extreme concentrations. Precision was best for methods N, D_1 and D_2.

TABLE 3

Precision of the methods for sensitivity manipulation by multidetection

	Method						
	AM_3	AM_2	AM_1	N	D_1	D_2	D_3
Procedure A[a]							
HCHO conc. (μg ml^{-1})	0.26	0.60	1.92	5.12	12.0	40.8	152
RSD (%)[b]	3.0	2.8	1.1	1.9	1.5	1.2	2.7
Procedure B[c]							
HCHO conc. (μg ml^{-1})	0.24	0.80	1.76	5.28	17.3	67.2	184
RSD (%)[b]	4.3	3.2	2.6	1.8	1.8	0.7	2.6
Procedure C[d]							
HCHO conc. (μg ml^{-1})	0.50	1.10	2.00	3.75	7.50	22.5	90.0
RSD (%)[b]	4.1	2.9	2.5	1.4	2.0	3.1	4.4

[a]Measurement of the absorbance at different times on the FIA peak. [b]Triplicate injections of 11 different samples. [c]Simultaneous monitoring of several wavelengths. [d]Several peaks obtained in the cyclic system.

Cyclic systems (M_p methods)

The manifold used is depicted in Fig. 2(b). The optimum values of the flow-injection variables were: flow rates $q_1 = q_2 = 0.42$ ml min^{-1}, $q_3 = 0.80$ ml min^{-1}; injected volume $V_i = 200$ μl; reactor lengths $L_1 = 25$ cm, $L_2 = 40$ cm, $L_3 = 140$ cm (0.5-mm inner diameter). One set of peaks per injected sample was obtained by monitoring at a single wavelength. The maxima and minima of such peaks provided the information required to implement this type of multidetection (Fig. 1b). Table 5 shows the features of the different calibration graphs used in each method as well as the parameters by which they were obtained. The programmed calibration ranges for the method are also collected in Table 5.

The accuracy and precision of the techniques are summarized in Tables 2 and 3. The smallest average errors are obtained for the conventional and dilution methods, whilst the smallest RSD corresponds to the conventional method and again increases noticeably for the extreme ranges (AM_3 and D_3).

Comparison of the results

The three multidetection techniques are compared from the points of view of their use in manipulation methods on the basis of a number of parameters. Multidetection based on the wavelength (M_λ) shows the widest determination range, cyclic systems the least. The three techniques have the same lower determination limit. The range of the manipulation factor for the M_λ and M_t methods is almost the same, that for cyclic systems (M_p) being somewhat smaller. A function (ϕ_p) covering the ranges of the seven calibration procedures was defined in order to compare the precision of the results:

TABLE 4

Features of the calibration graphs obtained in the method of sensitivity manipulation by multidetection based on simultaneous monitoring at several wavelengths

Calibration	Measured parameter[a]	Determination range[b] ($\mu g\ ml^{-1}$)	Programmed conc. range[b] ($\mu g\ ml^{-1}$)	Sensitivity[b] (μg^{-1})	Manipulation factor[b]
AM_3	Sum of the absorbances obtained at 25 wavelengths around the maximum (554—602 nm)	0.1—0.4	[HCHO] $\leqslant$ 0.35	2.007	23.8
AM_2	As above, at 7 wavelengths (572—584 nm)	0.3—1.3	0.35 < [HCHO] $\leqslant$ 1.0	0.628	7.5
AM_1	As above, at 3 wavelengths (576—580 nm)	0.7—3.0	1.0 < [HCHO] $\leqslant$ 2.5	0.271	3.2
N	Absorbance at 578 nm	2.0—8.0	2.5 < [HCHO] $\leqslant$ 7.5	0.084	1.0
D_1	Absorbance at 614 nm	7.0—30.0	7.5 < [HCHO] $\leqslant$ 28.5	0.025	0.30
D_2	Absorbance at 630 nm	26.0—106	28.5 < [HCHO] $\leqslant$ 90.0	0.0075	0.09
D_3	Absorbance at 642 nm	74.0—300	[HCHO] > 90.0	0.0027	0.03

[a] Absorbance measured each 2 nm. [b] As specified in Table 1.

TABLE 5

Features of the calibration graphs obtained in the method of sensitivity manipulation by multidetection based on several peaks obtained in a cyclic system

Calibration	Measured parameter	Determination range[a] ($\mu g\ ml^{-1}$)	Programmed conc. range[a] ($\mu g\ ml^{-1}$)	Sensitivity[a] (μg^{-1})	Manipulation factor[a]
AM_3	Sum of the absorbances of the first 6 peaks	0.1—1.1	[HCHO] $\leqslant$ 0.8	0.945	6.1
AM_2	Sum of the first 4 peaks	0.65—1.55	0.8 < [HCHO] $\leqslant$ 1.4	0.667	4.3
AM_1	Sum of the first 2 peaks	1.1—3.55	1.4 < [HCHO] $\leqslant$ 2.5	0.242	1.6
N	Absorbance of 2nd peak	1.6—5.5	2.5 < [HCHO] $\leqslant$ 5.0	0.156	1.0
D_1	Absorbance of 3rd minimum	3.5—11.5	5.0 < [HCHO] $\leqslant$ 10.0	0.077	0.4
D_2	Absorbance of 2nd minimum	5.0—40.0	10.0 < [HCHO] $\leqslant$ 35.0	0.027	0.1
D_3	Absorbance of 1st minimum	10.0—150	[HCHO] > 35.0	0.0042	0.03

[a] As specified in Table 1.

$$\phi_p = \left(\sum_{i=1}^{n} C_i/n\right)\left(\sum_{i=n}^{n} (\mathrm{RSD})_i/n\right)$$

which corresponds to the product of the average of the formaldehyde concentrations in the range (C_i) and the average of the relative standard deviations (for eleven samples). The values of this function for each procedure were $\phi_p(M_t) = 59$, $\phi_p(M_\lambda) = 95$, $\phi_p(M_p) = 53$, which indicates that methods M_t and M_p are more precise than M_λ. This means that the errors made in measuring the absorbance at a wavelength other than the maximum are more important than those arising from measuring the peak height at a different point on the flow peak from the maximum or from cycling the reacting sample through the detector. It can be concluded that the errors encountered in the conventional and dilution methods are smaller than those in the amplification methods with the exception of M_t, for which they are of the same order.

The sampling frequencies for methods M_λ and M_t are similar (about 25 h^{-1}), that for M_p being somewhat less for the amplification method owing to the need to obtain a larger number of peaks. Nevertheless, if other aspects are considered, method M_p offers important advantages over the other two techniques. First, it is instrumentally more straightforward; in fact, it uses a single conventional detector which need not be coupled on-line to a microprocessor (this is indispensable for methods M_t and M_λ, the latter also requiring a more sophisticated interface and more memory). The amount of analytical information provided by each technique varies greatly (M_t being the poorest). Method M_λ offers more information because it provides a peak for each wavelength used for monitoring; this is of relevance to simultaneous determinations, but not to the determination of a single species. In contrast, method M_p determines the physical and chemical evolution of the analyte in the system and involves kinetic aspects not detected in methods M_t and M_λ.

All three techniques make it possible to manipulate the analytical signal extensively in unsegmented flow systems. An advantageous result of the broad calibration range is the possibility of determining an analyte without prior dilution or concentration of the sample. The advantages inherent in the flow-injection technique as an automatic method of analysis are enhanced as a result of this avoidance of sample preconcentration or dilution.

This work was supported by the C.A.I.C.y.T. under grant No. 2012-83.

REFERENCES

1 T. Kuwana, R. Darlington and D. Leedy, Anal. Chem., 36 (1964) 2023.
2 Y. Talmi, Multichannel Image Detectors, Vols. I and II, ACS Symposium Series, American Chemical Society, Washington DC, 1979.
3 M. D. Luque de Castro and M. Valcárcel, Trends Anal. Chem., 5 (1986) 71.

4 J. Růžička and E. H. Hansen, Anal. Chim. Acta, 145 (1983) 1.
5 A. Ríos, M. D. Luque de Castro and M. Valcárcel, Anal. Chem., 57 (1985) 1803.
6 F. Lázaro, A. Ríos, M. D. Luque de Castro and M. Valcárcel, Anal. Chim. Acta, 179 (1986) 279.
7 D. J. Hooley and R. S. Dessy, Anal. Chem., 55 (1983) 313.
8 E. A. G. Zagatto, A. O. Jacintho, L. C. R. Pessenda, F. J. Krug, B. F. Reis and H. Bergamin F°, Anal. Chim. Acta, 125 (1981) 37.
9 R. Virtanen, Anal. Symp. Ser., 8 (1981) 375.
10 W. D. Basson and J. F. Van Staden, Fresenius' Z. Anal. Chem., 302 (1980) 370.
11 A. Fernández, M. D. Luque de Castro and M. Valcárcel, Anal. Chem., 56 (1984) 1146.
12 R. R. Miksch, D. W. Anthon, L. Z. Fanning, C. D. Hollowell, K. Revzan and J. Glauville, Anal. Chem., 53 (1981) 2118.
13 K. K. Stewart and A. G. Rosenfeld, Anal. Chem., 54 (1982) 2368.
14 J. K. Walker, Formaldehyde, R. E. Krieger, Huntington, NY, 1975, pp. 486—487.

Analytica Chimica Acta, 199 (1987) 29—40
Elsevier Science Publishers B.V., Amsterdam — Printed in The Netherlands

VERSATILE AUTOMATIC STOPPED-FLOW SYSTEM FOR ROUTINE ANALYSIS

A. LORIGUILLO, M. SILVA and D. PÉREZ-BENDITO*

Department of Analytical Chemistry, Faculty of Sciences, University of Córdoba, Córdoba (Spain)

(Received 9th December 1986)

SUMMARY

A versatile, automatic stopped-flow system featuring a mixing module and real-time data collection and treatment is presented. The mixing module is compatible with a number of spectrophotometers and spectrofluorimeters. The fast reaction between iron(III) and thiocyanate is used to evaluate the performance of the system and to develop a routine procedure for the determination of iron in wines, with a reaction time of 3 s. The calibration is linear over the range 1—30 $\mu g\ ml^{-1}$, with a r.s.d. of 0.9% ($n = 11$) for 10 μg Fe ml^{-1} and a high sample throughput (120 h^{-1}) is achieved.

The stopped-flow technique has normally been used to obtain basic information about fast chemical reactions (rate law, rate constants, activation energies etc.). It is useful for routine rapid chemical determinations, but can also be used with slow or equilibrium methods. The use of a computer-based stopped-flow system with automated control, data acquisition, data processing and solution preparation has resulted in significantly increased measurement throughput, precision, accuracy and flexibility [1—10]. Stopped-flow analysis is sufficiently versatile to accommodate a wide range of analytical procedures and often has advantages over other flow techniques such as flow injection analysis (FIA) and air-segmented continuous flow analysis (CFA) [8]. Thus, more precise (about 0.1%) and quantitative kinetic methods can readily be applied to very fast reactions (in the sub-second range) with greater sample throughput than afforded by FIA or CFA.

Several stopped-flow instruments are commercially available, but they are expensive. In order to reduce costs, a mixing flow module which can readily be fitted to any spectrophotometer or spectrofluorimeter and controlled by means an inexpensive on-line computer has been designed. This module is accommodated vertically above the detector. The mixing chamber, a straightforward commercial flow-cell, is also an observation chamber. The module also features a pneumatic propulsion system and a thermostatted chamber based on water recirculation. This automatic analyzer allows the use of reactions with half-lives in the millisecond range, as well as rapidly producing analytical results by use of computer programs developed for equilibrium, kinetic and differential kinetic methods.

0003-2670/87/$03.50

The simplicity of the automated modular stopped-flow system proposed herein allows the application of this technique, so far limited to methods based on fast reactions, to kinetic measurements on slow and equilibrium systems, with considerable gains in sample throughput, reproducibility and accuracy with respect to manual procedures, hence its special suitability for routine analyses. This last aspect was tested by using the module for the determination of iron in wines by the spectrophotometric thiocyanate method. Future experiments will be aimed at testing its suitability for routine applications in clinical, environmental and pharmaceutical chemistry.

DESCRIPTION OF THE INSTRUMENT

The stopped-flow system was designed with a number of criteria in mind. The mixing unit should be modular so that it can readily be fitted to and removed from any commercial detector such as a spectrophotometer or spectrofluorimeter. The readout system should easily be connected to the detector by means of commercially available hardware. No alteration of the original mechanical, optical or electronic configurations of the detector other than the incorporation and removal of the flow-cell from the stopped-flow module should be required. Finally, costs should be the minimum possible without detracting from its performance in kinetic and non-kinetic analysis.

Flow system

The flow system was designed by the authors and constructed and commercialized by QumiSur Instrumentation. Figure 1 shows its basic components: a mixing system, a syringe-drive system and a thermostatted chamber. These components are securely mounted on a vertical polymethylmethacrylate panel (42 × 19 × 1.5 cm) supported on a base of the same material (19 × 15 × 1.5 cm) bearing sample and reagent reservoirs at the back.

Mixing system. The mixing system consists of two drive syringes (a and b, Fig. 1), a stop syringe (c), 3-way stopcock delivery valves (d—f), a mixing/observation cell (g), and a connection system. The drive syringes are made from glass or teflon depending on the sample or reagents used and their capacity ranges from 2 to 5 ml. They are filled with reagents and sample solutions from reservoirs and the contents are rapidly expelled into the flow circuit by the syringe drive system. The vertical position avoids loss of liquids and bubble formation. The stopping device is a 1—2 ml syringe which rapidly stops the flow as the head of the plunger reaches the adjustable stopping block, on which a micro-switch for starting data acquisition is mounted. This block can be adjusted by means of a screw located on a guide which moves only in the vertical direction. This operation allows the volume of sample/reagent mixture delivered to be adjusted (it must be greater than the capacity of the mixing chamber). This volume can be varied between ca. 50 and 500 μl for sample or reagent according to need.

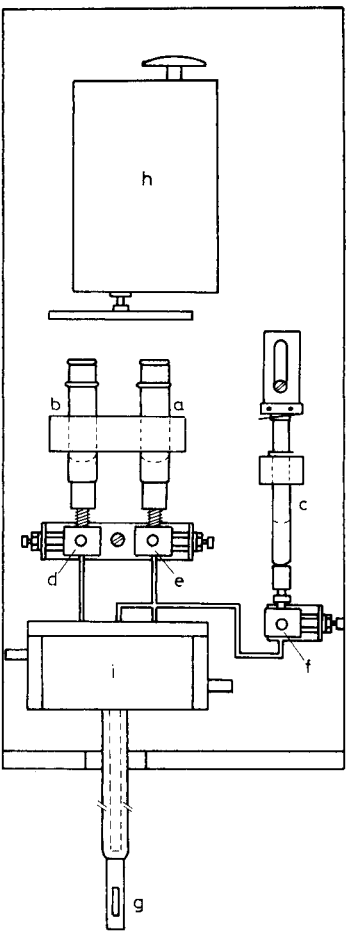

Fig. 1. General diagram of the stopped-flow mixing module: (a, b) drive syringes; (c) stop syringe; (d—f) 3-way stopcock delivery valves; (g) mixing/observation cell; (h) air piston; (i) thermostatted bath.

The 3-way stopcock delivery valves (Hamilton) feature a miniature system with a stream-switching mechanism. Two valves attached to the drive syringes allow the syringes to fill with sample and reagents, and allows the solutions to be rapidly propelled to the mixing/observation cell. The other valve permits the stop syringe to fill with the mixture from the observation cell and also permits its evacuation to waste. The mixing chamber and the observation cell form a single block consisting of a commercial flow-cell (Hellma) with two inlets (sample and reagent) and one outlet (reaction mixture). This system, made from quartz, has three windows intended to allow both photometric and fluorimetric measurements. This cell, with a inner volume of 100 μl and 3-mm path length provides fast and efficient mixing within a few

milliseconds. The different components of the mixing system are linked with teflon connectors and tubing (0.8-mm inner diameter).

Syringe drive system. The syringes are driven by an air piston (Camozzy) (h, Fig. 1) actuated by a manual pulse. This system provides air pressure up to 10 kg cm^{-2} and has a safety valve. This pneumatic system was chosen because of the rapid flow velocities afforded.

Thermostatted chamber. Temperature control is essential because the rate of most chemical reactions is strongly dependent on temperature. The device used in this stopped-flow unit is a 120-ml polymethylmethacrylate thermostatted bath (i, Fig. 1) operated by recirculating water. It is connected in series with the thermostatted detector cell compartment, so that only one thermostatting unit is needed. An acceptable operating range of 5—60°C, controlled to at least ±0.1°C, is achieved.

In order to avoid immersing the entire flow unit in the thermostatted bath, the connections between the drive syringes and the mixing/observation cell were also thermostatted. The length of these connections (teflon tubes) is critical because the propelling system has to introduce freshly thermostatted sample and reagent into the mixing/observation chamber. Thus, for a stop volume of 0.5 ml, the suitable length of each tube must be greater than 65 cm (0.8-mm inner diameter). These tubes are included as coils in the thermostatted bath. The bottom of the thermostatted bath and the mixing/observation cell were connected by a flexible tube which enveloped the teflon tubes from the drive syringes as well as the return tube to the stop syringe. The last tube, the length of which is not critical, was introduced into the flexible tube only for convenience.

Detection and read-out system

As stated above, the proposed stopped-flow system can be readily fitted to any spectrophotometer or spectrofluorimeter. However, these commercial detectors must be capable of following the analog signal change in the millisecond range according to the dead time of this stopped-flow system (see below). Detectors with this speed of observation are the most commonly used today.

The microprocessor and interface components for data acquisition are shown in Fig. 2. A Commodore 64K computer was chosen as read-out system in order to reduce hardware costs. Use of operative BASIC decreased its static memory to about 40K. The following peripherals were connected via its serial ports: a monitor (cathode ray tube, CRT), 16K ROM, 2K RAM disk drive (VIC-1541, Commodore) and a dot-matrix printer (Gemini-15X). The parallel port was an IEEE-488 interface (Binary System Precision) allowing the Commodore 64 to be fitted to the analog-to-digital converter (ADC).

For the ADC conversion, an 8-bit successive approximation ADC (Fluke 8840A) was used with a maximum throughput (number of samples handled per second) of 100 points s^{-1} and a resolution of ±1 μV (200-mV range).

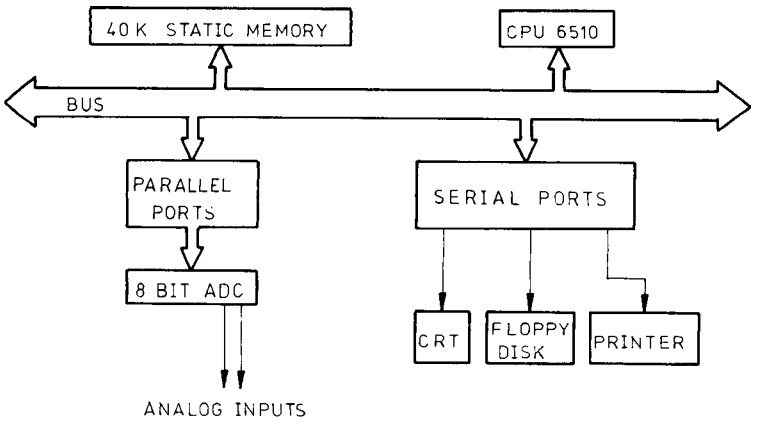

Fig. 2. Basic components of the computerized read-out system.

This resolution should be adequate for most applications. This converter contains a universal asynchronous receiver transmitter which is used to communicate across the guard to the IEEE-488 interface. The transmission speed is 62 500 baud. The timing is controlled through the real-time clock built into the Commodore 64.

The software was written in BASIC and resulted in a decrease in the sampling rate to about 20 points per second. Thus data can be collected at time intervals of about 50 ms. A Simons BASIC card was used to implement graphics on the Commodore 64. This graphics aid adds 114 new commands to BASIC, including programming aids and graphics commands.

Overall, the software developed was intended to avoid the external trigger mode by means of the microswitch system based on a simple subroutine program, to record signal vs. time plots, to calculate kinetic parameters such as rate constants and initial rates, as well as equilibrium parameters (maximum signal), and to store the signal/time data and results on disk.

PERFORMANCE TESTS

The reaction used for evaluation purposes was the complexation of iron(III) with thiocyanate, frequently used as a model reaction in stopped-flow techniques. This reaction has been widely studied in order to establish conditions under which it shows pseudo-first-order kinetics [3, 9, 11] as well as to obtain quantitative data [5, 8].

The working solutions were 5×10^{-4} M iron(III) nitrate and 0.01 M sodium thiocyanate, both diluted in 0.05 M sulphuric acid so that the thiocyanate concentration was at least 20-times that of iron(III) and therefore the reaction was first order in iron(III) [11]. The reaction temperature was maintained at 25 ± 0.1 °C and the course of the reaction was monitored spectrophotometrically at 460 nm.

Figure 3 shows the stopped-flow data recorded with the computerized data-acquisition system and displayed on the CRT. The data collection rate was 50 ms/point and the total absorbance change ca. 0.070. The curve was recorded in 0.6 s. From these data, and by using the linear plot of ln $(A_\infty - A_t)$ vs. time (where A_∞ is the final absorbance, A_t the absorbance at time t), the first-order rate constant was computed. The value found was 6.30 s^{-1}, with a relative standard deviation (r.s.d.) of 1.6% (n = 11). The initial rate related to iron(III) concentration was 0.173 mol l^{-1} s^{-1}, with a r.s.d. of 2.6%. The higher r.s.d. found in the measurement of the initial rate can be attributed to the relative low data accumulation rate (imposed by the inexpensive readout system).

One of the most important factors governing the performance of a stopped-flow system is the dead-time, t_d, which can be defined as the time taken by the solution to flow from the mixer to a point half way through the observation cell. Several methods have been described in the literature for the estimation of this parameter [12—14]. In this paper, the procedure proposed by Hiromi [14] was used; this procedure is based on the following expression: $t_d = V_d/f$, where V_d (ml) is the volume of the dead space between the centres of the mixer and the cell, and f is the flow velocity (ml s^{-1}).

In the proposed stopped-flow module, V_d is ca. 50 μl, as the mixer and observation cell are a single block with an inner volume of 100 μl. The flow velocity, closely related to the air pressure applied to the pneumatic syringe drive system, was calculated from the volume delivered by the drive syringes

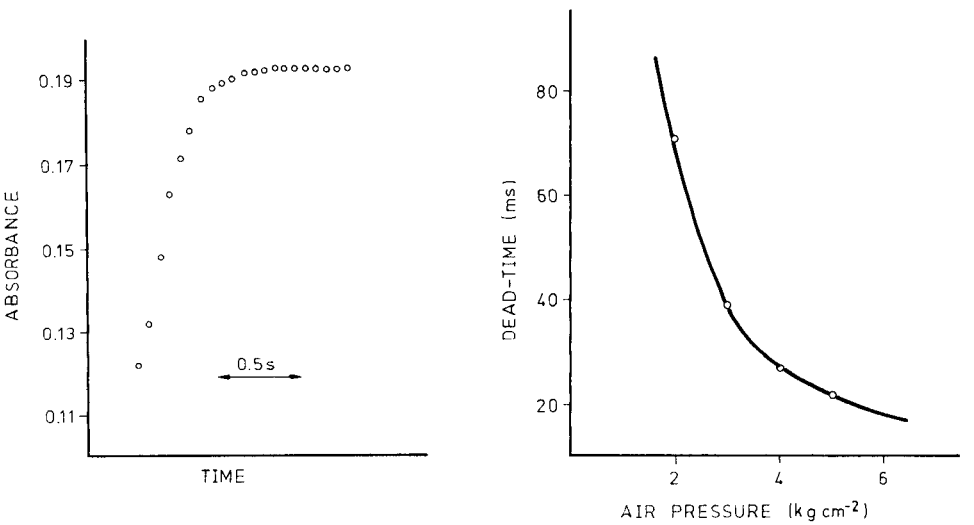

Fig. 3. Data points obtained from a kinetic run on the formation of iron(III)/thiocyanate complex.

Fig. 4. Plot of dead-time vs. air pressure applied by the pneumatic syringe drive system.

over a pre-determined time, measured to ±10 ms. Figure 4 shows the dependence of the dead-time on the air pressure applied by the pneumatic system. As can be observed, a dead-time shorter than 20 ms can be achieved with air pressures higher than 5 kg cm^{-2}.

Another factor considered in the performance test was the observable fraction, f(obs), which, according to Hiromi [14], is defined as the ratio of the observed extent of reaction to the total extent of reaction and is given by $f(\text{obs}) = 0.5^{t_d/t_{0.5}}$ where $t_{0.5}$ is the half-life of the reaction observed. Table 1 shows the maximum observable fraction of the reaction under study according to the value of the first-order constants (taking into account that the dead-time of the proposed stopped-flow module is about 20 ms). Given that f(obs) should be at least 75% for the kinetic data to be treated with acceptable precision, the reaction concerned should take place within ca. 100 ms ($k \approx 14\ s^{-1}$, see Table 1), if the proposed stopped-flow module is to be applied. In this case, it is evident that the proposed read-out system should be replaced with another featuring an analog-to-digital converter affording sampling rates of at least 1 ms/point.

Finally, in order to test the performance of the thermostatting system, the corresponding Arrhenius plot for the iron(III)/thiocyanate reaction was obtained over the range 10—25°C. The linearity of this plot indicated the efficiency of the system. The activation energy calculated from the slope was 54.2 kJ mol^{-1}, in agreement with other values reported for this parameter [15].

Reagents and procedures

The reagents used were of analytical-reagent grade and distilled water was used in the preparation of solutions. A standard solution (1000 μg ml^{-1}) of iron(III) was prepared by dissolving 1.000 g of pure iron metal in 50 ml of (1 + 1) nitric acid and diluting to 1 l with water. A 0.025 M thiocyanate solution was made by dissolving sodium thiocyanate in 2 M hydrochloric acid. The hydrogen peroxide used was 30% (v/v).

Two solutions were prepared in order to fill the drive syringes. For solution A, 1 ml of ethanol, 20 μl of 0.268 M EDTA and the volume of iron solution required to ensure a final concentration of iron between 1.0 and 30 μg ml^{-1} were added to a 10-ml volumetric flask and the mixture was diluted to the mark with water. Solution B was the 0.025 M thiocyanate. The air pressure within the syringe drive system was set at 3 kg cm^{-2} and the

TABLE 1

Relationship between the observable fraction, dead-time of the stopped-flow module (t_d) and first-order rate constant (k)

f(obs) (%)	99.9	99.0	95.0	90.0	75.0	50.0
$t_d/t_{0.5}$	0.0014	0.0144	0.074	0.153	0.416	1.000
k (s^{-1})	0.05	0.50	2.56	5.27	14.38	34.65

thermostatted system at 20 ± 0.1°C. Equal volumes of solutions A and B were mixed in the stopped-flow system and the reaction was followed at 460 nm (a Perkin-Elmer Lambda-5 spectrophotometer was used).

For the determination of iron(III) in wines, solution A contained sample plus 20 μl of 0.268 M EDTA per 10 ml of sample. For the determination of total iron, in a separate experiment, 100 μl of 30% hydrogen peroxide was added per 10 ml of wine sample in order to oxidize iron(II) to iron(III), before proceeding as above. The iron(II) content can be obtained by difference between the results obtained in the two experiments.

RESULTS AND DISCUSSION

Application of the stopped-flow system in routine analyses

In order to test the performance of the proposed stopped-flow system in routine analysis, it was applied to the kinetic determination of iron in wine samples. The iron(III)/thiocyanate reaction in an acidic medium was used in the same way as in the performance tests of the stopped-flow system. Among equilibrium methods, the extraction of the iron(III)/thiocyanate complex into diethyl ether is one of the standards for the determination of iron in wines [16]. This procedure also allows the speciation of iron in wines by conducting the reaction once in the presence of hydrogen peroxide to determine total iron and once in its absence to determine only iron(III).

As shown above, the proposed stopped-flow system is useful for monitoring reactions which take place in the millisecond range. When the iron(III)/thiocyanate reaction is used for the kinetic determination of iron in real samples the thiocyanate/iron ratio must be high (>50) in order to obtain the maximum signal as well as to avoid potential interferences. Under these conditions, the reaction is very fast, and only the final stages of the reaction can be monitored. Therefore the inexpensive readout system proposed herein yields irreproducible results. In order to obtain a linear segment of the rate plot and hence obtain better precision for the determination of iron, this rate was decreased by adding EDTA to the medium, which converts the reaction to that of ligand exchange. Thus, the reaction rate can be evaluated in about 3 s with good precision, without appreciable detriment to the sampling frequency.

In order to ensure the best conditions for the determination of iron in wines, some variables were studied. Initially, the experimental conditions used in the batch method for the determination of iron [16] were selected, i.e., the acidity was adjusted with 1 M hydrochloric acid and the temperature was 20°C. The influence of thiocyanate concentration was examined in the range $1.2–4.9 \times 10^{-2}$ M, while the composition of solution A was kept constant. A linear increase in the initial rate with increasing thiocyanate concentration was found. A concentration of 2.5×10^{-2} M was chosen. The effect of EDTA concentration was studied in the range $2.6–10.7 \times 10^{-4}$ M, at iron concentrations between 5 and 15 μg ml^{-1} ($0.8–2.4 \times 10^{-4}$ M). The initial rate

was constant for a given iron concentration, which confirmed that the EDTA added was enough to complex all iron present. Thus, 5.36×10^{-4} M (20 μl of 0.268 M EDTA per 10 ml of solution A) was selected for use in the determination of iron.

The figures of merit for the determination of iron using the kinetic procedure under the recommended procedure are shown in Table 2.

Determination of iron in wines

The iron content of wine and its evolution through the different stages involved in the aging of wine is a parameter of great relevance to wine makers insofar as concentrations above 10 μg ml^{-1} result in turbidity and colour changes adversely affecting the organoleptic properties of the wine. The oxidation state of iron in these samples depends on the storage conditions. Thus, bottled wines contain mainly iron(II), while aerated wines have higher iron(III) contents. The proposed stopped-flow system was applied to the determination of iron in various white and red wines from different wine-growing areas in Spain. In order to determine iron(II) and iron(III) in wines, two samples are needed. The iron(III) content is determined without pretreatment of the sample. Total iron is determined after addition of hydrogen peroxide. The iron(II) concentration is determined by difference. A 100-μl addition of 30% hydrogen peroxide per 10 ml of sample was enough to ensure complete oxidation of iron(II).

The flow chart for data processing (using the initial rate approach), calibration and measurement of the iron content in wine samples is shown in Fig. 5.

In order to detect possible interferences in the determination of iron in wines, the standard addition method was applied. The recoveries of iron(III) and total iron for several wines (Table 3) ranged from 97.0 to 103.6%. The r.s.d. values were 0.6% and 0.7% for iron(III) and total iron, respectively, for white wines.

The determination of iron in red wines by the batch procedure does not give good results. By use of the proposed kinetic procedure, this determination is feasible, although only total iron could be determined (average recovery, 96.8%; r.s.d. 0.6%). Because of the slight negative interference found

TABLE 2

Analytical figures of merit for the determination of iron by the stopped-flow technique

Linear range	1.0—30 μg ml^{-1}
Detection limit[a]	0.54 μg ml^{-1}
R.s.d.[b]	0.9%
Sampling frequency[c]	120 h^{-1}

[a] 3σ value (n = 30) for 10 μg Fe ml^{-1} [17]. [b] For 10 μg Fe ml^{-1} (n = 11). [c] Each sample analyzed in triplicate.

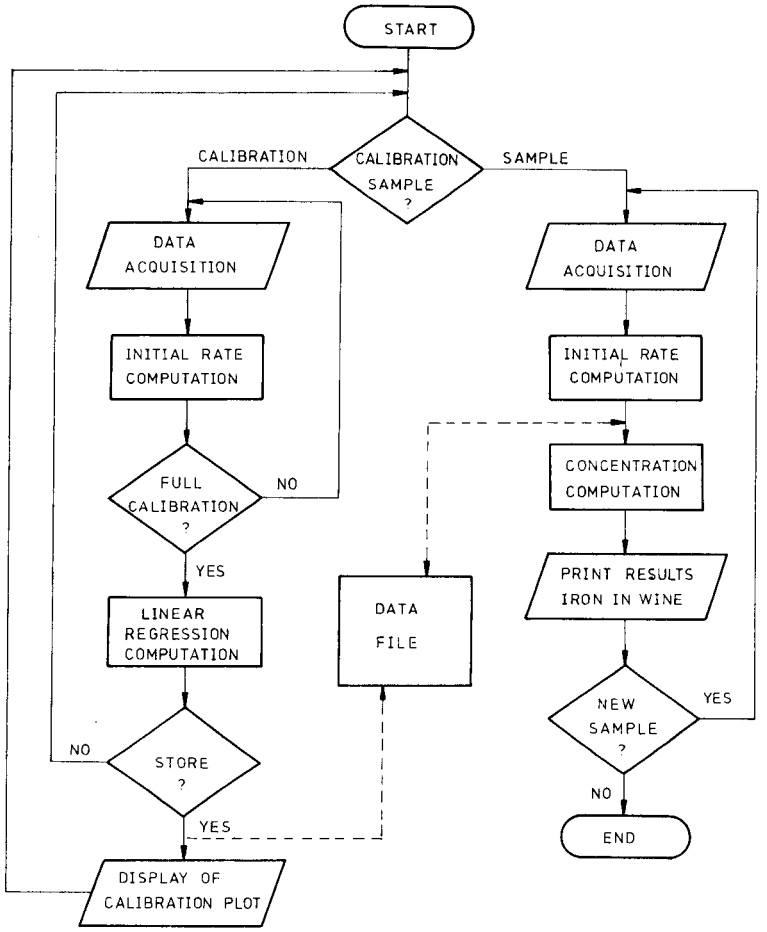

Fig. 5. Flow chart for calibration and the determination of iron in wines.

in the absence of oxidant, the iron(III) content was not determined. Table 4 shows the results obtained for the determination of iron(II), iron(III) and total iron in the wine samples analyzed. The data are in agreement with the results obtained by atomic absorption spectrometry (AAS).

The proposed stopped-flow system thus allows the determination of iron(III) and total iron at the $\mu g\ ml^{-1}$ level in most wine samples. The method compares favourably with its batch counterpart based on liquid/liquid extraction. It has a much higher sampling frequency (120 h^{-1} cf. 8 h^{-1}), does not require a blank measurement, and is much simpler to operate.

TABLE 3

Recovery of iron(III) and total iron added to white wines

Wine	Iron(III) (μg ml^{-1})			Total iron (μg ml^{-1})		
	Found	Added	Recovered[a]	Found	Added[b]	Recovered[a]
Montilla	1.4	—	—	3.0	—	—
	1.4	5.0	6.3 (99.1)	3.0	5.0	7.9 (99.8)
	1.4	10.0	11.1 (97.5)	3.0	10.0	12.6 (97.0)
	1.4	15.0	16.2 (98.8)	3.0	15.0	17.7 (98.3)
Jerez	1.9	—	—	3.7	—	—
	1.9	5.0	7.1 (102.9)	3.7	5.0	8.5 (97.7)
	1.9	10.0	12.3 (103.4)	3.7	10.0	13.6 (99.3)
	1.9	15.0	17.5 (103.6)	3.7	15.0	18.4 (98.4)
Rioja	2.3	—	—	5.8	—	—
	2.3	5.0	7.1 (97.3)	5.8	5.0	10.5 (97.1)
	2.3	10.0	12.0 (97.6)	5.8	10.0	15.5 (98.1)
	2.3	15.0	17.0 (98.3)	5.8	15.0	20.4 (98.2)

[a]Percentage recoveries are given in parentheses. [b]As iron(II).

TABLE 4

Determination of iron(II), iron(III) and total iron in wines

Wine	Iron concentration (μg ml^{-1})[a]			
	Iron(II)	Iron(III)	Total iron	AAS
Montilla (1 year)	3.6 ± 0.8	10.6 ± 0.8	14.2 ± 0.8	13.9
Montilla (2 year)	1.2 ± 0.4	3.5 ± 0.3	4.7 ± 0.4	
Montilla (fino)	1.6 ± 0.2	1.4 ± 0.1	3.0 ± 0.2	2.9
Moriles (fino)	1.6 ± 0.1	1.4 ± 0.1	3.0 ± 0.1	
Jerez (fino)	1.8 ± 0.1	1.9 ± 0.1	3.7 ± 0.1	3.8
Rioja (white)	3.5 ± 0.5	2.3 ± 0.1	5.8 ± 0.5	6.0
Valdepeñas (red)			10.0 ± 0.8	9.8
Jumilla (red)			6.0 ± 0.6	6.0
Rioja (red)			4.0 ± 0.8	3.8

[a]Average of four separate determinations ± s.d.

The authors are grateful to the C.A.I.C.y.T. (Project No. 0979/84) for financial support.

REFERENCES

1 D. Sanderson, J. A. Bittikofer and H. L. Pardue, Anal. Chem., 44 (1972) 1934.
2 G. E. Mieling, R. W. Taylor, J. English and H. L. Pardue, Anal. Chem., 48 (1976) 1686.
3 G. L. Mieling and H. L. Pardue, Anal. Chem., 50 (1978) 1333.
4 D. L. Krottinger, K. M. Walczak and H. V. Malmstadt, Am. Lab., 9 (1979) 51.

5 M. A. Koupparis, K. M. Walczak and H. V. Malmstadt, J. Autom. Chem., 2 (1980) 66.
6 J. L. Holtzman, Anal. Chem., 52 (1980) 989.
7 I. R. Bonnell and J. D. Defreese, Anal. Chem., 52 (1980) 139.
8 H. V. Malmstadt, K. M. Walczak and M. A. Koupparis, Int. Lab., 11(1) (1981) 32.
9 J. A. Alcocer, D. J. Livingston, G. F. Russell, C. F. Shoemaker and W. D. Brown, J. Autom. Chem., 5 (1983) 83.
10 I. A. G. Roos, L. P. G. Wakelin, J. Hakkennes and J. Coles, Anal. Biochem., 146 (1985) 287.
11 B. G. Willis, J. A. Bittikofer, H. L. Pardue and D. W. Margerum, Anal. Chem., 42 (1970) 1340.
12 P. M. Beckwith and S. R. Crouch, Anal. Chem., 44 (1972) 221.
13 N. Papadakis, R. B. Coolen and J. L. Dye, Anal. Chem., 47 (1975) 1644.
14 K. Hiromi, Recent Developments in the Stopped-flow Method for Study of Fast Reactions, in D. Glick (Ed.), Methods of Biochemical Analysis, Vol. 26, Wiley-Interscience, New York, 1980, pp. 137—164.
15 S. Lever and J. Crooks, Int. Lab., 15(8) (1985) 24.
16 Análisis de Alimentos, Servicio de Publicaciones del Ministerio de Sanidad y Consumo, Madrid, 1980, pp. 774.
17 W. R. Wolf and K. K. Stewart, Anal. Chem., 51 (1979) 1201.

Analytica Chimica Acta, 199 (1987) 41—47
Elsevier Science Publishers B.V., Amsterdam — Printed in The Netherlands

OPTIMIZATION OF SINGLE-COLUMN ANION CHROMATOGRAPHY WITH INDIRECT ULTRAVIOLET PHOTOMETRIC AND FLUORIMETRIC DETECTION

S. RAPSOMANIKIS and ROY M. HARRISON*

Institute of Aerosol Science, Chemistry Department, University of Essex, Colchester CO4 3SQ (Great Britain)

(Received 2nd March 1987)

SUMMARY

Optimization of single-column anion chromatography with indirect photometric and indirect fluorimetric detection is described. A simplex algorithm is used for signal maximization with eluent concentration, pH and flow rates as dependent variables. Absolute detection limits obtained for chloride, nitrite, nitrate and sulphate by indirect photometric detection were 1.0, 1.2, 1.4, and 2.0 ng, respectively. The use of single-beam indirect fluorimetric detection of these anions is also demonstrated. The method was applied to the detection of anions arising from gaseous acids or atmospheric aerosols.

The separation, identification and quantitation of anions such as chloride, nitrate, bromide, sulphate and cyanide is of interest in many fields. In agriculture, nitrate and phosphate are associated with fertiliser applications. Medicinal interests include analysis for fluoride and chloride as metabolic breakdown products of anaesthetic gases. Other areas of concern include industrial effluent control from the plating and photographic industries, acid deposition and purity of foodstuffs.

The determination of anions by ion chromatography involves injection of the sample into an eluent stream of buffer, exchange on an anion-exchange column, and detection. Two major detection methods have been developed depending on the capacity of the ion-exchange material of the chromatographic column, viz., suppressed conductivity detection [1, 2] and single-column ion chromatography with conductivity or indirect ultraviolet photometric detection [3—5]. Conductivity detection usually requires suppression of the conductivity of the eluent by converting it to non-conducting species. With the availability of columns with low ion-exchange capacities [6], it became possible to apply single-column ion chromatography by using low concentrations of eluent buffer and unsuppressed conductivity detection [3]. Indirect ultraviolet (uv) photometric detection involves the use of an uv-absorbing eluent at low concentrations and measurement of the signal decrease at the detector when non-uv absorbing sample ions replace the eluent ions [7].

0003-2670/87/$03.50

A sensitive and inexpensive method was needed for the analysis of anion mixtures arising from atmospheric acids and aerosols, because sampling times and volumes were restricted for better temporal resolution of variation of their atmospheric concentrations. In the present work optimization, by a modified simplex algorithm, of the sensitivity of an indirect uv detection system is described utilizing three different eluents and two columns. Also indirect fluorescence detection and optimization of its sensitivity is described.

EXPERIMENTAL

Equipment and materials

An LDC/Milton Roy Series III HPLC system was used. The uv monitor was equipped with a low-pressure mercury lamp and 254-nm or 280-nm cut-off filters depending on the eluent used. The fluorescence detector had a cadmium lamp (326 nm) and the appropriate excitation and emission filters. Two columns were used and compared, a Vydac 302 IC column (250 mm × 4.6 mm i.d.; Separations Group, Hesperia, CA 92345) and a Chrompak Iono-Sphere A (250 mm × 4.6 mm).

All chemicals and materials were used without further purification, unless otherwise stated. The eluents used were phthalate, salicylate, sulphobenzoate and anthranilate, adjusted to the appropriate pH (Orion 701 Ionanalyzer) with 0.1 M potassium hydroxide.

Filters for atmospheric sampling were loaded on an all-teflon filter pack [8] and aerosols were collected on the first stage on 1-μm pore size, teflon membrane filters (Whatman). Gaseous acids were collected on the second stage by nylon-66 1-μm pore size membrane filters (Gelman Sciences). Gaseous ammonia was collected on acid-impregnated Whatman 41 cellulose filters in the third stage. Details of filter treatment prior to use have been described elsewhere [9].

Optimization

Optimization of the response signals was done with a computer program based on the modified simplex algorithm of Nelder and Mead [10], but with several modifications to the original algorithm.

First, instead of maximization of a function, the response values are derived by experiment. Secondly, for the purpose of limiting the number of experiments, no major shrinkage is implemented. Instead the next-to-worst vertex is replaced by the new vertex. Thirdly, this version implements maximization of experimental values only. Fourthly, if a returned parameter is "out of bounds", an extremely low response is input so that the vertex does not interfere with the propagation of the algorithm. Fifthly, in accordance with the first modification, after the origin (vertex 0) has been chosen, the coordinates of the vertices forming the initial simplex do not need to be calculated. The initial simplex can be irregular and the choice of the coordinates is left to the experimenter. Finally, the step size for the variation of

each parameter in the initial simplex need not be fixed. A copy of the program, in C language, is available from the authors.

The algorithm is capable of dealing with a maximum of 15 parameters provided that (n + 1) vertices (n is the number of parameters) are formed initially. Each vertex represents an experiment with different values for each parameter. In the present study, four initial experiments were done (three parameters were investigated); in each experiment, different values of each parameter were used. In optimizing the indirect uv and indirect fluorescence signals, eluent flow rate, pH and concentration were investigated.

Preliminary experiments were done for each system with different non-continuous variables (e.g., different eluent and/or column) so that the origin of the algorithm (vertex 0) could be chosen. The values of the parameters for the other three vertices were chosen so that they were different from each other and produced responses sufficiently variable not to terminate the algorithm. Experiments for the formation of each vertex were done in triplicate (i.e., three injections) and the standard error was calculated as $[\Sigma(y_i - \bar{y})^2/n]^{1/2}$, where y is the response value. The algorithm was terminated, after inspection, when the difference in the response from the previous vertex fell below the standard error value [10].

The types of simplex algorithms utilized in analytical chemistry have been reviewed [11]. Optimization was done for the signal for 0.50 μg ml^{-1} nitrite present as sodium nitrite in aqueous solution, because no interferences from atmospheric input or contaminated glassware were expected. Limits of detection were estimated from calibration graphs, based on low-concentration standards, as the 3σ value for the baseline noise.

RESULTS AND DISCUSSION

In considering the optimization of the system available, it was possible to vary only certain parameters. Variation in small increments, as the simplex would have demanded, of wavelengths, bandwidths, cell path length and ion-exchange column length or loading, was not feasible. Optimization of peak signal (height of peak or depth of trough) proceeded for eluent pH, concentration and flow rate as variables. The boundaries of the simplex were set to ensure that elution of sulphate, which had the highest retention volume, did not exceed 30 min. If at the optimum conditions of sensitivity, baseline separation of the anions was not achieved, the next best conditions were chosen to obtain calibration graphs and estimate limits of detection.

The signal-to-noise ratio (S/N) in indirect photometric ion chromatography is proportional to the analyte ion concentration and inversely proportional to the eluent concentration and detector noise [12]. In practice, very low eluent concentrations would result in extremely large retention volumes for the anions, and at the limiting conditions analyte ions would not be displaced by eluent ions from the ion-exchanger. At a given pH, the retention

volume V_R is inversely proportional to the eluent concentration [4]. The pH at which the eluent is used controls the position of its dissociation equilibrium and hence the proportion of dissociated ions in solution. This in turn is inversely proportional to the retention volume of the analyte ions. Flow rates control the rate of ion exchange and hence the shape of the analyte peak front and the shape and sharpness of peak (or trough) produced by the analyte ion. Although analyte behaviour in ion chromatography is closely explained by theory [13], the simultaneous effect of the three parameters studied here on analyte signal does not seem to have been reported before.

Detection of anions by indirect fluorimetry, based on a cadmium lamp, is novel although a laser double-beam arrangement has been used in the detection of chloride and iodate by indirect fluorimetry [14]. At the working range of the instrument assembly used here, problems with baseline drift were not encountered and neither flicker nor shot noise were significant. Although the spectral geometries of the detectors for indirect fluorimetry and indirect photometry are different, considerations about eluent concentration, pH and flow rates are similar. The eluent concentration is inversely proportional to fluorescence efficiency, hence the S/N ratio could be improved by employing an eluent with higher fluorescence efficiency.

In practice the salicylate and anthranilate ions were used because of their ion-exchange capabilities. The cadmium lamp with a 326-nm excitation line was used with a 325-nm excitation filter because the absorption spectra of both ions fell within the 325—370 nm range (e.g., 325 nm excitation and 404 nm emission maxima for salicylate). The emission (fluorescence) filter used here was 370—700 nm.

TABLE 1

Optimum conditions and limits of detection for the determination of chloride, nitrite, nitrate and sulphate with indirect photometric and indirect fluorimetric detection

Column	Eluent	Conc. (mM)	pH	Flow rate (ml min^{-1})	Limit of detection (ng)[a]			
					Cl^-	NO_2^-	NO_3^-	SO_4^{2-}
Indirect photometric								
Vydac 302	Phthalate	0.7	4.6	1.13	1.5	2.0	2.2	3.5
	Salicylate	1.6	5.7	1.14	2.1	2.5	2.7	3.2
	Sulphobenzoate	1.0	4.1	1.50	1.0	1.2	1.4	2.0
IonoSphere A	Salicylate	2.7	5.2	1.32	25.0	42.0	66.0	82.0
	Sulphobenzoate	1.0	4.7	1.56	4.4	5.7	7.0	9.0
Indirect fluorimetric								
Vydac 302	Salicylate	1.7	4.8	1.68	5.0	5.5	6.5	8.0
	Anthranilate	1.4	5.4	1.89	7.8	9.1	9.6	12.2
IonoSphere A	Salicylate	2.5	6.2	2.15	32.0	39.0	58.0	78.0

[a] Absolute limits, calculated at 3σ of baseline noise [16], for 500- or 200-μl injections.

The results of the optimization study are given in Table 1. An example of the simplex optimization procedure is described in Table 2. The best limit of detection was achieved by using the Vydac column and the sulphobenzoate ion. The two columns had different ion-exchange capacities and, in agreement with theory, the Vydac column with an 0.1 meq g^{-1} ion-exchanger produced a better S/N ratio than the IonoSphere column which contained an ion-exchanger with 1.0 meq g^{-1} capacity (the operational eluent concentration for the Vydac column was less than that for the IonoSphere A column).

TABLE 2

Example of simplex optimization procedure for nitrite (250 ng) with the Vydac 302 column and salicylate ion for indirect photometric detection

	Eluent (mM)	pH	Flow rate (ml min^{-1})	Peak height (arbitrary units)
Vertex 0	1.35	5.4	1.50	2685
Vertex 1	0.40	4.0	2.50	1120
Vertex 2	1.00	4.5	1.00	2433
Vertex 3	0.80	5.0	2.00	2619
Reflection	1.70	5.9	0.50	4013
Expansion	3.00	7.8	−1.50	—[a]
Reflection	1.56	6.4	1.66	2491
Reflection	1.00	4.5	1.00	2462
Contraction	1.43	5.9	1.50	2982
Reflection	2.18	6.5	0.33	3973
Reflection	2.18	6.8	0.05	—[a]
Contraction	1.56	5.7	1.14	3981
Reflection	2.20	6.2	−0.18	—[a]
Contraction	1.60	5.99	1.08	3807

[a]Out of bounds.

TABLE 3

Atmospheric concentrations of gaseous acids and their particulate salts

Date	Location	Volume sampled (m^3)	Concentration[a] ($\mu g\ m^{-3}$)				
			HCl	HNO_3	Cl^-	NO_3^-	SO_4^{2-}
12.6.85	Library roof[b]	4.5	0.82	0.55	1.21	0.95	5.14
8.10.85	Chemistry Dept.[b]	4.0	0.90	<0.06	1.30	1.90	2.20
11.10.85	St. Osyth[c]	1.0	1.6	0.94	1.04	1.36	3.95
28.10.85	Playing fields[b]	2.0	2.92	2.34	3.87	<0.125	9.74
7.6.86	Playing fields[b] (a.m.)	1.3	0.73	0.77	0.79	3.43	7.46
7.6.86	Playing fields[b] (p.m.)	1.4	1.05	0.70	0.86	2.14	7.13
11.6.86	St. Osyth[c]	14.5	0.70	1.68	0.78	2.61	3.16
14.6.86	St. Osyth[c]	4.5	0.65	1.43	1.21	7.32	3.96
28.7.86	Playing fields[b]	1.2	1.71	3.10	3.42	16.12	19.40

[a]As acids and, for the anions, as particulate salts. [b]At Essex University. [c]In Essex.

The limits of detection reported here are an order of magnitude higher than those obtained in suppressed-conductivity ion chromatography but an order of magnitude lower than those produced in another study based on indirect photometric detection [15]. Results illustrating the application of the method to air samples are compiled in Table 3. The limits of detection obtained for indirect fluorimetric detection were slightly poorer than those obtained by indirect photometric detection (Table 1). The operational principles of the two methods are very similar. Figure 1 shows a chromatogram obtained by fluorimetric detection. Optimization proceeded in a similar manner to the photometric investigation; an eluent ion with higher fluorescence efficiency would have produced lower limits of detection, as discussed above.

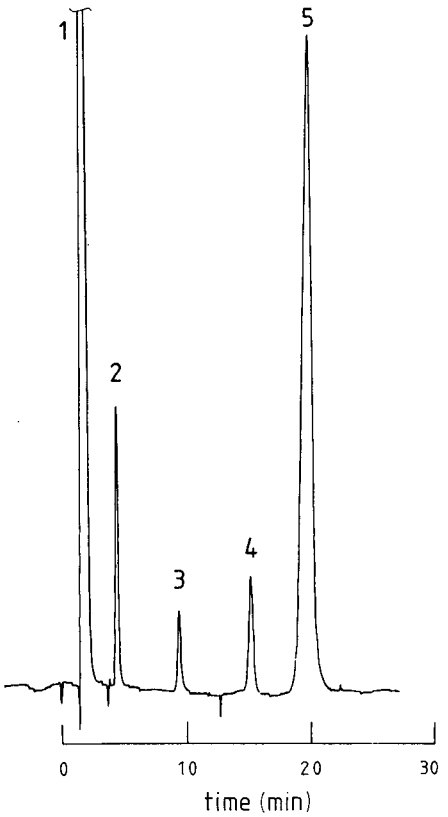

Fig. 1. Chromatogram of 0.5 mg l^{-1} each of chloride (peak 2), nitrate (peak 3) and 1.0 mg l^{-1} sulphate (peak 4) with fluorimetric detection. Peaks 1 and 5 are the void and system peaks, respectively. Conditions: Vydac 302 column with 1.7 mM salicylate at pH 4.8 as eluent with a flow rate of 1.68 ml min^{-1}.

REFERENCES

1 H. Small, J. S. Stevens and W. C. Bauman, Anal. Chem., 47 (1975) 1801.
2 C. A. Pohl and E. L. Johnson, J. Chromatogr. Sci., 18 (1980) 442.
3 M. S. Willison and A. G. Clarke, Anal. Chem., 56 (1986) 1037.
4 H. Small and T. E. Miller, Anal. Chem., 54 (1982) 462.
5 Z. Iskandarani and T. E. Miller, Anal. Chem., 57 (1985) 159.
6 D. P. Lee, Liq. Chromatogr., 2 (1984) 828.
7 H. Small and T. E. Miller, U.S. Patent, 1983, 4,414,842.
8 K. G. Anlauf, P. Fellin, A. A. Wiebe, H. I. Schiff, G. I. Mackay, R. S. Braman and R. Gilbert, Atmos. Environ., 19 (1985) 325.
9 S. Rapsomanikis, M. Wake and R. M. Harrison, Environ. Sci. Technol., submitted for publication.
10 J. A. Nelder and R. Mead, Comput. J., 7 (1965) 308.
11 S. N. Deming and L. R. Parker, Jr., Crit. Rev. Anal. Chem., 9 (1978) 187.
12 S. A. Wilson and E. S. Yeung, Anal. Chim. Acta, 157 (1984) 53.
13 D. R. Jenke, Anal. Chem., 56 (1984) 2674.
14 S. Mho and S. E. Yeung, Anal. Chem., 57 (1985) 2253.
15 B. Rössner and G. Schwedt, Fresenius' Z. Anal. Chem., 320 (1985) 566.
16 L. H. Keith, W. Crummett, S. Deegan Jr., R. A. Libby, J. K. Taylor and G. Wentler, Anal. Chem., 55 (1983) 2210.

Analytica Chimica Acta, 199 (1987) 49—57
Elsevier Science Publishers B.V., Amsterdam — Printed in The Netherlands

THE EFFECT OF SUBSTITUENTS ON THE EXTRACTION BEHAVIOR OF HYDROXAMIC ACIDS

MASSOUD HOJJATIE, TED CECCONIE and HENRY FREISER*

Strategic Metals Recovery Research Facility, Department of Chemistry, University of Arizona, Tucson, AZ 85721 (U.S.A.)

(Received 12th August 1986)

SUMMARY

The extraction behavior of several alkyl-substituted hydroxamic acids in chloroform solution with several metal ions is described. Among the *N*-phenylacylhydroxamic acids used, those with *o*-alkyl substituents on either the phenyl or acyl ring generally do not extract metals, apparently because of steric problems at the O=C—N—O$^-$ chelation site. An improved synthesis of substituted hydroxamic acids is reported.

Hydroxamic acids have been known for over a century and have been found useful in numerous applications [1, 2]. These compounds have been used as spectrophotometric reagents for the determination of several metal ions [3—5] and as extractants for the lanthanides [6—11].

Hydroxamic acids typically have been prepared from their acid chlorides and the appropriate hydroxylamines. These procedures require pyridine to be used as a scavenger for hydrochloric acid and treatment of the reaction product with aqueous ammonia to separate the ammonia-soluble material. These two factors have made the procedures both lengthy and tedious and have led to low yields [12—15].

As part of a systematic study of potential ligands for the separation of transition metals and the lanthanides, thirteen substituted hydroxamic acids were prepared. The procedure used for the synthesis of these compounds proved to be superior to existing ones both in terms of ease of product isolation and product yield. A representative group of the hydroxamic acids was chosen and studied as general metal extractants so that the role of the alkyl substituents on the extraction behavior of these compounds could be evaluated.

EXPERIMENTAL

Apparatus

An Eberbach box-type shaker was used to agitate the solutions in the extraction. An Orion Research 701A digital Ionalyzer was used for final pH measurement. A Perkin-Elmer 6500 ICP spectrometer was used for the

determination of the percentage of metal extracted. All melting points are uncorrected and were taken in open glass capillary tubes with a Thomas-Hoover melting point apparatus. Infrared spectra were obtained on a Perkin-Elmer 1800 infrared spectrometer. Proton-NMR spectra were measured at 60 MHz with a Varian EM-360L spectrometer and at 250 MHz with a Bruker WM-250 spectrometer on samples containing tetramethylsilane as internal standard. Elemental analysis was done by Atlantic Microlab, Atlanta, GA.

Reagents

A stock solution which contained Al(III) (3.5 mM), Cd(II) (0.085 mM), Cr(VI) (0.46 mM), Cu(II) (0.34 mM), Fe(III) (0.32 mM), Mn(II) (0.10 mM), Mo(VI) (0.32 mM), Ni(II) (0.70 mM), Pb(II) (0.85 mM), U(VI) (4.2 mM), V(IV) (0.49 mM), and W(VI) (0.65 mM) was prepared for the extraction studies. The concentrations of the various metals were chosen so that they could be easily detected by inductively-coupled plasma/atomic emission spectrometry (ICP/AES) and so that the ligand concentration after extraction would be essentially unchanged from its original value even if all of the metals were extracted under any one set of experimental conditions. Solutions of 0.500 M tartaric acid and 0.500 M tris(hydroxyamino)methane (Tris) were prepared to buffer the solutions during extraction. Chloroform (analytical-reagent grade) was washed three times with deionized water just prior to use. All other reagents were of analytical grade and used without further purification.

Preparation of hydroxamic acids

All hydroxamic acids were prepared from the appropriate hydroxylamines and acid chlorides. Hydroxylamines were prepared by reduction of appropriate aromatic nitro compounds with zinc dust in the presence of ammonium chloride [16], with some modifications. Acid chlorides were obtained commercially (Aldrich Chemical Company) or were prepared from treatment of the appropriate carboxylic acid (Aldrich Chemical Company) with purified thionyl chloride [17].

A typical procedure for the preparation of the hydroxamic acids is illustrated with 3,5-bis(trifluoromethyl)benzoyl-3,5-bis(trifluoromethyl)phenylhydroxylamine (3,5-FBFPHA) as follows.

Step 1. To a solution of ammonium chloride (10 g) in distilled water (400 ml), 3,5-bis(trifluoromethyl)nitrobenzene (10 g, 38 mmol) was added with stirring and the mixture was heated to 40°C. Zinc dust (12 g) was added during a 30-min period. The temperature of the mixture rose to 60°C. The mixture was stirred at 50—60°C for 3 h. After filtration and cooling, the residue was washed with ether and the combined filtrate was extracted with ether (4 × 50 ml). The combined ether layers were washed with saturated sodium chloride solution and dried with anhydrous magnesium sulfate. The drying agent was removed by filtration and the ether solution was concentrated in vacuo to provide a yellow oil (9.44 g, 84%). Infrared absorption

in the neat material occurred at 3449 cm^{-1} (NH, OH) and 1621 cm^{-1} (C=C, aromatic).

Step 2. In a three-neck round-bottomed flask equipped with a magnetic stirrer, a low-temperature thermometer and a dropping funnel, a solution of sodium hydrogen carbonate (5 g) in distilled water (4 ml) was combined with ether (50 ml) and the mixture was cooled to −5 to 0°C. 3,5-Bis(trifluoromethyl)hydroxylamine (3.5 g, 14 mmol) dissolved in ether (20 ml) was added to the above mixture. 3,5-Bis(trifluoromethyl)benzoyl chloride (3.95 g, 14 mmol) in ether solution (20 ml) was added dropwise at −5 to 0°C during a 30-min period. The orange mixture was stirred at −5 to 0°C for 1 h. Ether was removed in vacuo, saturated sodium hydrogen carbonate solution (50 ml) was added, and the mixture was stirred for 20 min. The product was extracted into dichloromethane (4 × 50 ml). The organic phase was washed with a saturated sodium chloride solution and dried with anhydrous magnesium sulfate. The solid was removed by filtration and the filtrate was concentrated to provide a white solid which was recrystallized from an ethanol/water mixture. Yield 5.9 g (79%); m.p. 218–220°C. ^{1}H-NMR ($CDCl_3$) δ 8.45, 8.25, 7.96 and 7.54 (aromatic protons), and δ 2.1 ppm (—OH). IR (KBr) 3270 cm^{-1} (—OH), and 1647 cm^{-1} (C=O). Calculated for $C_{17}H_7F_{12}NO_2$: 42.1%C, 1.4%H, 47.0%F, 2.9%N; found: 41.95%C, 1.5%H, 47.0%F, 3.0%N.

Extraction procedure

A series of stock aqueous solutions was prepared by combining 12.0 ml of the stock metal solution, 8.00 ml of 0.500 M tartaric acid, 8.00 ml of 0.500 M Tris for solution of pH 6.0 or above, and deionized water to give a total volume of 60.0 ml. A 10.0-ml volume of each aqueous phase was combined with an equal volume of a 0.100 M solution of the hydroxamic acid in chloroform. The phases were contacted for a 2-h period for the cases of *p*-ethylbenzoylphenylhydroxylamine (*p*-EBPHA) and *p*-tert-butylbenzoylphenylhydroxylamine (*p*-BBPHA) and for a 10-h period for the cases of *N*-*o*-tolylbenzohydroxamic acid (*o*-TBHA), *o*-tolyl-*m*-trifluoromethylphenylhydroxylamine (*o*-TFPHA), and *N*-*o*-tolyl-*p*-tert-butylbenzohydroxamic acid (*o*-TBBHA) by shaking the two phases in a 40-ml vial which was fitted with a polyethylene-lined plastic cap. The final pH of the aqueous phase was measured after phase separation. The concentration of each metal remaining in the aqueous phase was determined sequentially by using ICP/AES; the emission responses of the aqueous phases before and after extraction were compared. The instrumental conditions used were as described elsewhere [11]. The analytical wavelengths used for each metal were as follows: Al 396.152 nm; Cd 214.438 nm; Cr 205.552 nm; Cu 324.754 nm; Fe 238.204 nm; Mn 257.610 nm; Mo 202.030 nm; Ni 221.647 nm; Pb 220.353 nm; U 358.958 nm; V 310.230 nm; and W 207.911 nm. Background correction intervals were used in all cases to correct for any differences in background emission between the samples and blank solution. The percentage of metal extracted was calculated from the following equation:

$$\% \text{ Extracted} = [(B - A)/(B - \text{Blank})] \times 100$$

where B is the emission signal before extraction, A is the emission signal after extraction, and Blank is the emission signal of the blank.

RESULTS AND DISCUSSION

Preparation of the hydroxamic acids

The hydroxamic acids were prepared from the reaction of the appropriate phenylhydroxylamines and acid chlorides. Phenylhydroxylamines were prepared by reduction of aromatic nitro compounds with zinc dust in the presence of ammonium chloride [16]. The cited procedure was modified by extracting the product of the reduction into ether and drying it with magnesium sulfate. Hydroxylamines prepared by this method were more stable than those prepared by the literature method and could be stored up to four months without noticeable deterioration.

Hydroxylamines and acid chlorides were reacted at low temperature in ether in the presence of solid sodium bicarbonate. The literature procedures for the preparation of the hydroxamic acids require the use of pyridine as scavenger for hydrochloric acid [12—15]. The pyridine and pyridinium chloride side-product are difficult to remove entirely from the hydroxamic acid product and sometimes lead to brownish sticky materials and subsequent low yields. The procedure used to isolate the product involves an extraction into aqueous ammonia with a subsequent acidification step which is lengthy and tedious. The method presented here eliminates the need for troublesome post-treatment for the isolation of the by-products. Furthermore, this new method has an additional advantage in that sodium hydrogen carbonate is more innocuous than pyridinium salts.

Thirteen hydroxamic acids were prepared in high yields by using the above methods (Table 1). The structures of the compounds were confirmed by infrared, ^{1}H-NMR, and elemental analysis. Melting points were compared with those listed in the literature when known.

Extraction of several metals with the hydroxamic acids

To investigate the effect of alkyl substitution on the behavior of the hydroxamic acids, surveys were done to test the ability of *p*-BBPHA, *p*-EBPHA, *o*-TBHA, *o*-TFPHA, and *o*-TBBHA to extract various metal ions. In these studies, the percentage of metal (±10%) which would extract into 0.1 M solutions of the hydroxamic acids in chloroform was monitored over the pH range of approximately 0—10.

The extraction results for *p*-BBPHA and *p*-EBPHA are shown in Figs. 1 and 2, respectively. Both these compounds were capable of extracting all the metals studied except for Cr(VI). The extraction results for *o*-TBHA (Fig. 3) show that this compound was only capable of extracting Mo(VI), W(VI), Fe(III), and Cu(II) over the pH range studied. The amounts of Al(III), Cd(II), Cr(VI), Mn(II), Ni(II), Pb(II), and U(VI) extracted were not sig-

TABLE 1

Physical properties of the *N*-phenylacylhydroxamic acids $R-\underset{\underset{O}{\|}}{C}-N(OH)-R'$

Compound	Acronym	R	R′	Yield (%)	Melting point (°C)	
					Found	Lit.
$C_{13}H_{11}NO_2$	BPHA	C_6H_5	C_6H_5	96	120—121	121 [18]
$C_{14}H_{13}NO_2$	*o*-TBHA	C_6H_5	*o*-$CH_3C_6H_4$	93	108	104 [3]
$C_{14}H_{13}NO_2$	*o*-TPHA	*o*-$CH_3C_6H_4$	C_6H_5	90	101	101 [14]
$C_{14}H_{13}NO_2$	*m*-TPHA	*m*-$CH_3C_6H_4$	C_6H_5	84	93	93 [19]
$C_{14}H_{13}NO_2$	*p*-TPHA	*p*-$CH_3C_6H_4$	C_6H_5	95	116	116 [14]
$C_{14}H_{15}NO_2$	*p*-EBPHA	*p*-$CH_3CH_2C_6H_4$	C_6H_5	92	108—110	—
$C_{16}H_{17}NO_2$	*p*-IBPHA	*p*-$(CH_3)_2CHC_6H_4$	C_6H_5	71	112—114	—
$C_{17}H_{21}NO_2$	*p*-BBPHA	*p*-$(CH_3)_3CC_6H_4$	C_6H_5	85	135—136	—
$C_{18}H_{21}NO_2$	*o*-TBBHA	*p*-$(CH_3)_3CC_6H_4$	*o*-$CH_3C_6H_4$	65	140	—
$C_{14}H_{13}NO_3$	*p*-APHA	*p*-$CH_3OC_6H_4$	C_6H_5	69	130	130 [14]
$C_{14}H_{10}F_3NO_2$	*m*-FBPHA	*m*-$CF_3C_6H_4$	C_6H_5	80	75	76 [13]
$C_{15}H_{12}F_3NO_2$	*o*-TFPHA	*o*-$CH_3C_6H_4$	*m*-$CF_3C_6H_4$	73	119—120	—
$C_{17}H_7F_{12}NO_2$	3,5-FBFPHA	3,5-$(CF_3)_2C_6H_3$	3,5-$(CF_3)_2C_6H_3$	79	218—220	—

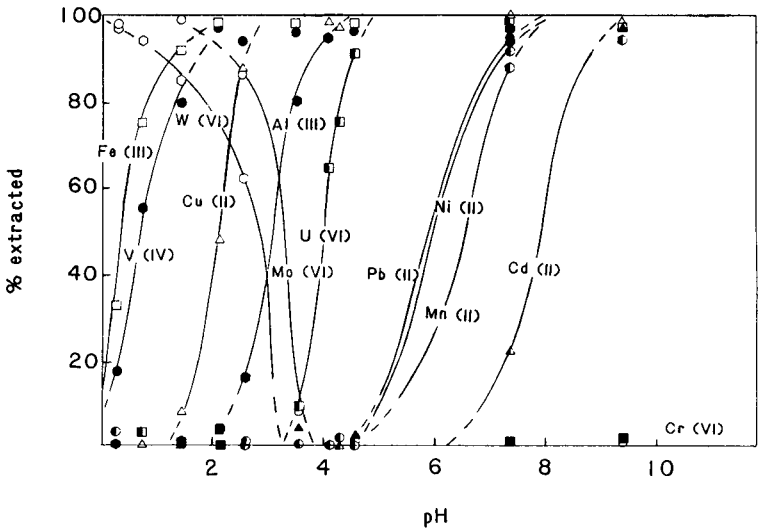

Fig. 1. Extraction behavior of *p*-BBPHA: (●) Al(III); (▲) Cd(II); (■) Cr(VI); (△) Cu(II); (□) Fe(III); (◐) Mn(II); (○) Mo(VI); (◐) Ni(II); (▲) Pb(II); (●) V(IV); (▮) U(VI); (○) W(VI).

nificantly different from 0% extraction. The extraction results for *o*-TFPHA are summarized in Fig. 4. This compound was capable of extracting only Mo(VI) and W(VI) in the pH range 0—4. The amounts of all other metals in the extracts were not significantly different from zero over the pH range 0.2—10.5. The results for extraction with *o*-TBBHA indicated that this compound was not capable of extracting any of the metals over the pH range 2.0—9.7.

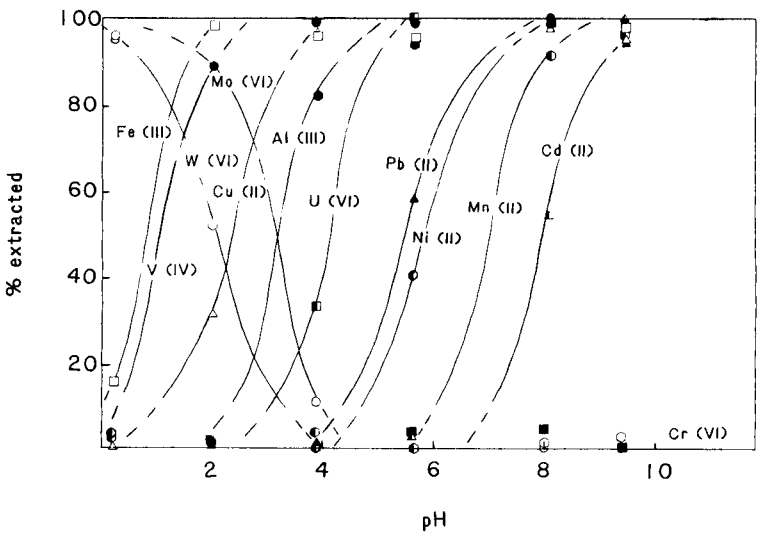

Fig. 2. Extraction behavior of *p*-EBPHA: (●) Al(III); (▲) Cd(II); (■) Cr(VI); (△) Cu(II); (□) Fe(III); (◐) Mn(II); (○) Mo(VI); (◐) Ni(II); (▲) Pb(II); (●) V(IV); (▮) U(VI); (○) W(VI).

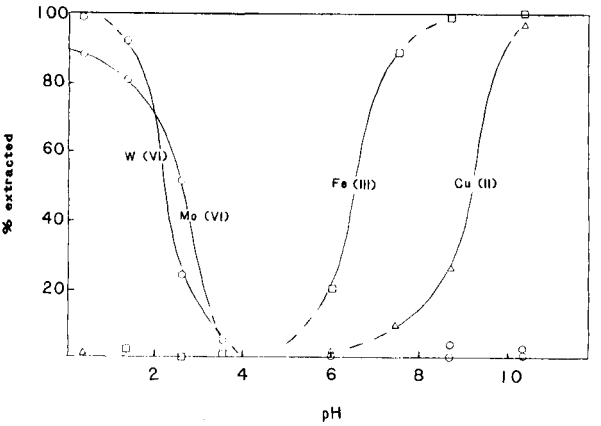

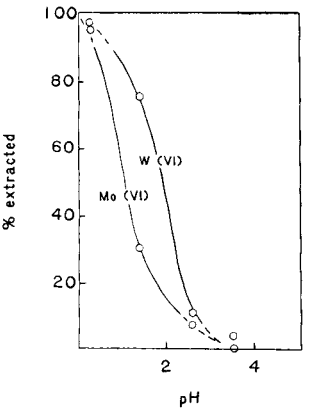

Fig. 3. Extraction behavior of *o*-TBHA: (△) Cu(II); (□) Fe(III); (○) Mo(VI); (○) W(VI).

Fig. 4. Extraction behavior of *o*-TFPHA: (○) Mo(VI); (○) W(VI).

The extraction behavior of the substituted hydroxamic acids, as with other chelating reagents which are weak acids, indicates a general increase of the amount of metal extracted with an increase in pH [20, 21]. For simple metal ions such as Al(III), Cd(II), Cu(II), Fe(III), Mn(II), Ni(II), and Pb(II), the extraction curves indicate that these metals are extracted as neutral chelates or self-adducts, as shown in the following equation:

$$M^{n+}_{(aq)} + (n + a)\,HL_{(org)} \rightleftharpoons ML_n \cdot aHL_{(org)} + nH^+_{(aq)}$$

The extraction results for both U(VI) and V(IV) also indicate an increase in extraction with an increase in pH, which is consistent with the extraction of the UO_2^{2+} and VO^{2+} complexes [20]. The extraction of Mo(VI) and W(VI) is seen to decrease with an increase in pH. This result is indicative of the extraction of these metals as MoO_2^{2+} and WO_2^{2+} species [20], as shown in the following equation:

$$2H^+_{(aq)} + MO^{2-}_{4(aq)} + 2HL_{(org)} \rightleftharpoons MO_2 \cdot L_{2(org)} + 2H_2O_{(aq)}$$

The extraction results for the hydroxamic acids were compared to results obtained for the parent compound, BPHA [2]. With BPHA, it was found that Cu(II), Fe(III), Co(II), Zn(II), Bi(III), Mn(II), and Al(III) were quantitatively extracted into 0.01 M BPHA in chloroform at pH values of 4—11, 2—3, 10—11, 9—11, 2—13, 10, and 6, respectively. It was also reported that significant amounts of other metals such as Pb(II) and Ni(II) (97%) and Cd(II) (78%) would be extracted under similar conditions in pH ranges of 7—11, 9—11, and 10—11, respectively. The extraction order observed was: Fe(III) ≈ Bi(III) > Cu(II) > Al(III) > Pb(II) > Zn(II) ≈ Ni(II) > Mn(II) ≈ Cd(II) ≈ Co(II).

The present studies indicate that the behavior of *p*-BBPHA and *p*-EBPHA, compounds which contain a single substituent on the *para* position of the

acyl ring, is similar to that of the parent compound BPHA in that the extraction order indicated by both *p*-BBPHA and *p*-EBPHA is the same as that for BPHA. The studies also indicate that an *o*-methyl substituent on either the *N*-phenyl (*o*-TBHA; *o*-TBBHA) or C-phenyl (*o*-TFPHA) ring results in a significant drop in the ability of the compounds to extract metals. Although these *o*-methyl-substituted compounds generally were ineffective at extracting the metals, both *o*-TBHA and *o*-TFPHA were found capable of extracting Ni(II) and Cu(II) when tartrate was absent in the aqueous phase [22].

The dramatic decrease in the extractability of the metals with the *o*-methyl-substituted compounds cannot be explained by changes in the acidic character caused by substitution. Although alkyl substituents on the *N*-phenyl ring lower the acidic character of the hydroxamic acids [13, 18, 19], these changes are not large. The changes in pK_a between BPHA (8.15) [6] and *o*-TBHA (8.40) [2] illustrate this fact. Moreover, *m*- and *p*-alkyl substituents on the C-phenyl ring also lower the acidic character of the hydroxamic acids [23], but compounds of this sort, such as *p*-BBPHA and *p*-EBPHA, were found to be good metal extractants.

It is reasonable to explain the reduced activity of the *o*-methyl extractants on the basis of steric hindrance which arises from interaction of the methyl group with its neighboring aromatic ring. Such an interaction would cause the O=C—N—O^- chelation site to be non-planar and result in a decrease in the chelate stability. It has been shown that planarity of the chelation ring is important for complexation to occur [12]. Although the introduction of trifluoromethyl groups was found to improve the extracting properties of the hydroxamic acids [13], such an introduction into an *o*-methyl-substituted compound as in *o*-TFPHA was found to be ineffective in causing such an improvement. Alkyl substituents in either the *meta* or *para* position of the phenyl rings would not lead to a steric hindrance problem because the substituent and neighboring aromatic ring are well separated spatially. Hence the extracting abilities of *p*-BBPHA and *p*-EPBHA are not hindered by steric effects.

Conclusions

Several substituted hydroxamic acids were prepared to investigate their use for the extraction of several metal ions. The substituents do not greatly alter the extractability of metals from that of BPHA unless they are in the *ortho* position. *Ortho* substitution greatly diminishes the ability of the hydroxamic acid to extract metals, probably because of steric effects.

The preparation of the hydroxamic acids was improved by replacing pyridine as hydrochloric acid scavenger with solid sodium hydrogen carbonate.

The authors thank Dr. S. Muralidahran of the Strategic Metals Recovery Research Facility for helpful discussions. This work was supported by a United States Department of Energy research grant.

REFERENCES

1 S. Shome, Analyst, 75 (1950) 27.
2 A. K. Majumdar, *N*-Benzoylphenylhydroxylamine and its Analogues, Pergamon, Oxford, 1972.
3 A. K. Majumdar and G. Das, Anal. Chim. Acta, 31 (1964) 147.
4 A. Bhaburi and P. Ray, Sci. Cult., 18 (1952) 95.
5 I. Alimarin, N. Borzenhova and N. Zakarina, Zavod. Lab., 28 (1961) 958.
6 D. Dyrssen, Acta Chem. Scand., 10 (1956) 353.
7 T. Sekine and D. Dyrssen, Talanta, 11 (1964) 867.
8 A. Reidel, J. Radioanal. Chem., 6 (1970) 75.
9 N. Poluektov, R. Lauer and V. Mishchenko, Zh Anal. Khim., 24 (1969) 1665.
10 S. Inoue, F. Ordonez and H. Freiser, Solv. Ext. Ion Exch., 3 (1985) 839.
11 T. Cecconie, M. Hojjatie and H. Freiser, Anal. Chim. Acta, 193 (1987) 247.
12 C. Armour and D. Ryan, Can. J. Chem., 35 (1957) 1454.
13 H. LeRoux and K. Fouche, J. Inorg. Nucl. Chem., 32 (1970) 3059.
14 S. Tandon and S. Bhattacharyya, Anal. Chem., 33 (1961) 1267; J. Chem. Eng. Data, 7 (1962) 553.
15 J. Shukla and S. Tandon, Indian J. Chem., 9 (1971) 279.
16 O. Kamm, Org. Synth. 4 (1925) 57.
17 K. Fleurke, C. Van der Stelt and W. Nauta, Recl. Trav. Chim. Pays-Bas, 81 (1962) 93.
18 R. Moshier and J. Schwarberg, Anal. Chem., 29 (1957) 947.
19 U. Priyadarshini and S. Tandon, J. Chem. Eng. Data, 12 (1967) 143.
20 J. Stary, Anal. Chim. Acta, 28 (1963) 132.
21 C. Fa-Chun, Q. Fernando and H. Freiser, Anal. Chem., 37 (1965) 361.
22 S. Muralidharan and M. Hojjatie, Strategic Metals Recovery Research Facility, University of Arizona, 1986, unpublished work.
23 D. Bjura and S. Tandon, Indian J. Chem., 8 (1970) 466.

Analytica Chimica Acta, 199 (1987) 59—76
Elsevier Science Publishers B.V., Amsterdam — Printed in The Netherlands

DETERMINATION OF NICKEL, COBALT, COPPER AND URANIUM IN WATER BY CATHODIC STRIPPING CHRONOPOTENTIOMETRY WITH CONTINUOUS FLOW

M. P. NEWTON and C. M. G. VAN DEN BERG*
Department of Oceanography, University of Liverpool, Liverpool L69 3BX (Great Britain)

(Received 3rd February 1987)

SUMMARY

The potential of cathodic stripping chronopotentiometry for the determination of trace metals in a continuous-flow system is investigated. An automated analyzer with a fast rate of data acquisition (250 kHz) is described. The cathodic scans are preceded by adsorptive collection of surface-active metal complexes on the hanging mercury drop electrode. The scans are done by passing a constant current of between 0.8 (in deaerated solution) and 60 μA (in solutions saturated with air) through the working electrode. Copper, uranium, and nickel can be determined in the presence of dissolved oxygen, but the sensitivity for nickel is then much reduced. The sensitivity of stripping chronopotentiometry in the presence of dissolved oxygen is similar to that of fast linear-sweep voltammetry in the absence of dissolved oxygen. The limits of detection were 0.1 nM Ni, 0.1 nM Co, 1.8 nM Cu and 1.6 nM U, when the measurements were preceded by 60-s stirred adsorption; in the presence of dissolved oxygen the limit of detection for nickel was higher at 0.6 nM, and cobalt could not be determined, as its peak was located on top of the oxygen peak. The determinations of copper and uranium were not adversely affected by dissolved oxygen. The limits of detection can be lowered further by using a prolonged collection period (up to 300 s). The technique was successfully tested by measuring nickel with continuous flow in water pumped on board of a small vessel in the Tamar estuary.

The electroanalytical chemistry of trace metals has progressed strongly with the development of cathodic stripping voltammetry (CSV) preceded by adsorptive collection of organic metal complexes. Thus, it is now possible to determine dissolved aluminium [1, 2], Cu, Pb and Cd [3], Fe, V, U, Zn, and Mo [4], manganese [5] and nickel [6], after addition of selective organic chelating compounds which allow complex adsorption on the electrode surface. The reduction step is very efficient because the complex is present in a monomolecular layer on the electrode surface, and the sensitivity therefore is very high; the limit of detection for most metals lies around 10^{-10} M after adsorptive collection for just 60 s on the hanging mercury drop electrode (HMDE).

Automation of multiple sample analysis by CSV is difficult, and the total measurement time is long, because of the need to remove dissolved oxygen

0003-2670/87/$03.50

from the solution. A study to assess the potential of cathodic stripping chronopotentiometry was therefore undertaken.

The origins of chronopotentiometry can be traced back to 1879 [7]. It differs from voltammetry in that the potential scan is made by using a controlled current rather than at a controlled rate, and the transition time (rather than the peak current) which elapses during the reduction (or oxidation) of dissolved material is recorded. Anodic stripping chronopotentiometry was used by Kemula and Strojek [8] to determine dissolved metals after plated deposition on a hanging mercury drop electrode (HMDE). The sensitivity of this method can be increased by using a low current. However, dissolved substances with reduction potentials more positive than that of the measured metal interfere if their reduction causes a current of similar magnitude to that applied during the scan, because this accelerates the scan rate and lowers the transition time. Thus the scan direction and rate are completely controlled by diffusion of chemical oxidizing or reducing agents to the electrode at a very low current through the circuitry when a high impedance is placed between the reference and working electrodes [8, 9].

Dissolved oxygen interferes with measurements by reductive stripping chronopotentiometry at small applied currents; its reduction slows down the scan, because of the reduction waves located at approximately 0 and −1 V. Eskilsson et al. [10] therefore used medium exchange with flow analysis and conducted the scan in 5 M calcium chloride, which is essentially free of dissolved oxygen.

In the present report, the interference by oxygen is overcome by applying an enhanced reduction current, as this makes the scan rate in stripping chronopotentiometry largely free from effects by dissolved oxygen. The scan rate is very fast in these conditions; each scan typically lasts 50—100 ms which necessitates a very fast rate of data acquisition by the monitoring equipment. The development of suitable monitoring equipment for stripping chronopotentiometry is described below. Measurements are made at a rate of 250 kHz, which is much faster than that used before (30 kHz [10]). The HMDE is used rather than a glassy carbon mercury film electrode [10], as the electrode surface is more readily and accurately reproduced. The potential of the system as a field instrument is tested by measurements of dissolved nickel in the Tamar estuary using continuous-flow analysis on board a small vessel.

EXPERIMENTAL

Instrumentation for stripping chronopotentiometry

The instrumental set-up comprised a laboratory-built "digitizer", a BBC model B computer (Acorn, 32K RAM) with printer, disc drives and monitor, and a HMDE (PAR model 303 A); the set-up is shown schematically in Fig. 1. The instrument contains an analogue board and digital circuitry. The analogue board (Fig. 2) consists of a potentiostat which controls the potential of the working electrode (WE) via the counter electrode (CE), a voltage follower

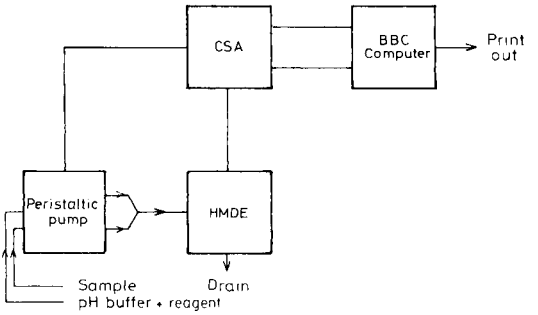

Fig. 1. Instrumental set-up for stripping chronopotentiometry.

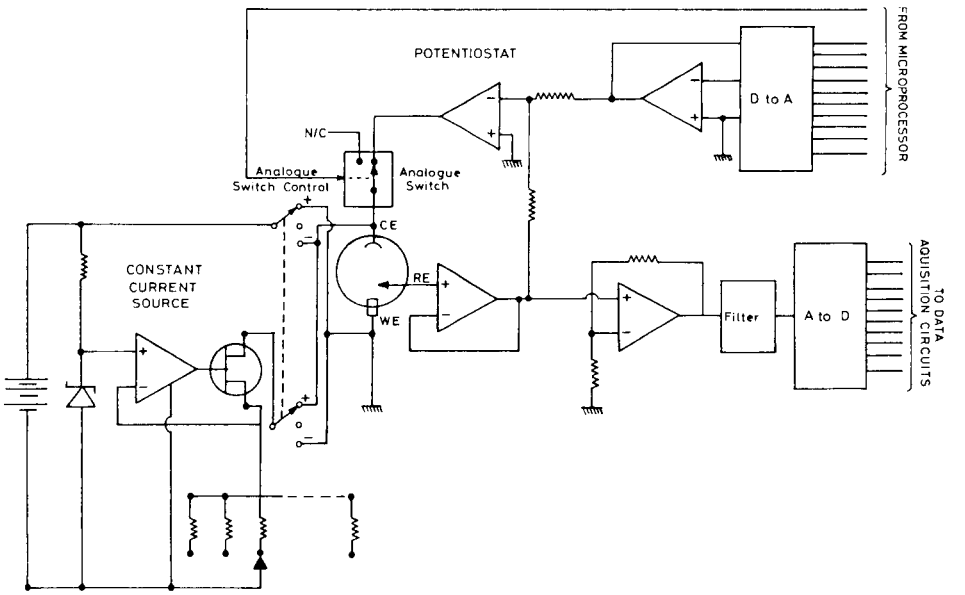

Fig. 2. Analogue board of the analyzer.

to measure the potential between the working electrode and the reference electrode (RE), and a constant-current source. The input impedance of the voltage follower was high ($>10^{12}$ ohm) to prevent current flow through the reference electrode; the leakage current via the analogue switch (switching time 250 ns) between the counter and reference electrodes was less than 0.5 nA. The power for the constant-current source was derived from a 9-V battery, and a mixture of fixed and variable resistors was used to give a total resistance range of 0.015—23 Mohm; thus currents were produced in the range of ±40 nA to ±80 μA.

A block diagram of the digital circuitry is presented in Fig. 3. The cell potential between the reference and working electrodes is read at regular time intervals (4 μs) by the 10-bit A/D converter (ADC EH-10B1, nominal conversion time 4 μs, typical conversion time 3.6 μs). The output of the A/D converter is used as a memory address, so that the total scan range (0 to −1.5 V) is subdivided in a kbyte (1024) of equal intervals of approximately 1.5-mV width. Each time a potential reading falls in one of these potential intervals, its memory location is incremented. Thus a delay (= transition time) in the potential scan produces high counts at that potential interval, which is represented by a peak in a plot of counts (= time elapsed) against potential, as shown schematically in Fig. 4. The area of the peak is equal to the transition time. Each reading takes 3.8 μs and a new reading is taken every 4 μs (= length of one count) or at multiples thereof. Two 2K × 8-bit RAM chips are used in parallel to store the data, having a storage capacity of 2^{16} (65 536) counts per 1.5-mV interval. Every 200 μs, the microprocessor (Intel 8085) compares

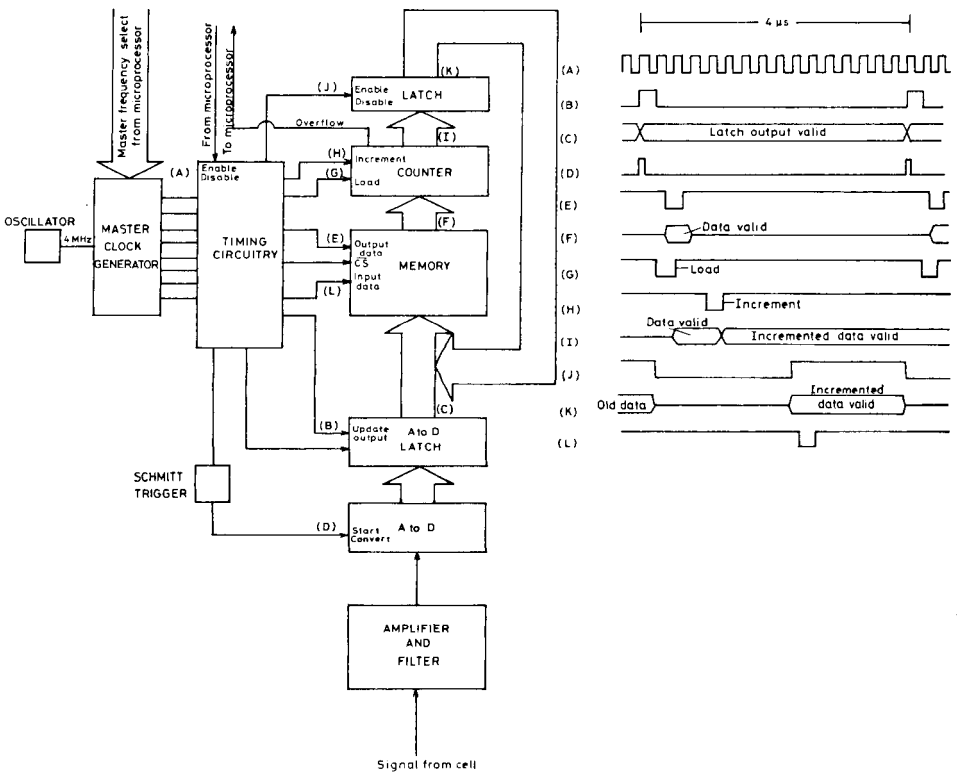

Fig. 3. Block diagram of the digital circuitry of the analyzer: (A) master frequency; (B) update A/D latch; (C) A/D latch output; (D) A to D start-convert pulse; (E) memory output data; (F) data out; (G) load counters; (H) increment counters; (I) data on output of counters; (J) enable signal for latch; (K) data on output of latch; (L) write incremented data into memory.

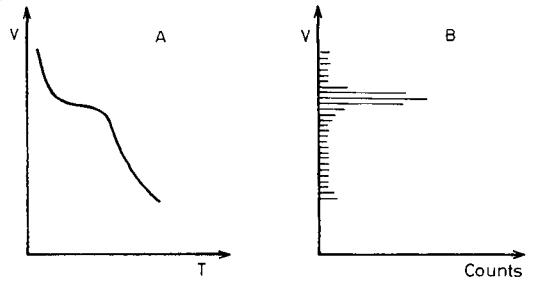

Fig. 4. Schematic representation of a scan of an adsorbed metal complex. (A) Potential vs. time; (B) digitized output of the analyzer, in the form of potential vs. counts.

the cell potential with the required end-potential, at which the scan is finally stopped. The data are then transferred to the BBC computer. The HMDE and relays in the peristaltic pump and the magnetic stirrer (when used) were controlled by a microprocessor-controlled interface in the digitizer of the system.

Software

The machine-code program for the analyzer was written in Intel 8085 assembly language on the BBC computer, and then converted to machine code using the Romas assembler. During the start-up of the instrument, this machine-code program is downloaded from disc into 4K of RAM on the microprocessor board and executed. The parameters for the measurement (initial and end potential, rate of data acquisition, collection time, quiescence time, and the number of repeat measurements) are entered at the keyboard and transferred to the analyzer at the start of the measurements. The analogue/digital converter is started at the end of each collection period immediately prior to the scan and continues to sample the potential until the end-potential has been reached; then the data are transferred to the BBC computer. The peak area (= the transition time) was calculated by deducting the averaged counts of the extrapolated baseline from the total number of counts over a preset potential interval encompassing the peak; the limits of this potential interval were set by visual inspection of the scan on the monitor, and normally no adjustment was found to be necessary during repeated analyses over a limited concentration range. Placement of the limits was facilitated by computer software which provided their graphical representation as vertical lines superimposed on the scan on the monitor.

Other equipment

Comparative results by cathodic stripping voltammetry were obtained with a PAR 174A polarograph, and a PAR model 305 magnetic stirrer, using the same HMDE as for chronopotentiometry. The HMDE was fitted with a flow cell (PAR model 310) for continuous-flow work. The peristaltic pump used for automated continuous-flow measurements was a Gilson Minipuls, with a

4-channel pump-head; this pump was fitted with a relay for on/off control by the analyzer. All tubing connected to the peristaltic pump was teflon (0.8 mm i.d.).

Reagents

The following aqueous stock solutions were prepared. For nickel and cobalt, the pH buffer stock solution was 1 M boric acid/0.4 M ammonia (Aristar) (giving a pH in seawater of 8.5), and the reagent solution was 0.1 M dimethylglyoxime (DMG) in 0.25 M sodium hydroxide (Aristar). For copper the pH buffer stock solution was 1 M 4-(2-hydroxyethyl)-1-piperazineethane sulphonic acid (HEPES) and 0.5 M ammonia (giving a seawater pH of 7.7), and the reagent was 0.1 M quinolin-8-ol (oxine) in 0.25 M hydrochloric acid. For uranium, the pH buffer was 1 M 1,4-piperazinebis(ethane sulphonic acid) (PIPES) and 0.5 M ammonia (giving a pH of 6.8 in seawater), and the reagent stock solution was 0.1 M quinolin-8-ol.

Standard metal solutions were prepared by dilution from atomic absorption standard solutions (BDH), except uranium for which an aqueous 0.005 M stock solution was prepared by dissolving spectroscopic-grade U_3O_8 (Johnson Matthey Chemicals) in concentrated nitric acid (Aristar) and diluting with distilled water. Contaminating trace metals in the pH buffers were removed by equilibration with 10^{-4} M manganese(IV) oxide followed by filtration [3]. The reagent solution for nickel determinations by continuous flow contained 6×10^{-3} M DMG and 0.3 M borate pH buffer.

Seawater used for laboratory experiments was collected from the Channel during a cruise with the NERC research vessel Frederick Russell, in November 1984, and stored in a 10-l polyethylene container, and from the Menai Straits by pumping near the Marine Sciences Institute in Menai Bridge, and stored in a 50-l polyethylene container. The seawater was filtered (0.45-μm oxoid) and UV-irradiated for 2 h before usage.

Procedures

The analytical parameters were as described in the literature. Briefly, nickel and cobalt were measured after addition of 2×10^{-4} M DMG [6] and 0.01 M borate buffer to the sample; borate buffer (pH 8.5) was used rather than the recommended ammonia buffer [6] to avoid the possible precipitation of magnesium hydroxide in seawater at pH >9. Copper was measured with 10^{-4} M quinolin-8-ol and 0.01 M HEPES buffer [3], and uranium with 2×10^{-5} M quinolin-8-ol and 0.01 M PIPES buffer [11]. Quinolin-8-ol rather than catechol [4] was selected for copper and uranium, as catechol is unstable in the presence of dissolved oxygen. The solutions were deaerated before CSV by purging with argon; deaeration was done before stripping chronopotentiometry only when indicated.

The procedure for discrete (individual) samples was as follows: 10 ml of the sample was pipetted into the cell, pH buffer and chelating agent were added to the required concentrations, and the solution was deaerated (for

CSV only); the stirrer was started, the potentiostat was switched on at the required adsorption potential, and a new mercury drop was extruded which was the beginning of the collection period of between 30 and 120 s; then the stirrer was stopped and a quiescence period of 10 s was allowed whereafter the scan was initiated.

The following procedure was used for automated continuous-flow determination of labile nickel in seawater: water was transported by peristaltic pump at a rate of ca. 2 ml min^{-1} from the outlet of the pumped seawater supply on board the vessel; the reagent (buffer + DMG) flow was merged with that of the sample in a T-junction at a volumetric ratio of 1:30 (reagent/sample); mixing was ensured by passing the solution through a tight loop, and a reaction time of ca. 30 s was allowed before the solution reached the HMDE. Each measuring cycle started with the extrusion of a new mercury drop, and pumped collection took place for 45 s at an adsorption potential of −0.7 V; then the pump was stopped, a quiescence time of 2 s was allowed, and the scan for reductive stripping chronopotentiometry was initiated; typically, this took <0.1 s, after which the pump was restarted. The calculation of the peak area by the BBC computer took much longer (45 s) as the program did not fit in the memory and segments had to be loaded from disc; the total analysis time therefore was about 90 s. The memory capacity of the BBC computer is presently being upgraded by the installation of 128K sideways RAM which can hold the entire calculating program and should decrease the data treatment time to <5 s and the total time to <52 s.

The applied current during the scan usually was 10 μA, but different settings were used depending on the oxygen concentration and the length of the quiescence time; a much smaller current (1 μA) could be used for discrete, deaerated samples in the polarographic cell, whereas a larger current (>20 μA) was used in the continuous-flow system if the scan was done without stopping the sample flow.

Field study

Field tests of the analyzer were conducted on board the "sea-truck", of the Institute of Marine and Estuarine Research in Plymouth, a vessel of 12-m length with a plastic hull and shallow draft (0.5 m), and fitted with a submersible centrifugal pump which was used to sample the water while the vessel was in transit [12]. Salinity and turbidity were measured continuously in this pumped water supply, and the outflow was subsampled by using a peristaltic pump. A piece of nylon plankton netting (ca. 100-μm particle cut-off size) was wrapped around the inlet of the teflon tube (0.8-mm inner diameter) leading to the peristaltic pump to prevent particles from blocking the exit tube just under the HMDE in the PAR flow cell. The pumping time between subsampling and the water/reagent mixture reaching the HMDE was about 90 s.

RESULTS

Measurement of copper, uranium and nickel in seawater

Copper and uranium were measured by using stripping chronopotentiometry in seawater in the presence of dissolved oxygen, with quinolin-8-ol as the absorptive chelating agent. Typical scans for copper are shown in Fig. 5. The peak potential for copper was at —0.52 V, about 0.07 V more negative than with CSV [3] as a result of the fast scan rate in the chronopotentiometric method. The current used for these scans was 4 μA, which produced an averaged scan rate of ca. 3 V s^{-1}, compared with a scan rate of 10 mV s^{-1} in CSV. This measurement was done without deaeration of the sample; a broad reduction wave for oxygen in this condition was located at —0.8 V.

Measurements of uranium were tested at various scan rates at between 5.2 and 9.1 μA, as shown in Fig. 6A. At the fastest scan rate, the baseline was relatively flat, whereas at the lowest the uranium peak appeared on the shoulder of the oxygen wave. The peak potential of uranium shifted by 0.2 V in a negative direction from the slowest to the fastest scan, the latter being equivalent to an average rate of 7.5 V s^{-1}. Figure 6B shows the result for a lower level of uranium (10 nM rather than 14 nM) but with a longer stirred adsorption time (240 s rather than 60 s).

The peak areas of copper and uranium increased linearly with the metal concentrations when standard additions were made; only at relatively high metal levels (>80 nM for Cu and >30 nM for U) the increase diminished as a result of saturation of the drop surface. This result is similar to that obtained by CSV [3, 11]. Reductive stripping chronopotentiometry differs in this aspect from chronopotentiometry for which the increase in the transition time (at constant applied current) is non-linear with the dissolved reactant concentrations [13]; in stripping chronopotentiometry, the transition time

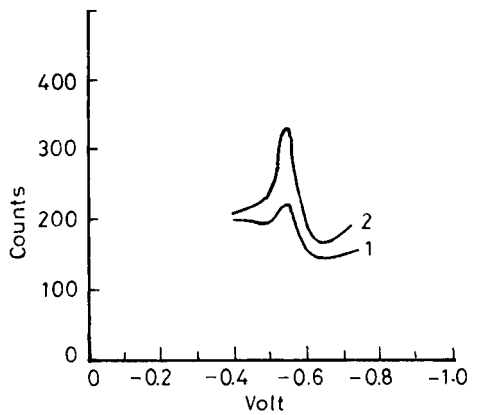

Fig. 5. Measurement of labile copper in seawater by stripping chronopotentiometry in the presence of dissolved oxygen. Scans: (1) 5 nM Cu; (2) 15 nM Cu. Conditions: 4×10^{-5} quinolin-8-ol, 0.01 M HEPES, 60-s stirred collection at —0.4 V; current setting 4 μA.

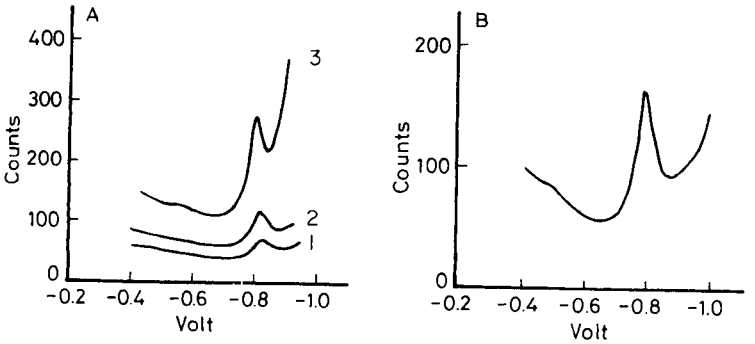

Fig. 6. Measurement of dissolved uranium in seawater. (A) 60-s stirred collection of 14 nM uranium with scans at different constant currents: (1) 9.1 μA; (2) 7.0 μA; (3) 5.2 μA. (B) 240-s stirred collection of 10 nM uranium with scan at 7.0 μA. Conditions: 2×10^{-5} M quinolin-8-ol, 0.01 M PIPES (pH 6.8), and 10^{-4} M EDTA; deposition potential = −0.4 V.

depends on the reduction of a previously adsorbed complex rather than on reactant diffusion to the electrode during the scan.

The nickel peak appears at the beginning of the oxygen wave when nickel is measured by stripping chronopotentiometry in seawater saturated with air (Fig. 7). Nickel had to be measured at a high current (>10 μA) as its reduction wave coincided with that for dissolved oxygen at lower current settings. The potential limits and the baseline within which the peak area was calculated are also indicated in Fig. 7. The increase in the peak height with standard nickel additions was linear up to about 400 nM (Fig. 8A) whereafter the slope diminished as a result of saturation of the drop surface; identical results were obtained from the comparative experiments with CSV. In stripping chronopotentiometry, the peak potential of nickel was found to shift in a positive direction with increasing nickel concentration (Fig. 8B). This positive peak shift was probably caused by the lowering of the scan rate during the reduction of adsorbed nickel at enhanced nickel concentrations.

Interferences

Interference as a result of competitive adsorption of complexes of other metal ions or of surface-active organic material in natural water samples is the same as with CSV and is therefore not treated here in detail. Copper and uranium have different optimal pH values (7.7 and 6.9, respectively), and do not interfere with each other in those conditions, unless one of these metals is present at an unusually high concentration (>200 nM). Competitive adsorption of surface-active organic materials is diminished by maintaining a short collection period (<60-s stirring), or by prior ultraviolet-irradiation of the sample. The latter treatment is essential to release copper and nickel from organic complexes in natural waters in order to measure the total dissolved rather than the labile metal concentration [3, 14].

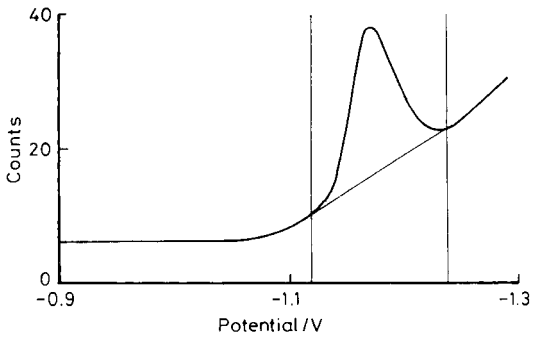

Fig. 7. Measurement of dissolved nickel (9 nM) in air-saturated seawater. Conditions: 2×10^{-4} M DMG, 0.01 M borate buffer; 60-s collection at −0.7 V, scan at 30 μA. The vertical lines are the potential limits within which the peak area was calculated.

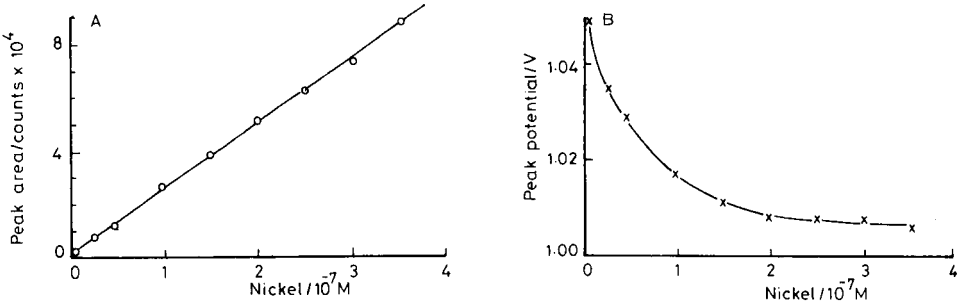

Fig. 8. Variation of the peak area (A) and peak potential (B) with nickel concentration. Conditions: 60-s stirred collection at −0.7 V; the deaerated solution contained 2×10^{-4} M DMG in seawater at pH 8.6; the current setting was 1 μA.

Dissolved oxygen produced a large reduction peak at −1.1 V when air-saturated seawater was tested (Fig. 9). It was not possible to scan past the oxygen wave at currents <3 μA unless a smaller mercury drop was used. The oxygen peak shifted strongly in a negative direction at higher currents: the peak potential was −1.13 V at 3.7 μA, −1.17 V at 7 μA, −1.22 V at 15.2 μA, −1.27 V at 23 μA, −1.34 V at 39 μA, and −1.39 V at 66 μA. It is therefore possible to diminish interference by oxygen by selecting a current at which the peak is separated from the metal being quantified. The nickel peak, for instance, appeared on top of the oxygen peak at a current of 5.6 μA, whereas at currents >10 μA the peaks were separated. The reduction of nickel is apparently more reversible than that of oxygen: at 15 μA the nickel peak potential was at −1.12 V, whereas that of oxygen was at −1.22 V.

The concave shape of the background counts between −0.2 and −0.7 V (Fig. 9) was ascribed to the capacitance current. The capacitance of the electrode is not constant as the double-layer capacitance varies with the potential

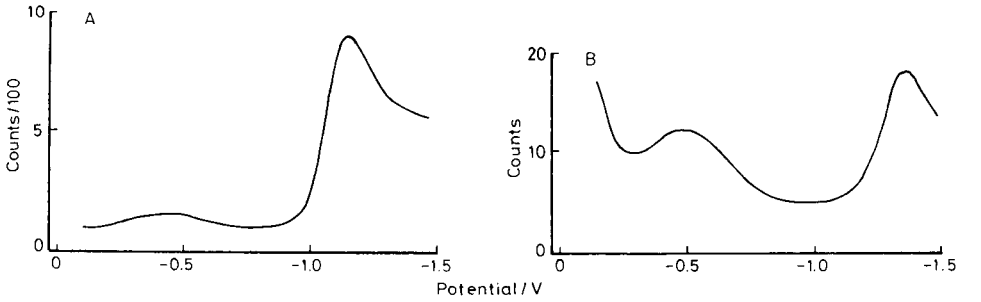

Fig. 9. Scans showing the reduction wave of dissolved oxygen at different applied currents: (A) 3.7 μA; (B) 39 μA.

and goes through zero at —0.5 V in chloride solutions of similar composition as seawater [15]. The background current therefore has a sigmoidal shape, where part of the capacitance contribution to the baseline at potentials below about —1 V is masked by the reduction of oxygen (Fig. 9). The shape of the baseline is out of phase with the actual capacitance as a result of the fast scan rate, and the broad hump can be seen to shift to more negative potentials with a further increase in the current (Fig. 9A, and B, note the different vertical scales). The reduction peak for copper is located on this broad hump as can be seen from its asymmetric appearance in Fig. 5.

At low current settings, the scan rate at potentials more positive than —1 V is affected by the reduction of dissolved oxygen, the waves appearing at around —0.5 V and —0.85 V; this reduction causes a background current of between 1.0 μA (at —0.3 V) and 1.8 μA (at —0.7 V) in unstirred conditions, which consumes part of the reduction current applied during the scan. Nevertheless, dissolved metal concentrations can be evaluated by means of standard additions to the sample containing dissolved oxygen, because the effect is constant. At low applied currents, the scan rate could vary from sample to sample if the dissolved oxygen concentration varied strongly, but this effect is diminished by selecting a current much larger than that caused by the first reduction step of oxygen. Thus the area of the copper peak shown in Fig. 5 (measured at 4 μA) decreased by only 20% when the solution was deaerated.

The determination of nickel in air-saturated water is affected more than copper by dissolved oxygen because its reduction peak is located near the second reduction wave of oxygen (H_2O_2/H_2O). A high current therefore needs to be applied which diminishes the sensitivity. The nickel peak is considerably enhanced, and the baseline is nearly flat, when the solution is deaerated and a lower current is selected, as shown in Fig. 10. Nevertheless, nickel concentrations could be evaluated accurately by standard additions in the presence or absence of dissolved oxygen.

Experiments with cobalt showed that this element can be determined by stripping chronopotentiometry simultaneously with nickel after deaeration of the solution. However, cobalt is affected more strongly by dissolved

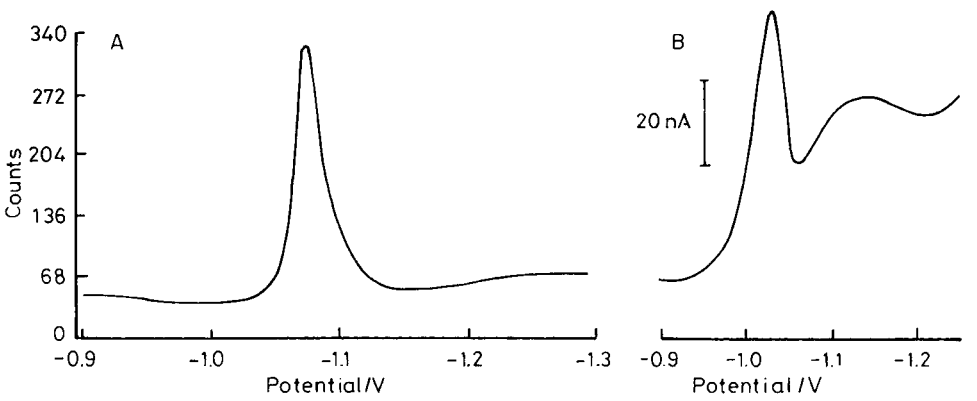

Fig. 10. Comparison of the measurement of nickel by stripping chronopotentiometry (A) and CSV (B). Conditions: 9 nM nickel in deaerated seawater, containing 2×10^{-4} M DMG; scans preceded by 60-s collection at 0.7 V. The chronopotentiometric current setting was 5.6 μA.

oxygen, as its peak potential is 0.1 V more negative, and low levels of cobalt can therefore only be determined after deaeration of the sample.

Results obtained for copper (4—10 nM), uranium (3—14 nM), nickel (3—7 nM) and cobalt (5—10 nM) by stripping chronopotentiometry with internal standard additions were verified by CSV with the same HMDE but after deaeration of the sample. Good agreement was obtained between the two techniques; the results were identical within the normal experimental standard deviation.

The effect of varying the applied current

The total reducible charge, σ, accumulated on the HMDE can be evaluated from the product of the applied cathodic current, i_c, and the transition time, τ, which is obtained from the peak area (in counts) multiplied by the counting time (4 μs); thus $\sigma = i_c\tau$.

The product of $i_c\tau$ should be constant at varying currents when the adsorbed charge of complexed metal is constant. However, in air-saturated samples, some of i_c is consumed by the reduction of dissolved oxygen, so the scan is driven by the residual current, i_r. This residual current cannot be measured directly during the scan, but variations in it can be evaluated from the scan rate, which depends directly on the current (at constant capacitance); the scan rate can be obtained from $1/B$, where B is the average height of the baseline under the peak. Thus, in an attempt to correct the transition time for variations in the scan rate at low currents as a result of variable dissolved oxygen levels, a new parameter was calculated, the compensated peak area, from the peak area/B.

The peak area, the compensated peak area, the charge (σ), the peak height and the peak potential were measured for the stripping chronopotentiometry

of nickel in the presence and absence of dissolved oxygen and at various current settings. The results are presented in Table 1. Both the peak areas and peak heights obtained for nickel in deaerated seawater showed a considerable increase when the current was lowered (Table 1). Higher currents were needed in the presence of oxygen, and the peak area was commensurately smaller. The charge decreased with increasing current, dropping from 162 nC at 15 μA to 77 nC at 42 μA. This decrease may be caused by a small but increasing degree of inefficiency of the reduction of adsorbed nickel at enhanced scan rates. The nickel reduction became also increasingly irreversible at faster scan rates, as is apparent from the peak potential which shifted from −1030 mV at 0.8 μA to −1214 mV at 42 μA; the peak potential was located at −1030 mV when the scan was done by linear-sweep CSV at a scan rate of 50 mV s^{-1}.

The compensated peak area, though far less variable than the peak area at varying scan rates, was not as stable as expected, perhaps because of the difficulty of estimating the average scan rate under the nickel peak. The variability diminished at greater scan rates because of the shift of the oxygen peak away from that of nickel, but in these conditions the scan rate is not much affected by variations in the dissolved oxygen concentration, so that calculation of the compensated peak area is no longer required.

Comparison of stripping chronopotentiometry with CSV

The sensitivity of stripping chronopotentiometry was compared with that of CSV by running scans on the same solutions and with the same HMDE, the solutions having been deaerated before the CSV tests. In Fig. 10, the measurement of 9 nM Ni by linear-sweep CSV and by stripping chronopotentiometry can be compared; the measurement of the same nickel concentration in air-saturated seawater by stripping chronopotentiometry can be seen in Fig. 7. The reduction of nickel is rather irreversible so that the sensitivity in CSV

TABLE 1

Effects of varying the current for the stripping chronopotentiometric scan on the reduction of adsorbed complexes of nickel with DMG.

[The solution (seawater) contained 9 nM Ni, 2 × 10^{-4} M DMG and 0.01 M borate pH buffer; each scan was preceded by 60-s stirred adsorption at −0.7 V]

Applied current (μA)	Peak area (counts)	Peak height (counts)	Compensated area ×100	σ (nC)	E_p (mV)
Deaerated					
0.8	48 841	2336	89	152	−1030
5.65	6016	274	117	136	−1080
15	2708	109	36	162	−1115
Not deaerated					
20	1474	53	46	118	−1133
30	752	22	47	90	−1170
42	459	12	51	77	−1214

does not benefit from using the differential pulse modulation. It can be seen that as a result of the sloping baseline obtained in CSV (Fig. 10), the stripping chronopotentiometric scan was much more sensitive, whereas the chronopotentiometric scan in presence of dissolved oxygen (Fig. 7) was similar to that obtained by CSV.

The relative standard deviation of the measurement of 9 nM nickel by stripping chronopotentiometry was 2.2% without deaeration, and 1.4% after deaeration (n = 8). The limit of detection for nickel as calculated from 3× (peak area/noise) was 0.6 nM Ni in air-saturated seawater (current setting 15 μA) whereas after deaeration it was 0.2 nM Ni at 5.6 μA and 0.1 nM Ni at 0.8 μA (determined after 60-s stirred collection). This compares favourably with a limit of detection of 0.6 nM Ni (3× signal/noise) for linear-sweep CSV at the same HMDE. Cobalt could be determined by stripping chronopotentiometry only after deaeration, and its limit of detection was similar to that of nickel.

Comparison of the determinations of copper and uranium by stripping chronopotentiometry and CSV is less favourable than that of nickel to the former method. The reduction of copper, after its adsorption as a complex with quinolin-8-ol, is quite reversible and its peak height is considerably enhanced by using the differential-pulse (DP) modulation. Thus the sensitivity for copper by stripping chronopotentiometry was found to be similar to that obtained by linear-sweep CSV, but quite inferior to that of DPCSV. The limit of detection by stripping chronopotentiometry was 1.8 nM for copper and 1.6 nM for uranium (n = 8); the corresponding limits by DPCSV are 0.2 nM for both metals [3, 11].

It may be possible to enhance the sensitivity of stripping chronopotentiometry for metals with a reversible reduction by using pulsed-current techniques, but this would adversely affect the application of stripping chronopotentiometry as a field technique. The fast, single scan (lasting from 50 to 100 ms) presently applied in these experiments was relatively insensitive to engine vibrations and ship motion. This time span would inevitably become longer if current modulations were used to take advantage of the reversible reduction of certain metals, and the scan would be more likely affected by environmental factors; its sensitivity as a laboratory instrument, however, could probably be enhanced by current modulation.

The sensitivity of cathodic stripping chronopotentiometry with the HMDE in the presence of dissolved oxygen compares well with the results recently obtained with a mercury-film carbon electrode where medium exchange was used so that the scan could be done in the absence of dissolved oxygen [10]; a limit of detection of 0.5 nM Ni (3× their standard deviation) was obtained in those conditions after 70-s adsorption, as compared to our results of 0.6 nM Ni in the presence of dissolved oxygen, and 0.1 nM Ni in its absence, after 60-s adsorption. Furthermore, the linear range of the HMDE is longer than that of the solid electrode; the peak area obtained with the HMDE increased linearly with the adsorption time until at least 300 s, as compared with a

linear range of <50 s with the solid flow cell [10]. By extending the collection time to 300 s, the limit of detection with the HMDE in the presence of dissolved oxygen could therefore be reduced to 0.1 nM, or 0.02 nM Ni after deaeration.

Field application of continuous-flow stripping chronopotentiometry

The instrument was converted to continuous-flow analysis by attaching a flow cell to the capillary. Convective collection was achieved by pumping the merged reagent and sample flows to the HMDE (Fig. 1) where the liquid jetted from a distance of ca. 1 mm to the mercury drop. Each scan was initiated after a quiescence period of two seconds to allow the water movement to slow down; during the quiescence period, water from the bulk (≈50 ml) of the flow cell became mixed with the solution immediately surrounding the HMDE. Each scan, therefore, was done in the presence of the bulk concentration of dissolved oxygen which could differ from the more variable concentration present in the pumped supply; the scan rate was thus protected from strong fluctuations in the dissolved oxygen concentration which could occur during passage through an estuary. A further stabilizing factor was the well-known permeability of the teflon tubing (inner diameter 0.8 mm) to oxygen; it was observed from the oxygen peak that previously deaerated seawater contained oxygen after passage through the teflon tubing.

The Tamar river has a very pronounced turbidity maximum at around a salinity of 0.2. Dissolved, labile nickel was measured in this estuary during four consecutive runs across the turbidity maximum in order to investigate the fast removal processes which are thought to occur in this region [16]. The first run was upstream starting from a salinity of around 17; the last run was in the downstream direction and was continued until a salinity of 31 was reached. The speed of the vessel was 6 knots during the major part of the transects, but was increased to 9 knots on the final, downstream passage at salinity >12 at 21:30. The turbidity (calibrated in ppm of suspended particles) was measured continuously in addition to the measurements by stripping chronopotentiometry and the salinity.

The variation in the labile nickel concentration is given along with the salinity as a function of the time in Fig. 11A; the labile nickel concentration can be seen to drop strongly each time the turbidity maximum (at salinity = 0.2) is passed in either direction, the labile nickel concentration being higher away from the turbidity maximum. The labile nickel and the turbidity are plotted against the salinity in Fig. 11B; the salinity scale has been expanded in a negative direction at salinities below 0.2 in order to separate the data in the freshwater region, which is of special importance because of the turbidity maximum; time was used to separate the data with a unit value equal to the measuring time of stripping chronopotentiometry (ca. 2 min). It can be seen (Fig. 11B) that the drop in the labile nickel concentration coincides with the turbidity maximum. The nickel levels increase strongly downstream with a maximum at intermediate salinities (18—21), and then drop again as a result

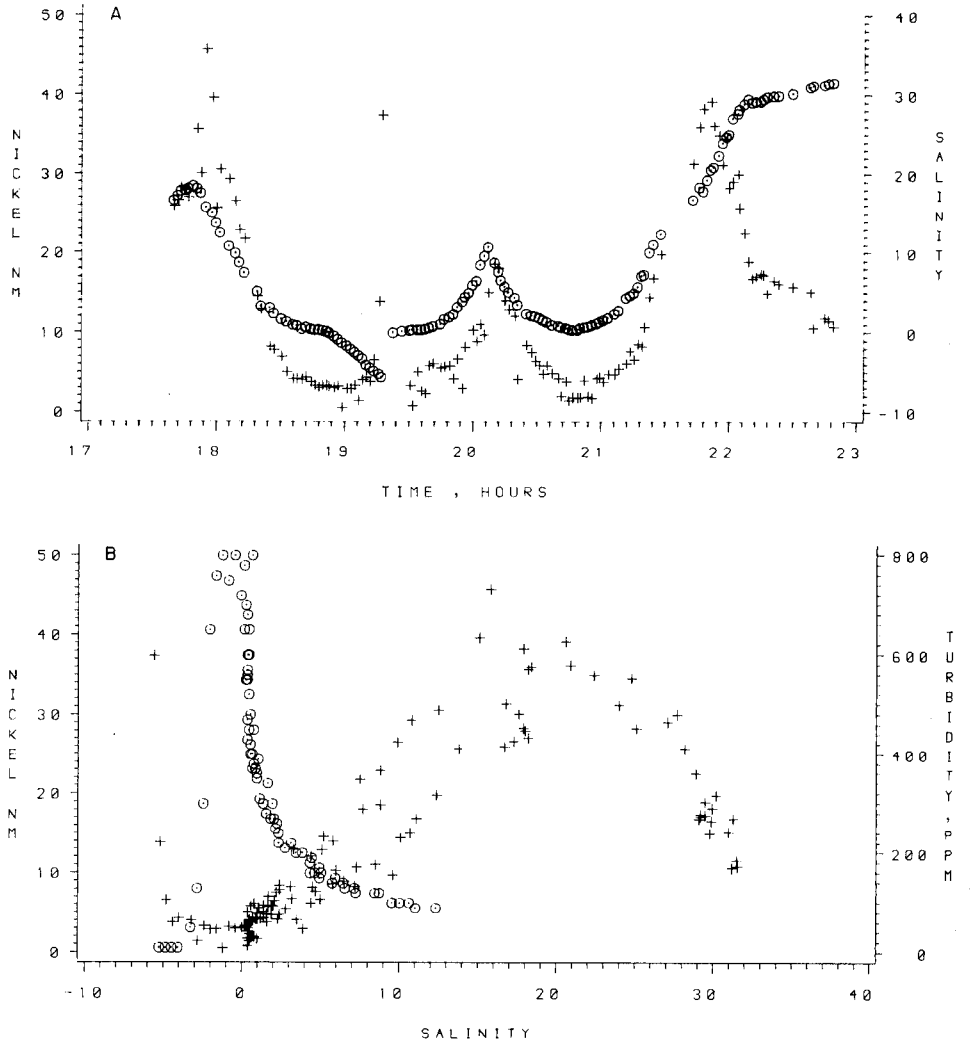

Fig. 11. Continuous-flow measurement of dissolved nickel (nM) in the Tamar estuary. (A) Dissolved nickel (+) and salinity (○) as functions of time. (B) Dissolved nickel (+) and turbidity (○) as functions of salinity.

of dilution of estuarine water with high-salinity seawater. This result is similar to that observed (in less detail) for copper and zinc in this estuary [16]; the increase at intermediate salinities is probably caused by a combination of re-injection of pore waters and desorption from particles. A study into the processes governing these effects is presently under way.

Some hysteresis is apparent in the nickel data obtained during the upstream and downstream runs; this effect is caused by the time lapse between sub-sampling the pumped water supply, and the water/reagent mixture reaching

the electrode (60 s plus a reaction time of 30 s) to which has to be added the adsorption time (45 s), giving a total delay of 135 s between sampling (including the salinity measurement) and the nickel measurement. The change in the salinity and the nickel concentration were sufficiently fast at salinities <18 to cause the apparent hysteresis in Fig. 11B.

The results of this study in the Tamar estuary indicated that reductive stripping chronopotentiometry is a robust field technique. The measurements were not noticeably affected by the presence of large amounts of particles [coarse (>100 μm) particles had been removed by pre-filtering the sample flow], or by likely variations in the dissolved oxygen concentration as apparent from the constant scan rate (constant baseline) throughout the estuary.

The present rate of about 30 measurements per hour was limited largely by the slow data treatment in the computer used, but could be improved by increasing the memory capacity of the computer (see Experimental). It should then be possible to increase the measuring frequency to between 60 and 90 per hour, depending on the collection time.

Conclusions

Because of the nature of the stripping chronopotentiometric scan, the sensitivity of the cathodic method is similar to, or better than, that of linear-sweep CSV, whereas a reversibly reduced metal such as copper can be determined with greater sensitivity by differential-pulse CSV. Stripping chronopotentiometry is especially useful as a field technique, as it can be used in the presence of dissolved oxygen, and as the fast scan makes the measurement less sensitive to vibrations and movement of the electrode.

The authors are grateful for assistance with software development and laboratory experiments by P. J. M. Buckley. The manuscript was typed by V. C. Hughes and the drawings prepared by J. Murphy. The research was financially supported by NERC grants GR3/5873 and GR3/4788.

REFERENCES

1 J. Wang, P. A. M. Friar and J. S. Mahmoud, Anal. Chim. Acta, 172 (1985) 57.
2 C. M. G. Van den Berg, K. Murphy and J. P. Riley, Anal. Chim. Acta, 188 (1986) 177.
3 C. M. G. Van den Berg, J. Electroanal. Chem., 215 (1986) 111.
4 C. M. G. Van den Berg, Sci. Total Environ., 49 (1986) 89 (and references therein).
5 J. Wang and J. S. Mahmoud, Anal. Chim. Acta, 182 (1986) 147.
6 B. Pihlar, P. Valenta and H. W. Nürnberg, Fresenius' Z. Anal. Chem., 307 (1981) 337.
7 P. Delahay and G. Mamantov, Anal. Chem., 27 (1955) 478.
8 W. Kemula and J. W. Strojek, J. Electroanal. Chem., 12 (1966) 1.
9 S. Bruckenstein and J. W. Bixler, Anal. Chem., 37 (1965) 786.
10 H. Eskilsson, C. Haraldsson and D. Jagner, Anal. Chim. Acta, 175 (1985) 79.
11 C. M. G. Van den Berg and M. Nimmo, Anal. Chem., 59 (1987) 924.
12 A. W. Morris, A. J. Bale and R. J. M. Howland, Estuarine Coastal Shelf Sci., 14 (1982) 649.
13 R. Neeb, Inverse Polarographie und Voltammetrie, Verlag Chemie, Weinheim, 1969, p. 63.

14 C. M. G. Van den Berg and M. Nimmo, Sci. Total Environ., 60 (1987) 185.
15 I. M. Kolthoff and J. J. Lingane, Polarography, 2nd edn., Interscience, New York, 1952, p. 139.
16 D. R. Ackroyd, A. J. Bale, R. J. M. Howland, S. Knox, G. E. Millward and A. W. Morris, Estuarine Coastal Shelf Sci., 23 (1986) 624.

Analytica Chimica Acta, 199 (1987) 77—83
Elsevier Science Publishers B.V., Amsterdam — Printed in The Netherlands

DETERMINATION OF CAPROLACTAM BY ADSORPTIVE VOLTAMMETRY AFTER SEPARATION BY THIN-LAYER CHROMATOGRAPHY

ZUZANA TOCKSTEINOVÁ and MILOSLAV KOPANICA*

UNESCO Laboratory of Environmental Electrochemistry, J. Heyrovský Institute of Physical Chemistry and Electrochemistry, Czechoslovak Academy of Sciences, Jilská 16, 110 00 Prague 1 (Czechoslovakia)

(Received 14th February 1987)

SUMMARY

Caprolactam (2-oxohexamethyleneimine) can be determined in wastewaters and natural waters by adsorptive stripping voltammetry after separation of the product of the reaction between caprolactam and *p*-(*N*,*N*-dimethylamino)benzene-*p'*-azobenzoyl chloride. When a hanging mercury drop electrode is used with an accumulation time of 60 s in stirred solution, caprolactam can be determined from a lower limit of 0.2 μg ml^{-1}. With a 360-s accumulation time, linear calibration plots are obtained for 8×10^{-10}—8×10^{-9} mol l^{-1} caprolactam. The effect of interfering sample components is eliminated by the TLC separation.

A method for the determination of low concentrations of caprolactam (2-oxohexamethyleneimine) is necessary for control of industrial wastewaters in areas where synthetic fabrics are produced. The aim of this work was to establish an electrochemical method for the determination of low amounts of caprolactam, preferably involving preconcentration of the analyte on the surface of the working electrode. Because caprolactam is electrochemically inactive, its determination in such a way required a suitable derivatization procedure. Because nitrosation of caprolactam proceeds with low efficiency and the product is not stable enough for reliable usage, other procedures were examined. It was found that the product of the reaction between caprolactam and *p*-(*N*,*N*-dimethylamino)benzene-*p'*-azobenzoyl chloride is electrochemically active and can be determined by the application of adsorptive stripping voltammetry.

EXPERIMENTAL

Reagents and equipment

A 1×10^{-3} M solution of caprolactam was prepared by dissolving the compound (Riedel de Haën, F.R.G.) in water. A 5×10^{-3} M solution of *p*-(*N*,*N*-dimethylamino)benzene-*p'*-azobenzoyl chloride (Technological University, Pardubice, Czechoslovakia) was prepared by dissolving in benzene. All other

0003-2670/87/$03.50

solutions were prepared from reagent-grade chemicals; twice-distilled water (quartz apparatus) was used throughout.

The polarographic analyzer (PA-4; Lab. přístroje, Praha) was used in the three-electrode configuration. A static mercury drop electrode (SMDE-1, Lab. přístroje, Praha) served as working electrode, Ag/AgCl electrode as reference electrode and a platinum wire as the auxiliary electrode. Dissolved oxygen was removed from the sample solutions by nitrogen. A Pye-Unicam 8800 spectrophotometer was used as required.

Silufol UV-254 plates (Sklo Union, Kavalier, Czechoslovakia) were used for the thin-layer chromatographic separations.

Procedure

Approximately 5 ml of the aqueous solution of caprolactam (0.02—1.00 mg ml^{-1}) was evaporated to dryness in vacuum. The residue was dissolved in 2 ml of the reagent solution, and the mixture was boiled for 10 min on a water bath, using a reflux condenser. The solution was then evaporated to dryness and the residue was immediately dissolved in 2 ml of benzene. A portion (20 μl) of the resulting solution was placed on the Silufol plate and dried with air. Then the elution was started, in the ascending direction; the mobile phase was benzene/ethyl acetate (12:3). The orange band (R_f = 0.61) was cut out and the coloured derivative was eluted with 5 ml of methanol. This solution of the product was diluted with 20 ml of 0.1 M acetate buffer, pH 4.5, and transferred to the electrolysis cell. The conditions for adsorptive stripping voltammetry were as follows: differential pulse voltammetry (5 pulses per second, duration of pulses and interval between pulses 100 ms), accumulation potential 0 V, accumulation time 60—360 s, stirred solution during accumulation, rest period 15 s, potential scan from 0 to —1.0 V at 20 mV s^{-1}. The peak potential of the separated product was —0.30 V.

RESULTS

Reaction of caprolactam with p-(N,N-*dimethylamino)benzene*-p'-*azobenzoyl chloride*

The reagent *p*-(*N*,*N*-dimethylamino)benzene-*p'*-azobenzoyl chloride (I) has been reported to react with amines and phenols [1] with formation of coloured products which are suitable for the spectrophotometric determination of these compounds. Similarly, caprolactam was found to react with reagent I in benzene medium according to the reaction

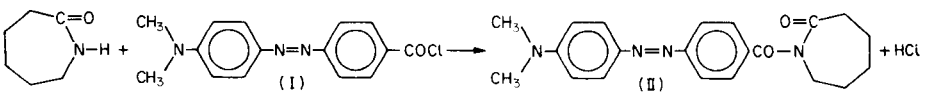

The product of this reaction, *N*-[*p*-(*N'*,*N'*-dimethylamino)benzene-*p'*-azobenzoyl] caprolactam (II), had practically the same ultraviolet/visible spectrum as reagent I with an absorbance maximum at ca. 480 nm. The

product of the reaction was therefore identified by mass spectrometry; compound II was identified as the major component in the reaction mixture after boiling reagent I and caprolactam in benzene (see Procedure). Besides this product, the hydrolyzed (carboxylic acid) form of the reagent was also identified in the reaction mixture. The existence of this compound can most probably be ascribed to the presence of water in the reaction mixture. The results of mass spectrometric measurement also provided evidence for compounds III and IV,

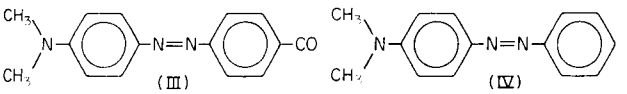

(III) (IV)

present as trace impurities in the reaction mixture.

Separation of the product of the reaction between caprolactam and the reagent

The electrochemical activity of both the reagent and the product of the above reaction, caused by the presence of the N=N bond in both substances, made it necessary to separate these compounds before the voltammetric step. Because thin-layer chromatography (TLC) is experimentally simple and relatively fast, the conditions for this mode of separation were examined.

It was found that a mixture containing reagent I and product II were well separated by using the one-dimensional ascending technique with a development time of 10 min. The optimum mobile phase was a mixture of benzene and ethyl acetate (12:3). Under these conditions, the R_f value of the product (II) was found to be 0.61. The presence of the hydrolyzed form of the reagent caused the development of the band with a R_f value of 0.39. Detection of the separated component was simple because the band of product II was intensely coloured (orange). After TLC separation, this band was cut out and the separated product was dissolved in methanol.

Voltammetry of the separated product

In preliminary experiments, it was found that in acetate buffer solution (pH 4.5) with 20% (v/v) methanol, the product of the reaction (II) yielded a well-developed d.c. polarographic wave with a half-wave potential of −0.30 V (vs. Ag/AgCl). Results obtained by cyclic voltammetry at a hanging mercury drop electrode (HMDE) in the potential interval between 0 and −1.20 V showed that the studied compound yielded cathodic and anodic peaks.

The corresponding cathodic (i_{pc}) and anodic (i_{pa}) peak currents increased with increasing polarization rate in the range from 100 mV s^{-1} to 600 mV s^{-1}, while the ratio i_{pa}/i_{pc} remained less than 1. If the time delay before the cathodic scan was prolonged, a significant increase of the i_{pc} value was observed. These findings suggested that the product of the electrode reaction is adsorbed on the surface of the HMDE at a potential close to 0 V. To verify this, normal-pulse voltammetric (NPV) curves were recorded with varied initial potentials

(E_{in}) in the range from +0.10 to —0.10 V. The results showed that maximal peak current was obtained when the E_{in} value was kept at 0 V. Figure 1 shows the NPV curve of the product (II) together with the normal-pulse polarographic (NPP) curve obtained under identical conditions with a DME. The NPV current is about six times higher than that obtained in NPP, because much more of the substance is adsorbed on the surface of the stationary electrode than is adsorbed on the surface of a DME with identical surface area.

The results given above showed that adsorptive stripping voltammetry (AdSV) could be applied for the determination of caprolactam.

Adsorptive stripping voltammetry of the separated product

Because of the preconcentration of the analyte on the surface of the HMDE, the application of AdSV enables measurements to be made with much less sample and thus to achieve the TLC separation with a lower concentration of the sample solution. In the examination of the effect of different experimental parameters on the AdSV response of the product (II), in all cases 0.05 mg of caprolactam was processed as described in the given Procedure. In acetate buffer medium containing 20% (v/v) methanol, the peak potential was —0.30 V. The i_{pc} value depended on the accumulation potential (E_{acc}) and the accumulation time (t_{acc}). It was confirmed that the optimum accumulation potential was 0 V.

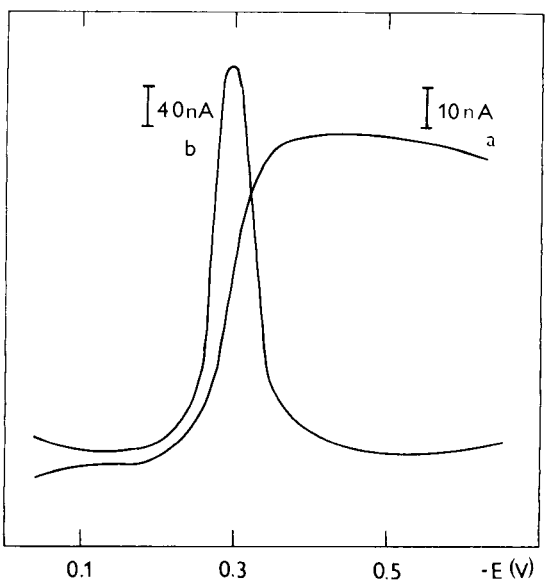

Fig. 1. NPP and NPV curves for product II in a supporting electrolyte of 0.1 M acetate buffer containing 20% (v/v) methanol. (a) NPP curve, drop time 2 s, polarization rate 2 mV s^{-1}; (b) NPV curve, HMDE, polarization rate 2 mV s^{-1}. E_{in} = 0 V; concentration of product II, 1 × 10^{-6} mol l^{-1}.

The peak current increased with prolonged accumulation time and reached a limiting value. Linear dependences of the peak current on the concentration of the product (II) were found in the concentration range 8×10^{-10}—1×10^{-7} mol l^{-1}. For the lower concentration range, 8×10^{-10}—8×10^{-9} mol l^{-1}, the accumulation time used was 360 s and for the higher concentration range, the accumulation time was 150 s. The slopes of the regression lines were 0.63 nA nM^{-1} for the lower concentration range and 0.21 nA nM^{-1} for the higher concentration range, with correlation coefficients of 0.9928 and 0.9998, respectively. The peak current vs. concentration dependence was studied with varied amounts of caprolactam, as in the Procedure. The resulting linear dependence gave evidence of the reproducible recovery of caprolactam under the recommended conditions and verified that the measured current corresponding to the electrode reaction of product II depended linearly on the caprolactam concentration.

Influence of pH. Figure 2 shows the dependence of peak current, i_p, and peak potential, E_p, on pH. These data were obtained by AdSV measurement of solutions with identical starting concentrations of caprolactam, when both the accumulation potential and time were kept constant. The variation of i_p and E_p with pH can be caused by the protonation of the product of the electrode reaction, but the influence of hydrogen ion concentration on the extent of adsorption may also affect the peak currents. A pH of 4.5 was chosen with regard to the necessity of applying an accumulation potential of 0 V; lower pH values resulted in less well developed peaks with more positive peak potentials.

Significant enhancement of peak currents with decreasing concentration of supporting electrolyte has been reported in AdSV determination of some organic compounds [2]. In the present case, no influence of supporting electrolyte concentration (in the range 0.001—0.5 M) on the values of the peak current was observed.

Influence of surface-active substances. The interfering effect of surface-active substances in AdSV is usually serious because of competition for the adsorption sites. In the determination of caprolactam as in the recommended procedure, the peak currents were doubled when the test solution contained Triton X-100 in an 800-fold weight ratio to the amount of the analyte (Fig. 3). A similar, but less pronounced effect was caused by tribenzylamine. Gelatin, however, caused serious distortion of the peaks. Similar effects have been observed in the differential-pulse polarographic determination of benzylpenicillenic acid after addition of Triton X-100 [3]. A possible explanation of the observed phenomenon is that at high Triton X-100 concentrations, a film rather than a monomolecular layer is formed on the surface of the HMDE; the hydrophobic properties of this film may facilitate the adsorption of product II on the electrode surface and thus enhancement of the peak current is observed.

Efficiency of the reactions. The efficiency of the formation of product II was evaluated by analyzing a series of aqueous caprolactam solutions as in

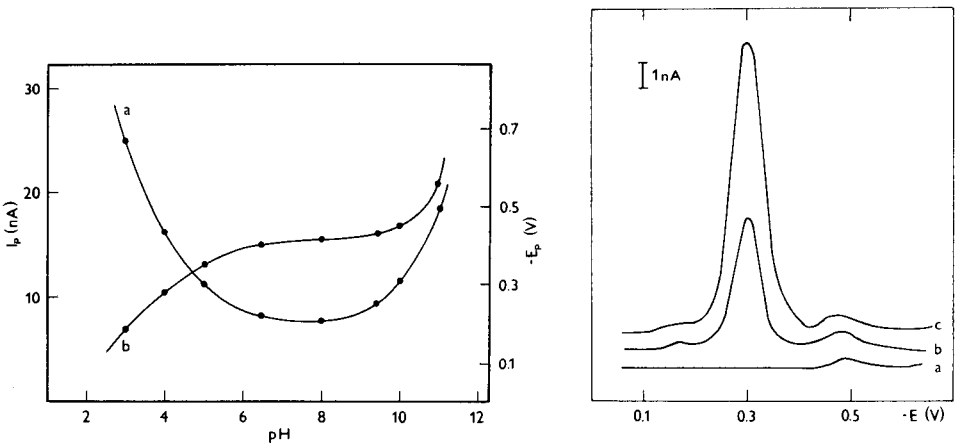

Fig. 2. Dependence of the cathodic peak current (a) and peak potential (b) of the AdSV curves of product II on pH. Supporting electrolyte, 0.1 M acetate buffer containing 20% (v/v) methanol; concentration of product II, 3.2×10^{-8} mol l^{-1}; HMDE, $E_{acc} = 0$ V, $t_{acc} = 150$ s, stirred solution, $t_{rest} = 15$ s, scan rate 20 mV s^{-1}.

Fig. 3. Effect of Triton X-100 on AdSV curves of the product (II) of reaction: (a) supporting electrolyte; (b) supporting electrolyte and 6.4×10^{-9} mol l^{-1} product II; (c) as (b) after addition of an 800-fold amount of Triton X-100. Conditions as for Fig. 2 with pH 4.5.

the given procedure (the method of standard addition was used). The amount of caprolactam in the original aqueous solutions (at a concentration of 10^{-3} mol l^{-1}) was also determined spectrophotometrically [4] by using the reaction with ninhydrin after hydrolysis with a methanolic solution of sodium hydroxide. Comparison of the results obtained showed a mean 98% recovery of caprolactam in the proposed procedure.

The method was also tested for some polluted water samples with known amounts of caprolactam added (0.05—0.5 mg l^{-1}). In all cases, the results obtained agreed well with the amount of added caprolactam. Evaluation of the data again depended on the method of standard addition.

Conclusion

Adsorptive stripping voltammetric determination of the product of the specified reaction was found to be sensitive enough to permit combination of this method with standard TLC techniques, by which low volumes of the sample solution (20—100 μl) can be separated in relatively short times (10—15 min).

When an accumulation period of 60 s is applied in stirred solution, caprolactam can be determined in aqueous samples with a lower determination limit of 0.2 μg ml^{-1}. Under these conditions, it is sufficient to start the TLC separation with only 20 μl of the mixture of reagent and sample in benzene.

Because the analyte is separated by TLC, all interferences are eliminated and the proposed method can be applied in the analysis of wastewaters and natural waters.

The authors are indebted to Dr. V. Hanuš of this Institute for interpretation of the MS data.

REFERENCES

1 J. Churáček, J. Říha and M. Jureček, Fresenius' Z. Anal. Chem., 249 (1970) 120.
2 J. Wang, Am. Lab., 17 (1985) 41.
3 M. Jemal and A. M. Knevel, Anal. Chem., 50 (1975) 1917.
4 P. Burša, Ph.D. Thesis, Technological University, Pardubice, Czechoslovakia, 1986.

Analytica Chimica Acta, 199 (1987) 85—91
Elsevier Science Publishers B.V., Amsterdam — Printed in The Netherlands

AN AMPEROMETRIC SENSOR FOR CARBON DIOXIDE BASED ON IMMOBILIZED BACTERIA UTILIZING CARBON DIOXIDE

HIROAKI SUZUKI

Fujitsu Laboratories Ltd., 10-1 Morinosato-Wakamiya, Atsugi 243-01 (Japan)

EIICHI TAMIYA and ISAO KARUBE*

Research Laboratory of Resources Utilization, Tokyo Institute of Technology, 4259 Nagatsuta-cho, Midori-ku, Yokohama 227 (Japan)

(Received 9th December 1986)

SUMMARY

A biosensor consisting of a CO_2-utilizing autotrophic bacterium (strain S-17, *Pseudomonas* type) and an oxygen-sensing electrode was constructed for the amperometric determination of CO_2. The correlation between current decrease and CO_2 concentration was linear in the range 5—200 mg l^{-1} CO_2. The optimum temperature and pH for operation of the biosensor were 30°C and 5.5, respectively. The sensor did not respond to other volatile compounds except for acetic acid. The sensor could be operated continuously for about a month.

The determination of carbon dioxide is very important in some industrial processes and in environmental and clinical analyses. The pCO_2 electrode was first developed for the measurement of CO_2 in blood by Stow et al. [1] and was subsequently improved by Severinghaus and Bradley [2]. This potentiometric pCO_2 device has found widespread use in biological and industrial applications, and has been used as the sensing element in enzyme electrodes [3]. The response characteristics of the pCO_2 electrode have been evaluated from many viewpoints [4], but major problems are associated with the potentiometric method of detection. Various ions and some organic and inorganic volatile acids affect the potential of the inner pH electrode and the gas-permeable membrane of the pCO_2 electrode [3—8]. In addition, the precision of the conventional potentiometric pCO_2 electrode is somewhat restricted because of the Nernstian type of response. In contrast, the amperometric oxygen electrode generates a current directly determined by the chemical reaction, hence it theoretically possesses far greater sensitivity. By combining a biochemical reaction which consumes oxygen with an oxygen electrode, several amperometric biosensors with excellent sensitivity have been constructed [9]. The purpose of the study reported herein was to develop a novel microbial amperometric CO_2 sensor based on an autotrophic bacterium and to evaluate the characteristics of the sensor.

0003-2670/87/$03.50

EXPERIMENTAL

Reagents and bacteria

All chemicals were of reagent grade and were used without further purification. Solutions were prepared with distilled/deionized water. Standard aqueous 1 M solutions of potassium carbonate, sodium acetate, sodium formate, butanol, and 0.05 M KH_2PO_4/NaOH buffer solutions of different pH were prepared.

The autotrophic bacterium, which can grow with only carbonate as the source of carbon, was obtained from The Fermentation Research Institute, Japan. This bacterium was isolated from soil obtained in Akita Prefecture, Japan, and is named S-17. It is thought to belong to the genus *Pseudomonas*; S-17 is a 1 × 4—5-μm Gram-negative rod and grows both autotrophically (utilizing only carbonate as the C-source) and heterotrophically (growing with some organic compounds) on common nutrient media. Usually S-17 is incubated under aerobic conditions, but can also grow slowly under anaerobic conditions. Optimum temperature and pH for growth are 20—34°C and pH 4.0—8.6, respectively. In this study, S-17 was autotrophically incubated under aerobic conditions at 30°C for approximately one month on the inorganic medium shown in Table 1. For comparison, it was also incubated in an organic medium composed of 0.3% nutrient broth and 0.2% peptone in distilled water. In both cases, similar numbers of bacteria were harvested after the incubation period. The present experiments were done with autotrophically grown S-17 except for the case mentioned in Fig. 5.

Procedure for CO_2 determination

A CO_2 sensor was constructed as shown in Fig. 1. Bacterial cells retained on a cellulose nitrate membrane (Toyo Roshi Co.; pore size 0.45 μm) were placed around the platinum cathode of a galvanic-type oxygen-sensing electrode (Ishikawa Seisakujo Co., Tokyo; diameter 1.7 cm). The bacteria solution was placed dropwise onto the cellulose nitrate membrane with slight suction so that the bacteria were retained. The cathode and the immobilized cells were then totally covered with a Millipore polytetrafluoroethylene (PTFE) membrane (pore size 0.5 μm, type FH) secured with a rubber O-ring. The PTFE membrane acts as a gas-permeable membrane.

TABLE 1

Composition of the inorganic medium

Compound	Amount (mg l^{-1})	Compound	Amount (mg l^{-1})	Compound	Amount (mg l^{-1})
KH_2PO_4	400	NaCl	50	$FeCl_3 \cdot 6H_2O$	8.7
K_2HPO_4	500	$MnCl_2 \cdot 4H_2O$	1	$CoCl_2$	0.005
$Na_2SO_4 \cdot 7H_2O$	50	$CaCl_2 \cdot 2H_2O$	5	$Na_2MoO_4 \cdot 2H_2O$	0.002

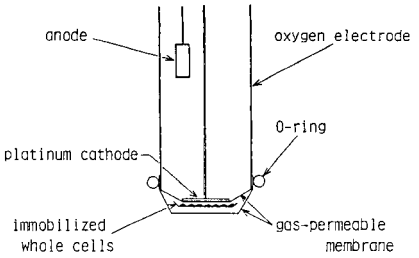

Fig. 1. Construction of the CO_2 sensor.

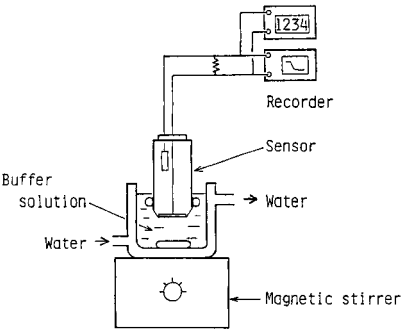

Fig. 2. Schematic diagram of the sensor system.

When a sample solution containing CO_2 is injected into the external buffer solution, CO_2 permeates through the gas-permeable membrane, and is assimilated by the bacteria. The respiratory rate of the bacteria is consequently increased, causing the consumption of oxygen. If the decrease in the oxygen concentration is measured with an oxygen-sensing electrode, the concentration of CO_2 can be measured indirectly. Thus, an amperometric CO_2 sensor can be constructed.

Figure 2 shows a schematic diagram of the system. The sensor was placed in a thermostatically controlled, circulating water jacket and, in most experiments, the temperature was maintained at 30°C. The cell contained a total volume of 50 ml of buffer (0.05 M KH_2PO_4/NaOH), usually at pH 5.5. The current output of the oxygen-sensing electrode was measured with a digital multimeter (Takeda Riken, model TR6843) and the time response was recorded with an electronic polyrecorder (Toa Electronics, Model EPR-200A). CO_2 was supplied by acidification of a potassium carbonate solution mixed with the same buffer as contained in the cell, so as not to create a change in oxygen concentration. Because the CO_2 solution was continuously stirred, the CO_2 concentration came to a certain equilibrium state which could not be described by a simple formula. Then 100 μl of potassium carbonate solution was injected into the sensor cell from a microsyringe at constant time intervals. In most experiments, the pH of the buffer solution was kept constant at 5.5.

For comparison, the same experiments as described above were repeated with a conventional potentiometric pCO_2 electrode (Jyoko Co., Tokyo), and the concentration of K_2CO_3 was correlated to the CO_2 concentration. The CO_2 sensor was stored in the buffer solution at 4°C when not in use.

RESULTS AND DISCUSSION

Characteristics of the system

Figure 3 shows the current/time response of the CO_2 sensor to the addition of various concentration of CO_2 (from potassium carbonate). This experiment was done by injecting 100 μl, 200 μl, and 300 μl of the 1 M carbonate into 50 ml of the buffer solution (30°C, pH 5.5). The concentrations noted in Fig. 3 are the final concentrations in the buffer solution. As shown, the current decreased rapidly with maximum response 2—3 min after the injection; then the current increased gradually because of the escape of CO_2 to the air.

Because the sensor utilizes a microbial element, it must be operated at constant optimum temperature. The dependence of the current decrease of the sensor on temperature is shown in Fig. 4. In this experiment, the temperature of the buffer solution (pH 5.5) was increased stepwise and the current output of the CO_2 sensor was measured at each temperature for an injection giving 2 mM carbonate. Reflecting the optimum growth temperature for S-17 of 30—34°C, the response of the sensor was low for temperatures below 30°C, and exhibited a maximum in the range 30—32°C, gradually decreasing above this level. The experiment was not continued to temperatures above 34°C because of the risk of killing the bacteria. Based on this result, all other experiments were done at 30°C.

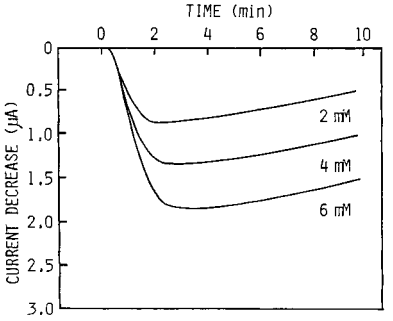

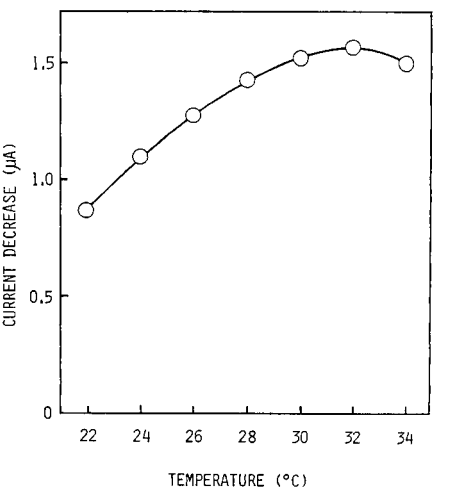

Fig. 3. Time response of the CO_2 sensor. The curves correspond to 2 mM, 4 mM, and 6 mM potassium carbonate, respectively. Conditions: 0.05 M KH_2PO_4/NaOH buffer pH 5.5, 30°C.

Fig. 4. Dependence of current decrease on temperature for 2 mM carbonate in the 0.05 M buffer (pH 5.5).

The concentration of dissolved CO_2 is greatly affected by a change in pH and so the CO_2 determination must be done at a constant buffered pH. CO_2 and H_2CO_3 reach an equilibrium state depending on pH:

$$CO_2 + H_2O \leftrightarrow HCO_3^- + H^+; HCO_3^- \leftrightarrow H^+ + CO_3^{2-}$$

However, in these experiments, the CO_2 concentration could not easily be determined because the buffer solution was stirred for the purpose of saturating it with oxygen. As is well known, at lower pH values the concentration of CO_2 is increased. But if the pH were too low, the rate of CO_2 production in the buffer would exceed the rate of CO_2 assimilation by the bacterium, and the current decrease would not then be a true reflection of the CO_2 concentration. As a compromise between the CO_2-generating ability of the buffer solution and the experimental error incurred through loss of unassimilated CO_2, the pH value was set at 5.5.

Calibration

Calibration curves of potassium carbonate concentration vs. current decrease are shown in Fig. 5. Two types of CO_2 sensor prepared from either autotrophically grown S-17 or heterotrophically grown S-17 were compared. The procedure described above was followed, and 3 min after injection of the carbonate solution, the current decrease of the oxygen-sensing electrode was measured. For concentrations of carbonate below 6—8 mM, the current decrease was approximately proportional to the carbonate concentration,

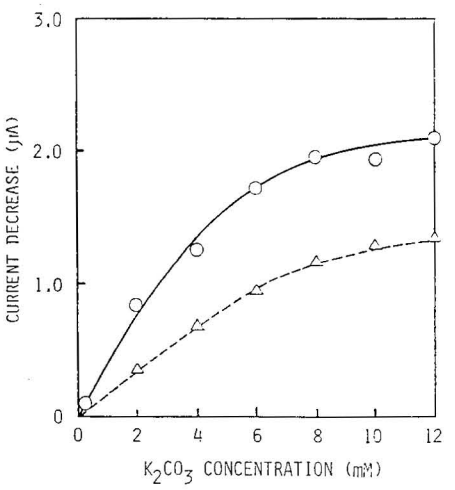

Fig. 5. Dependence of the current decrease on concentration of potassium carbonate: (○) autotrophically grown S-17; (△) heterotrophically grown S-17. Conditions: 0.05 M KH_2PO_4/NaOH buffer (30°C, pH 5.5).

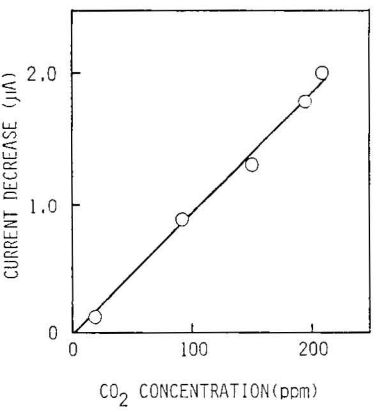

Fig. 6. Calibration curve for the CO_2 sensor. Conditions: 0.05 M KH_2PO_4/NaOH buffer, pH 5.5, 30°C.

but at higher concentrations the response reached a plateau because of saturation of the system with CO_2. The sensor based on autotrophically grown S-17 possessed greater sensitivity than the one based on heterotrophically grown S-17. The initial rate of carbon dioxide utilization did not depend on the carbonate concentration at values higher than 8 mM. The rate of CO_2 utilization appears to be limited by the uptake or metabolism of CO_2 by the microbial cells.

Figure 6 shows the calibration curve for the biosensor. The CO_2 concentration was determined separately by repeating the experiment with a conventional potentiometric pCO_2 electrode. A calibration graph was then constructed relating the CO_2 concentration measured potentiometrically to the current decrease of the amperometric CO_2 sensor. The linear range of the sensor extended up to 200 mg l^{-1} CO_2 (ca. 5 mM). The upper limit of the linear range was governed by saturation of CO_2 in the buffer solution and not by biochemical kinetics. The points plotted in Fig. 6 correspond to the lower concentration range of the upper curve in Fig. 5, obtained with autotrophically grown cells. Considering that the current fluctuation resulting from experimental errors is within 0.05 μA, the proposed sensor could detect a variation of 5 mg l^{-1} CO_2 in the lower concentration range.

Selectivity and stability

Selectivity of the microbial sensor was also examined. Various aqueous solutions of compounds such as acetic acid, citric acid, formic acid, ethanol and butanol were added to the sensor system. Organic acids were added as their sodium salts so as not to affect the pH of the solution. Though the sensor responded slightly (37% of the response to CO_2) to acetic acid, all the other compounds produced no observable response within the margin of experimental error. The response to acetate is perhaps due both to the volatility of the compound and its possible utilization by the bacteria. The fact that formic acid was not detected is noteworthy.

Stability of the sensor was also tested. The output current of the sensor fell at a rate of approximately 0.07 μA day^{-1} for the first six days, but thereafter remained at a constant value of 1.0 μA for more than three weeks. This was considered to be very satisfactory for its application in practical use, especially in a flow cell configuration. The stability of the CO_2 sensor with heterotrophically grown S-17 was very poor, with a lifetime of only 7—10 days. With the autotrophically grown S-17, the stability was greatly improved, probably as a result of materials accumulated during the incubation stage.

We thank Dr. Maeda of the Fermentation Research Institute for providing us with S-17 and Mr. J. M. Dicks for helpful discussion in compiling this report.

REFERENCES

1 R. W. Stow, R. F. Baer and B. F. Randall, Arch. Phys. Med. Rehabil., 38 (1957) 646.
2 J. W. Severinghaus and A. F. Bradley, J. Appl. Physiol., 13 (1958) 515.
3 G. G. Guilbault and F. R. Shu, Anal. Chem., 44 (1972) 2161.
4 M. A. Jensen and G. A. Rechnitz, Anal. Chem., 51 (1979) 1972.
5 R. K. Kobos, S. J. Parks and M. E. Meyerhoff, Anal. Chem., 54 (1982) 1976.
6 M. E. Lopez, Anal. Chem., 56 (1984) 2360.
7 J. M. Cooley and B. Kratochvil, Can. J. Chem., 56 (1978) 2452.
8 D. Midgley, Analyst, 100 (1975) 386.
9 I. Karube and S. Suzuki, Ion-Selective Electrode Reviews, Vol. 6, Pergamon, Oxford, 1984, p. 15.

Analytica Chimica Acta, 199 (1987) 93—97
Elsevier Science Publishers B.V., Amsterdam — Printed in The Netherlands

MICROBIAL ELECTRODE SENSOR FOR VITAMIN B_{12}

ISAO KARUBE*, YONGXIANG WANG[a], EIICHI TAMIYA and MASAHIRO KAWARAI

Research Laboratory of Resources Utilization, Tokyo Institute of Technology, Nagatsuta-cho, Midori-ku, Yokohama 227 (Japan)

(Received 24th February 1987)

SUMMARY

A microbial sensor consisting of immobilized *Escherichia coli* 215 and an oxygen electrode is described for the determination of vitamin B_{12}. When the sample solution is injected into the microbial electrode system, the increased consumption of oxygen by the micro-organisms causes a decrease in the dissolved oxygen around the porous membrane of the oxygen electrode and the current decreases gradually with time until a steady state is reached. The response time for a rate measurement is 2 h. When 0.5 mg of *Escherichia coli* 215 is immobilized, a linear relationship is obtained between the current decrease and the vitamin B_{12} concentration between 5×10^{-9} and 25×10^{-9} g ml^{-1}.

The determination of vitamin B_{12} is important in various fields such as clinical analysis, food processing and fermentation process [1]. Vitamin B_{12} has previously been determined by microbioassay [2], and this has often proved to be advantageous because of its selectivity, sensitivity and ability to yield reproducible results. However, microbioassay is time-consuming and requires complicated procedures [3]. Hence a simple method for the determination of vitamin B_{12} is desirable.

A variety of microbial electrodes consisting of immobilized micro-organisms and electrochemical devices have been developed for applications to microbioassays for determinations of nystatin [4], phenylalanine [5, 6], and vitamin B_1 [7]. *Escherichia coli* 215 requires vitamin B_{12} for growth [8] and oxygen is consumed in its respiration. Therefore, vitamin B_{12} can be determined by the microbial sensor approach with use of immobilized micro-organisms such as *E. coli* 215 and an oxygen electrode. In this study, a rapid electrochemical microbioassay for vitamin B_{12} is described.

EXPERIMENTAL

Materials

Hart infusion agar was purchased from Eiken Chemical Co. Yeast extract was obtained from Difico Laboratories, and vitamin B_{12} from Kanto Chemical Co. Other reagents were commercially available materials of analytical or laboratory grade. Distilled water was used for all procedures.

[a]Present address: Institute of Microbiology, Academia Sinica, Beijing, China.

0003-2670/87/$03.50

Culture of micro-organisms

Escherichia coli 215, donated by Prof. R. Matsuno, Kyoto University, was used for the assay of vitamin B_{12}. It was maintained in Hart infusion agar and transferred to a fresh medium (pH 7.0) containing 0.5% yeast extract, 1% glucose, 0.3% KH_2PO_4, 0.7% K_2HPO_4, 0.05% sodium citrate, 0.05% NaCl and vitamin B_{12} (10 g l^{-1}). The cells were cultivated for 16 h at 30°C. The cells were harvested by centrifugation (8000*g* × 10 min) at 5°C and washed three times with a phosphate buffer (0.1 mol l^{-1}, pH 7.0).

Vitamin B_{12} sensor apparatus

The cells were suspended in phosphate buffer (0.1 mol l^{-1}, pH 7.0) and the cell content was adjusted to an absorbance at 660 nm of 0.48—0.50. The suspension containing 0.5 mg of wet cells was dripped on to a porous acetylcellulose membrane (Millipore type HA, 0.45-μm pore size, 25-mm diameter, 150-μm thickness) with slight suction. The oxygen electrode (Ishikawa Seisakujo Co., Model U-1) consisted of a teflon membrane (12.5-μm thickness), a platinum cathode, a lead anode and sodium hydroxide electrolyte. The porous membrane containing the bacteria was attached to the surface of the teflon membrane of the electrode, and was held in position with an O-ring. The measurement system for vitamin B_{12} is shown in Fig. 1.

Procedures

A portion (25 ml) of double-strength assay medium (pH 7.0) containing 0.1% sodium citrate, 0.2% $(NH_4)_2SO_4$, 0.1% NaCl, 0.6% KH_2PO_4, 1.4% K_2HPO_4 and 1% glucose (all by weight), and 25 ml of a sample solution containing appropriate amounts of vitamin B_{12}, were placed in a beaker as

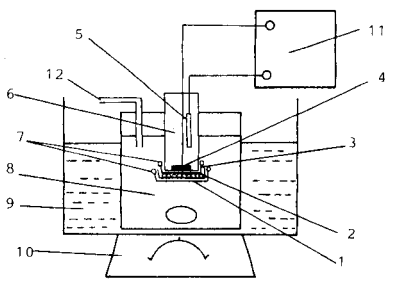

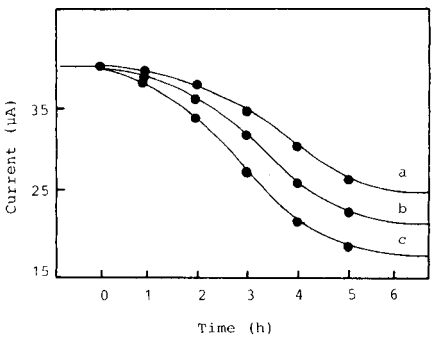

Fig. 1. Schematic diagram of the microbial sensor system: (1) Acetylcellulose membrane; (2) immobilized cells; (3) teflon membrane; (4) cathode (Pt); (5) anode (Pb); (6) electrolyte; (7) O-ring; (8) assay medium; (9) water bath; (10) stirrer; (11) recorder; (12) air.

Fig. 2. Response curves of the sensor for vitamin B_{12} in a pH 7.0 medium at 35°C. The microbial electrode was inserted into the assay medium containing various vitamin B_{12} concentrations: (a) 5 × 10^{-9}; (b) 10 × 10^{-9}; (c) 20 × 10^{-9} g ml^{-1}. (0.5 mg of microbial cells was immobilized on the acetylcellulose membrane.)

measuring cell and incubated at 35°C. The microbial electrode was inserted into the measuring cell (Fig. 1). The electrode current was continuously displayed on a chart recorder (TOA Electronics, Model EPR-200A).

RESULTS AND DISCUSSION

Response of the electrode

Escherichia coli 215 requires vitamin B_{12} for its growth [8], and the sensor functions by monitoring the decrease in dissolved oxygen. Figure 2 shows typical response curves of the sensor at various vitamin B_{12} concentrations. The current at zero time corresponds to the assay medium being saturated with oxygen. This current shows the endogenous respiration level of the immobilized micro-organisms. When the sample solution containing vitamin B_{12} is injected into the system, vitamin B_{12} permeates through the porous membrane and is assimilated by the immobilized micro-organisms. This causes an increased oxygen consumption by the immobilized micro-organisms with a consequent decrease in dissolved oxygen around the membranes. As a result, the sensor current decreases markedly with time until a steady state is reached. The steady state indicates the equilibrium consumption of oxygen by the micro-organisms stimulated by diffusion of vitamin B_{12} from the sample solution. The steady-state currents depend on the concentration of vitamin B_{12}.

The time required for the determination of vitamin B_{12} by the steady-state method, however, is long. Therefore, a rate assay was used for the determinations described here. The rate of current decrease depended on the concentration of vitamin B_{12}.

Influence of glucose concentration. The concentration of glucose used in the assay medium affects the growth of the bacteria and therefore the rate of current decrease. As shown in Table 1, the current decrease increased with an increase in glucose concentration above 1.0%. Thereafter, an assay medium containing 1.0% of glucose was used for the determination of vitamin B_{12}.

Influence of cell content on the calibration graph. The respiration activity of micro-organisms, as measured by the current, is affected by the concentration of *E. coli* cells in the membrane. Therefore, the effect of bacterial concentration on the response of vitamin B_{12} was examined. As shown in Fig. 3, when 0.5 mg of wet cells was used in the sensor, a linear relationship

TABLE 1

Effects of glucose concentration on the response (rate of current decrease) of the vitamin B_{12} sensor[a]

Glucose conc. (% w/v)	0.2	0.5	0.8	1.0	2.0
Rate ($\mu A\ h^{-1}$)	4.0	5.1	5.5	5.8	5.8

[a]Tests conducted with vitamin B_{12} (20×10^{-9} g ml^{-1}), at pH 7.2 and 35°C.

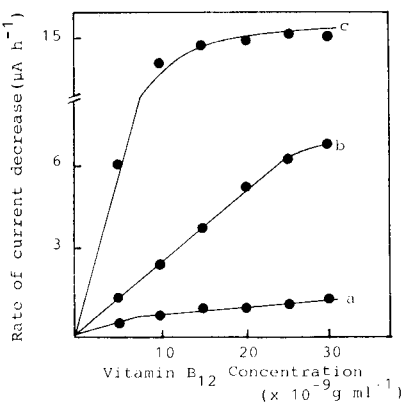

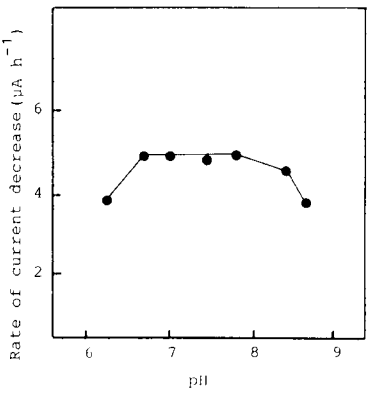

Fig. 3. Effect of membrane cell content on the calibration graphs: (a) 0.2 mg; (b) 0.5 mg; (c) 2 mg (wet cells).

Fig. 4. Effect of pH on response of the sensor for vitamin B_{12} (20×10^{-9} g ml^{-1}). The experimental conditions were the same as for Fig. 3b, except for the pH.

was obtained between the rate of the current decrease and the vitamin B_{12} concentration between 5×10^{-9} and 25×10^{-9} g ml^{-1}. The current decrease increased with increasing initial bacterial cell concentrations. However, the sensitivity was not satisfactory at high initial cell concentrations. Therefore, a membrane containing 0.5 mg of absorbed wet cells was employed for the electrode.

Influence of pH and temperature. The influences of pH and temperature on the microbial electrode were examined because these factors affect the respiration activity of micro-organisms. A standard solution of vitamin B_{12} (20×10^{-9} g ml^{-1}) was used for these experiments. As shown in Fig. 4, the rate of current decrease reached a plateau between pH 6.7 and 7.8. Therefore, a phosphate buffer of pH 7.0 was employed for further studies.

With regard to the influence of temperature on the current output of the microbial electrode, the amount of dissolved oxygen in the phosphate buffer solution decreases with increasing temperature. Therefore, the results were corrected for dissolved oxygen content at various temperatures. As shown in Fig. 5, the rate of current decrease of the microbial electrode was almost constant from 28°C to 39°C. However, the rate of current decrease decreased for temperatures above 39°C because of the thermal inactivation of the enzymes in the bacteria. The low rate of current decrease occurring below 28°C may be attributed to the relatively dormant state of the bacteria in the membrane.

Re-usability of the microbial electrode

Figure 6 shows the long-term stability of the microbial sensor. Stable responses to the standard solution (vitamin B_{12}; 20×10^{-9} g ml^{-1}) were observed for 25 days when the immobilized bacteria membrane was stored

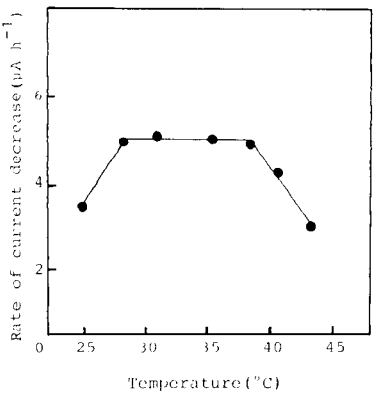

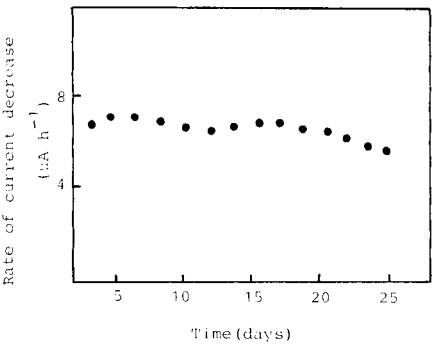

Fig. 5. Effect of temperature on the response of the sensor. The assay medium was kept at pH 7.2 and the current was measured for a bioassay time of 2 h. A vitamin B_{12} level of 20×10^{-9} g ml^{-1} and 0.5 mg of wet cells were employed.

Fig. 6. Time stability of the sensor; the current was measured at 35°C and pH 7.0 for a vitamin B_{12} level of 20×10^{-9} g ml^{-1}.

at −25°C. During this period, the decrease in the response of the sensor was about 8%. The microbial electrode could therefore be used for a relatively long time for the determination of vitamin B_{12}.

As many bacteria require specific compounds for their growth, it follows that the bioassay of amino acids, vitamins and antibiotics is possible by using appropriate bacteria. Generally, microbioassays of such biologically active materials are done by turbidimetric and titrimetric methods. These methods, however, require a lengthy incubation with the bacteria [3].

In this study, a rapid electrochemical microbioassay for vitamin B_{12} is proposed. The rate of current decrease depends on the concentration of vitamin B_{12} in the sample solution, and vitamin B_{12} below 25×10^{-9} g ml^{-1} may be determined directly from the current decrease. The bioassay can be completed within 2 h. This general method can undoubtedly be extended to the determination of other vitamins and amino acids produced by bacterial metabolism.

The authors are grateful to Prof. R. Matsuno, Kyoto University, for his kind gift of the bacterial strain.

REFERENCES

1 H. R. Skeggs, in P. Gyorgy and W. N. Pearson (Eds.), The Vitamins — Chemistry, Physiology, Pathology, Methods, Vol. 7, Academic, New York, 1967, p. 277.
2 D. L. Mollin, B. B. Anderson and J. F. Burman, Clin. Haematol., 5 (1976) 521.
3 T. M. Berg and H. A. Behagen, Appl. Microbiol., 23 (1972) 531.
4 I. Karube, T. Matsunaga and S. Suzuki, Anal. Chim. Acta, 109 (1979) 39.
5 I. Karube, T. Matsunaga, N. Teraoka and S. Suzuki, Anal. Chim. Acta, 119 (1980) 271.
6 T. Matsunaga, I. Karube, N. Teraoka and S. Suzuki, Anal. Chim. Acta, 127 (1981) 245.
7 T. Matsunaga, I. Karube and S. Suzuki, Anal. Chim. Acta, 98 (1978) 25.
8 T. Kamikubo, Vitamins, 11 (1956) 43.

Analytica Chimica Acta, 199 (1987) 99—109
Elsevier Science Publishers B.V., Amsterdam — Printed in The Netherlands

DESCRIPTIONS OF MOLECULAR SHAPE APPLIED IN STUDIES OF STRUCTURE/ACTIVITY AND STRUCTURE/PROPERTY RELATIONSHIPS

ROBERT H. ROHRBAUGH and PETER C. JURS*

152 Davey Laboratory, Department of Chemistry, The Pennsylvania State University, University Park, PA 16802 (U.S.A.)

(Received 23rd February 1987)

SUMMARY

Three-dimensional molecular shape is often an important determinant of the physicochemical properties or biological activities of chemical compounds. A set of six descriptors that code the shapes of molecules by calculating the areas of three orthogonal projections is developed. The descriptors are applied to a series of tests of their applicability on diverse problems in studies of structure/activity and structure/property relationships. Correlation of these descriptors with the physicochemical properties of several sets of compounds, and with biological activity values for several sets of compounds, shows that the indexes contain much information about molecular shape.

Structure/activity and structure/property relations have been widely reported in recent years [1—6]. In many cases, the biological activity or physicochemical property of interest is related to the three-dimensional shape of the tested compounds. Numerically encoding the three-dimensional shape of a chemical compound is a difficult task which may be approached in several ways.

One way to represent three-dimensional shape is to use a set of indexes, each of which encodes a certain aspect of the overall shape of the molecule. In some instances, this may be preferable to using a single index description of shape. By decomposing the overall description of shape into several complementary aspects, unnecessary information which may otherwise obscure the truly useful information is eliminated.

A second method used to encode shape information involves the use of steric substituent constants. These constants are designed to encode the structural differences between compounds of a congeneric series in order to seek correlations with differential reactivity. One of the first steric parameters to be widely utilized was Taft's steric substituent parameter, E_s, which was based on kinetic data for acid hydrolysis of esters [7]. Others have reported modified versions of Taft's approach [8, 9]. Verloop et al. [10] have also developed a set of substituent constants known as STERIMOL parameters, which represent the steric dimensions of the substituent with respect to the axis of connection to the parent compound.

0003-2670/87/$03.50

A third commonly used approach to the representation of shape information is to compare the shape of the test compound to that of a standard compound. The standard compound is usually defined as the structure with the highest observed activity. The shape of the standard compound is assumed to mirror the shape of the receptor cavity involved. Each test compound is compared to the standard based on some criterion, and the differences are used as a measure of dissimilarity. The degree to which a test compound is dissimilar to the standard is then used to aid in generating a quantitative description of the activity of the compound. Shape-descriptive methods which are based on such comparisons include the minimum topological difference [11], minimum steric difference [12], investigated receptor site [13], and molecular shape analysis [14].

DESCRIPTION OF METHOD

The shape parameters presented here are of the multiple-index type. Six indexes are calculated, including three parameters to encode information about three mutually perpendicular perspectives of the compound, and three normalized indexes. These parameters are related to Amoore's approach to describing molecular shape by using orthogonal projections [15].

The indexes are calculated by using a two-dimensional version of the point-encoded algorithm described by Stouch and Jurs [16]. In order to perform the calculations, the three-dimensional atomic coordinates of the compound must be available. These coordinates are usually calculated by using molecular mechanics methods [1, 17]. Once the molecular geometry has been defined, the structure is oriented in three-dimensional space according to some well-defined criterion. The molecule is then viewed from three orthogonal directions defined by the X, Y, and Z coordinate axes. For each perspective, the coordinates are compressed into the plane defined by the remaining two axes. For the perspective along the Z axis, the Z coordinates would be disregarded and the molecule projected onto the X/Y plane. A simple analogy, from which the name was derived, would be to obtain the shadow which results from directing parallel rays of light along the axis of perspective. The area of this projection will be used as an index of molecular shape.

The first index calculated is the area of the shadow of the molecule projected on a plane defined by the X and Y axes ($S1$). The second index is the area projected onto the Y-Z plane ($S2$), and the third index is the area projected onto the X-Z plane ($S3$). Figure 1A illustrates this process for toluene. Each area is also normalized by dividing the index by the area of the rectangle defined by the maximum dimensions of the projection on the plane ($S4$, $S5$, and $S6$). The six indexes for toluene are illustrated in Fig. 1B.

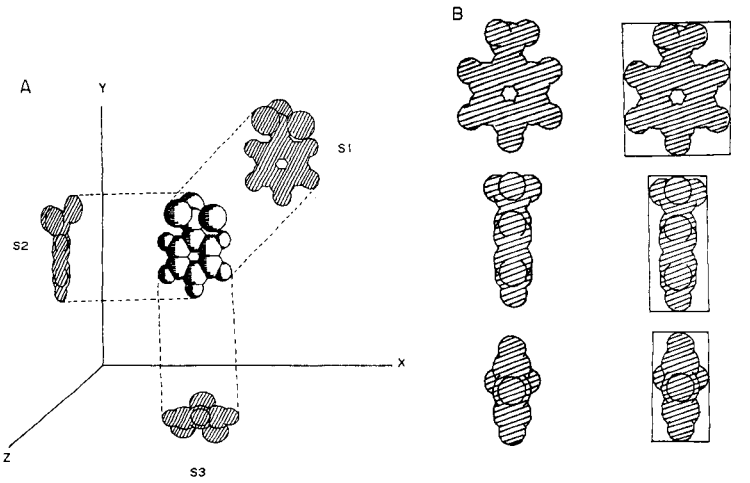

Fig. 1. (A) Illustration of the calculation of shadow areas for toluene. (B) The six shadow areas for toluene: left-hand column shows $S1$, $S2$, and $S3$; right-hand column shows $S4$, $S5$, and $S6$.

Calculation

The actual calculation of the areas is achieved by assembling a grid of an arbitrary density (e.g., five divisions/linear Å). This grid is placed over the shadow of interest, as shown in Fig. 2. The size of the grid is determined from the maximum dimensions of the molecule. The grid is constructed to fit as tightly as possible around the shadow in order to eliminate unnecessary calculations. Next, the grid is scanned and each intersection is checked to see if it is within the van der Waals radius of any of the atoms in the molecule. This method assumes that the atoms of the molecule are rigid spheres with the van der Waals radii listed in Table 1. If the point is within the van der Waals radius of any atom, then that intersection is considered to be inside the shadow. The running sum of intersections inside the shadow is kept, and the total is divided by the square of the grid density. The resulting number gives an accurate approximation of the area of the projection.

After the first shadow area ($S1$) has been calculated, the molecule is rotated about the X axis by 90 degrees. The grid is resized and placed over the new projection. The grid is again scanned and the second area ($S2$) calculated. The third index ($S3$) is calculated by additionally rotating the molecule about the Y axis by 90° and scanning the resultant projection. The normalized indexes ($S4$—$S6$) are calculated at each step by dividing the shadow area by the total area defined by the maximum dimensions of the molecule.

Substituent shadow areas are calculated in a similar manner. The structure of the substituent is entered with a marker indicating the R-group of the compound. When the grid is scanned, a radius of zero is assigned to the

TABLE 1

Van der Waals radii

Atom type	Radius (Å)	Atom type	Radius (Å)
C (sp^3)	1.70	N (sp)	1.60
C (sp^2)	1.70	N (aromatic)	1.60
C (sp)	1.77	S (singly bonded)	1.80
C (allenyl)	1.70	S (doubly bonded)	1.80
C (aromatic)	1.77	F	1.50
O (singly bonded)	1.52	Cl	1.75
O (doubly bonded)	1.50	Br	1.85
N (sp^3)	1.55	I	1.97
N (sp^2)	1.55		

R-group of the compound. In this manner, only the area associated with the substituent is calculated.

An obvious determinant of the utility of this method is the proper choice of an initial starting orientation. In order to compare similar molecules, a standard orientation must be defined. For most cases presented in this paper, this orientation was defined to be the molecule situated such that its first and second largest moments of inertia were aligned with the X and Y axes, respectively. In many cases, however, another configuration may be more descriptive of the property of interest. It is for this reason that the indexes were designed so that orientation could be tailored to the specific problem being investigated. Some examples of alternative orientations would be to align a certain substructural unit or functional group with the axes, or to align the molecule with respect to some electronic property (e.g., dipole moments).

The effect of different initial orientations on the values calculated for the shadow areas was assessed using two separate methods. First, shadow areas were calculated for three structurally different sets of compounds: 143 polynuclear aromatic hydrocarbons, 86 simple olefins, and 201 *N*-nitroso compounds. For each set of compounds, the shadow areas were calculated for two different orientations, and the correlations between the two series of shadow areas were examined. The results are given in Table 2. The correlations obtained demonstrate that the shadow-area values are strongly dependent on the initial orientation used.

Secondly, shadow areas for toluene were calculated for the molecule in fifty systematically varied orientations. The relative standard deviation to the mean was 16% for $S1$, 23% for $S2$, and 20% for $S3$. The high relative standard deviations indicate the dependence of the shadow areas on the initial orientation.

The effect of grid density on the calculation was also examined. The studies showed that a grid density of approximately five divisions per linear Å

TABLE 2

Simple, pairwise correlations of shadow areas for polynuclear aromatic hydrocarbons (PAHs), olefins, and *N*-nitroso compounds using two different orientations

	PAHs[a]	Olefins[b]	*N*-Nitroso compounds[c]
*S*1	0.999	0.987	0.978
*S*2	0.691	0.925	0.815
*S*3	0.634	0.575	0.680
*S*4	0.757	0.001	0.447
*S*5	0.985	0.828	0.511
*S*6	0.985	0.602	0.460

[a]Moments-of-inertia orientation and orientation in which PAH is in position of maximum length-to-breadth ratio. [b]Moments-of-inertia orientation and orientation in which double bond and largest substituent on double bond are in *X*/*Y* plane. [c]Moments-of-inertia orientation and orientation in which *N*-nitroso group is in the *X*/*Y* plane.

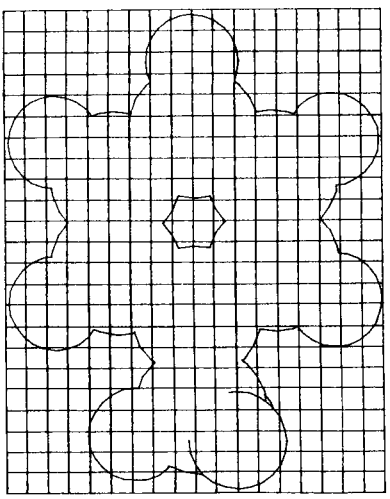

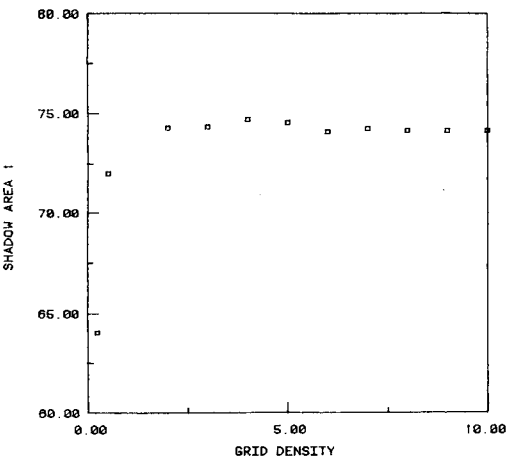

Fig. 2. Calculation of shadow areas using grid.

Fig. 3. Shadow area 1 (*S*1) vs. grid density for pyrene. *S*1 is given in Å^2. Grid density is given in units of division per Å.

is sufficient to calculate an accurate area. Using higher densities results in an increase in calculation time, without a proportional increase in accuracy. Figure 3 shows a plot of calculated shadow area (*S*1) versus grid density for pyrene. The plot shows the calculated area leveling off rapidly at a density of approximately three to four divisions per linear Å.

All computations reported here were performed on the Penn State Chemistry Department's PRIME 750 computer. The ADAPT software system [1]

was used for structure entry and modeling, descriptor generation, data analysis, and graphic output.

APPLICATIONS

Structure/property studies

Olefins. Shadow areas were calculated by using both the moment-of-inertia orientation and a user-defined orientation for 86 olefins taken from earlier work [18]. The user-defined orientation involved placing the two carbons of the double bond and the first carbon of the largest substituent on the double bond in the X/Y plane. The shadow areas were correlated with several physical properties (some experimental, some calculated) for the 86 olefins. The experimental properties used included boiling point and gas-chromatographic retention indexes [18]. Various physicochemical properties were calculated, including molecular surface area and volume, moments of inertia, logarithm of the partition coefficient, log P, molecular connectivities, and molar refraction. Molecular surface area and volume were calculated by using Pearlman's algorithm [19]. The three molecular moments of inertia were calculated by using the moment of inertia tensor [20]. These numbers can give information regarding the extent of the molecule. The logarithmic partition coefficient (log P) of the compound between octanol and water was calculated by using the fragment addition method of Hansch and Leo [21]. This value is a measure of the hydrophobicity of the compound. Molecular connectivities (X), as reported by Randić [22] and later by Kier and Hall [23], were calculated. These indexes are based on graph theory and encode only topological information about the compounds. Finally, molar refraction was calculated by using the fragment addition method reported by Vogel [24]. All the properties studied can be loosely classified as bulk property descriptors. Table 3 gives the results of the correlation analysis.

The high correlations obtained indicate that the shadow areas contain information regarding the bulk properties of the olefins. These include not only size (surface area, volume, and moment of inertia), but also electronic (total sigma charge and molar refraction) and topological (molecular connectivities) information. It is important to note that although the correlations are similar for both orientations, the numbers and types of indexes used to obtain these correlations are different.

N-Nitroso compounds. *N*-Nitroso compounds represent a well studied class of chemical carcinogens. Shadow areas were calculated for 201 *N*-nitroso compounds [25, 26]. The moment-of-inertia orientation and an orientation defined by aligning the *N*-nitroso group in the X/Y plane were used. The shadow areas were tested for correlations with the same physical properties as described above. High correlations (>0.90) were obtained for molecular polarizability, molecular connectivities, molecular volume, and molar refraction. As with the olefins, the information contained in the shadow indexes correlates well with size, electronic and topological information.

TABLE 3

Correlations of shadow areas with other structural descriptors for 86 olefins

Descriptor	Mom. inertia orientation		Double bond orientation	
	Terms used[a]	Correlation	Terms used	Correlation
Kovats' retention index	1, 2, 3, 6	0.90	1, 2, 6	0.92
Boiling point	1, 2, 3, 6	0.91	1, 3, 6	0.93
Molar refraction	1, 2, 3, 4, 5, 6	0.98	1, 2, 3, 4, 6	0.98
Volume	1, 2, 3, 4, 5, 6	0.99	1, 2, 3, 4, 6	0.99
Total sigma charge			1, 2, 3	0.95
First moment of inertia	1, 2, 3, 4, 6	0.96	1, 2, 4, 5, 6	0.95
Second moment of inertia	1, 2, 3, 4, 5	0.96		
Log P	1, 2, 3	0.90	1, 2, 3	0.99
X_0	1, 2, 3, 4, 5	0.95	1, 2, 3, 4	0.97
X_1			1, 2, 3	0.96
Surface area	1, 2, 3, 5, 6	0.99	1, 2, 3, 4	0.99

[a] 1 = $S1$, 2 = $S2$, 3 = $S3$, 4 = $S4$, 5 = $S5$, 6 = $S6$.

Volume correlation. The area of each projection ($S1$, $S2$, $S3$) can be viewed as being the area of a rectangle with dimensions of $1 \times w$, $1 \times h$, and $h \times w$, respectively. The square root of the product of the three areas yields the volume of a box with dimensions $1 \times w \times h$ (Fig. 4). This value was tested for correlation with the molecular volume as calculated using Pearlman's algorithm [19] on several diverse classes of compounds. The results are given in Table 4. The values calculated correlate highly with the molecular volume, despite the obvious simplifications made in the calculation.

It was also noted that this value was less sensitive to the initial orientation of the structure. Using 50 different orientations for toluene, a relative standard deviation to the mean of only 6% was observed for the square root of the product of $S1$, $S2$, and $S3$. This value is significantly lower than the relative standard deviations reported earlier for the individual shadow areas.

Pitzer's acentric factor. Shadow areas were calculated for a set of 60 hydrocarbons for which Pitzer's acentric factors have been reported [27]. The acentric factor (AF) is related to the vapor pressure of the compound in the following manner:

$$AF = -\log (P'_R) - 1.00$$

where P'_R is the reduced vapor pressure at the reduced temperature. In theory, the acentric factor is related to the spherical symmetry of a molecule [28]. In this sense, it is to a degree a measure of one aspect of the shape of a compound.

The following equation was developed which relates the acentric factor to several shadow areas:

$$AF = 0.0051(S1) + 0.0040(S2) - 0.069$$

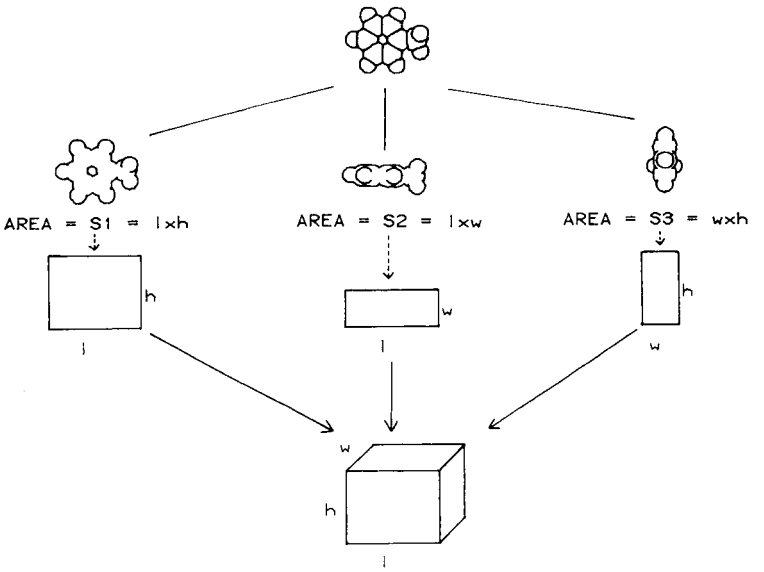

Fig. 4. Example of molecular volume calculation.

TABLE 4

Correlations of volume and shadow areas

	Correlation	Orientation
Olefins		
Mom. orient.	0.91	
User orient.	0.96	C=C—R in *X*-*Y* plane, R = largest subst.
N-*Nitroso compounds*		
Mom. orient.	0.97	
User orient.	0.96	N—N=O moiety in *X*-*Y* plane
PAHs		
Mom. orient.	0.96	
User orient.	0.95	L/B orientation

The statistics found, $r = 0.95$, $F = 241$, $n = 60$ and $s = 0.045$, indicate that the shadow areas are collectively encoding information similar to that found in the acentric factor (i.e., shape information).

Structure/activity studies

Taft steric parameters. The shadow areas of 19 alkyl substituents were calculated and used to estimate the corresponding E_s parameter. Taft's parameter, E_s, is a measure of the effect that a substituent has on the rate of the hydrolysis of ethyl esters. The parameter is based on the assumption that the acid hydrolysis of the esters is affected only by the steric characteristics

of the substituent, and that all other effects are minor. The substituents used were obtained from Taft [7]. The alkyl groups were chosen in order to minimize any contribution to the parameter from electronic effects. The following equation relating E_s to shadow areas was obtained:

$$E_s = 0.14(S3) - 2.12$$

for which the statistics were $r = 0.88$, $F = 56$, $n = 18$ and $s = 0.48$. The correlation is fairly high, indicating that the shadow areas contain information similar to the E_s parameters for the tested alkyl substituents.

Benzimidazole derivatives. Previous studies of the displacement of dihydrosafrole metabolite from its complex with cytochrome P-450 using benzimidazole derivatives have suggested that the mechanism is shape/size sensitive [29]. Shadow areas were calculated for 21 benzimidazole derivatives and also for the substituents which distinguish the derivatives. These values were then used to predict the activity of the compound. The activity is measured as the negative logarithm of the rate of displacement. Two separate regression analyses were done. The first regression used the shadow areas of the molecule, and the following equation was obtained:

$$-\log (\text{rate}) = -0.034(S1) - 0.015(S2) - 1.84(S5) + 6.93$$

for which $r = 0.96$, $F = 67$, $n = 21$ and $s = 0.17$.

The second equation was developed by using the shadow areas of the substituents. A similar equation was obtained:

$$-\log (\text{rate}) = -0.036(S1) - 2.06(S5) + 0.010(S2) + 5.33$$

for which $r = 0.96$, $F = 63$, $n = 21$ and $s = 0.17$. In each case, an equation was developed which accurately describes the variance observed in the activity data. The standard deviations of the regressions are less than 10% of the activity values used, indicating a good fit.

Structure/taste. Twenty compounds previously investigated by Iwamura for taste potency were studied [30]. The compounds were derivatives of 3-nitroaniline (6-substituted) and 3-cyanoaniline (6-substituted). Shadow areas were calculated and used to estimate the sweet taste intensity ($\log A$) of the compounds. An orientation was used such that the aromatic ring was in the X/Y plane. The following relationship was developed:

$$\log A = 0.17(S1) + 9.28(S4) - 0.11(S3) - 9.47$$

for which $r = 0.97$, $F = 84$, $n = 20$ and $s = 0.18$. The regression model has a high multiple correlation coefficient, a significant F-statistic and a low standard deviation. Iwamura's best equation using STERIMOL parameters was a two-variable equation with $r = 0.90$ and $s = 0.32$. For this set of compounds the shadow area parameters have provided a better model for estimation of a measured property than the STERIMOL parameters.

DISCUSSION

As demonstrated by the examples above, the shadow-area shape indexes do contain information which can be useful in a variety of applications of structure/property and structure/activity relationships. The correlations obtained in the study with olefins and *N*-nitroso compounds show that the shadow areas include information about the bulk properties of compounds. In addition, the relationships developed between the shadow areas and Taft's E_s parameter, Pitzer's acentric factor, and molecular volume suggest that there is indeed shape-related information present in the new parameters. Finally, the structure/activity relationships developed using the shadow areas for the benzimidazole derivative and for taste potency illustrate the potential of applications of the shadow areas to real-world problems.

The indexes developed have also been demonstrated to be useful as both molecular and substituent descriptors. This method could be adapted to be a shape-similarity measure by comparing the three projections of two molecules and calculating the overlap area of each projection.

Despite the excellent results obtained, there are several problems still to be addressed. For example, which initial orientation to use is not always obvious. Additional schemes for aligning the compounds may be developed based on existing knowledge of the system being studied. Also, further studies are needed on the applicability to other types of compounds and other types of chemical properties and activities.

It should be noted that these parameters are developed under the assumption of a rigid molecular structure. In most cases, this is an invalid assumption because chemical compounds exhibit dynamic behavior. In addition, the method presumes that atoms can accurately be described as hard spheres. Again, this is a simplification which may cause problems in interpreting the parameters. For these reasons, care should be used when determining the suitability and reliability of these or any numbers based on these assumptions. However, the above-mentioned drawbacks are inherent in any attempt to describe the three-dimensional geometry of a molecule, and until a simple alternative approach can be developed, such methods will no doubt continue to be used.

Conclusions

The set of six new shape parameters called shadow areas developed for use in structure/activity and structure/property relationship studies encode the information contained in three mutually perpendicular perspectives. With the flexibility to define the orientation of importance, the ability to be used as molecular or substituent parameters, and the potential to be used comparatively, these parameters have been shown to be useful in a variety of applications. Future work will be aimed at expanding these applications, studying alternative orientation schemes, and testing the limitations of the parameters.

REFERENCES

1 A. J. Stuper, W. E. Brugger and P. C. Jurs, Computer-Assisted Studies of Chemical Structure and Biological Function, Wiley-Interscience, New York, 1979.
2 Y. C. Martin, Quantitative Drug Design. A Critical Introduction, M. Dekker, 1978.
3 E. C. Olson and R. E. Christofferson (Eds.), Computer-Assisted Drug Design, ACS Symp. Ser. 112, American Chemical Society, Washington, DC, 1979.
4 E. J. Ariens (Ed.), Drug Design, Vol. IX, Academic, New York, 1980.
5 L. Golberg (Ed.), Structure-Activity Correlation as a Predictive Tool in Toxicology, Hemisphere, Washington, DC, 1983.
6 J. K. Seydel (Ed.), QSAR and Strategies in the Design of Bioactive Compounds, VCH, Deerfield Beach, FL, 1985.
7 R. W. Taft, in M. S. Newman (Ed.), Steric Effects in Organic Chemistry, Wiley, New York, 1956, pp. 556—675.
8 C. K. Hancock, E. A. Myers and B. J. Yager, J. Am. Chem. Soc., 83 (1961) 4211.
9 S. H. Unger and C. Hansch, Prog. Phys. Org. Chem., 12 (1976) 91.
10 A. Verloop, W. Hoogenstraaten and J. Tipker, in J. Ariens (Ed.), Drug Design, Academic, New York, 1976, pp. 165—207.
11 A. T. Balaban, A. Chiriac, I. Motoc and Z. Simon, in G. Berthier, M. J. S. Dewar, H. Fischer, K. Fukui, G. G. Hall, H. Hartman, H. H. Jaffé, J. Jortner, W. Kutzelnigg, K. Ruedenberg and E. Scrocco (Eds.), Lecture Notes in Chemistry, Vol. 15, Springer, Berlin, 1980.
12 Z. Simon, A. Chiriac, I. Motoc, S. Holban, D. Ciubotaru and Z. Szabadai, Stud. Biophys., 55 (1976) 217.
13 I. Motoc, Z. Naturforsch., Teil A, 38 (1983) 1342.
14 A. J. Hopfinger, J. Am. Chem. Soc., 102 (1980) 7196.
15 J. E. Amoore, Cold Spring Harbor Symp. Quant. Biol., 30 (1965) 623.
16 T. R. Stouch and P. C. Jurs, J. Chem. Inf. Comp. Sci., 26(1) (1986) 4.
17 N. L. Allinger and Y. H. Yuh, Molecular Mechanics, Operating Instructions for MM2 and MMP2 Programs, 1977 Force Field, Quantum Chemistry Program Exchange, QCPE Program No. 395, 1980.
18 R. H. Rohrbaugh and P. C. Jurs, Anal. Chem., 57 (1985) 2770.
19 R. S. Pearlman, in S. H. Yalkowsky, A. A. Sinkula and S. C. Valvani (Eds.), Physical Chemical Properties of Drugs, M. Dekker, New York, 1980, pp. 321—347.
20 H. Goldstein, Classical Mechanics, Addison-Wesley, Cambridge, MA, 1950, pp. 146—156.
21 C. Hansch and A. Leo, Substituent Constants for Correlation Analysis in Chemistry and Biology, Wiley-Interscience, New York, 1979, pp. 18—43.
22 M. Randić, J. Am. Chem. Soc., 97 (1975) 6604.
23 L. B. Kier and L. H. Hall, Molecular Connectivity in Chemistry and Drug Research, Academic, New York, 1976.
24 A. I. Vogel, Elementary Practical Organic Chemistry, Part 2: Qualitative Organic Analysis, Wiley, New York, 1966, pp. 24—25.
25 W. Lijinsky, in T. K. Rao, W. Lijinsky and J. L. Epler (Eds.), Genotoxicology of *N*-Nitroso Compounds, Plenum, New York, 1984, Chaps. 1, 10.
26 R. Preussmann and B. W. Stewart, in C. E. Searle (Ed.), Chemical Carcinogens, 2nd edn., American Chemical Society, Washington, DC, 1984, Chap. 12.
27 C. A. Passut and R. P. Danner, Ind. Eng. Chem. Process Des. Dev., 12 (1973) 365.
28 K. S. Pitzer, J. Am. Chem. Soc., 77 (1955) 3427.
29 M. Murray, C. B. Marcus and C. F. Wilkinson, Quant. Struct. Activity Relat., 4 (1985) 19.
30 H. Iwamura, J. Med. Chem., 23 (1980) 208.

Analytica Chimica Acta, 199 (1987) 111—118
Elsevier Science Publishers B.V., Amsterdam — Printed in The Netherlands

LASER-EXCITED IONIC FLUORESCENCE SPECTROMETRY OF RARE-EARTH ELEMENTS IN THE INDUCTIVELY-COUPLED PLASMA

M. E. TREMBLAY, B. W. SMITH and J. D. WINEFORDNER*
Department of Chemistry, University of Florida, Gainesville, FL 32611 (U.S.A.)
(Received 6th May 1987)

SUMMARY

A pulsed tunable dye laser pumped with an excimer laser is used to excite ionic fluorescence of the rare earth elements in the inductively-coupled plasma. Because several fluorescence lines were observed after laser excitation, it was possible to draw partial energy-level diagrams for most of the rare earths. Non-resonance fluorescence lines were used for all measurements in order to minimize spectral interferences. Detection limits at given excitation wavelengths are reported for each element. Laser-excited ionic fluorescence eliminates the problem of spectral interferences which has been associated with the determination of the rare earths by atomic emission spectrometry in the inductively-coupled plasma.

Several researchers have used the technique of inductively-coupled plasma emission spectrometry (ICP/ES) for the determination of the rare earths [1—6]. However, because of the complex characteristics of emission spectra of rare earths in ICP/ES, it can be difficult to determine trace concentrations of one rare earth in the presence of a complex mixture of the others. In order to minimize spectral interferences caused by high concentrations of matrix elements such as yttrium, calcium and iron in ICP/ES, it is often necessary to isolate the rare earth prior to its determination by emission spectrometry. Several procedures based on chemical separation [1, 2] and ion exchange [2, 3] have been reported for the separation of these elements. However, such procedures can be time-consuming and can also introduce error through contamination.

Although the emission of the rare earth in the ICP has been amply described, the ionic fluorescence characteristics of the rare earth in the ICP have never been reported to our knowledge. This paper reports on the ionic fluorescence of the rare earth elements by pulsed dye laser excitation in the ICP. Because of the striking simplicity of the rare earth fluorescence spectra, which results from narrow-bandwidth dye-laser excitation, it is possible to reduce greatly or even eliminate spectral interferences in a mixture of all the rare earths. It should also be possible to measure the rare earth concentrations without prior separation from other elements present in the sample.

This report includes several different fluorescence processes for the rare earths which include: resonance fluorescence, Stokes direct line fluorescence,

0003-2670/87/$03.50

anti-Stokes direct line fluorescence, Stokes stepwise fluorescence, and anti-Stokes stepwise fluorescence. These various fluorescence processes have been explained in detail by Omenetto and Winefordner [7]. The use of non-resonance fluorescence eliminates any source scatter problem which is primarily reserved for resonance fluorescence, and permits freedom from spectral line interferences.

EXPERIMENTAL

Reagents

All standard stock solutions of rare earths were prepared by dissolving an appropriate amount of the rare earth oxide (Spex Industries) in a minimal volume (3—5 ml) of hot hydrochloric acid and then adding enough water to make 100 ml of 1000 μg ml^{-1} solution [8]. Working standards were made by serial dilution of the stock solutions.

Lasers

Excimer laser. The dye pumping source in the set-up is a rare-gas halide excimer laser (Model TE-861-S; Lumonics, Ontario, Canada) operated with XeCl at 308 nm. A maximum energy output of 60 mJ per pulse was obtained at a repetition rate of 25 Hz. The laser-beam energy was monitored before each measurement with a power meter (Model 380105 Scientech, Boulder, CO).

Dye laser. A frequency-doubled (KDP) tunable dye laser (Model EDP-330; Lumonics) was used to cover the desired spectral range. 4,4′-Diphenylstilbene (DPS) dye in dioxane allowed tunability between 396 and 418 nm, while Rhodamine (R610) in methanol with frequency doubling allowed tunability between 297 and 308 nm. Wavelength selection was done with an automatic scanning unit (Compuscan, Lumonics, Model EDP-60).

Instrumentation

The ICP was a standard 27-MHz commercial model (Model HFP-1500 Plasma Therm, Kresson, NJ). Typical operating parameters were: incident power of 0.6—1 kW, plasma support argon gas flow rate 12—15 l min^{-1}, auxiliary argon gas flow rate of 0.5—1.1 l min^{-1}, and viewing height above the load coil 15 mm. A concentric nebulizer (Meinhard, Santa Ana, CA) with a nebulizing gas pressure of 32 psig produced a solution uptake of 1.1 l min^{-1}. The diameter of the dye laser in the plasma was approximately 3 mm.

The resulting fluorescence from the laser-irradiated volume was focused as a 1:1 image on the entrance slit of the 0.35-m monochromator (Heath, Benton, Harbor, MI). A 3-mm slit height and a 150-μm slit width were used. Neutral density filters were used to increase the linear dynamic range. A photomultiplier tube (PMT; R928; Hamamatsu) was used to measure the fluorescent radiation. The output of the PMT was terminated with a 1000-ohm load resistor and fed into a gated integrator and boxcar averager

(Model SR-250; Stanford Research System, Palo Alto, CA) which was triggered by a photodiode positioned to collect a portion of the laser radiation. The gate width was set at 200 ns and the gate delay at 34 ns. The output signals of the gated integrator and boxcar averager were displayed on a chart recorder and measured with a personal computer. A block diagram of the experimental system is shown in Fig. 1.

RESULTS AND DISCUSSION

Laser-excited atomic and ionic fluorescence of several elements is possible in the ICP [9—12]. However, there seem to be no reports of laser-excited fluorescence of rare earths.

Calibration curves were constructed for the laser-excited ionic fluorescence of all the rare earths except for promethium and samarium, which were not available, and holmium because no ionic fluorescence was detected for this element. The calibration curves are not given for all the rare earths, but the detection limits are reported in Table 1. All measurements were obtained at non-resonance fluorescence lines. The use of non-resonance instead of resonance fluorescence resulted in a decrease in the detection limit by a factor of up to 10-fold primarily because of the minimization of scattered radiation from the source. The detection limit is defined as 3 times the standard deviation of the blank solution (water) divided by the sensitivity (the slope of the calibration plot). The standard deviation was evaluated by

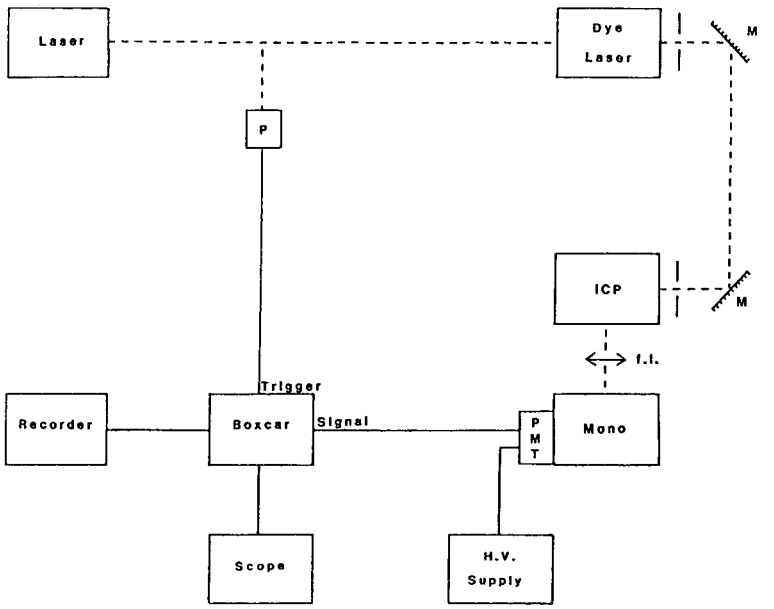

Fig. 1. Block diagram of experimental system for laser-excited ionic fluorescence of the rare-earth elements in the inductively-coupled plasma.

TABLE 1

Fluorescence transitions and detection limits for the rare earth elements in the inductively-coupled plasma

Rare Earth element	Excitation wavelength (transition, cm^{-1})[a]	Fluorescence wavelength (nm) (transition, cm^{-1})[a]	Fluorescence process	Detection limit (ng ml^{-1})	Detection limit by ICP/ES (ng ml^{-1})[b]
La	403.169 (2592—27388)	379.083 (1016—27388)	AS-DLF[c]	170	10
Dy	407.798 (828—25343)	394.470 (0—25343)	AS-DLF[c]	400	10
Gd	407.844 (4841—29353)	354.580 (1159—29353)	AS-DLF[c]	75	14
Ce	407.585 (4911—29439)	401.239 (4523—29439)	AS-DLF[c]	400	48
Er	404.835 (7150—31844)	374.265 (5133—31844)	AS-DLF[c]	260	10
Nd	406.109 (3802—28419)	428.452 (5086—28419)	S-DLF[d]	470	50
Pr	406.134 (5108—29724)	405.654 (5079—29724)	AS-DLF[c]	240	37
Tb[g]	403.306 (?)	400.557 (?)	?	650	23
Lu	302.054 (12435—45532)	296.332 (11796—45532)	AS-DLF[c]	85	1.0
Tm	301.530 (237—33392)	313.136 (0—31927)	S-SWF[e]	140	5.2
Yb	303.111 (0—32982)	297.056 (0—33654)	AS-SWF[f]	25	1.8
Eu	305.494 (1669—34394)	290.668 (0—34394)	AS-DLF[c]	72	2.7

[a]Energy levels in cm^{-1}; the numbers in parentheses are the lower and upper levels. [b]From Winge et al. [6]. [c]Anti-Stokes direct line fluorescence. [d]Stokes direct line fluorescence. [e]Stokes stepwise fluorescence. [f]Anti-Stokes stepwise fluorescence. [g]Energy levels were not identified for Tb.

collecting 1000 data points at 25 Hz with a personal computer. The high spectral selectivity is evident because the blank signal was the same whether water or a 100 μg ml^{-1} solution of all other rare earths was aspirated into the plasma.

In most cases, the sensitivity of the Stokes or anti-Stokes direct line fluorescence exceeds that of the Stokes or anti-Stokes stepwise fluorescence. Even though the direct line fluorescence signals were usually more intense than the stepwise fluorescence signals, collisional activation/deactivation caused several stepwise fluorescence signals to be intense. The dominant factor which affects the sensitivity of either direct line or stepwise fluorescence process appeared to be the transition probability of the fluorescence line. The results given in Table 1 indicate that for all rare earths, the limits of

detection for ionic fluorescence are approximately 10 times worse than the best values reported for ICP/ES [6] with a pneumatic nebulizer.

In all measurements, no spectral interference occurred when 100 $\mu g\ ml^{-1}$ of each of the rare earths were measured together. In conventional ICP/ES, spectral interferences in mixtures of rare earths are serious problems, which necessitate some form of separation prior to the measurements. The unique spectral selectivity associated with laser-excited fluorescence is due to the rather narrow spectral bandwidth of the laser, the number densities of the lower levels of the rare-earth species, and the quantum efficiencies of the respective fluorescence transitions.

The analytically useful range or linear dynamic range is taken as the detection limit to the upper concentration where the signal deviates by no more than 5% from linearity. The linear range is approximately 3 or 4 orders of magnitude. The strong curvature at approximately 700 $\mu g\ ml^{-1}$, as shown in Fig. 2, is observed for all the rare earths studied and is probably due to the combined effects of primary source absorption, self-absorption of fluorescence and reabsorption of fluorescence radiation (post filter effect).

The pertinent transitions for each rare earth are shown in simplified ionic energy level diagram in Fig. 3 (A—K). The transitions shown were selected from Corliss and Bozman [13]. An ionic energy level diagram of terbium is not included because it was not possible to identify the energy levels of the transitions corresponding to the fluorescence lines observed. The transitions reported do not represent the complete fluorescence spectrum within the wavelength range studied, because weaker lines could be observed at higher instrumental gain settings. Although many other ionic fluorescence spectra were observed at different excitation wavelengths, only one ionic energy level diagram per element is given in this report. The most sensitive absorption line for a particular element was not always used. The use of transitions not involving the ground ionic state was not necessarily a disadvantage because the lower ionic energy levels appeared to be highly

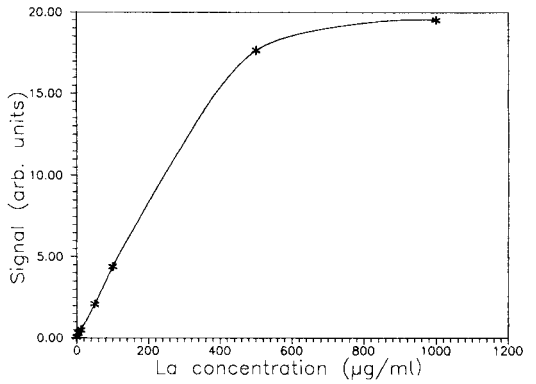

Fig. 2. Calibration curve for lanthanum ion.

populated. These excited lower levels may in fact be nearly as highly populated as the ground ionic state as a consequence of the high temperature of the ICP.

In all cases, when the fundamental wavelength from the dye laser was used to excite the fluorescence, the pumped transition appeared to be optically saturated to a considerable degree, i.e., increasing the laser power increased the non-resonance fluorescence signal up to a plateau. Therefore, the analytical signal is only weakly dependent upon laser fluctuations. However, the transitions were not saturated when frequency doubling was used.

The imprecision (%RSD) of the technique at low concentrations was approximately 5%. This was determined by measuring the relative standard deviation (RSD) at a concentration ten times greater than the detection limit. At concentrations much greater than the detection limit, the RSD is approximately 3%

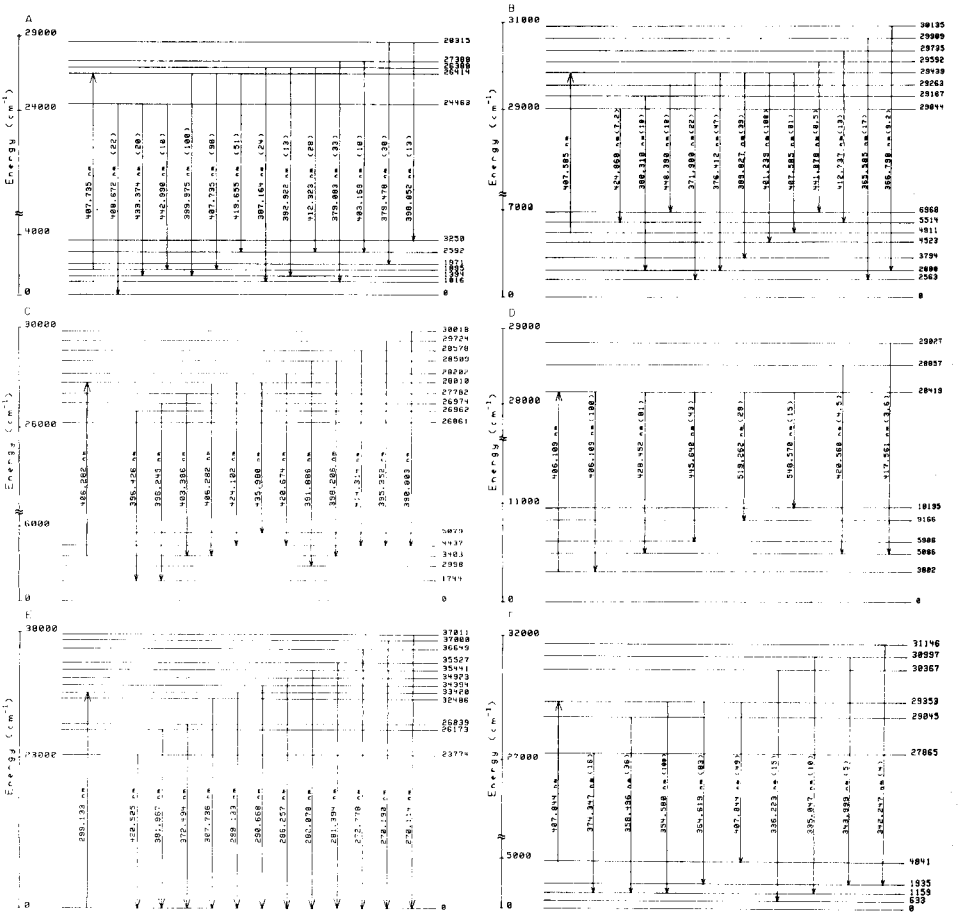

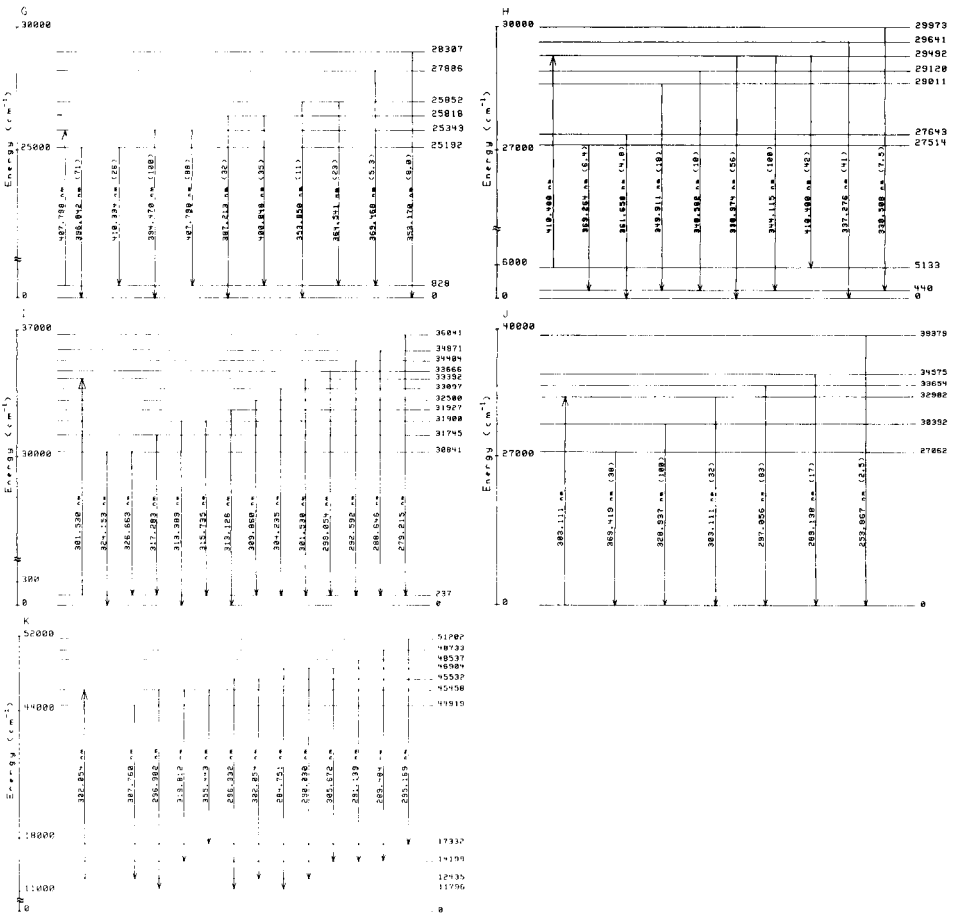

Fig. 3. Partial energy level diagrams. Wavelengths are also indicated in nm, and relative intensities in parenthesis. (A) Lanthanum ion; (B) cerium ion; (C) praseodymium ion; (D) neodymium ion; (E) europium ion; (F) gadolinium ion; (G) dysprosium ion; (H) erbium ion; (I) thulium ion; (J) ytterbium ion; (K) lutetium ion.

Conclusions

The detection limits obtained by laser-excited ionic-fluorescence spectrometry were adequate for the trace determination (<1 μg ml^{-1}) of any rare earth in a complex mixture of all other rare earths (100 μg ml^{-1}) without spectral interferences. This technique should not require separation of the rare earths from other matrix elements which would most likely be required for ICP/ES because of severe spectral interferences.

From this study, it can be concluded that the intensity of the ionic fluorescence depends on three features: (1) the spectral irradiance of the laser (until saturation of the pumped transition is reached; (2) the fluorescence transition probability; and (3) the population density of ions in the lower level from which the absorption process is initiated.

The spectral selectivity offered by this method as well as the good tunability of the dye laser makes laser-excited ionic fluorescence spectrometry the method of choice for the determination of rare earths when high sensitivity, low detection limits and high selectivity are desired. However, the relatively high cost of the excitation system and the restriction to single-element detection (although scanning of the dye laser is possible) will surely limit the use of the laser-ICP system to special situations where more conventional approaches are lacking in some figures of merit.

This research was supported by AF-AFOSR-86-0015.

REFERENCES

1 S. J. Buchanan and L. S. Dale, Spectrochim. Acta, Part B, 41 (1986) 237.
2 H. Qing-Kie, T. C. Huques, M. Haukka and P. Hannaker, Talanta, 32 (1985) 495.
3 J. G. Crock and F. E. Lytle, Anal. Chem., 54 (1982) 1329.
4 A. Bolton, J. Hwang and A. V. Bolt, Spectrochim. Acta, Part B, 38B (1983) 165.
5 I. B. Brenner, A. E. Watson, T. W. Steele, E. A. Jones and M. Goncalves, Spectrochim. Acta, Part B, 36 (1981) 785.
6 R. K. Winge, V. J. Peterson and V. A. Fassel, Appl. Spectrosc., 33 (1979) 206.
7 N. Omenetto and J. D. Winefordner, Appl. Spectrosc., 26 (1972) 555.
8 M. L. Parsons, B. W. Smith and G. E. Bentley, Handbook of Flame Spectroscopy, Plenum, New York, 1975.
9 H. Uchida, M. A. Kosinski and J. D. Winefordner, Spectrochim. Acta, Part B, 38 (1983) 5.
10 H. G. C. Human, N. Omenetto, P. Cavalli and G. Rossi, Spectrochim. Acta, Part B, 39 (1984) 1345.
11 N. Omenetto and H. G. C. Human, Spectrochim. Acta, Part B, 39 (1984) 1333.
12 M. S. Epstein, S. Nikdel, J. D. Bradshaw, M. A. Kosinski, J. N. Bower and J. D. Winefordner, Anal. Chim. Acta, 113 (1980) 221.
13 C. H. Corliss and W. R. Bozman, Natl. Bur. Stand. (U.S.), Monogr., 53 (1963).

Analytica Chimica Acta, 199 (1987) 119—127
Elsevier Science Publishers B.V., Amsterdam — Printed in The Netherlands

INDUCTIVELY-COUPLED PLASMA/ATOMIC EMISSION SPECTROMETRY OF SULFUR WITH A VACUUM SCANNING SPECTROMETER AND ITS APPLICATION TO THE ANALYSIS OF COAL LIQUEFACTION CATALYSTS

MASAAKI KUBOTA*, RAUL A. REIMER[a], KUNIKO TERAJIMA, YUJI YOSHIMURA and AKIO NISHIJIMA

National Chemical Laboratory for Industry, Higashi 1-1, Yatabe, Tsukuba, Ibaraki 305 (Japan)

(Received 16th March 1987)

SUMMARY

Inductively-coupled plasma/atomic emission spectrometry with a high-resolution vacuum scanning monochromator is described for the determination of sulfur at 180.734 nm. The behavior of the signal-to-background ratio is investigated as functions of RF power, argon gas flow rate and observation height above the load coil. Under the operating conditions selected, the detection limit is 3 $\mu g\ l^{-1}$. The Se I 196.090-nm line is chosen as internal standard, because the S/Se line pair exhibited the least change with carrier gas flow rate and acid concentration of solution. Sulfur in Ni—Mo and Co—Mo/Al_2O_3 catalysts used for coal liquefaction is determined as S(—II) and S(VI) species. The total amount of the species agreed well with the sulfur value obtained by the conventinal combustion method.

Inductively-coupled plasma/atomic emission spectrometry (ICP/AES) has been used for the determination of sulfur (or sulfate) in waters [1, 2], brine [2], biological samples [3] and polymeric materials [4]. Sensitive sulfur spectral lines occur at 180.734, 182.036 and 182.626 nm [5], measurement of these lines is hampered by strongly absorbing oxygen bands (Schumann-Runge system, bandheads at 183.01 and 181.56 nm [6]). Kirkbright et al. [7] purged the monochromator and optical pathway between the plasma torch and the entrance slit with nitrogen. Under their operating conditions, the 182.036-nm line exhibited the greatest intensity and the best detection limit of the three sulfur lines investigated. Similar nitrogen-purged monochromator systems were utilized by other groups [3, 4, 8, 9], and Wallace [8] and Morita et al. [3] reported that the 180.734-nm line gave the greatest sensitivity.

This paper describes the determination of sulfur at the 180.734-nm line with the aid of a vacuum scanning monochromator, and its application to

[a]Present address: Yacimientos Petroliferos Fiscales, Avda, Calchaqui KM. 23500, Florencio Varela, Buenos Aires, Argentina.

0003-2670/87/$03.50

the determination of sulfate and sulfide in catalysts used for coal liquefaction.

EXPERIMENTAL

Instrumentation

The RF power generator used was a Shimadzu excitation source model ICPS-2H operating at 27.12 MHz with a 3-turn load coil. The spectrometer was a 1-m vacuum scanning monochromator, Shimadzu model CTM-100, with a photomultiplier (Hamamatsu R106UH) and a 1024-channel linear photodiode-array detector (Tracor Northern TN-1224-4I). The spectrometric system consisted of the monochromator, a wavelength-scanning controller connected with a minicomputer (FACOM U-1100), a strip-chart recorder for recording of output signal from the photomultiplier and a multichannel analyzer (Tracor Northern TN-1710) with an I/O plotter for data acquisition from the photodiode-array detector.

In order to attain high resolution, the monochromator, equipped with a 3600 line mm^{-1} holographic grating and variable curved slits, was designed so as to minimize coma aberration by selecting a smaller off-axis angle (2.8875°). The reciprocal linear dispersion was 0.22 nm mm^{-1} at 250 nm. The Hg 313.155- and 313.183-nm lines from a mercury lamp can be completely separated under the conditions of a 10-μm entrance and 20-μm exit slit width even if the entrance slit height is increased to 10 mm. When a narrow entrance slit is used to attain a large signal-to-background ratio (SBR), the signal-to-noise ratio (SNR) was improved by increasing the entrance slit height, because the photomultiplier voltage could be decreased to the range where the detector noise was not dominant. Thus, the use of a narrow slit width (10 μm) and large slit height (10 mm) was effective for improving the detection capability.

The inside of the monochromator and the optical pathway between the two lenses were kept at a constant pressure of ca. 1×10^{-3} torr, and argon was supplied to the optical pathway between the first lens and the plasma torch to allow operation in the vacuum-ultraviolet region. The temperature of the monochromator could be adjusted to 30 ± 1°C by controlling the temperature of the thermostat housing. The basic characteristics of the photodiode-array detector have been reported previously [10]. The detector provides a poorer response than the photomultiplier tube (PMT) especially in the vacuum region. Thus, in this study, the PMT was used for emission measurements, unless otherwise stated.

Reagents

A stock solution of 1000 μg ml^{-1} sulfur was prepared by dissolution of analytical reagent-grade diammonium sulfate in deionized distilled water. Commercially available stock solutions (1000 μg ml^{-1}) of yttrium, selenium, zinc, etc., were employed to prepare internal standard solutions.

Sample preparation

The samples chosen for investigating the applicability of the present method were Ni—Mo and Co—Mo catalysts supported on γ-Al_2O_3 which were prepared for studies of their catalytic performance for coal liquefaction. These catalysts included fresh specimens presulfurized in a hydrogen sulfide/hydrogen gas stream at 400°C for 5 h and spent catalysts used for 50-h treatment of coal-derived liquids. The spent catalysts were washed with tetrahydrofuran in a Soxhlet extractor. All the catalysts were crushed in an agate mortar and dried by heating at 80°C for 2 h. Each catalyst (100 mg) was treated with 20 ml of (1 + 5) hydrochloric acid and heated on a hot plate for 30 min. The mixture was filtered. For the determination of sulfur-(VI), 10 ml of 200 μg Se ml^{-1} solution was added to the filtrate, and diluted with water to 100 ml before ICP determination. For the determination of sulfur (—II), the residue and filter paper were heated on a hot plate for 30 min with 10 ml of (1 + 1) nitric acid, the solution was filtered, and the filtrate was treated as above.

RESULTS AND DISCUSSION

Wavelength scans around several sensitive sulfur lines demonstrated that the S I 180.734-nm line gave the highest emission intensity with the present experimental system. The effects of plasma operating parameters on the signal and SBR were investigated to select suitable conditions for sulfur measurements at 180.734 nm. The parameters included the RF power, the flow rates of the auxiliary, carrier and purge gases and the observation height. The experimental conditions are listed in Table 1. The results obtained by varying the RF power, carrier gas flow rate and observation height, while other parameters were maintained as listed in Table 1 are given in Fig. 1. The SBR was nearly constant when the auxiliary gas flow rate was increased from 0.3 to 1.2 l min^{-1}, although the signal and background were slightly decreased on increasing the gas flow rate. Argon purge-gas flow rates of > 2.5 l min^{-1} were required to maintain a constant sample signal. A flow rate of 2 l min^{-1} was selected, because plasma instability was observed at flow rates >3 l min^{-1}.

Detection limit and precision

The detection limit, defined as the analyte concentration required to yield a net signal equivalent to three times the standard deviation of a blank value (3σ), was measured at the plasma operating conditions selected above. Table 2 compares the value obtained with literature values [1—3, 7, 8, 11]. The present result (3 ng ml^{-1}) is 3—8 times lower than recent literature values [2, 3]. This may be because the measurements in this study were made under the appropriate slits and plasma conditions. The curved slits allowed the use of a larger entrance slit height (10 mm) without decreasing the resolution. When the larger slit height was used, a signal for a 10 μg ml^{-1}

TABLE 1

Experimental conditions

RF power	1.2 kW	Observation height	15 mm above load coil
Entrance slit width	10 μm	Sample uptake rate	2.0 ml min^{-1}
slit height	10 mm	Scanning speed	0.047 nm min^{-1}
Exit slit width	20 μm	Integration time	10 s
slit height	15 mm		
Argon flow rate			
Plasma gas	11.5 l min^{-1}		
Auxiliary gas	1.2 l min^{-1}		
Carrier gas	1.0 l min^{-1}		
Purge gas	3.0 l min^{-1}		

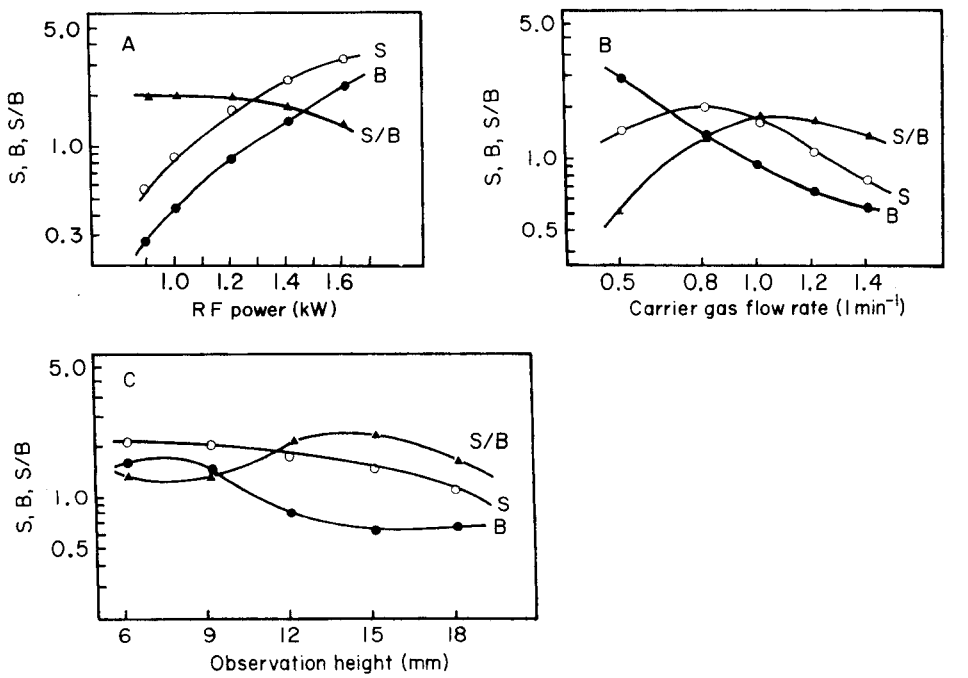

Fig. 1. Effects of RF power (A), carrier-gas flow rate (B) and observation height (C) on the signal (S), background (B) and signal-to-background ratio (S/B) of the S I 180.734-nm line.

sulfur solution was detected at PMT voltages above 500 V. Though it was necessary to use higher voltages for concentrations lower than 1 μg ml^{-1}, the supply of 700 V was enough to attain signals equal to those obtained with a smaller slit height (4 mm) and higher PMT voltage (800 V). Signal-to-noise ratios at 700 V were nearly one and half times better than the ratios at 800 V. The precision was evaluated by ten repetitive runs (10-s

TABLE 2

Detection limits for sulfur[a]

Detection limit (μg ml^{-1})		Reference
Reported	Based on 3σ	
1.7	—	7
0.05	—	8
0.024 (2σ)	0.036	11
0.079 (as SO_4^{2-})	0.026	1
0.070 (as SO_4^{2-})	0.023	2
0.006—0.010 (2σ)	0.009—0.015	3
0.003	0.003	Present work

[a]All workers used the 180.731-nm line except Kirkbright et al. [7] who used the 180.036-nm line.

integration per run) on working standard solutions. The relative standard deviations were 0.84, 0.55 and 0.41% at sulfur concentrations of 0.1, 0.5 and 1.0 μg ml^{-1}, respectively. The calibration graph was linear over a concentration range of four orders of magnitude.

Internal standard

Internal standardization has been used in analytical emission spectrometry as a means of compensating for changes in analyte signal as well as for improving measurement precision. In ICP/AES with internal standardization, the proper choice of operating parameters is essential in order to obtain a substantial improvement in analytical performance [12, 13]. Also considerable attention must be given to the correct choice of internal standard. Barnett et al. [14, 15] proposed guidelines for the choise based on consideration of the excitation energy, ionization energy, etc. According to Salin and Horlick [16], use of the line pair Ca(II)/Sr(II) provided an improvement in precision, while that of Ca(II)/Ar(II) degraded precision. Yttrium and scandium have been most commonly employed as standard elements [2, 17—19]. Brenner et al. [2] reported that the use of the Sc(II) 361.384-nm line for internal standardization resulted in an overall improvement in short- and long-term precision for the determination of sulfate in the presence of variable and large quantities of salts. However, the excitation potentials of the yttrium and scandium lines are much lower than that of sulfur and the combination of ionization potential and excitation potential for either the Y or Sc line is greater than the excitation potential of the S(I) 180.734-nm line (Table 3 [5]).

A survey was made, therefore, to select suitable internal standard lines. The photodiode array was used for the experiment, because the choice of lines can be made easily and rapidly by the simultaneous observation of many spectral lines over a wide wavelength region. The B(I) 182.641 nm,

TABLE 3

Spectral lines of sulfur and internal standards

Line	Wavelength (nm)	Excitation potential (eV)	Ionization potential (eV)
S(I)	180.734	6.85	10.35
Y(II)	371.029	3.52	6.51
B(I)	182.641	6.79	8.29
Zn(II)	206.191	6.01	9.39
Se(I)	196.090	6.32	9.75
Sc(II)	361.384	3.45	6.54

Se(I) 196.090 nm and Zn(II) 206.191 nm lines, for which excitation potentials are nearly equal to the sulfur line potential, were selected (see Table 3). A suitable internal standard line would be one which responds in a similar way to the sulfur line when plasma and sample conditions change. The carrier gas flow rate was varied from 0.5 to 2.0 l min^{-1}, and signal intensities of the sulfur and an internal standard line were measured alternately by slew scanning. Figure 2 shows the variation of the intensity ratios of the S line to the internal standard lines with the gas flow rate. It was evident that changes were significant for the line pairs S(I)/Zn(II) and S(I)/Y(II), because the atomic lines and ionic lines behave differently [20]. Comparing the line pairs S(I)/B(I) and S(I)/Se(I), the latter was less sensitive to changes in the carrier gas flow rate. The effect of the hydrochloric and nitric acid concentration of solutions on the intensity ratios of S(I)/Y(II) and S(I)/Se(I) is illustrated in Fig. 3. For comparison, the effect of perchloric acid concentration is also given in the range below 2% (v/v). A slight change in the ratio was found for the line pairs S(I)/Y(II), whereas the ratio remained nearly constant for the line pair S(I)/Se(I) over the acid concentration range investigated. Based on these experimental results, the Se I 196.090-nm line was selected as the internal standard line.

Application to the analysis of catalysts

Table 4 shows the effect of acid composition on the sulfur value obtained by using selenium as the internal standard. The results obtained with nitric acid (1 + 1) and mixtures of nitric and hydrochloric acid agreed well with the value found by the conventional combustion method with an infrared absorption detector. Relative standard deviations (n = 10) of the nitric acid dissolution/selenium internal standard method were 0.40 and 0.36% on the samples which contained 4.25 and 8.40% (w/w) sulfur, respectively, while relative standard deviations for the yttrium internal standard method were 0.62 and 0.48% for the same two samples.

Recently, Schultz et al. [21] found that presulfurization contributed to

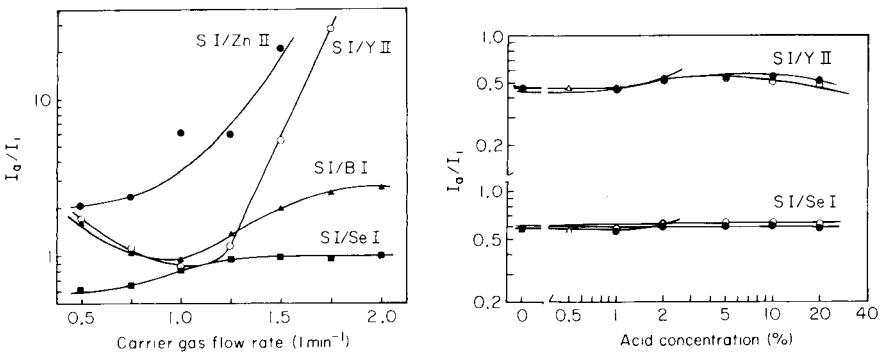

Fig. 2. Effects of carrier-gas flow rate on the intensity ratios of the S 180.734-nm/Y(II) 371.029-nm, S(I)/Zn(II) 206.191-nm, S(I)/B(I) 182.641-nm and S(I)/Se(I) 196.090-nm line pairs.

Fig. 3. Effects of acid concentration on the intensity ratios of the S(I) 180.734-nm/Y(II) 371.029-nm and S(I)/Se(I) 196.090-nm line pairs: (•) HCl; (○) HNO_3; (△) $HClO_4$.

TABLE 4

Effect of composition of acid solutions on the results for total sulfur

Volume ratios in mixture			Sulfur found[a] (% w/w)
HCl	HNO_3	H_2O	
1	0	1	1.1
10	1	9	9.0
5	1	4	9.2
1	1	0	9.0
0	1	1	9.2

[a]Combustion method gave 9.1% (w/w).

the enhancement of the hydrogenation activity of molybdenum catalysts supported on γ-alumina, i.e., the hydrogenation activity of the oxide (MoO_3) catalysts was lower than that of the sulfided (MoS_2) catalysts. It is known that MoS_2 is not decomposed by water but attacked by nitric acid or aqua regia [22]. In the sulfur 2*p* spectrum of a spent catalyst obtained by x-ray photoelectron spectroscopy, the S(VI) peak which might originate from sulfates disappeared on treating the catalyst with hydrochloric acid (1 + 1), whereas the S(—II) peak from sulfides had constant intensity. Thus, determinations of the S(VI) and S(—II) species in Ni–Mo and Co–Mo supported catalysts were done by the procedure described. The results for S(VI) (HCl-soluble) and S(—II) (HNO_3-soluble) are listed together with the concentrations of nickel, molybdenum and cobalt as oxides in Table 5. The concentration ratios for the HCl-soluble to the HNO_3-soluble in the spent catalysts were higher than those in the fresh catalysts. This implies that the

TABLE 5

Results for sulfur in fresh and spent catalysts (% w/w)

Catalyst		NiO^a	CoO^a	$MoO_3{}^a$	Sulfur found (% w/w) ICP/AES			Combustion method
					HCl soln.	HNO_3 soln.	Total	
Ni—Mo/Al_2O_3 (10.8)[b]	fresh	4.35	—	13.9	1.46	7.49	8.95	9.11
	spent	3.46	—	13.2	1.61	5.19	6.80	6.74
Ni—Mo/Al_2O_3 (22.5)[b]	fresh	4.39	—	15.0	1.30	7.10	8.40	8.69
	spent	3.46	—	12.7	1.97	4.73	6.70	6.16
Co—Mo/Al_2O_3 (10.8)[b]	fresh	—	4.00	15.8	1.81	6.86	8.67	8.77
	spent	—	3.20	12.1	1.59	3.98	5.57	6.02

[a]% (w/w) in catalyst. [b]Medium pore diameter (nm).

catalysts used for coal liquefaction show a decrease in the MoS_2 content, causing a decrease in the hydrogenation activity.

In Table 5, the sulfur values found by the combustion method are also given. Considering that the precision of the combustion method is ca. 5% in the authors' laboratory, it was concluded that good agreement was attained between the total amounts of sulfur obtained from HCl- and HNO_3-soluble material and the values determined by the combustion method.

The present study has demonstrated an improvement in the detection capability for sulfur with the aid of a high-resolution vacuum spectrometer and the applicability of ICP/AES to the determination of two sulfur species in real samples by the utilization of the appropriate sample preparation procedure. The samples analyzed contained rather high concentrations of sulfur. It is, however, expected that sulfur compounds could be determined at trace levels by ICP/AES using the scanning vacuum spectrometer system. In addition, it is thought that the use of the selected conditions should permit simultaneous determinations of major constituents of catalysts (sulfur, nickel, cobalt, molybdenum, etc.) and ash constituents (calcium, magnesium, iron, titanium, etc.) deposited on the spent catalyst, because the plasma conditions chosen here do not differ significantly from those suitable for the measurement of most metals.

REFERENCES

1 D. L. Miles and J. M. Cook, Anal. Chim. Acta, 141 (1982) 207.
2 I. B. Brenner, H. Eldad, S. Erlich and N. Dalman, Anal. Chim. Acta, 166 (1984) 51.
3 M. Morita, T. Uehiro and K. Fuwa, Anal. Chim. Acta, 166 (1984) 283.
4 G. DiPasquale and B. Casetta, At. Spectrosc., 5 (1984) 209.
5 A. N. Zaidel', V. K. Prokof'ev, S. M. Raiskii, V. A. Slavnyi and E. Ya. Shreider, Tables of Spectral Lines, IFI/Plenum, New York, 1970.
6 R. W. B. Pearse and A. G. Gaydon, The Identification of Molecular Spectra, 4th edn., Chapman and Hall, London, 1976.

7 G. K. Kirkbright, A. F. Ward and T. S. West, Anal. Chim. Acta, 62 (1972) 241.
8 G. F. Wallace, At. Spectrosc., 1 (1980) 38.
9 J. W. McLaren and S. S. Berman, Spectrochim. Acta, Part B, 40 (1985) 217.
10 M. Kubota, Y. Fujishiro and R. Ishida, Spectrochim. Acta, Part B, 37 (1982) 849.
11 T. Hayakawa, F. Kikui and S. Ikeda, Spectrochim. Acta, Part B, 37 (1982) 1069.
12 S. A. Myers and D. H. Tracy, Spectrochim. Acta, Part B, 38 (1983) 1227.
13 M. H. Ramsey and M. Thompson, Analyst, 110 (1985) 519.
14 W. B. Barnett, V. A. Fassel and R. N. Kniseley, Spectrochim. Acta, Part B, 23 (1968) 643.
15 W. B. Barnett, V. A. Fassel and R. N. Kniseley, Spectrochim. Acta, Part B, 25 (1970) 139.
16 E. D. Salin and G. Horlick, Anal. Chem., 52 (1980) 1578.
17 G. J. Schmidt and W. Slavin, Anal. Chem., 54 (1982) 2491.
18 Y. Endo and N. Sakao, Bunseki Kagaku, 30 (1981) 433.
19 H. Uchida, Y. Nojiri, H. Haraguchi and K. Fuwa, Anal. Chim. Acta, 123 (1981) 57.
20 H. Kawaguchi, T. Ito, K. Ota and A. Mizuike, Spectrochim. Acta, Part B, 35 (1980) 199.
21 G. W. Schultz, H. Shimada, Y. Yoshimura, T. Sato and A. Nishijima, Bull. Chem. Soc. Jpn., 58 (1985) 1077.
22 J. W. Mellor, A Comprehensive Treatise on Inorganic and Theoretical Chemistry, Vol. XI, Longmans Green, London, 1931.

Analytica Chimica Acta, 199 (1987) 129—135
Elsevier Science Publishers B.V., Amsterdam — Printed in The Netherlands

DIFFERENTIAL DETERMINATION OF ANTIMONY(III) AND ANTIMONY(V) BY INDIRECT SPECTROPHOTOMETRY WITH CHROMIUM(VI) AND DIPHENYLCARBAZIDE, AFTER REDUCTION OF ANTIMONY(V)

NORINOBU YONEHARA*, TOSHIAKI FUJI, HAYAO SAKAMOTO and MASAAKIRA KAMADA

Department of Chemistry, Faculty of Science, Kagoshima University, Korimoto, Kagoshima 890 (Japan)

(Received 11th November 1986)

SUMMARY

Antimony(III) is determined indirectly through its reaction with excess of chromium(VI), the excess being quantified with diphenylcarbazide and measurement at 540 nm. Antimony(V) is reduced to antimony(III) with sodium sulfite in hydrochloric acid solution; excess of sulfite is eliminated by boiling. The subsequent determination of antimony(III) gives the concentration of total antimony, and antimony(V) is found from the difference between the results before and after reduction. Antimony in its different oxidation states can be determined in the range 0.04—0.7 mg l^{-1} within an error of about 10%.

Antimony(III) reacts rapidly and quantitatively with chromium(VI) in acidic solutions. An indirect spectrophotometric determination of antimony-(III), which is rapid and reasonably sensitive without extraction, has been based on this reaction followed by reaction of the excess of chromium(VI) with diphenylcarbazide (DPC) and measurement of the resulting absorbance at 540 nm [1]. In the present communication, this procedure is extended to provide differential determination of antimony(III) and antimony(V) and its sensitivity is improved by using 5-cm cells. Total antimony is determined after reduction of antimony(V) to antimony(III) with sulfurous acid, and antimony(III) alone is determined without the reduction procedure. The difference between the two results gives the concentration of antimony(V). By the proposed method, antimony can be readily determined in its different oxidation states at 0.1 mg l^{-1} levels.

EXPERIMENTAL

Apparatus and reagents

A Hirama Model 6B spectrophotometer was used. Deionized/distilled water and analytical reagent-grade chemicals were used throughout.

0003-2670/87/$03.50

Standard antimony(V) solution (1.00 g l^{-1}) was prepared by dissolving potassium pyroantimonate in water; more dilute working solutions were prepared by simple dilution. Sodium sulfite solution (2 M) was prepared by dissolving 25 g of anhydrous sodium sulfite in 100 ml of water; this solution is saturated at less than about 18°C. The standard antimony(III), potassium dichromate and DPC solutions were prepared as described previously [1].

Procedure A (for the determination of antimony(III))

To 20.0 ml of sample solution containing up to 16 μg of antimony(III) in a glass-stoppered tube were added 2.0 ml of 1.0 M sulfuric acid and 0.20 ml of 2.9×10^{-4} M potassium dichromate. Then 0.4 ml of 4.1×10^{-2} M DPC was added as quickly as possible (20—30 s) and mixed thoroughly. The absorbance was measured at 540 nm in 5-cm glass cells against a water reference.

Procedure B (for the determination of antimony(III))

This procedure was the same as procedure A, except that the sulfuric acid solution and, in this case, 0.050 ml of the DPC solution were added in that order, the volume was adjusted to 22.4 ml with water, and then the dichromate solution was added.

Procedure C (for the determination of total antimony)

To 30.0 ml of sample solution containing up to 40 μg of antimony in a 200-ml glass beaker, were added 40 ml of concentrated hydrochloric acid and 0.5 ml of 2 M sodium sulfite. The solution was evaporated to less than 20 ml at 200°C on a hot-plate. The remaining solution was diluted to exactly 50 ml with water. A 20-ml aliquot of this solution was treated as in procedure A, except that 2.0 ml of water was added instead of sulfuric acid.

In preliminary tests of the reduction process, 20.0 ml of the standard solution of antimony(V) and 50 ml of concentrated hydrochloric acid were mixed; this solution was treated with sulfite, etc. as described above.

RESULTS AND DISCUSSION

Calibration graphs for antimony(III) and effect of reaction variables

A series of standard solutions of antimony(III) was treated as in procedure A; the resulting graph (Fig. 1, curve 1) provides better sensitivity than the earlier procedure [1] largely because of the longer cell used. The effects of reaction variables for procedure A are similar to those previously reported for a 1-cm cell [1]. The limit of determination was 0.02 mg l^{-1}. The relative standard deviation for 8 replicate determinations of 0.35 mg l^{-1} antimony(III) was 1.0%. The calibration graph for procedure B (Fig. 1, curve 2) deviates from a stoichiometric relationship at higher concentrations of antimony(III), because of the competitive reaction of antimony(III) and DPC for chromium(VI); the higher the concentration of DPC (curves 2—5) or temperature

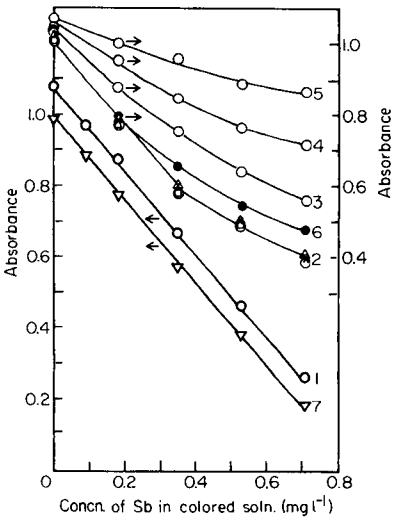

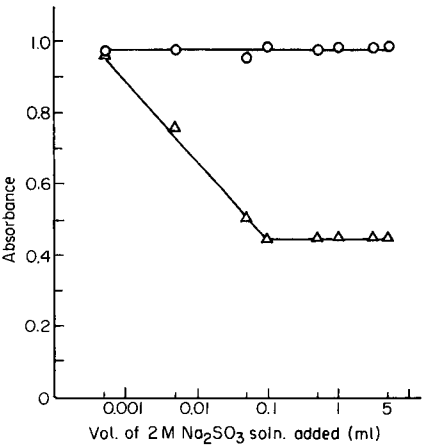

Fig. 1. Calibration graphs and effects of DPC and sulfuric acid concentrations and temperature. Curves: (1) by procedure A; (2—6) by procedure B; (7) by procedure C. Temperature: (1—5 and 7) 19°C; (6) 30°C. Concentration of sulfuric acid: (×) 0.020 M; (△) 0.040 M; (○, •) 0.090 M; (□) 2.30 M. Concentration of DPC: (1, 5, 7) 7.3×10^{-4} M; (2, 6) 9.1×10^{-5} M; (3) 1.8×10^{-4} M; (4) 3.6×10^{-4} M. Concentration of chromium(VI): 5.1×10^{-6} M.

Fig. 2. Effect of amount of sodium sulfite on reduction of antimony(V): (○) blank; (△) 25 μg of antimony(V) in the initial solution. For the addition of <0.1 ml of 2 M sodium sulfite, 1 ml of an appropriately diluted solution was used. Other conditions as in procedure C.

(curve 6), the larger the deviation. An increase in the DPC concentration or temperature increases the rate of the DPC/chromium(VI) reaction, thus reducing the chromium(VI) concentration available to antimony(III). No significant changes in the sensitivity of the method were observed when the concentration of sulfuric acid was changed in the range 0.020—2.30 M (curve 2).

Reduction of antimony(V) to antimony(III) and removal of the excess of reducing agent

Three reducing agents were examined for the reduction of antimony(V) and for convenient removal of their excess. Ascorbic acid and hydrazine sulfate were not satisfactory, because the excess could not be removed completely so that some chromium(VI) was reduced. Sodium sulfite seemed to be the most suitable; the reduction proceeded readily in hydrochloric acid solution and the excess of sulfur dioxide was easily removed by boiling. The effect of the amount of sodium sulfite added was examined in the range 0.0005—5 ml of 2 M solution. The results are shown in Fig. 2. In the absence

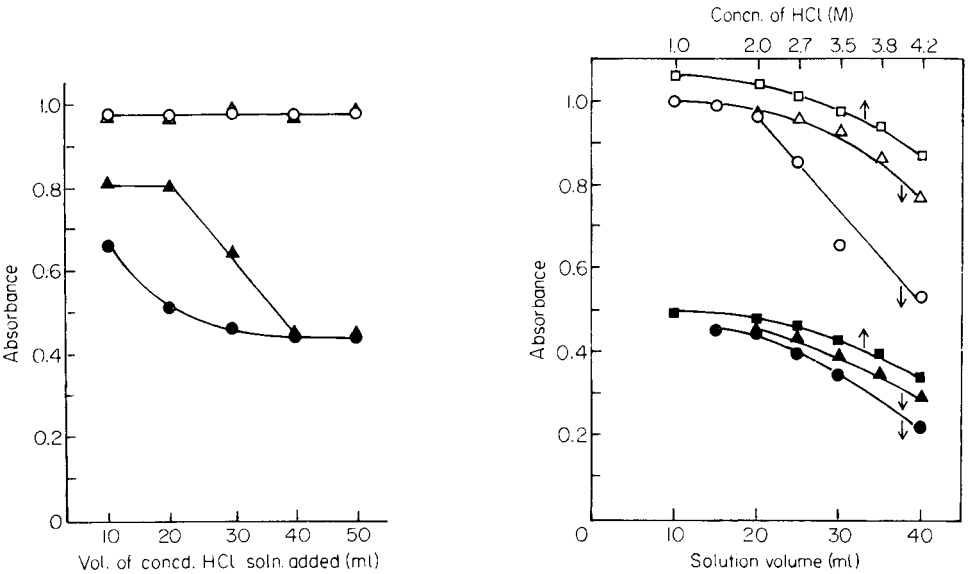

Fig. 3. Effect of amount of concentrated hydrochloric acid on reduction of antimony(V) and removal of excess of sodium sulfite: (○, △) blank; (●, ▲) 25 μg of antimony(V) in the initial solution. Sulfite (2 M) added: (○, ●) 5.0 ml; (△, ▲) 0.5 ml. Other conditions as in procedure C.

Fig. 4. Effect of volume of solution after evaporation. Curves: (○, △, ●, ▲) by procedure C (except for the volume of solutions after evaporation); (○, △) blank; (●, ▲) 25 μg of antimony(V) in the evaporated solution; (○, ●) 5.0 ml of 2 M sodium sulfite; (△, ▲) 0.5 ml of 2 M sodium sulfite; (□) blank and (■) 10 μg antimony(III), both treated as in procedure A in the presence of hydrochloric acid.

of antimony(V), the absorbances remained constant at the value expected, which shows that the excess of sulfur dioxide had been completely removed in procedure C. When >0.1 ml of 2 M sodium sulfite was added, antimony(V) was completely reduced to antimony(III).

Figure 3 shows the effect of the amount of concentrated hydrochloric acid added. For these tests, the volume of the solution was adjusted to 70 ml with water before boiling. The excess of sulfur dioxide was completely removed in the range of hydrochloric acid tested; the absorbances of the reagent blank remained constant. However, the addition of >40 ml of concentrated hydrochloric acid was required to reduce antimony(V) completely. Figure 4 shows the effect of the volume of the solution after evaporation. The absorbances of both the blank and 25 μg antimony(V) obtained after evaporation of the solution to 20 ml show that both the reduction of antimony(V) and the removal of excess of sulfur dioxide were complete. However, the larger the volume of the solution in the 20—40 ml range (i.e., before dilution to 50 ml), the lower the absorbance. This behavior seems to depend mainly on the effect of the acid concentration on the color development,

although the elimination of sulfur dioxide is obviously incomplete when 5 ml of 2 M sodium sulfite is used. The concentration of hydrochloric acid in the evaporated solutions, determined titrimetrically, was about 6 M regardless of the volumes of the solutions, probably because of the formation of an azeotropic mixture. The acid concentrations in the final colored solutions obtained by treating each of the evaporated solutions according to procedure C are indicated in Fig. 4; these acidities are related to the volumes on the lower axis. The influence of the hydrochloric acid concentration on the color development was examined by treating blank and antimony(III) solutions according to procedure A, except that hydrochloric acid in the concentration range indicated in Fig. 4 was added without sulfuric acid. The behavior was similar to that described above, i.e., the solution should be evaporated to <20 ml, because the removal of sulfur dioxide is complete and the acid concentration has less effect on the color development (Fig. 4).

A calibration graph was obtained for a series of standard solutions of antimony(V) by procedure C; the resulting graph is shown in Fig. 1 (curve 7). The limit of determination was 0.04 mg l^{-1} and the relative standard deviation for 8 replicate determinations of 0.35 mg l^{-1} antimony(V) was 3.4%.

Effects of standing times and temperature on the interferences of arsenic(III) and vanadium(IV)

The interferences of diverse ions and their elimination were discussed previously [1]. Arsenic(III) and vanadium(IV), which can reduce chromium(VI), interfered seriously with the determination of antimony(III). The

TABLE 1

Effects of arsenic(III) and vanadium(IV) on the determination of 0.20 mg l^{-1} antimony(III) by procedures A and B

Acid	Proc.	Standing time (min)	Sb(III) found (mg l^{-1})					
			In the presence of 5 mg l^{-1}					
			As(III)			V(IV)		
			1°C	19°C	30°C	1°C	19°C	30°C
H_2SO_4 (0.09 M)	A	0.5	0.25	0.25	0.27	0.18	0.25	0.33
		2.0	0.30	0.30	0.35	0.21	0.34	0.43
		5.0	0.34	0.39	0.42	0.25	0.47	0.71
	B		—	0.20	0.23	—	0.24	0.38
HCl (2.0 M)	A	0.5	0.34	0.49 (0.31)[a]	0.59	0.20	0.22 (0.23)[a]	0.26
		2.0	0.67	0.76 (0.50)[a]	0.82	0.21	0.26 (0.27)[a]	0.35
		5.0	0.82	0.94	0.97	0.25	0.34	0.45
	B		—	0.45	0.40	—	0.42	0.38

[a] Antimony(V) was treated by procedure C in the presence of arsenic(III) or vanadium(IV).

effects of these two ions were also examined for the present procedures A, B and C; antimony(III) solutions containing arsenic(III) or vanadium(IV) and sulfuric acid (0.09 M) or hydrochloric acid (2.0 M) were treated with the DPC solution at various standing times after the addition of chromium(VI) in procedure A. As shown in Table 1, shorter standing times and lower temperatures are preferable for the elimination of interferences in procedure A. Arsenic(III) showed less interference on procedure B than that on procedure A, while the effect of vanadium(IV) was less on procedure A than on procedure B.

In order to examine the effects of these ions for procedure C, the antimony(III) solutions were first treated in the presence of 2.0 M hydrochloric acid, without the evaporation procedure, as in procedures A and B. Rather large interferences were observed with arsenic(III) in both the procedures A and B and with vanadium(IV) in procedure B, but the interference of arsenic(III) was greatly decreased in procedure C involving evaporation. Procedure A combined with evaporation (i.e., procedure C) is preferable for determining total antimony.

Differential determination of antimony(III) and antimony(V)

Antimony(III) and total antimony were determined by using mixed solutions containing known amounts of antimony(III) and antimony(V). Antimony(V) was calculated from the difference between the two results. The results shown in Table 2 indicate a maximum error of ±0.02 mg l^{-1} for antimony(III), whereas some values for total antimony show larger errors.

Geothermal water, taken from a deep geothermal drill hole at Kirishima in Japan, was analyzed by the present method. The results are shown in Table 3, together with those obtained previously [1]. The value for total antimony

TABLE 2

Recovery of total antimony and antimony(III) in prepared mixtures

Mixture taken (mg l^{-1})			Found (mg l^{-1})		
Total Sb	Sb(III)	Sb(V)	Total Sb	Sb(III)	Sb(V)
0.20	0.10	0.10	0.23	0.10	0.13
0.30	0.10	0.20	0.35	0.10	0.25
	0.20	0.10	0.26	0.18	0.08
0.40	0.10	0.30	0.42	0.10	0.32
	0.20	0.20	0.39	0.18	0.21
	0.30	0.10	0.38	0.29	0.09
0.50	0.10	0.40	0.55	0.11	0.44
	0.20	0.30	0.52	0.18	0.34
	0.30	0.20	0.48	0.28	0.20
	0.40	0.10	0.53	0.40	0.13
0.60	0.30	0.30	0.65	0.30	0.35

agrees with that obtained by atomic absorption spectrometry [2]. Antimony-(III) seems to have been oxidized to antimony(V) during storage for about 4 years.

TABLE 3

Determination of antimony in geothermal water[a]

	Total Sb (mg l^{-1})	Sb(III) (mg l^{-1})	Sb(V) (mg l^{-1})
Proposed method	0.15	0.04	0.11
Previous method	—	0.20[b]	—
Atomic absorption	0.15[b]	—	—

[a]Sample taken at Kirishima, Japan, January 1982. [b]Determined in 1982.

REFERENCES

1 N. Yonehara, Y. Nishimoto and M. Kamada, Anal. Chim. Acta, 172 (1985) 183.
2 M. Yamamoto, K. Urata, K. Murashige and Y. Yamamoto, Spectrochim. Acta, Part B, 36 (1981) 671.

Analytica Chimica Acta, 199 (1987) 137—145
Elsevier Science Publishers B.V., Amsterdam — Printed in The Netherlands

A SIMPLE STOPPED-FLOW METHOD WITH CONTINUOUS PUMPING FOR THE SPECTROPHOTOMETRIC FLOW-INJECTION DETERMINATION OF BORON IN PLANTS

M. A. Z. ARRUDA and E. A. G. ZAGATTO*

Centro de Energia Nuclear na Agricultura da Universidade de S. Paulo, Caixa Postal 96, 13400 Piracicaba, São Paulo (Brazil)

(Received 22nd January 1987)

SUMMARY

An alternative way of stopping a processed sample inside a flow-through detector is proposed. A commutating device permits the peristaltic pump to operate continuously, thus avoiding problems associated with the pump inertia often found in analyzers requiring pump stoppage. The feasibility of the approach is demonstrated by improving the spectrophotometric determination of boron in plants, which is based on a relatively slow reaction. Effects of commutating times, flow rates, manifold dimensions and reagent concentrations are studied. With the same analytical frequency (60 h^{-1}) and azomethine-H consumption (2.1 mg per sample) of the original procedure, the proposed system provides better sensitivity because of a three-fold increase in the sample-processing time and the absence of significant sample dispersion. Reproducible results (r.s.d. for typical samples usually less than 1%) are in agreement with those obtained with the original procedure.

The impact of the flow-injection concept [1] in the field of automated analytical chemistry and its overall acceptance [2, 3] can be explained by the favourable characteristics of the flow-injection analyzer. Its simplicity and versatility are often emphasized [3]. The stopped-flow analyzers require pump stoppages and microprocessor-control but are also essentially simple, and are useful in connection with relatively slow chemical reactions, mainly enzymatic assays [4—6]. Recently, Krug et al. [7] emphasized the performance of a commutating device and pointed out the feasibility of achieving alternating and intermittent streams with commutation.

Commutation can also be useful in a flow-injection stopped-flow analyzer with continuous pumping [7], thus avoiding the problems associated with the inertia of peristaltic pumps. As higher flow rates are used, the wash time is greatly reduced. For a given period [3], the available time for chemical reactions is then increased because this period can be almost entirely exploited for the reaction development. Because molecular diffusion has very little effect on the sample dispersion [8], long stop periods are feasible. If the processed sample is stopped in the flow-through detector, the gradual development of the reactions can be monitored [4]. As precise timing is easily attained, the

0003-2670/87/$03.50

measurement related to the end of the stop period reflects the required analyte concentration.

This paper deals with a flow-injection stopped-flow analyzer with continuous pumping which is further used in connection with the earlier-suggested [9] flow-injection spectrophotometric determination of boron in plant material.

EXPERIMENTAL

Reagents, standards and samples

All reagents were of analytical grade; distilled-deionized water was always used. Azomethine-H was synthesized as described by Mazaheri [10]. All solutions, including samples and standards, were stored in polyethylene vials.

Colour reagent A (Fig. 1) was prepared daily by dissolving 0.5 g of azomethine-H and 2 g of ascorbic acid in about 40 ml of warm water (ca. 50°C), and making the volume up to 100 ml with water [9]. Preliminary tests indicated that the analytical signal undergoes a reduction of about 30% if a two-day-old reagent is used. Also, small differences in peak heights, usually less than 10%, were observed when the commercially available azomethine-H (Merck, Darmstadt) was used. Sample carrier stream (C, Fig. 1) was prepared with the same acidity as the samples (0.1 M in HCl) to minimize problems with the blank value [11]. Buffer/masking reagent B was prepared by dissolving 132 g of diammonium hydrogenphosphate and 25 g of disodium-EDTA in 500 ml of water.

Boron standards, also 0.1 M in HCl and covering the 0.00—3.00 mg l^{-1} range, were prepared by dilutions of a 100 mg B l^{-1} (as boric acid) stock solution.

The samples were mineralized by a procedure similar to that used earlier [9], involving dry ashing of 5 g of ground leaves at 550°C, for 2—4 h, addition of 10 ml of 1 M HCl, filtration and dilution to 100 ml with water.

The flow-injection system

The stopped-flow analyzer consisted of an Ismatec mp13GJ4 peristaltic pump, a B352 Micronal three-piece commutator with built-in T-shaped perspex connectors and polyethylene coils (inner diameter, 0.8 mm; winding diameter, 2 cm), a model 25 Beckman spectrophotometer provided with a 178-OS Hellma flow cell (inner volume, 80 μl; optical path, 10 mm) and a Beckman 24/25 ACC recorder.

The flow diagrams of the flow-injection systems with either a three-piece or a two-piece [7, 12] commutator are shown in Fig. 1. In the situations specified, the sample is aspirated through a coiled sampling loop, the excess being discarded. The colour and buffer/masking reagents recycle outside the analytical path, while the sample carrier stream and a pressure-compensating stream of water are aspirated towards waste. The reagent transmission lines between the commutator and the confluence points are filled with trapped

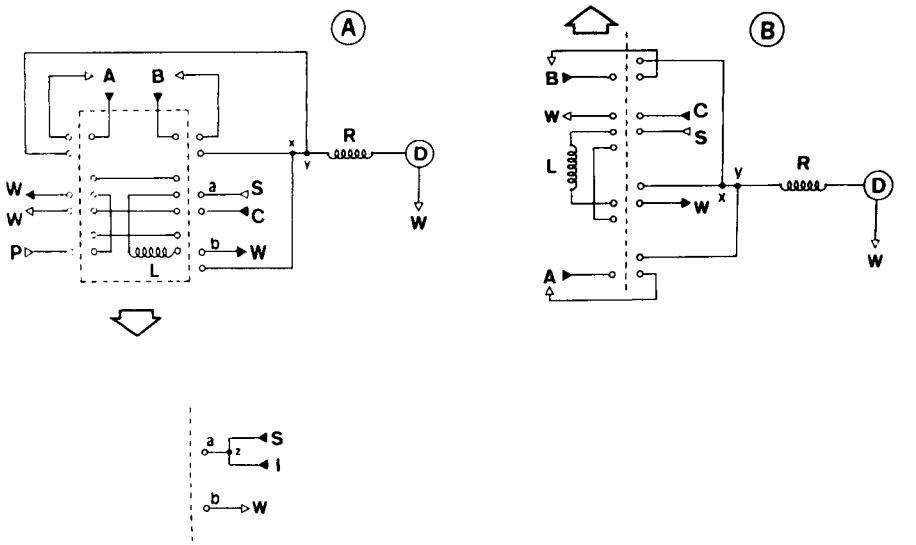

Fig. 1. Flow diagrams of the stopped-flow systems suggested for the determination of boron in plants. S, sample, aspirated at 10.0 ml min^{-1}; L, 400-cm sampling loop; C, sample carrier stream (10.0 ml min^{-1}); B, buffer/masking reagent (2.5 ml min^{-1}); A, colour reagent (2.5 ml min^{-1}); R, 50-cm coiled reactor; D, spectrophotometer at 417 nm; x, y and z, confluence points; W, waste. Vectors indicate where the peristaltic pump is applied; triangles indicate flow directions and arrows the commutator movement. The modifications required to investigate interferences are indicated in the lower part of Fig. 1A which shows the convergent tubes directing the sample (S) and interferent (I) solutions (5.0 ml min^{-1}) towards the commutation point a and the point b connected to the waste line. Fig. 1A refers to the three-piece commutator used for this work and Fig. 1B, to a two-piece one. In the system shown in B, the pressure-compensating stream P is not required. For details, see text.

reagents. When the commutator is switched to the alternate position, the sampling loop is intercalated in the sample carrier stream and the reagents are directed towards the analytical path. At the x confluence point, the buffer/masking reagent is added to the sample zone, the colour reagent being added at the next confluence point (y). The reactions involved, discussed elsewhere [9, 13], proceed inside the main reactor and the flow cell. As the sample zone is transported, the previous processed sample is discarded. When the commutator is operated back to the position specified in Fig. 1 to start another cycle, the sample zone is stopped, allowing the detector to quantify the increasing formation of the coloured condensation species. The absorbance related to the end of the stop period, which is proportional to the boron content in the sample, constitutes the basis of the measurements. In contrast to the zone-trapping approach [7, 14], the reagents are not consumed during the stoppage of the sample zone.

The need for two separate reagents was confirmed after mixing equal volumes of the A and B solutions: after two hours, the azomethine-H condensation [9] was evident, the solution becoming more intensely coloured, yet less reactive. Although in the original procedure [9], the confluence points for addition of the A and B reagents were separated by a 50-cm coil, the x-y distance can be reduced at will, as demonstrated in preliminary tests involving interference studies. In the present procedure, the x-y distance was zero and an X-shaped connector was employed for the addition of both reagents.

The flow rates were kept as high as possible, the ratios between them being the same as in the original work. The length of reactor, R, was chosen as 50 cm. The baseline was then always smooth, indicating the favourable mixing conditions of the flow-injection system. It should be stressed that increasing the reactor length increases the wash time and the required injected volume for the same degree of dispersion [3]. However, the precision decreased with a short (15-cm) reactor.

Procedures

The flow-injection system of Fig. 1 was used in a factorial experiment involving variations in commutation times (10—100 s), in the length of the sampling loop (50—400 cm) and in the peristaltic pump speed (33—150% of the pumping speed indicated in Fig. 1). Boron standards in the 0.00—3.00 mg l^{-1} range were used, reagent A being 0.5% (w/v) in azomethine-H. For each situation, carry-over was evaluated by injecting a 30.0 mg B l^{-1} standard solution and recording the analytical signal corresponding to a blank solution injected after it.

The influence of the azomethine-H concentration, in the 0.25—1.0% (w/v) range, was investigated by using the same system; loop L was 400 cm long and the sampling and injecting times (t_{STOP} and t_{GO}) were 50 and 10 s, respectively.

After the azomethine-H concentration had been selected as 0.5% (w/v), the effects of the potential interferents [9, 13] were studied. For this experiment, the system of Fig. 1 was used; the sample aspiration tube was replaced by two convergent tubes which merged before the inlet of the sampling loop (point z of Fig. 1A. lower portion). Pumping was applied to both tubes, so that two convergent streams with identical flow rates were established. One stream consisted of boron standards (0.00—6.00 mg l^{-1}) and the other consisted of different solutions with a potential interfering species (50.0 and 500 mg Al l^{-1}, 2.00 and 10.0 mg Zn l^{-1}, 10.0 or 100 mg Fe(III) l^{-1}, 2.00 or 10.0 mg Cu l^{-1}, 30.0 or 300 mg Na l^{-1}, 50.0 or 500 mg P l^{-1}), all solutions being also 0.1 M in HCl. Disodium-EDTA concentrations of 0.0—2.5 and 5.0% (w/v) in the B reagent were tested. The possibility of reducing buffering capacity was investigated by using 0.66 M triammonium phosphate solution, also 5% (w/v) in disodium-EDTA, as the B reagent. Boron standards were prepared with different acidities (0.09, 0.10 or 0.11 M HCl).

After dimensioning, the flow-injection system was applied to real analysis. Precision was evaluated as the relative standard deviation of seven successive

measurements of a typical sample (26.3 $\mu g\ g^{-1}$, B, dry basis). Accuracy was assessed by running some already analyzed [9] samples.

RESULTS AND DISCUSSION

In the flow-injection system of Fig. 1, only the portion of the sample zone stopped inside the flow cell is quantified. The selection of this portion is similar to the selecting step of the zone-sampling process [7, 15] with the flow cell of the analyzer being analogous to the resampling loop associated with zone sampling. Therefore, images of the concentration/time functions at the detector may be achieved [7, 16, 17] by stepwise varying of the resting time of the commutator in the injection position (t_{GO}). Curves (a), (b) and (c) in Fig. 2 correspond to different injected volumes. Only the portions of the outputs related to t_{GO} values higher than 7 s are shown because when this time interval was too short, carry-over effects became more pronounced. Carry-over effects have not been discussed in detail in previous papers dealing with zone sampling because, in such processes, the selected portion of the sample zone is removed from its original path and introduced into another carrier stream. In the present process, the outer portions of the processed zone remaining in physical contact with the portion stopped inside the flow cell constitute the main source of carry-over.

In the proposed system (Fig. 1), carry-over was calculated as 0.8% and 0.05% for washing periods of 7 s and 9 s, respectively. When t_{GO} was higher

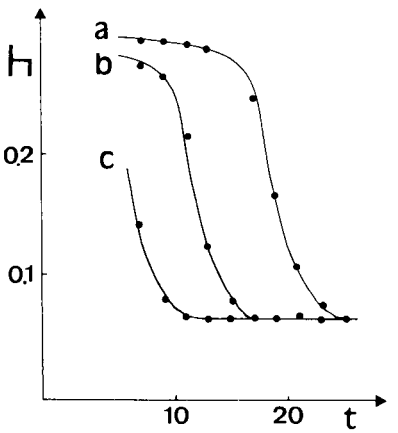

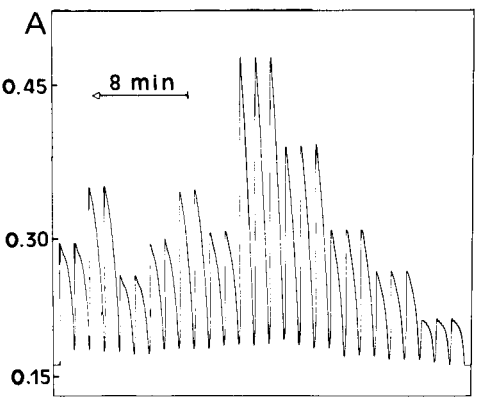

Fig. 2. Effect of the t_{GO} period. A 3.00 mg B l^{-1} standard solution is injected into the system of Fig. 1A by means of 400-cm (a), 200-cm (b) and 50-cm (c) sampling loops. The recorded peak height (h) is given as absorbance.

Fig. 3. Recorder output of a routine run for boron determination in plants. From the left, the signals correspond to five standard solutions (0.00, 0.50, 1.00, 2.00 and 3.00 mg B l^{-1}) injected in triplicate and six solubilized samples, in duplicate.

than 11 s, the carry-over was less than 0.01%. However, the washing period should be as small as possible, in order to minimize reagent consumption and the mean available time for reaction development. As a compromise between all these features, t_{GO} was fixed at 10 s. For an analytical frequency of 60 measurements per hour, a washing period of 10 s means that 83.3% of the flow-injection period is used for development of the chemical reactions. The carry-over may be also reduced by increasing the pumping speed, which means an increase in the total volume flowing through the detector during the wash period. However, the pumping speed cannot be increased at will: when it was increased in 50%, the precision deteriorated, the relative standard deviation of the measurements being usually around 10%. This drop in reproducibility at higher flow rates is probably due to insufficient time for mixing. It should be reported that when flow rates were higher, leaking at the manifold connections was observed because of excessive hydrodynamic pressure.

With the flow rates specified in Fig. 1 and a t_{GO} period of 10 s, a 400-cm long sampling loop was required to minimize sample dispersion (Fig. 2). This loop is not fully emptied during the injection time, therefore although a sampling loop is used the injection process approximates the time-based injection [7]. In this case, the size of the sampling loop is not so relevant a factor in dispersion.

The resting time of the commutator in the position specified in Fig. 1, t_{STOP}, has a marked effect on the recorded peak height (Table 1) because slow chemical reactions are involved. Therefore, the sensitivity increases with higher t_{STOP} values. A t_{STOP} of 50 s was chosen, taking into account the boron content in the samples and the desired sampling rate. For sample lots with low boron contents, a 90-s stop period is actually used in routine work. It is important to mention that the blank value undergoes a slight increase with t_{STOP} (Table 1); this is due to the azomethine-H condensation [9] in neutral media. This confirms again the impossibility of having both the A and B reagents in the same solution.

As in the original procedure [9], it was proved that there is an almost linear relationship between the slope of the calibration plot and the concentration of azomethine-H. Therefore, another possibility of increasing the analytical signal is to increase the azomethine-H concentration in the A reagent. However, this increase is limited by the absorbance of this reagent. With

TABLE 1

Effects of the t_{STOP} period with t_{GO} = 10 s

t_{STOP}[a]	10	20	30	40	50	60	70	80	90	10(
Slope[b]	0.006	0.024	0.071	0.089	0.104	0.116	0.128	0.137	0.145	(
Blank[c]	0.018	0.027	0.029	—	0.042	0.044	—	—	—	(

[a] Resting time (s) of the commutator in the position specified in Fig. 1A. [b] Slope of the calibration plot, expressed in variation of the peak height (A) per variation of the boron concentration in the sample (mg l^{-1}). [c] Peak height (absorbance) related to the 0.00 mg B l^{-1} standard solution.

the azomethine-H concentration of 0.5% selected for this work, the absorbance corresponding to the baseline was 0.15 (Fig. 3) and the azomethine-H consumption was 2.1 mg per sample which is equivalent to that of the earlier work [9].

The buffer capacity of the system cannot be reduced. When the phosphate concentration in the B reagent was reduced to 0.66 M, the same final pH of 7.2 was attained but the baseline absorbance became more dependent on the sample acidity. When the hydrochloric acid concentration in the standards was varied from 0.09 to 0.11 M, the baseline absorbance decreased by about 60%. This confirms the strong dependence between baseline level and pH [9]. This effect can be overcome by using a buffer with higher capacity (2 M phosphate). Slight differences in the slope of the calibration plot (ca. 2%) were observed when the sample acidity was changed from 0.09 M to 0.11 M. Therefore, care should be taken in the preparation of sample and standards in order to minimize the variability in sample acidity.

According to Capelle [13], the reaction rate is decreased when the sodium concentration in the sample increases. In the flow-injection system, this means a decrease in peak height. With the suggested procedure, sodium levels in the leaves of up to 200 $\mu g\, g^{-1}$ (neglecting the sodium losses during sample preparation) can be tolerated, the signal attenuation being less than 1%.

The proposed procedure is slightly affected by interfering ions (Table 2). It should be stressed that the interfering levels reported here are well above the levels usually found in plant leaves [18, 19]. As already reported [13], increasing the disodium-EDTA concentration is not very effective in improving the selectivity. However, when the disodium-EDTA concentration was changed from 2.5% to 5.0% (w/v), the sodium interference underwent a slight decrease (Table 2) and the selectivity against Zn, Cu and Fe(III) was improved. Without disodium-EDTA, the baseline was always too high (absorbance >0.5) and interference effects were unacceptable. A 5% (w/v) disodium-EDTA solution was therefore chosen. It should be reported that citrate addition (about 0.1 M as ammonium citrate) to reagent B [20] was not effective in aluminium masking, yet it enhanced the blank value because of formation of coloured species with iron and aluminium. Although the presence of large amounts of aluminium does not have a pronounced effect on the analytical results (Table 2), it produces a distortion in the recorded peak. This effect, noticed also in test-tube experiments, is due to fast precipitation of aluminium followed by the relatively slow formation of the soluble complex which occur in a neutral phosphate solution containing aluminium and disodium-EDTA. The addition of iron(III) produces a slight increase in the blank value because of formation of the coloured soluble complex. Blank running is therefore essential. This is accomplished by replacing reagent A (Fig. 1) by a 2% (w/v) ascorbic acid solution and running the samples again. Finally, it is important to note that the Al, Zn, Cu, Fe(III) and pH interferences are proportional to the boron content (see Table 2).

TABLE 2

Effects of possible interfering ions. Data express peak heights (absorbance) and are referred to the system of Fig. 1A with the modifications indicated in the lower part of the figure; t_{GO} and t_{STOP} values were 10 s and 50 s, respectively; EDTA means disodium-EDTA concentrations (w/v) in reagent B (for details, see text)

Solution I ($mg\ l^{-1}$)		6.00 mg B l^{-1}[a]		1.00 mg B l^{-1}[a]		Blank
		2.5% EDTA	5% EDTA	2.5% EDTA	5% EDTA	5% EDTA
—		0.303	0.310	0.085	0.090	0.042
30.0	Na	0.303	0.306	0.085	0.089	0.041
300	Na	0.274	0.285	0.056	0.064	0.017
50.0	P	0.303	0.306	0.085	0.089	0.042
500	P	0.303	0.306	0.085	0.089	0.041
2.00	Zn	0.303	0.310	0.085	0.090	0.042
10.0	Zn	0.298	0.309	0.085	0.090	0.042
2.00	Cu	0.298	0.310	0.083	0.090	0.042
10.0	Cu	0.289	0.310	0.081	0.090	0.041
10.0	Fe	0.293	0.304	0.082	0.086	0.041
100	Fe	0.284	0.293	0.077	0.083	0.041
50.0	Al	0.303	0.310	0.085	0.090	0.040
500	Al	0.274	0.270[b]	—[b]	—[b]	—[b]

[a] Boron concentrations in the S solution (Fig. 1A, lower portion). [b] Distorted peaks.

TABLE 3

Boron contents ($\mu g\ g^{-1}$) in plant leaves, as determined by the suggested stopped-flow and by the earlier [9] procedures

Sample	Procedure	
	Earlier	Stopped-flow
1	21.6	20.6
2	13.8	11.4[a]
3	27.8	27.0
4	15.0	15.4
5	—	5.6[a]
6	21.5	18.8
7	31.6	32.5

[a] With a t_{STOP} period of 90 s.

The suggested procedure is remarkably stable: after 8 hours of continuous operation, only minor changes in the coefficients of the calibration equation (usually less than 5%) were detected. However, baseline drift and modifications in the coefficients of the calibration equation were sometimes observed. Longer warm-up periods and periodic recalibrations are thus recommended. From successive measurements of a typical sample (26.1 $\mu g\ g^{-1}$ B, dry basis),

the standard deviation of the recorded signal was calculated as 0.8%. The accuracy can be assessed by examining the data in Table 3. The sensitivity enhancement relative to the earlier work [9] is mainly due to the three-fold increase in the sample processing time and to the absence of significant sample dispersion.

Partial support of this project by FAPESP (Fundacao de Amparo a Pesquisa do Estado de S. Paulo), by CNPq (Conselho Nacional de Desenvolvimento Cientifico e Tecnologico) and by FINEP (Financiadora de Estudos e Projetos) is greatly appreciated. The authors express their gratitude to F. J. Krug and to H. Bergamin Fº for critical comments, to R. C. Barbosa for her collaboration in the earlier stages of this research, and to Ms. D. Athie for linguistic improvement.

REFERENCES

1 J. Ružička and E. H. Hansen, Anal. Chim. Acta, 78 (1975) 145.
2 E. H. Hansen, D.Sc. Thesis, Lyngby, Technical University of Denmark, 1986.
3 M. Valcárcel and M. D. Luque de Castro, Analisis por inyeccion en flujo, Publicaciones del Monte de Piedad y Caja de Ahorros de Cordoba, Cordoba, Spain, 1984.
4 J. Ružička and E. H. Hansen, Anal. Chim. Acta, 106 (1979) 207.
5 B. J. Compton, J. R. Weber and W. C. Purdy, Anal. Lett. Part B, 13 (1980) 861.
6 P. J. Worsfold and H. Hughes, Analyst, 109 (1984) 339.
7 F. J. Krug, H. Bergamin Fº and E. A. G. Zagatto, Anal. Chim. Acta, 179 (1986) 103.
8 J. Ružička and E. H. Hansen, Flow Injection Analysis, Wiley-Interscience, New York, 1981.
9 F. J. Krug, J. Mortatti, L. C. R. Pessenda, E. A. G. Zagatto and H. Bergamin Fº, Anal. Chim. Acta, 125 (1981) 29.
10 A. Mazaheri, Commun. Soil Sci. Plant Anal., 7 (1976) 331.
11 H. Bergamin Fº, B. F. Reis and E. A. G. Zagatto, Anal. Chim. Acta, 97 (1978) 427.
12 S. S. Jørgensen, K. M. Petersen and L. A. Hansen, Anal. Chim. Acta, 169 (1985) 51.
13 R. Capelle, Anal. Chim. Acta, 24 (1961) 555.
14 F. J. Krug, B. F. Reis, M. F. Gine, E. A. G. Zagatto, J. R. Ferreira and A. O. Jacintho, Anal. Chim. Acta, 151 (1983) 39.
15 B. F. Reis, A. O. Jacintho, F. J. Krug, E. A. G. Zagatto, H. Bergamin Fº and L. C. R. Pessenda, Anal. Chim. Acta, 123 (1981) 221.
16 E. A. G. Zagatto, M. F. Gine, E. A. N. Fernandes, B. F. Reis and F. J. Krug, Anal. Chim. Acta, 173 (1985) 289.
17 E. A. G. Zagatto, O. Bahia Fº and H. Bergamin Fº, Anal. Chim. Acta, 198 (1987) 153.
18 E. Malavolta, personal communication.
19 M. Pinta, Atomic Absorption Spectrometry, Adam Hilger, London, 1975.
20 W. D. Basson, R. G. Bohmer and D. A. Stanton, Analyst 94 (1969) 1135.

Analytica Chimica Acta, 199 (1987) 147—155
Elsevier Science Publishers B.V., Amsterdam — Printed in The Netherlands

THE S_2 EMISSION CHARACTERISTICS OF SEVERAL ORGANIC SULFUR COMPOUNDS OBTAINED BY MOLECULAR EMISSION CAVITY ANALYSIS AND PYROLYSIS

KOICHI NAKAJIMA*

Faculty of Liberal Arts, Hosei University, 2-17-1 Fujimi, Chiyoda-ku, Tokyo 102 (Japan)

TAKEO TAKADA

Department of Chemistry, College of Science, Rikkyo University, 3-34-1 Nishi-Ikebukuro, Toshima-ku, Tokyo 171 (Japan)

(Received 30th December 1986)

SUMMARY

Emission profiles of several organic sulfur compounds are investigated by modified molecular emission cavity analysis (MECA). Thiourea, 1,3-diethylthiourea, *S*-methylcysteine and taurine are pyrolyzed in a hydrogen stream and the pyrolytic products are determined by gas chromatography. The S_2 emission mechanism is discussed on the basis of emission profiles and the composition of the pyrolytic products. Although some compounds give multipeaked responses, the splitting disappears when a worn surface cavity is used or oxalic acid is added to the sulfur compound in the cavity. When the emission profile from thiourea is compared with that from 1,3-diethylthiourea, it is clear that the multipeaked response is due to quenching by degradation products of the latter compound. The main product of pyrolysis is hydrogen sulfide. The emission intensity is related to the yield of hydrogen sulfide in pyrolysis. As methylmercaptan was not detected in the pyrolysis products, it is suggested that the quenching by the organic fragments results from their hydrogen consumption rather than their reaction with sulfur species. The S_2 emission from sulfur-containing compounds is rapidly complete in the presence of oxalic acid, and it is suggested that such compounds are subject to reductive breakdown in the cavity.

If a sulfur compound is introduced into a relatively low-temperature, fuel-rich hydrogen flame and a cold object (shield or cavity) is placed near the flame core, an intense blue emission from S_2 is observed near the surface of the object [1]. This enhancement of the intensity is known as the Salet phenomenon. This emission is useful for selective and sensitive determination of sulfur compounds, but it has several limitations [2]. Each sulfur-containing compound has a different emissivity. The emission intensity is very dependent on the strength with which each sulfur atom is bound in the molecule, and, because of the low temperature of the cool flames, there is a limited amount of energy available for the dissociation of each sulfur atom in the sample molecules. The presence of non-sulfur-containing organic compounds in a sample causes a decrease in the S_2 emission intensity [3—5]. Therefore, the determination of sulfur compounds is quite troublesome; a calibration

0003-2670/87/$03.50

graph is necessary for each compound and a sulfur compound must be separated completely from a quencher. Although conversion of sulfur-containing compounds to sulfur dioxide is a method of escaping from these limitations, it prevents, for example, the simultaneous determination of several sulfur compounds. If the emission and/or quenching mechanisms can be identified, these limitations may be resolved, thus extending the utility of such S_2 emissions.

Molecular emission cavity analysis (MECA) has several advantages compared with the conventional nebulization flame technique or flame photometric detection in gas chromatography. This technique can introduce the cavity to an arbitrary flame position, thus it is easier to investigate the effect of flame composition and/or the flame temperature on the S_2 emission. A solvent which could depress the emission [4] can be evaporated prior to introducing the cavity into the flame. By adding other compounds (which would enhance or quench the S_2 emission) to the cavity with the sample, the effect of such additives on the S_2 emission is readily investigated.

In previous papers, the S_2 emission behavior from several sulfur compounds has been studied by modified MECA [6, 7]. A hydrogen/oxygen flame was used, and the cavity introduction procedure was different from that used by Belcher et al. [8]. But it is impossible to clarify the emission mechanism only from results obtained by MECA. It is essential to identify the species which are formed in the flame, in order to investigate the emission mechanism. As it is difficult to identify the species produced in the flame in-situ, several kinds of sulfur-containing organic compounds were decomposed by heating in a stream of hydrogen, and their degradation products were identified by gas chromatography. This paper describes some of the information regarding the S_2 emission mechanism on the basis of the emission profiles in MECA and the composition of the pyrolytic products of several sulfur-containing organic compounds.

EXPERIMENTAL

Apparatus

The S_2 emission intensity was measured by MECA. The sample was injected into a cavity at the end of a rod held in a sample holder assembly, as shown in Fig. 1. The silica cavity (8 mm deep, 6-mm diameter) was pitched at 8° below the horizontal with the center of the cavity 20 mm above the top of the burner. Belcher et al. [8] introduced the cavity into a flame by turning the cavity holder assembly, but in this procedure, a rapid emission (small t_m value, i.e., the time from inserting the cavity into the flame to achieving maximal intensity) may escape detection. Therefore, in this study, the cavity was reproducibly positioned, by sliding the assembly horizontally on an optical bench, into a nitrogen-sheathed oxyhydrogen flame in line with the detector.

Hydrogen (4 l min^{-1}) and oxygen (0.2 l min^{-1}) were supplied to a total-consumption burner through the fuel (outer) and the nebulizer (inner) inlets,

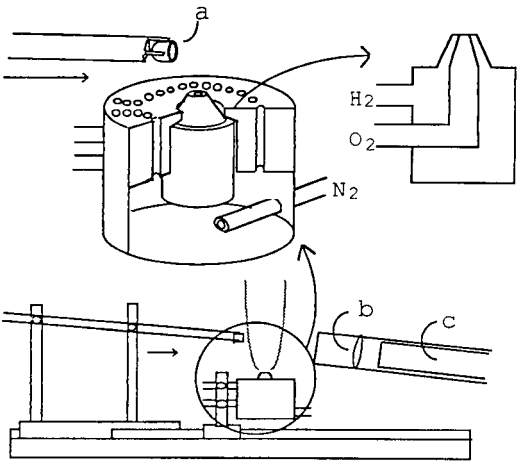

Fig. 1. Arrangement of apparatus for modified MECA: (a) cavity; (b) interference filter; (c) photomultiplier tube.

respectively. The burner was modified so that nitrogen (6 l min^{-1}) could flow around the oxyhydrogen flame to prevent air entering the flame from its surroundings. Generally, introduction of air or oxygen into a hydrogen flame extinguishes the blue S_2 emission owing to the formation of sulfur-oxygen compounds, the increase of flame temperature or decrease in hydrogen atom concentration [8]. In the previous paper [6], when oxygen was introduced to a hydrogen flame, if the oxygen immediately reacted with hydrogen at the top of the burner, the S_2 emission was not affected by the oxygen and intense S_2 emission was observed from sulfur-containing compounds. The temperature and composition of this flame could be controlled exactly and regularly through adjustment of the hydrogen and oxygen flow rates, because the effect of secondary air was negligible [6].

Sample solutions (5 μl) were injected into the cavity from a microsyringe and the solvent was evaporated by a hot air blower, after which the cavity was introduced into the flame. The S_2 emission was viewed through an interference filter (half-bandwidth 18 nm) at 394 nm and recorded on a Shimadzu Chromatopack C-R3A (a data-processing device for gas chromatography) connected to the output of the photomultiplier tube (R268, HTV).

The pyrolyzer used was a Shimadzu PYR-1A. Sample solution (10 or 20 μl) was deposited in a platinum boat and the solvent was evaporated before introduction of the sample holder into a silica tube (6-mm diameter, 170 mm long) in an electric furnace. The sample was pyrolyzed at 800°C in a stream of hydrogen (100 ml min^{-1}) which was used as the surrounding and carrier gas. The effluent gas was collected in a 100- or 50-ml glass syringe and 1-ml aliquots were examined by gas chromatography. Sulfur-containing compounds (H_2S and CH_3SH) and light hydrocarbons in the pyrolytic products were detected by flame photometric and flame ionization detection, respectively. The two gas chromatographs and the conditions used are described in Table 1.

TABLE 1

Equipment and parameters for gas chromatography

	FPD[a]	FID[b]
Gas chromatograph	Shimadzu GC-4BM	Ohkura Model 701
Column	Teflon 3 mm i.d. × 6 m	SUS 3 mm i.d. × 2 m
Packing[c]	APS-1000, 40—60 mesh	Unibeads-1S, 80—100 mesh
Temperature	70°C	70°C
Carrier flow rate	N_2, 70 ml min^{-1}	He, 40 ml min^{-1}
Hydrogen	50 ml min^{-1}	0.5 kg cm^{-2}
Air	60 ml min^{-1}	1.2 kg cm^{-2}

[a]Flame photometric detector. [b]Flame ionization detector. [c]Gaskuro Kogyo.

A Shimadzu TGA-30M was used for thermogravimetric analysis of thiourea and 1,3-diethylthiourea. About 10 mg of solid sample was introduced into the platinum cell and the weight loss was measured at a heating rate of 20°C min^{-1} in an atmosphere of nitrogen (30 ml min^{-1}).

Reagents

All water used was distilled. Thiourea (Wako), 1,3-diethylthiourea (Tokyo Kasei), *S*-methylcysteine (Aldrich), taurine (Kanto) and oxalic acid (Kanto) were of analytical-reagent grade and were used without further purification. Stock solutions (500 μg S ml^{-1} for sulfur compounds and 0.25 M for oxalic acid) of each compound were prepared by dissolving the compounds in water or 99.5% (v/v) ethanol. These solutions were further diluted to give the concentrations required in the experiments.

RESULTS AND DISCUSSION

The S_2 emission profiles of thiourea, 1,3-diethylthiourea, *S*-methylcysteine and taurine (250 ng S) were observed by MECA by using a nitrogen-sheathed oxyhydrogen flame, and are shown in Fig. 2. In MECA, a single emission peak is normally observed from a compound containing a single sulfur grouping [9, 10], but multipeaked responses have also been observed. Multipeaked responses were obtained from 30—300 ng S in 1,3-diethylthiourea. The intensity of the second peak increased with the concentration of 1,3-diethylthiourea, but the first changed very little. When 1,3-diethylthiourea or *S*-methylcysteine was mixed with oxalic acid (0.25 M, 5 μl) within a cavity, however, the resulting emission response (Fig. 2, c, e) was a rapid single peak, and the emission intensity was greater than that in the absence of oxalic acid. A transparent silica cavity commonly becomes translucent and rough with prolonged use. When the cavity had such a worn surface, 1,3-diethylthiourea gave a single peak.

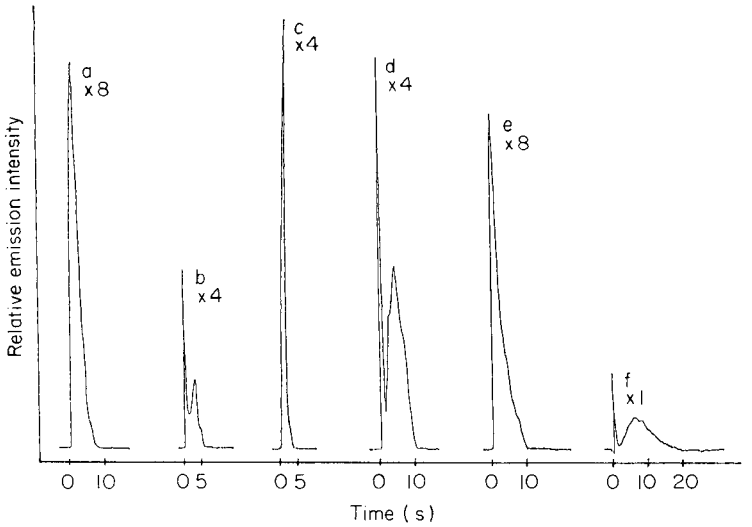

Fig. 2. Emission/time profiles from several sulfur compounds: (a) thiourea, 250 ng S; (b) 1,3-diethylthiourea, 250 ng S; (c) 1,3-diethylthiourea, 250 ng S + 0.25 M oxalic acid, 5 μl; (d) *S*-methylcysteine, 250 ng S; (e) *S*-methylcysteine, 250 ng S + 0.25 M oxalic acid, 5 μl; (f) taurine, 250 ng S. (×8 etc. indicates the factor by which the peak height should be multiplied.)

A possible reason for peak-splitting is that the second peak is formed by the delayed decomposition of a portion of the sample deposited in a corner of the cavity, as there would be a temperature gradient within the cavity. In this case, if breakdown is caused by thermal decomposition, a compound with a high decomposition temperature would always give a multipeaked response. However, from the thermogravimetric measurements, the decomposition temperature of thiourea, which gives a single peak, was higher than that of 1,3-diethylthiourea which gives multiple peaks. Therefore, it is clear that the peak-splitting cannot be attributed to the difference of temperature of the cavity and the decomposition temperature of the compound.

Multipeaked responses like that shown in Fig. 2 have been also observed from several other compounds [4, 8, 10, 11]. Some of these were explained by the mode of breakdown, i.e., the decomposition reaction sequence [10]. However, as the amount of thiourea in the cavity increased, the peak height increased slightly, but further peaks also appeared [8]; this effect may arise from the interaction of some of the initial decomposition products with undecomposed sample, to form a less volatile compound [10]. But, from the results of thermogravimetric measurements on thiourea and 1,3-diethylthiourea, it was found that no such less volatile compound was formed.

The S_2 emission profile is affected not only by the binding energy of sulfur in a compound, because the emission profile of 1,3-diethylthiourea (Fig. 2b)

was different from that of thiourea (Fig. 2a). Because the presence of oxalic acid or the use of a worn-surface cavity gave a large emission intensity and a single peak response, the multiple peaks are presumably a result of quenching by the degradation products. Generally, the presence of non-sulfur-containing organic compounds in a sample quenches the S_2 emission from a sulfur compound [3—5]. These suppressions may be caused by the same process. Sugiyama et al. [12] suggested that the decrease in the emission intensity can be attributed to inactivation of the excited S_2* species by its combination or collision with organic compounds and/or organic degradation products. If the excited S_2* species reacts with organic fragments, a compound such as methylmercaptan, methyl sulfide or dimethyl disulfide should be produced in the flame.

As it is difficult to detect these compounds in situ, pyrolysis was used as a quasi-flame system. Several sulfur-containing compounds (5—10 μg S) were pyrolyzed at 800°C in a hydrogen stream (100 ml min^{-1}), because the temperature of the flame used in MECA was 800—900°C. The degradation products were collected in a syringe, and the composition of the gaseous products was determined by gas chromatography. The results are shown in Table 2. The main product was hydrogen sulfide. Methylmercaptan was produced in *S*-methylcysteine pyrolysis, as well as a large amount of methane. But it appears doubtful that the methylmercaptan was produced by the reaction of sulfur and degradation products, because methylmercaptan was not detected in the pyrolytic products from 1,3-diethylthiourea which gave a smaller emission response than *S*-methylcysteine.

When a large amount of a compound (mg level) was pyrolyzed, however, methylmercaptan was produced by all the sulfur compounds. Therefore, the S_2 emission may be quenched by the reaction or collision of sulfur with organic fragments, when the amounts of such fragments in the cavity are large. However, in practice, as the suppression is caused by a small amount of sample (sub-ng level), it must be supposed that the quenching arises from another process.

The results in Fig. 2 and Table 2 show that a compound which formed a large amount of hydrogen sulfide gave a much more intense emission than those that formed a small amount of hydrogen sulfide. The amount of hydrogen sulfide formed by thiourea pyrolysis increased with an increase in the hydrogen flow rate through the heating chamber (Fig. 3). It was previously reported [7] that the S_2 emission intensity in MECA increased with an increase in the hydrogen flow rate of the flame. Therefore, it is probable that the amount of hydrogen sulfide produced by pyrolysis is closely connected with the S_2 emission intensity in the flame.

It has been suggested that an S_2 molecule is excited by the recombination reaction of hydrogen atoms [13]:

$$2H\cdot + S_2 \rightarrow S_2^* + H_2$$

Sugiyama et al. [14] suggested that a sulfur-containing compound is first

TABLE 2

Composition of gaseous products formed by pyrolysis of sulfur compounds

Compound	Sulfur species[a]		Hydrocarbon[b]		
	H_2S[c]	CH_3SH[c]	CH_4[d]	C_2H_6[d]	C_2H_4[d]
Thiourea	53 000	0	29[d]	0[d]	0[d]
1,3-Diethylthiourea	16 000	0	74	34	130
S-methylcysteine	21 100	600	255	15	38
Taurine	750	0	34	22	57

[a] 5 μg S (500 μg S ml^{-1}, 10 μl); sample was pyrolyzed, and gaseous products were collected in a 100-ml syringe. [b] 10 μg S (500 μg S ml^{-1}, 20 μl); sample was pyrolyzed, and gaseous products were collected in a 50-ml syringe. [c] Arbitrary units. [d] μl l^{-1}.

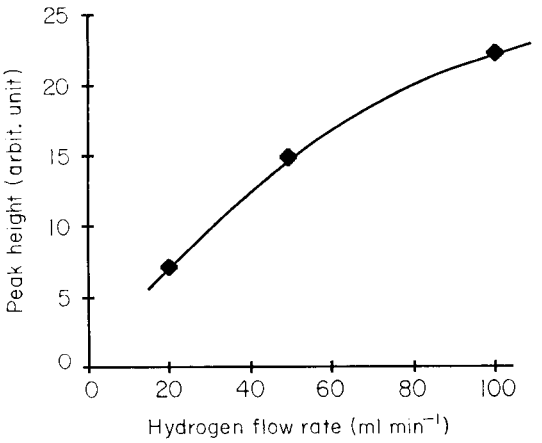

Fig. 3. Effect of hydrogen flow rate on the yield of hydrogen sulfide in the pyrolysis of thiourea (2.5 μg S).

converted to hydrogen sulfide in the flame, followed by the formation of S_2:

$$\text{S-compound} \xrightarrow{n\text{H}} H_2S; \quad H_2S \rightarrow S; \quad S + S \rightarrow S_2$$

The above results support this process, and suggest that the amounts of hydrogen atoms have an effect not only on the S_2 excitation process but also on the formation of hydrogen sulfide. Therefore, the quenching by the organic fragments may be explained on the basis that they consume hydrogen atoms and hinder the formation of hydrogen sulfide.

As shown in Fig. 2, the S_2 emission from 1,3-diethylthiourea is more rapidly completed in the presence of oxalic acid than in its absence, which means that oxalic acid promotes the breakdown of 1,3-diethylthiourea.

Although the role of oxalic acid is not clear, the result shows that the sulfur-containing compound apparently undergoes a reductive breakdown. The emission profile from thiourea was more slowly completed than that from 1,3-diethylthiourea, as shown in Fig. 2. This suggests that sulfur compounds undergo both reductive and thermal breakdown. As thiourea would be little affected by the degradation products, if only reductive breakdown took place, then the emission should be completed more rapidly than that from 1,3-diethylthiourea.

The emission was initiated immediately after introduction of the cavity into the flame. But the cavity does not instantly achieve a high temperature. Therefore, the S_2 emission is initiated by reductive breakdown, and thermal breakdown occurs relatively slowly as the cavity heats up. Therefore, the multipeaked response may be attributed to reductive breakdown for the first peak and thermal breakdown for the second peak. If it is assumed that 1,3-diethylthiourea consumes a lot of hydrogen atoms during the reductive breakdown, this can explain why only the second peak intensity increased with the amount of sample. The rate of reductive breakdown is dependent on the concentration of hydrogen atoms but not on the amount of sample; however, the rate of thermal breakdown is dependent on the heating rate of the cavity and on the amount of sample. As the rate of reductive breakdown would be decreased with an increase in the hydrogen atom consumption by organic fragments, the multipeaked response would be observed.

Conclusions

It is suggested that the formation of excited S_2 molecules follows the formation of hydrogen sulfide. Hydrogen atom consumption by organic fragments may be responsible for the quenching and the observed multipeaked response. It was found that the S_2 emission is initiated by reductive breakdown of the compound in the cavity, and that thermal decomposition occurs relatively slowly as the cavity heats up in the flame. This suggests that the emission profile is also affected by the flame composition and temperature.

The presence of oxalic acid with a sulfur-containing compound promotes the breakdown of the compound and enhances the S_2 emission intensity. It is well known that a coating of phosphoric acid on the cavity enhances the S_2 emission intensity; it was suggested that the coating would reduce the rate of hydrogen atom recombination [11, 15]. Oxalic acid is not refractory, however, and the effect of oxalic acid may not be the same as that of phosphoric acid. Although the effects of oxalic acid and worn surfaces have not been explained completely, several causes can be considered. For the oxalic acid effect, these may be carbon particles deposited on the surface or hydrogen atom and/or some radical formation by the reaction of hydrogen with oxalic acid; the effect of worn surfaces may be due to an increase in the catalytic surface area. Work is still in progress to clarify the reasons for these effects.

The authors thank Prof. H. Hagiwara, Prof. S. Saitou and Prof. H. Kurita for their help and advice.

REFERENCES

1 C. Veillon and J. Y. Park, Anal. Chim. Acta, 60 (1972) 293.
2 S. O. Farwell and R. A. Rasmussen, J. Chromatogr. Sci., 14 (1974) 224.
3 W. E. Rupprecht and T. R. Phillips, Anal. Chim. Acta, 47 (1969) 439.
4 R. Belcher, S. L. Bogdanski, S. A. Ghonaim and A. Townshend, Anal. Lett., 7 (1974) 133.
5 M. Dressler, J. Chromatogr., 270 (1983) 145.
6 K. Nakajima and T. Takada, Bunseki Kagaku, 33 (1984) 183.
7 K. Nakajima and T. Takada, Bunseki Kagaku, 33 (1984) 271.
8 R. Belcher, S. L. Bogdanski and A. Townshend, Anal. Chim. Acta, 67 (1973) 1.
9 M. Q. Al-Abachi, Proc. Anal. Div. Chem. Soc., 14 (1977) 251.
10 M. Burguera, S. L. Bogdanski and A. Townshend, CRC Crit. Rev. Anal. Chem., 10 (1980) 185.
11 R. Belcher, S. L. Bogdanski, D. J. Knowles and A. Townshend, Anal. Chim. Acta, 77 (1975) 53.
12 T. Sugiyama, Y. Suzuki and T. Takeuchi, J. Chromatogr., 80 (1973) 61.
13 A. G. Gaydon, The Spectroscopy of Flames, Chapman and Hall, London, 1974, p. 309.
14 T. Sugiyama, Y. Suzuki and T. Takeuchi, J. Chromatogr., 77 (1973) 309.
15 T. J. Cardwell and P. J. Marriott, Anal. Chim. Acta, 121 (1980) 175.

Analytica Chimica Acta, 199 (1987) 157—160
Elsevier Science Publishers B.V., Amsterdam — Printed in The Netherlands

Short Communication

THE pH-STATIC ENZYME SENSOR
An ISFET-based Enzyme Sensor, Insensitive to the Buffer Capacity of the Sample

BART H. VAN DER SCHOOT* and PIET BERGVELD

Department of Electrical Engineering, Twente University, P.O. Box 217, 7500 AE Enschede (The Netherlands)

(Received 21st May 1987)

Summary. An ISFET-based urea sensor is combined with a noble-metal electrode which provides continuous coulometric titration of the products of the enzymatic reaction. The sensor thus becomes independent of the buffer capacity of the sample; and because the enzyme is operating at a constant pH, the linear response range is expanded.

Enzyme sensors based on the measurement of pH consist basically of a pH-sensitive electrode to which an enzyme-loaded membrane is attached. The conversion of substrate in the immobilized enzyme membrane results in a local change in pH which can then be measured. The pH-sensitive electrode used is usually a glass membrane electrode or an ISFET. In 1980, Caras and Janata [1] described the first ISFET-based enzyme sensor sensitive to penicillin. The name ENFET was introduced for this sensor.

The response of enzyme sensors based on the measurement of pH is sensitive to the buffering capacity of the sample. Furthermore, these electrodes have a non-linear response for two reasons. First, the buffering capacity of the sample solution is pH-dependent; this implies that pH changes in the immobilized enzyme membrane depend on the initial pH of the sample solution. A second, and perhaps even more important reason for the non-linear response is the pH-dependent enzyme kinetics. It is well known that each enzyme has its own optimal pH value at which its activity is greatest. Thus, at high substrate concentrations, the pH changes in the enzyme membrane may become so large that the enzyme is actually inhibiting its own performance. The complex response characteristics of these enzyme electrodes have been the subject of a number of papers (see, e.g. [2, 3]) and the general conclusion is that the practical applicability is limited.

Recently, ISFET-based sensors have been developed for the performance of coulometric acid/base titrations on a very small scale. This is achieved through the application of a noble-metal electrode that is arranged closely around the pH-sensitive gate of the ISFET. Through the electrolysis of water, H^+ or OH^- ions are formed, depending on the direction of the current from this electrode to a distantly located counter electrode. In this way, a

0003-2670/87/$03.50

simple pH-actuator is added to the ISFET and local pH changes can be generated. The practical value of this technique has been shown in a system for titrations in microliter samples [4] and in a new type of carbon dioxide sensor with excellent long-term stability [5]. In this communication, the first results of the application of such a system in an enzyme sensor are presented. Through the use of a feedback system, the products of the reaction in the immobilized enzyme membrane are continuously titrated. In this way, the pH in the membrane is kept equal to that of the sample solution and thus the enzyme is operating at a constant pH. Therefore, it seems appropriate to call this sensor a pH-static enzyme sensor. The amount of current that is needed for the coulometric neutralization of the reaction products is proportional to the substrate concentration. The application of this technique for the improvement of the response of enzyme electrodes has also been proposed by Chandler and Eddowes [6].

Experimental

A cross-section of the pH-static enzyme sensor is shown in Fig. 1. The membrane consists of a cross-linked mixture of albumin and urease. The Ta_2O_5 gate oxide of the ISFET is silanized with 3-aminopropyltriethoxysilane. Bovine albumin (25 mg; Sigma A-7030) and 25 mg of urease (EC 3.5.1.5, Sigma Type IX, U-4002) were dissolved in 0.5 ml of 25 mM phosphate buffer, pH 7. To this solution, 0.2 ml of glutaraldehyde (2% in water) was added and a drop of this mixture was deposited over the surface of the sensor/actuator chip that was encapsulated with an epoxy resin. After some hours, the cross-linking reaction was complete and the sensors were ready for use.

The sensor that is thus created can of course also be operated like a "normal" ENFET, i.e., without the use of the generating electrode. In that

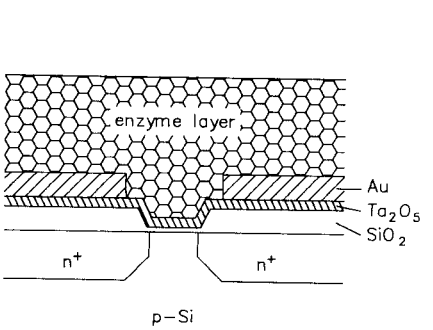

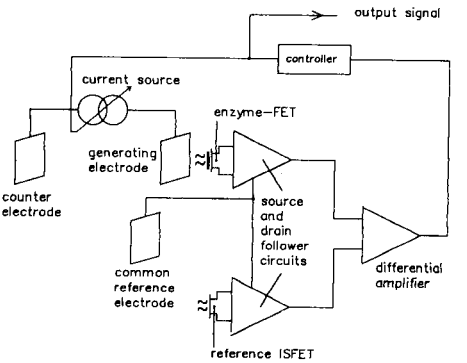

Fig. 1. Schematic cross-section of the pH-static enzyme sensor. The enzyme membrane is deposited over the entire structure.

Fig. 2. Coulometric control system in which the pH in the enzyme membrane is kept equal to that in the sample solution.

case, pH changes are measured as a function of substrate concentration. Measurements were made in phosphate buffers of various concentrations at pH 7. The buffer solutions were contained in an ordinary 100-ml glass beaker and were not stirred. The substrate concentration was changed through the addition of small aliquots of a concentrated urea solution.

If the sensor is to be operated in the pH-static mode, the control system outlined in Fig. 2 is used. In this system, the pH in the enzyme membrane is continuously compared to that of the sample solution as it is measured with the reference ISFET. If urea is added to the solution, the pH in the enzyme membrane will rise and the controller will then activate the current source that is connected to the generating electrode. The operation of the system is such that the alkaline products of the enzymatic reaction, i.e., ammonia, are constantly neutralized.

Results

Figure 3 shows that the response of the ENFET is dependent on the buffer capacity of the sample solution. The pH-sensitivity of the ISFET's used for these experiments was approximately 50 mV/pH. It can be seen that the output values level off when the response is about 100 mV. This change in output voltage corresponds to a pH value of ca. 9 in the immobilized enzyme membrane.

When the pH-static mode is used (Fig. 2), the amount of current required to provide continuous neutralization is linearly related to the substrate concentration (Fig. 4). The response is almost independent of the buffer capacity of the sample. A second important advantage of this method is that the linear range can be expanded. Without continuous neutralization, the response levels off at high substrate concentrations (Fig. 3). In the case of the pH-static sensor, however, the enzyme operates at constant pH and its activity is not inhibited by its own products. It must be noted that in the

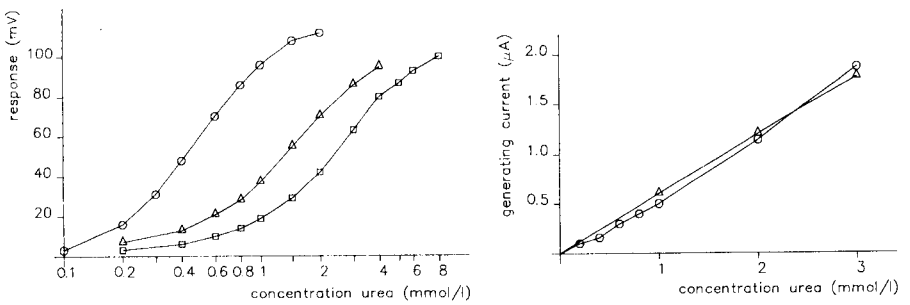

Fig. 3. The sensitivity and dynamic range of the urea-ENFET depend on the buffer capacity of the sample. Buffer concentration (mmol l^{-1}): (○) 1; (△) 5; (□) 10.

Fig. 4. The output of the pH-static enzyme sensor is independent of the sample buffer capacity and the dynamic range is expanded. Buffer concentration (mmol l^{-1}): (○) 1; (△) 5.

case of the normal ENFET, the response to added urea is logarithmic so that Fig. 3 is plotted on a semilogarithmic scale in the conventional manner. In contrast, the coulometric response with the pH-static sensor is linearly related to urea concentration (Fig. 4). Comparison of these two figures show that the linear response ranges for the 1 and 5 mmol l^{-1} buffers are clearly expanded with the latter method of measurement.

Conclusion

The first results obtained with the pH-static enzyme sensor show that this method of controlling the internal membrane pH is a practical solution for the problem of buffer dependence. However, various technological problems have yet to be solved. The results are fairly reproducible but it was found that albumin is not the most suitable membrane material. Because the pH-sensitive gate area of the ISFET and the generating electrode cannot be physically located in the same point, there is necessarily a small distance between the two. Therefore, during the application of the coulometric compensation current, a pH gradient is formed in the membrane. The pH directly at the surface of the generating electrode is considerably lower than the pH at the ISFET gate where it is kept equal to the bulk pH of the solution. Through these lateral pH differences, deformations occur in the protein layer and the response time of the sensor is increased. The construction of the sensor must therefore be optimized by choosing a different geometry or other membrane materials.

The integration of an enzymatic membrane with a sensor/actuator system offers the possibility of controlling the internal membrane pH. Of course, the method is not limited to keeping the membrane pH equal to that of the sample solution. It should also be possible to control the membrane pH in such a way that an enzyme is always operating at its optimal pH value.

Part of this work was financed within the Dutch Biosensor Stimulation Programme by the Centre for Micro-Electronics Twente. B.H.v.d.S. thanks the Royal Netherlands Academy of Arts and Sciences for the award of a fellowship.

REFERENCES

1 S. Caras and J. Janata, Anal. Chem., 52 (1980) 1935.
2 S. D. Caras, J. Janata, D. Saupe and K. Schmidt, Anal. Chem., 57 (1985) 1917.
3 M. J. Eddowes, Sensors and Actuators, 7 (1985) 97.
4 B. H. van der Schoot and P. Bergveld, Sensors and Actuators, 8 (1985) 11.
5 B. H. van der Schoot and P. Bergveld, Proc. 2nd International Meeting on Chemical Sensors, Bordeaux, France, July, 1986, Université Bordeaux 1, ISBN 2-906257-00-1, 1986, pp. 665—668.
6 G. K. Chandler and M. J. Eddowes, Proc. 2nd International Meeting on Chemical Sensors, Bordeaux, France, July, 1986, Université Bordeaux 1, ISBN 2-906257-00-1, 1986, pp. 531—533.

Analytica Chimica Acta, 199 (1987) 161—165
Elsevier Science Publishers B.V., Amsterdam — Printed in The Netherlands

Short Communication

ANODIC RESPONSE TO OXYGEN OF AN ELECTROCHEMICAL DETECTOR IN HIGH-PERFORMANCE LIQUID CHROMATOGRAPHY AND FLOW-INJECTION ANALYSIS

J. B. F. LLOYD

Home Office Forensic Science Laboratory, Priory House, Gooch Street North, Birmingham B5 6QQ (Great Britain)

(Received 1st May 1987)

Summary. A strong anodic response associated with the presence of oxygen in liquid chromatography and flow-injection solvent streams is found to occur at the porous-graphite electrodes of a commonly available detector cell. Removal of oxygen lowers the residual current and improves the detection limits considerably in oxidatively-detected analyses.

Under the usual conditions of electrochemical detection in the reductive mode, whether in flow-injection analysis or in high-performance liquid chromatography (HPLC), oxygen produces a strong cathodic response and must be removed from the solvent if low (cathodic) residual currents and, hence, detection limits are to be obtained. It is shown here that a similar effect in an anodic sense can occur under some conditions with oxidative detection, the sensitivity of which also may be improved by the use of deoxygenated solvents.

Experimental

Reagents and solvents were of Aristar grade (BDH) or HPLC grade (Rathburn, Walkerburn, U.K.).

The chromatograms were run on 150 mm × 4.5 mm columns of 3-μm ODS-Hypersil (Shandon) with deoxygenated samples and solvent (methanol/aqueous phosphate, pH 3; 100:55, v/v) as described previously [1]. (Gentle refluxing is used to deoxygenate the solvent.) For flow-injection work, the column was replaced with a 70-cm length of 0.4 mm i.d. stainless-steel tubing. All of the steel tubing used in the system had been passivated with nitric acid, and the chromatography columns had been extracted with EDTA at pH 7 to remove heavy metal impurities.

Usually the oxidative detector was an Environmental Sciences Associates (ESA) unit, model 5100A (Severn Analytical, Gloucester). This was fitted with a dual "coulometric" cell containing two porous-graphite working electrodes in series (part 5010), or with a cell containing a porous-graphite and a glassy carbon (wall-jet) working electrodes in series (part 5012). The quoted

0003-2670/87/$03.50

electrode potentials are with reference to the proprietary reference electrodes in the cells, stated in the manual to be dependent on the H_2/H^+ couple. In each series of experiments, the cells were conditioned at the highest potential setting to be used. Other procedures gave no significant advantage either in performance or in stabilization time. In some experiments, a Metrohm wall-jet detector (model 656) was used.

Reductive-mode detection was with a modified Princeton Applied Research flow cell detector (model 310) and accessory instrumentation [1]. The hanging mercury drop size was 6 mg.

Results and discussion

When an aerated sample is injected into a deoxygenated HPLC system operated with electrochemical reductive detection, an intense and characteristically broadened peak from the reduction of oxygen is produced. If the sample is purged with nitrogen, the peak is eliminated [2].

A corresponding peak, at the same retention time, appears when the experiment is repeated with oxidative detection at the porous-graphite electrode of the ESA cell, just as though the response is due to the oxidation of oxygen. This is shown in Fig. 1. Below electrode potentials in the region of +0.8 V (chromatogram B), the peak shape is similar to the reductive response, but at higher potentials the peak becomes increasingly distorted and the baseline is displaced as in the +1.0 V example (chromatogram C). No peak is seen when the sample is deoxygenated (chromatogram A). An inverted response occurs if a deoxygenated sample is injected into an aerated chromatography system.

The response is detectable over all the positive potential range. This is shown by the flow-injection results summarized in Fig. 2, curve A, where the variation with potential of peak heights from injections of aerated solvent samples into a deoxygenated solvent stream are plotted. Peak heights rather than areas are used because in the region of the distortion the peaks could not sensibly be integrated. At negative potentials, the response disappears into the reduction wave of oxygen. The variation with electrode potential of the residual current at a porous-graphite electrode in a solvent stream before and after deoxygenation is also shown in Fig. 2. At negative potentials, differences occur because of the oxygen reduction. At positive potentials up to +0.7 V the differences are small, but from this point there is a rapid anodic increase in the residual current from the aerated solvent (curve B), but a negligible increase from the deoxygenated solvent (curve C). The respective values at +1.0 V are 14.6 μA and 0.35 μA. That the increase apparently is much greater than the increase in the aerated sample peak heights (curve A) is probably a spurious effect related to the peak distortion. At less negative potentials, however, the peak heights considerably exceed the residual currents from the aerated solvent, even though the oxygen concentrations in the aerated solvent stream and in the samples injected into the deoxygenated stream were similar (in equilibrium with the laboratory atmosphere) and the

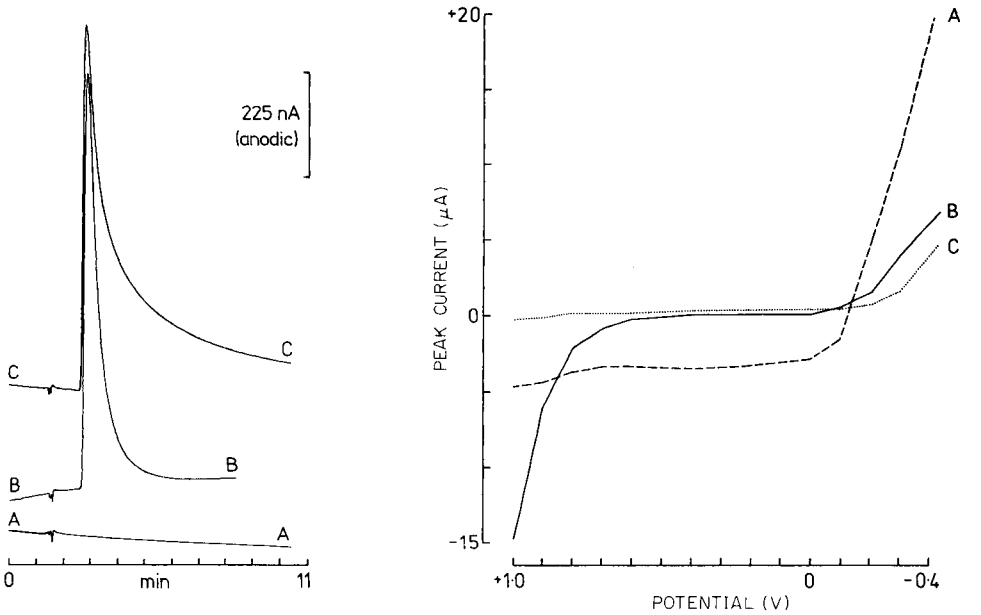

Fig. 1. Liquid chromatograms in deoxygenated solvent with detection at an ESA porous-graphite electrode at +0.8 V (A and B) and +1.0 V (C) vs. a proprietary reference electrode. The sample in each case was the blank solvent, which was either nitrogen-purged (A) or aerated (B and C).

Fig. 2. Flow-injection results showing the variation of peak height with potential of a porous-graphite electrode from the injection of aerated solvent samples (10 μl) into a deoxygenated solvent stream (A), and the variation of the residual current from aerated (B) and deoxygenated (C) solvent streams.

oxygen concentration at the peak maxima was decreased by flow-dispersion. Possibly in the continual presence of oxygen, the electrode becomes passivated to oxygen. Evidently this occurs in the cathodic region too, as Fig. 2 shows. A similar effect has been reported at glassy-carbon electrodes [3].

Each of the five porous-graphite electrodes that have been used (four in the dual cells, and one in the porous-graphite/glassy-carbon cell) have exhibited qualitatively similar effects. Although they have varied considerably in magnitude between different electrodes, the effects have always been significant to the HPLC application of the electrodes. The data in Fig. 2 are from an intermediate case. There seems to be no marked dependence on the history of an electrode, or on the methanol content and pH of the solvent within the ranges limited by the conditions typical of reversed-phase chromatography on bonded-phase columns. An oxygen peak monitored reductively at the mercury electrode, or oxidatively at a porous-graphite electrode, is not perceptibly varied in amplitude by an oxidatively-responding upstream electrode which,

therefore, causes no significant depletion of oxygen. Neither did the installation of an electrochemical guard cell, to oxidize any solvent impurities, affect the results. The response could be detected only weakly at the ESA glassy-carbon electrode, and not at all at the Metrohm glassy-carbon electrode.

The voltammetric response of the porous-graphite cells to oxidizable compounds appears not to be significantly affected by oxygen. Thus, hydrodynamic voltammograms of hydroquinone (100 pmol flow-injections) in aerated and deoxygenated solvents displayed anodic waves with half-heights at +0.42 V and +0.43 V, respectively. Diphenylamine (50 pmol injections) gave respective results of +0.66 V and +0.67 V. However, the wave heights under the aerated conditions were decreased by 8% and 9%, respectively, possibly because of a direct reaction with oxygen in an adsorbed or bound state on the electrode surface.

The origin of the sensitivity to oxygen is a matter of speculation. Perhaps the anodic corrosion that can occur at graphite electrodes [4] is involved. In the present case, this would be particularly favoured by the large surface area of the electrodes, and might be increasingly promoted at increasingly negative potentials by the presence of oxygen. Whether or not this is so, it is unquestionable that because of the usual dependence of the noise level and drift in a baseline signal on the magnitude of the residual current, detection limits at this type of electrode can be enhanced substantially if oxygen is removed from the system. An example is shown in Fig. 3, where chromatograms of samples

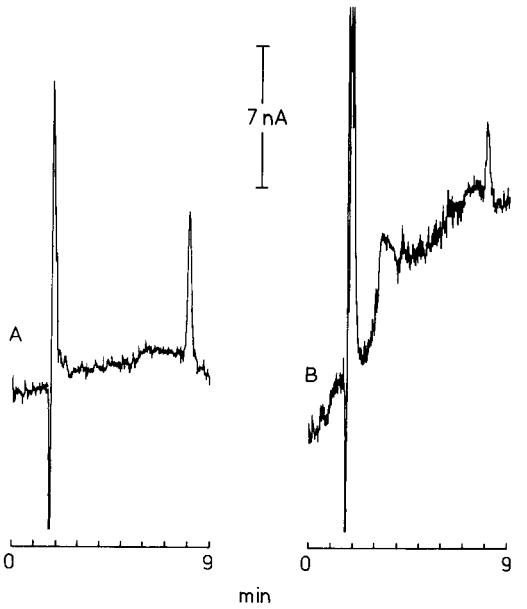

Fig. 3. Liquid chromatograms, with detection at +0.8 V, of diphenylamine (100 fmol, 16.9 pg), under deoxygenated (A) and aerated (B) conditions. The peak for diphenylamine is at 8 min.

containing diphenylamine (100 fmol, 16.9 pg) are compared under deoxygenated (A) and aerated (B) conditions. Apart from the reduced noise level and drift in the deoxygenated case, the increased response to the analyte is also apparent.

REFERENCES

1 J. B. F. Lloyd, Anal. Chim. Acta, 154 (1983) 121.
2 K. Bratin and P. T. Kissinger, Talanta, 29 (1982) 370.
3 A. B. Ghawji and A. G. Fogg, Analyst, 111 (1986) 157.
4 J. P. Randin, in J. O'M. Bockris, B. E. Conway, E. Yeager and R. E. White (Eds.), Comprehensive Treatise of Electrochemistry, Vol. 4, Plenum, New York, 1981, Chap. 10.

Analytica Chimica Acta, 199 (1987) 167—171
Elsevier Science Publishers B.V., Amsterdam — Printed in The Netherlands

Short Communication

DETERMINATION OF MERCURY TRACES BY DIFFERENTIAL-PULSE STRIPPING VOLTAMMETRY AFTER SORPTION OF MERCURY VAPOUR ON A GOLD-PLATED ELECTRODE

FRITZ SCHOLZ*, LUTZ NITSCHKE and GÜNTER HENRION

Wissenschaftsbereich Analytik, Sektion Chemie, Humboldt-Universität, 1040 Berlin, Hessische Straße 1-2 (German Democratic Republic)

(Received 3rd October 1986)

Summary. Trace mercury is reduced with tin(II) to mercury metal, which is volatilised by bubbling air through the solution. A certain fraction of this mercury is sorbed on a rotating gold disk electrode and stripped in a thiocyanate solution. The detection limit is about 30 ng Hg(II) in solution; the relative standard deviation is 6% for 100 ng Hg(II) (n = 7). The detection limit for mercury in air is 1.7 ng l^{-1} with a preconcentration time of 10 min.

The determination of traces of toxic metals such as mercury in biological materials, natural waters and in air has become increasingly important. Anodic stripping voltammetry (ASV) is a well established technique for quantifying traces of heavy metal ions. In organic trace analysis, adsorptive stripping is often used for the preconcentration of organic substances [1, 2] but there are few examples of the application of adsorptive stripping in organic trace analysis [3].

Mercury, which should be very suitable for adsorptive stripping, has so far been preconcentrated in ASV only by reductive electrodeposition. Wax-impregnated graphite [4, 5], glassy carbon [6, 7] and carbon paste [8] have been used as the electrode materials in ASV of mercury. Sipos et al. [9, 10] applied gold electrodes in a differential pulse method (DPASV) for mercury. They used twin gold disk electrodes and worked in the subtractive mode to avoid interferences from copper which otherwise seemed to be impossible. Johnson and co-workers [11, 12] devoted much effort to the electrochemistry and determination of mercury. Lindstrom [13] described DPASV with gold electrodes in a flow-injection determination of mercury, obtaining a detection limit for mercury in aqueous solutions of approximately 5×10^{-10} mol l^{-1}. At the 2 μg l^{-1} Hg(II) level, the reproducibility was better than 2%. Goto et al. [14] applied the semidifferential method in the ASV of Hg(II) at a gold disk electrode and reported the same detection limit of 5×10^{-10} mol l^{-1}.

In the case of electrodeposition of mercury, underpotential deposition plays an important role. As long as the deposition conditions ensure the

0003-2670/87/$03.50

formation of less than a monolayer, a single peak is obtained for mercury oxidation. Accordingly, these requirements must be fulfilled to get reliable results. In this communication, a special version of adsorptive stripping is reported for the determination of mercury. The main principle, which has been described recently [15], is the sorption of mercury from the gaseous phase on a gold-plated disk electrode.

Because of its strong affinity for mercury, gold has long been used for the collection of mercury vapour in chemical analysis. The first analytical application was the Eschka method for the gravimetric determination of milligram amounts of mercury [16, 17]. In 1878, a gold cathode was used for the electrogravimetric determination of mercury [17, 18]. Later, gold wool served as the collector for mercury vapour in numerous procedures based on cold-vapour atomic absorption spectrometry (AAS) [19]. It is rather surprising that nobody seems to have used this process of collection in voltammetric work. The only electrical method which utilises the mercury collection on gold is the Jerome method [20]; the conductivity changes of a thin gold layer on an insulator, which occur after mercury sorption, are used to determine mercury in gases.

In the proposed method, mercury is determined by anodic stripping voltammetry after preconcentration by sorption of mercury vapour onto a gold rotating disk electrode. The mercury is stripped after transference of the electrode to a suitable solution.

Experimental

Reagents. The mercury(II) solutions were stabilized with nitric acid and potassium dichromate as described by Feldman [21]. All chemicals were of analytical-reagent grade.

The gold bath for plating contained 0.9 g of potassium dicyanoaurate (prepared from hydrogen tetrachloroaurate [22]), 1.0 g of potassium cyanide, 0.5 g of sodium carbonate and 1.0 g of disodium hydrogenphosphate diluted to 100 ml with water.

Equipment. Measurements were done with a computerized electrochemical system (ECM-700; ZWG der AdW der DDR, Berlin) connected to a printer (model 1154, Robotron, DDR). A type 1.200002 pump (Reglerwerk Dresden) served for aspiration of air. The driving device for the syringe to add the mercury-saturated air was a Lineomat (MLW, DDR).

The best results were obtained with an electrode prepared by plating a 2.5-μm layer of gold onto a platinum disk electrode (10-mm diameter).

Determination of mercury in liquid samples. Mercury(II) was first reduced to the metal as in the procedure for cold-vapour atomic absorption spectrometry. The sample was diluted with water, 25 ml of concentrated sulfuric acid and 5 ml of concentrated nitric acid were added to a volume of 100 ml. This solution was prepared in the flask shown in Fig. 1. Then 20 ml of a solution containing 3% (w/v) sodium chloride and 3% (w/v) hydroxylammonium sulphate was added, followed by continuously dropwise add-

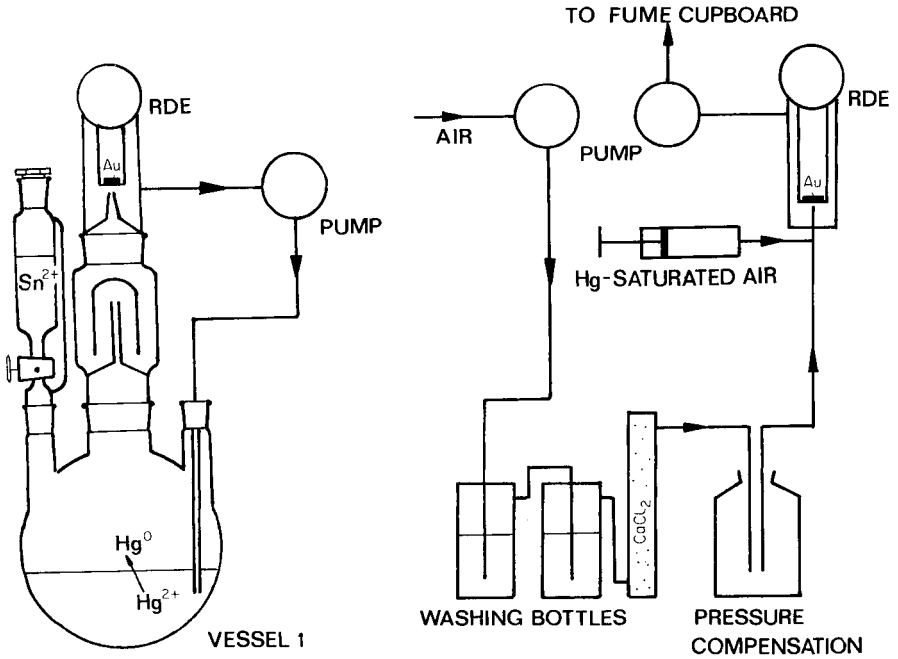

Fig. 1. Apparatus for the volatilisation and sorption of mercury vapour from solution.

Fig. 2. Apparatus for air analysis.

ition of 10 ml of a 10% (w/v) tin(II) sulphate solution. The pump was switched on, so that air was bubbled through the solution and was cycled through the system. After passing through a trap to collect any droplets sprayed from the solution, the air was led through a narrow jet (1.0 mm internal diameter) onto the rotating gold electrode (1500 rpm) where sorption took place. The sorption time was 5 min for the range 20—200 ng of mercury and 2 min for higher amounts.

After a constant sorption time, the pump was switched off and the electrode was transferred to the electrolytic cell which contained 50 ml of a saturated potassium sulphate solution with 30 mg l^{-1} ammonium thiocyanate. Mercury was then stripped by scanning from 0.0 V to +0.55 V vs. SCE. The best differential-pulse voltammograms were obtained with 10-mV staircase ramp, 50-mV pulse amplitude, and 5-ms pulse duration. The anodic stripping curve was stored and after each measurement the electrode was cleaned for 1 min at +0.7 V (vs. SCE). The baseline was then recorded, stored and subtracted from the stripping curve. Background subtraction was essential in obtaining clearly defined peaks.

Determination of mercury in air. The equipment used is shown in Fig. 2. For calibration, mercury-free air was essential; this was obtained by bubbling air through several washbottles filled with acidic potassium permanganate solution. After a sorption time of 10 min at a flow rate of 56 l h^{-1}, air so

treated gave no stripping signal for mercury. Mercury-saturated air was obtained as described by Dumarey et al. [23] and injected as required from the syringe.

Results and discussion

When mercury was determined in solution, the sorption did not depend markedly on the rotation speed of the gold-plated electrode and was independent of the rotation speed in the range 600—2400 rpm. To avoid the need for careful positioning of the jet in relation to the electrode, the electrode was rotated at 1500 rpm. The dependence of the ASV signal on sorption time is shown in Fig. 3. The calibration graph is sigmoidal (Fig. 4) because of adsorption/desorption processes in the low concentration range and peak broadening at high concentrations. When glass apparatus is used, the detection limit is about 30 ng of mercury. For 100 ng of mercury(II), the relative standard deviation was about 6% (n = 7). Replacement of glassware by quartz vessels and miniaturisation of the system would decrease the detection limit, as it does in the cold-vapour AAS method.

To obtain reliable results, it was necessary to condition the electrode daily by polarizing between 0.0 V and 0.7 V (vs. SCE) repeatedly until reproducible background curves were obtained. Then, prior to each measurement, the electrode was washed with 5 M hydrochloric acid and diethyl ether.

For the determination of mercury in air, a sorption time of 10 min with an air flow rate of 56 l h^{-1} gave a usable calibration for the range 10—140 ng of mercury (Fig. 5). The 3σ detection limit was calculated to be 1.7 ng l^{-1}

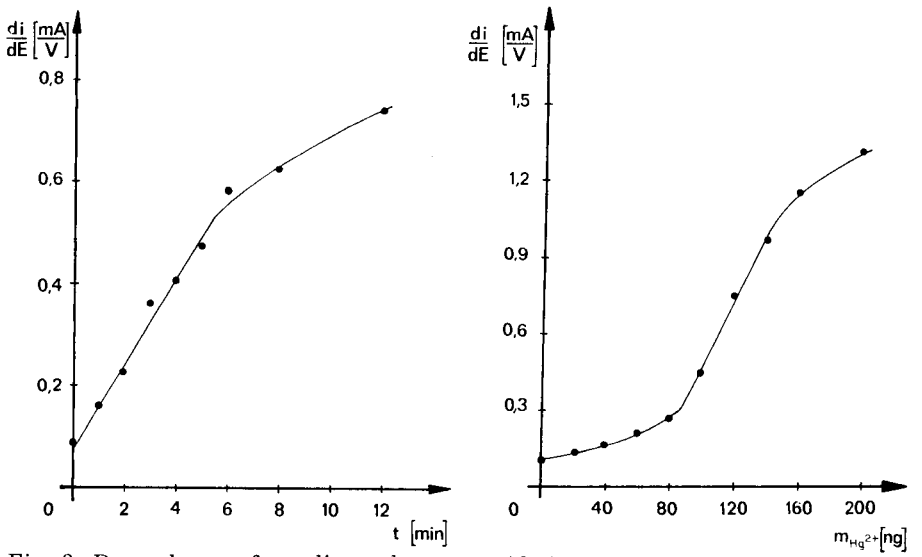

Fig. 3. Dependence of anodic peak current (derivative) on sorption time for 40 ng of mercury.

Fig. 4. Calibration curve for analysis of solutions.

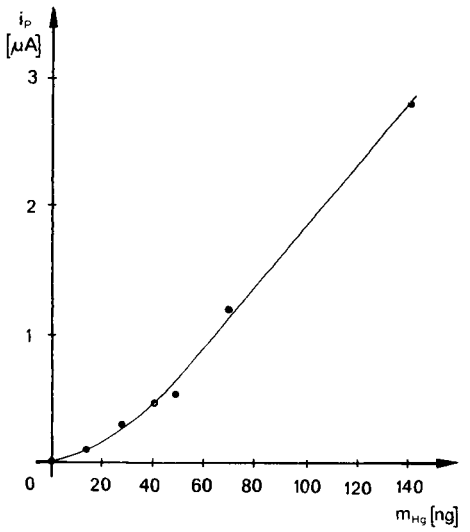

Fig. 5. Calibration curve for air analysis (10-min sorption time, 56 l h^{-1} flow rate).

mercury in air. The procedure allows fast convenient determinations of mercury at very low concentrations.

REFERENCES

1 J. Wang, Int. Lab., 15(8) (1985) 68.
2 R. Kalvoda, Anal. Chim. Acta, 138 (1985) 11.
3 M. Friedrich and H. Ruf, J. Electroanal. Chem., 198 (1986) 261.
4 S. P. Perone and W. J. Kretlow, Anal. Chem., 37 (1965) 968.
5 R. Fukai and L. Huynh-Ngoc, Anal. Chim. Acta, 83 (1976) 375.
6 T. Miwa and A. Mizuike, Jpn. Analyst, 17 (1968) 448.
7 D. Jagner, Anal. Chim. Acta, 105 (1979) 33.
8 L. Ulrich and P. Ruegsegger, Fresenius' Z. Anal. Chem., 277 (1975) 349.
9 L. Sipos, P. Valenta, H. W. Nürnberg and M. Branica, J. Electroanal. Chem., 77 (1977) 263.
10 L. Sipos, J. Golimowski, P. Valenta and H. W. Nürnberg, Fresenius' Z. Anal. Chem., 298 (1979) 1.
11 L. A. Schadewald, T. R. Lindstrom, W. Hussein, E. E. Evenson and D. C. Johnson, J. Electrochem. Soc., 131 (1984) 1583.
12 R. W. Andrews, J. H. Larochelle and D. C. Johnson, Anal. Chem., 48 (1976) 212.
13 T. R. Lindstrom, Dissertation, Iowa State University, Ames, IA, 1980.
14 M. Goto, K. Ikenoya and D. Ishii, Bull. Chem. Soc. Jpn., 53 (1980) 3567.
15 F. Scholz, L. Nitschke and G. Henrion, Z. Chem., 25 (1985) 441.
16 A. Eschka, Z. Anal. Chem., 11 (1872) 344.
17 G. Lunge, Chemisch-technische Untersuchungsmethoden, Vol. 2, Springer, Berlin, 1900, p. 172.
18 F. W. Clarke, Ber., 11 (1878) 1409.
19 See, e.g., A. M. Ure, Anal. Chim. Acta, 76 (1975) 1.
20 R. T. McNerney, Int. Lab., 13(7) (1983) 56.
21 C. Feldman, Anal. Chem., 46 (1974) 99.
22 Gmelins Handbuch der anorganischen Chemie, Systemnr. 62, Verlag Chemie, Weinheim, 1954, 743.
23 R. Dumarey, E. Temmerman, R. Dams and J. Hoste, Anal. Chim. Acta, 170 (1985) 337.

Analytica Chimica Acta, 199 (1987) 173—176
Elsevier Science Publishers B.V., Amsterdam — Printed in The Netherlands

Short Communication

DETERMINATION OF CYANURIC ACID IN SWIMMING POOL WATER BY DIFFERENTIAL PULSE POLAROGRAPHY

J. STRUYS* and P. M. WOLFS

Laboratory for Inorganic Chemistry, National Institute of Public Health and Environmental Hygiene, P.O. Box 1, 3720 BA Bilthoven (The Netherlands)

(Received 5th November 1986)

Summary. A reliable differential pulse polarographic method is described for the determination of cyanuric acid (1,3,5-triazine-2,4,6-triol) in pool water. Cyanuric acid in the range 10^{-5}—10^{-3} M is determined by means of the peak at ca. —60 mV (vs. Ag/AgCl/3 M NAcl). The high sensitivity of the polarographic technique allows ten-fold dilution of samples, thus avoiding matrix effects. It it shown that the peak can be attributed to formation of insoluble mercury(I) cyanurate, $Hg_2(HC_3N_3O_3)$, at the mercury electrode.

Cyanuric acid (I) is recommended for the stabilization of the chlorine content in swimming pool water. Stabilization can be achieved either by adding cyanuric acid to pool water with the chlorine (as hypochlorite or chlorine solution) or by introduction of chlorinated cyanurates, directly as a single

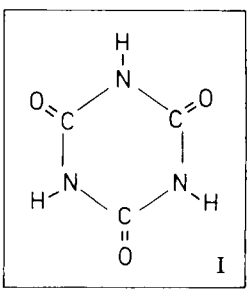

I

chemical. The mechanism of stabilization of the residual chlorine may be written as follows:

chlorinated cyanurates + $H_2O \rightleftharpoons$ cyanuric acid + HOCl

Chlorinated cyanurate is an organic chloramine having one, two or three chlorine atoms attached to the nitrogen atoms of the symmetric triazine ring. As chlorine bound to the triazine ring is less susceptible to destruction by sunlight, chlorinated cyanurates provide a reservoir of chlorine atoms. In public pools in The Netherlands, the application of this stabilizer is allowed, provided that the total cyanurate concentration in pool water is 20—50 mg l^{-1}

0003-2670/87/$03.50

at pH 6.8—7.8. According to the regulations for use of the stabilizer, the free residual chlorine should exceed 2.0 mg l^{-1} in order to maintain sufficient bactericidal power. Obviously, application of the cyanurate stabilizer requires a reliable method of analysis, as the concentration of cyanuric acid must be measured in addition to physicochemical and bacteriological tests warranting the quality of water in public pools and sauna institutes.

The commonest method recommended for testing the cyanuric acid content of pool water is turbidimetry of melamine cyanurate [1]. This method suffers from a substantial blank signal and from variable slopes of the calibration plots. An alternative which is free from matrix effects in the relevant concentration range and easy to apply, was therefore sought.

In this communication, a reliable method is presented for determinations of cyanuric acid at $\geqslant 1$ mg l^{-1} levels in pool water and water in saunas. A differential-pulse polarographic method was chosen because of its high sensitivity, which permitted 10-fold dilution of the water samples and so eliminated most matrix effects at cyanuric acid concentrations as low as 1 mg l^{-1}. Literature dealing with polarographic behaviour of cyanuric acid is very scarce. Zhantalai and Slisarenko [2] described a d.c. polarographic method. They obtained anodic waves with a limiting current proportional to the cyanuric acid concentration, but at the higher concentrations, the half-wave potential shifted to more negative values. This shift can probably be attributed to the formation of insoluble mercury(I) salts or stable mercury(II) complexes [3].

Experimental

Differential pulse polarograms were recorded with a PAR-374 polarographic analyzer. All measurements were done with a static mercury drop electrode (SMDE) in a three-electrode cell (PAR-303). Deaeration was done with purified nitrogen. The reference electrode was a Ag/AgCl (3 M NaCl) electrode.

Standard solutions of cyanuric acid (1,3,5-triazine-2,4,6-triol; Aldrich) in the range 1.3—130 mg l^{-1} were prepared with twice-distilled water. The supporting electrolyte was a phosphate buffer of pH 7.2, which was prepared from analytical-grade chemicals (0.0425 M KH_2PO_4/0.029 M NaOH) and twice-distilled water.

Cell solutions consisted of 0.5 ml of standard cyanuric acid solution or pool-water sample and 4.5 ml of phosphate buffer. Polarograms were run in the potential range between —0.005 V and 0.11 V, and the peak appearing at about —60 mV (vs. Ag/AgCl/3 M NaCl) was used. The scan rate was 2.08 mV s^{-1} (slow); the mercury drop time was 0.93 s. Other operating conditions were as follows: sensitivity, low; pulse amplitude, 100 mV average length (data smoothing), 16; peak sensitivity, high; drop size (PAR 303), large.

All samples were treated with 1 ml of 0.1 M sodium thiosulphate per liter of pool water in order to neutralise the available chlorine, converting all chlorinated cyanurates to cyanuric acid.

Results

Cyanuric acid in twice-distilled water. Standard solutions containing cyanuric acid in the range 10^{-5}—10^{-4} M were analysed as described above; the cell concentration was in the range 0.13—1.3 mg l^{-1}. Good linearity between peak height and concentration was obtained ($r^2 = 0.995$, $n = 10$) but the intercept was rather high (0.869×10^{-6} A) with respect to the slope (0.288×10^{-6} A μM^{-1}). This procedure was therefore not suitable for samples with concentrations lower than 1 mg l^{-1}. Results with standard solutions in the range 10^{-4}—10^{-3} M provided better calibration data: $r^2 = 0.999$ ($n = 10$), intercept 0.101×10^{-6} A and slope 0.381×10^{-6} A/10 μM. However, irregular polarograms were obtained when the concentration of cyanuric acid in the electrolysis cell exceeded 5×10^{-5} M, although the peak height was linear with the concentration up to 10^{-3} M. Therefore, pool waters with concentrations exceeding 50 mg l^{-1}, were diluted by an appropriate factor, before 0.5 ml was added to 4.5 ml of the base electrolyte, so that the concentrations in the cell were below the 5×10^{-5} M level.

Cyanuric acid in tap water and pool water. With standard solutions prepared from tap water, similar results were obtained. A pool-water sample collected from a public swimming pool where no stabilizers had been used, was spiked with 18.4 mg l^{-1} cyanuric acid. This sample was analysed with use of a calibration graph and with a standard addition method (3 additions). The mean values were 18.5 and 18.9 mg l^{-1}, respectively, with a distribution variance of about 1% ($n = 10$). The influence of sodium thiosulfate, which was added to the pool waters, was shown to be negligible by comparing standard cyanuric acid samples in distilled water with and without 10^{-4} M sodium thiosulfate.

Cyanuric acid in pool water of four sauna institutes. Samples were collected in both whirlpools and swimming pools of four sauna institutes, which were known to use cyanuric acid. The results are summarised in Table 1. Matrix effects were not apparent for any sample.

Discussion

Differential pulse polarography seems to be a reliable method for the determination of cyanuric acid in pool water. The detection limit is far below the concentrations usually found when cyanuric acid is applied in swimming pools. This high sensitivity allows dilution of samples, which may be necessary to avoid matrix effects.

The polarographic behaviour was investigated because the anodic wave at about —60 mV may be masked by interfering reactions, e.g., the shift of the mercury wave caused by the presence of chloride ions. Shifts of the peak potential in the negative direction with increasing cyanuric concentrations (ca. 27 mV for a ten-fold concentration increase) indicated a reaction with mercury to form an insoluble salt or a stable complex with the triazine ring, rather than oxidation of cyanurate. Cyanuric acid (H_3Cy) is a weak acid with dissociation constants of 1.16×10^{-7}, 1×10^{-11} and 1×10^{-13},

TABLE 1

Concentrations of cyanuric acid in swimming pools and whirlpools of four sauna institutes. Results were obtained with the standard addition method and from a calibration graph (in parentheses)

Institute	Cyanuric acid found (mg l^{-1})	
	Swimming pool	Whirlpool
1	0 (0)	13 (13)
2	7 (6)	29 (30)
3	113 (109)	7 (7)
4	7 (6)	0 (0)

respectively [1]. If an insoluble salt $Hg_mH_{3-m}Cy$ is formed after the anodic reaction $2\ Hg \rightarrow Hg_2^{2+} + 2e^-$, the stoichiometric number m can be evaluated from the shift of the peak potential, analogously to the treatment of the formation of insoluble mercury(I) halides [3]. A plot of peak potential (at constant pulse amplitude) against the logarithm of the cyanuric acid concentration in the range 10^{-5}—10^{-6} M gave a good linear relationship ($r^2 = 0.97$) which indicated that $m = 2$. This means that the anodic wave relies on the formation of $Hg_2(HCy)$. This evaluation was done with polarograms pertaining to the low concentration range specified because at higher concentrations ($>5 \times 10^{-5}$ M) the peak shape was distorted. The likelihood of the formation of $Hg_2(HCy)$ was confirmed by chemical tests. A mercury(I) nitrate solution added to a cyanuric acid solution gave a white precipitate. When mercury(I) ions and cyanuric acid were mixed in various proportions and the cyanuric acid remaining in the supernatant liquid was determined polarographically, the results indicated that the precipitate was formed from mercury(I) and cyanuric acid in a 2:1 ratio. When the precipitate was filtered, dried, weighed and dissolved in 1 M nitric acid, and the concentration of mercury was determined by atomic absorption spectrometry, the results corresponded to a 1.9:1 ratio, confirming the previous tests.

REFERENCES

1 G. C. White, Handbook of Chlorination for Potable Water, Waste Water, Cooling Water, Industrial Processes and Swimming-pools, Van Nostrand, New York, 1972, pp. 499—505.
2 B. P. Zhantalai and V. P. Slisarenko, Zavod. Lab., 39 (1973) 6.
3 J. Heyrovsky and J. Kuta, Principles of Polarography, Academic, New York, 1966, pp. 167—178.

Analytica Chimica Acta, 199 (1987) 177—180
Elsevier Science Publishers B.V., Amsterdam — Printed in The Netherlands

Short Communication

DETERMINATION OF SURFACE-ACTIVE COMPOUNDS IN PRECIPITATION STUDIES BY AC POLAROGRAPHY

N. BATINA and B. ĆOSOVIĆ

Center for Marine Research, Rudjer Bošković Institute, P.O.B. 1016, 41001 Zagreb (Yugoslavia)

DJ. TEŽAK

Laboratory of Physical Chemistry, Faculty of Sciences, P.O.B. 163, University of Zagreb (Yugoslavia)

(Received 20th December 1986)

Summary. The simple procedure is based on measurement of the capacity current of the mercury electrode by a.c. polarography after adsorption of the surfactant. Nonionic surfactants of the Triton-X series were studied in connection with precipitation of colloidal silver iodide. Useful results were achieved in the 10^{-4}—10^{-7} mol dm^{-3} range for Triton X-100, X-305 and X-705 by adjusting the sorption time, the type of molecular transport to the electrode and the dilution ratio.

Various types of surface-active substances, both ionic and nonionic, as well as some macromolecular compounds are easily determined in aqueous solutions by means of their adsorption on suitable electrodes. The adsorption involves displacement of water molecules by organic molecules which produces a measurable decrease of the electrode double-layer capacity. The use of the mercury electrode is advantageous because of its reproducibly renewable surface. Alternating current (a.c.) polarography can be used to measure either the capacity of the electrode double-layer or the capacity current. This simple methodology has been widely applied in environmental analysis, polymer analysis, process control, etc. [1]. Direct measurement of surfactants by electrochemical methods has proved useful in the determination and characterization of organic matter in natural and polluted waters [2—7].

Numerous investigations have been reported on colloid stabilization caused by nonionic or ionic surfactants [8—11]. In such studies, it is important to determine the amount of adsorbed surfactants on the colloid particles and the equilibrium concentration of the surfactant in the bulk solution. The advantages of the electrochemical method are its simple procedure and relatively high sensitivity in comparison with spectrophotometric determination. Here, the proposed method is illustrated for the precipitation of silver iodide in the presence of nonionic surfactants of the Triton-X series.

0003-2670/87/$03.50

Experimental

Before the examination of the solutions, the colloidal silver iodide was separated by centrifugation on a Beckman ultracentrifuge at 2600*g* for 20 min.

The concentrations of the surfactant in the supernatant liquids were measured by using a.c. polarography. Sodium perchlorate (0.1 mol dm^{-3}) was added as supporting electrolyte. Measurements were made with a phase-selective polarograph (Metrohm E506). A hanging mercury drop electrode (HMDE; Metrohm) with a surface area of 2.57×10^{-2} cm^2 was used as the working electrode, with a saturated calomel reference electrode and a platinum-wire auxiliary electrode. All measurements were done at room temperature and without deaeration of the solution. In order to increase the sensitivity, surfactants were accumulated on the electrode surface at a potential of —0.6 V prior to the potential scan.

These measurements are very sensitive to trace amounts of adsorbable impurities. Therefore special precautions are needed to obtain clean glassware and water and chemicals of high purity.

Results and discussion

Typical capacity current/potential curves for Triton X-305 are presented in Fig. 1. The surfactant was preconcentrated on the electrode at —0.6 V for 300 s without stirring. Calibration curves were constructed by plotting the decrease of the capacity current, Δi, measured at —0.6 V from the value in the supporting electrolyte, versus the bulk concentration of surfactant. Calibration curves obtained for different Tritons (Triton X-705, X-305 and X-100) under the same experimental conditions are presented in Fig. 2. Clearly, the sensitivity of the method increases with increasing molecular weight of the surfactant; as little as 10^{-7} mol dm^{-3} Triton X-305 and Triton X-705 can be determined.

In this work, colloidal silver iodide was prepared with excess of silver nitrate in the presence of Triton X-305. Therefore, the effect of silver ions on the measured signal was studied. Capacity current/potential curves for different concentrations of Triton X-305 obtained with and without silver ions present are shown in Fig. 3. At the higher concentrations of Triton X-305, silver ions have no effect on the measured capacity current, but a slight effect was observed when 10^{-3} mol dm^{-3} Ag^+ was added to 0.99×10^{-7} mol dm^{-3} Triton X-305. Down to about 2×10^{-7} mol dm^{-3} Triton X-305 can thus be determined in the supernatant solution even in the presence of silver ions.

Because Tritons are strongly adsorbed on the mercury electrode, the rate-determining step is usually the time needed for the surfactant molecules to reach the electrode surface. Prolonging the diffusion time from 30 s to 300 s increases the sensitivity for Triton X-100 by about an order of magnitude and a further increase is obtained by stirring the solution for only 60 s (Fig. 4).

These results show that the procedure for surfactant determination can be used in two ways. A direct measurement of surfactant over a wide concentration range is possible by using a series of calibration curves as illustrated in

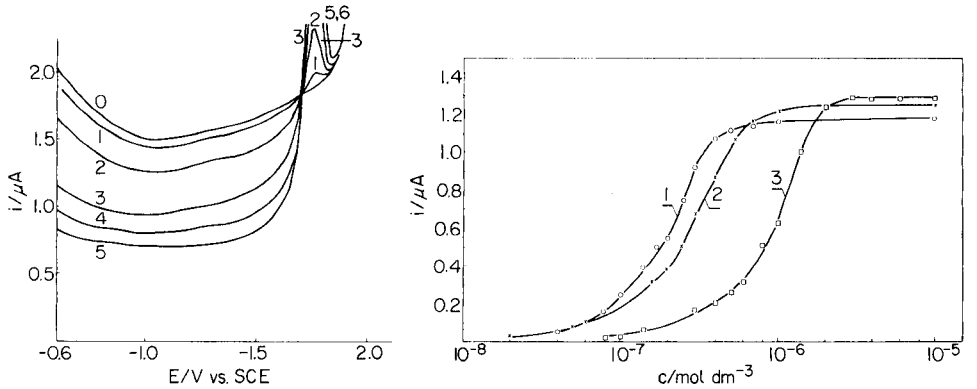

Fig. 1. Capacity current/potential curves for Triton X-305 on the HMDE in 0.1 mol dm^{-3} $NaClO_4$. Concentration of Triton X-305: (0) 0, (1) 6 × 10^{-8}, (2) 2 × 10^{-7}, (3) 4 × 10^{-7}, (4) 5.4 × 10^{-7}, (5) 1 × 10^{-6} mol dm^{-3}. Accumulation time 300 s, diffusion-controlled transport.

Fig. 2. Calibration curves: (1) Triton X-705; (2) Triton X-305; (3) Triton X-100. Conditions as in Fig. 1.

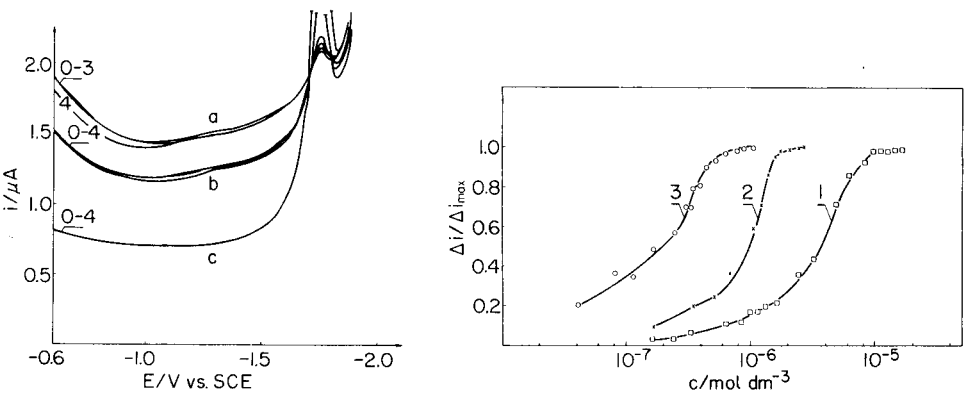

Fig. 3. Capacity current/potential curves for different concentrations of Triton X-305: (a) 0.99 × 10^{-7}, (b) 2.70 × 10^{-7}, (c) 9.86 × 10^{-7} mol dm^{-3}. Silver nitrate present: (0)0, (1) 10^{-6}, (2) 10^{-5}, (3) 10^{-4}, (4) 10^{-3} mol dm^{-3}.

Fig. 4. Calibration curves for Triton X-100 in 0.5 mol dm^{-3} NaCl obtained with different transport conditions: (1) diffusion for 30 s; (2) diffusion for 300 s; (3) stirring for 60 s.

Fig. 4. Alternatively, the concentration range of surfactant can be adjusted by appropriate dilution so that only one calibration curve is needed. If other ions present in the supernatant solution interfere in the voltammetric measurement, the dilution procedure is advantageous because the concentrations of interferences are also decreased by dilution.

In a typical procedure, the colloid was separated by centrifugation and the supernatant liquid was diluted so that the concentration of Triton fell within the range of the calibration curve (see Fig. 2). Sodium perchlorate was added just prior to voltammetry. The capacity current/potential curves of samples of diluted supernatant solutions containing 10^{-4}—10^{-5} mol dm^{-3} Triton X-305 were very similar to those shown in Figs. 1 and 3. The concentration of surfactant in the supernatant liquid was evaluated from the decrease of the capacity current by means of the calibration curve, with correction for the dilution factor. The amount of surfactant adsorbed on the colloidal particles was calculated as the difference between the initial concentration of Triton and the equilibrium concentration in the supernatant liquid. Adsorption isotherms were then constructed by plotting the adsorbed quantity against the equilibrium concentration of surfactant. Such results have been utilized in investigating the effects of Tritons on the growth and aggregation of silver iodide sols [12].

Financial assistance from the Self-Managed Community of Interest for Scientific Research of S. R. Croatia and the National Bureau of Standards, Washington, DC (Grant NBS 579) is acknowledged.

REFERENCES

1 H. Jehring, Elektrosorptionanalyse mit der Wechselstrompolarographie, Akademie, Berlin, 1974.
2 H. W. Nürnberg and P. Valenta, in E. D. Goldberg (Ed.), The Nature of Seawater, Dahlem Konf., Berlin, 1975, pp. 87—136.
3 Z. Kozarac, V. Žutić and B. Ćosović, Tenside Deterg., 13 (1976) 260.
4 W. Davison and M. Whitfield, J. Electroanal. Chem., 75 (1977) 763.
5 B. Ćosović and V. Vojvodić, Limnol. Oceanogr., 27 (1982) 361.
6 Z. Kozarac, D. Hršak and B. Ćosović, Environ. Sci. Technol., 17 (1983) 268.
7 B. Ćosović, in W. Stumm (Ed.), Chemical Processes in Lakes, Wiley, New York, 1985, pp. 55—80.
8 R. J. Akers, Rep. Prog. Appl. Chem., 60 (1975) 605.
9 R. F. Eirich, J. Colloid Interface Sci., 58 (1977) 423.
10 P. D. Bisio, J. C. Cartledge, W. H. Keesom and C. J. Radke, J. Colloid Interface Sci., 78 (1980) 225.
11 Dj. Težak, V. Hrust, S. Heimer, B. Težak and M. Wrischer, Croat. Chem. Acta, 53 (1980) 397.
12 Dj. Težak, N. Batina and B. Ćosović, Croat. Chem. Acta, 59 (1986) 813.

Analytica Chimica Acta, 199 (1987) 181—183
Elsevier Science Publishers B.V., Amsterdam — Printed in The Netherlands

Short Communication

SIMULTANEOUS DETERMINATION OF LEAD, COPPER, CADMIUM AND ZINC IN PURE ZIRCONIUM METAL BY DIFFERENTIAL-PULSE ANODIC STRIPPING VOLTAMMETRY

S. S. DHAKTODE
Siddharth College of Arts, Science & Commerce, Fort, Bombay 400 023 (India)
(Received 30th December 1986)

Summary. Zirconium metal (ca. 1 g) was dissolved in hydrofluoric acid, excess of which was removed by fuming with sulphuric acid. An aliquot of this solution was treated with sodium citrate and adjusted to pH 4.5. Lead, copper and cadmium were deposited on the hanging mercury drop electrode by applying a potential of —0.8 V vs. Ag/AgCl for 1 min and anodic stripping voltammograms were recorded; the anodic peaks appeared at —0.51, —0.14 and —0.67 V, respectively. In a separate run, zinc was deposited at —1.2 V and the stripping peak appeared at —1.1 V. Standard additions were used to quantify these impurities at levels in the low mg kg^{-1} range, with relative standard deviations of 5—11%.

Zirconium materials are important in nuclear technology and high demands are placed on their purity. Among the many trace impurities present in these materials, lead, copper, cadmium and zinc can be determined by electrochemical stripping techniques at a mercury electrode [1, 2]. To achieve this for pure zirconium metal, it is necessary to establish a suitable decomposition procedure which allows the use of a relatively large sample (about 1 g) to attain a sufficiently low limit of determination, and to find an electrolyte, which effectively suppresses the hydrolysis of zirconium. Differential-pulse anodic stripping voltammetry (DPASV) after dissolution of samples in hydrofluoric/sulphuric acids is shown to be satisfactory.

Experimental

Reagents. AristaR-grade sulphuric acid and AnalaR-grade hydrofluoric acid (BDH) were used in dissolving zirconium metal. A 1.0 M solution of sodium citrate was prepared in double-distilled water and subjected to controlled-potential electrolysis at —1.2 V for 48 h at a mercury pool cathode to remove metallic impurities.

Apparatus. Differential-pulse anodic stripping voltammograms were recorded at a hanging mercury drop electrode (HMDE; Metrohm). A PARC-174A polarograph was used for DPASV; cell temperature was maintained at 25°C.

Preparation of sample solution. Zirconium metal (ca. 1.0 g) was dissolved in 10 ml of hydrofluoric acid in a platinum dish [3]. The solution, after

0003-2670/87/$03.50

cooling was evaporated several times with small amounts of concentrated sulphuric acid to remove the hydrofluoric acid completely. The residue was dissolved in concentrated sulphuric acid, transferred to a 100-ml volumetric flask and diluted to the mark with double-distilled water; the sulphuric acid concentration being kept at 5% (v/v). The same procedure was adopted for the sample blank and for the sample with a suitable standard addition. The blank and sample solutions must be prepared immediately before the stripping, as zirconium tends to hydrolyse.

Polyethylene containers, which had been cleaned with AnalaR-grade nitric acid (1 +1) and rinsed with double-distilled water, were used for storage of stock solutions of supporting electrolyte and sample.

Determination of trace metals by DPASV. An aliquot (5 ml) of the sample solution was placed in a 10-ml volumetric flask and 2.5 ml of 1.0 M sodium citrate was added. The pH was adjusted to 4.5 and the solution was diluted to the mark with water. This solution was transferred to the electrolysis cell. After pre-electrolysis at the HMDE for 1.0 min and a rest period of 30 s, the anodic stripping voltammogram was recorded (scan rate 5 mV s^{-1}, pulse amplitude 50 mV). The voltammograms showed stripping peaks for Pb, Cu, Cd and Zn at −0.51, −0.14, −0.67 and −1.1 V (vs. Ag/AgCl) respectively (Fig. 1). The deposition potential for Pb, Cu and Cd was −0.80 V; for zinc, it was −1.2 V in a separate experiment.

Results and discussion

In view of the complex matrix after the sample pretreatment, the standard addition method must be used rather than direct calibration. Standard additions were selected so that the total amount of each metal was approximately doubled. The results of stripping voltammetric determinations for Pb, Cu, Cd and Zn are given in Table 1.

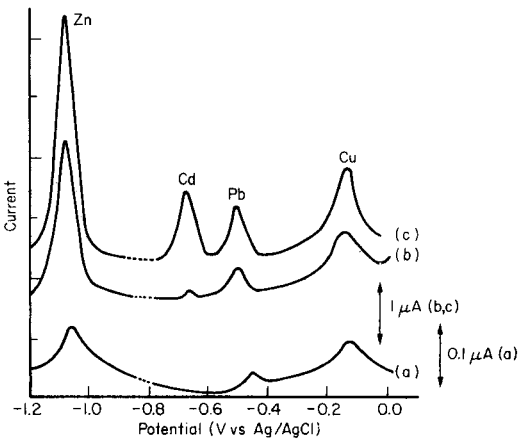

Fig. 1. Stripping voltammograms: (a) sample blank; (b) 5 ml of sample solution; (c) sample + standard addition of Zn (0.55 μg), Cd (0.4 μg) Pb (0.35 μg) and Cu (0.4 μg) in 10 ml of solution. Conditions as in Experimental.

TABLE 1

Determination of Pb, Cu, Cd and Zn in zirconium metal[a]

Metal	Pb	Cu	Cd	Zn
Average content (mg kg^{-1})	7	8	1	20
RSD (%)	5	10	—	11

[a]Average and relative standard deviation for 5 separate determinations.

The effects of probable impurities such as Ni, Co, Sn, As, Mn and Cr were investigated. When these impurities were present at low mg kg^{-1} levels, they did not interfere with the determination.

Stripping voltammetry at the HMDE can be complicated by the formation of intermetallic compounds in the mercury drop [4, 5]. For example, copper is known to form Cu—Zn [6] and Cu—Cd intermetallic compounds when the metals are present in solution at high concentrations. In the present study, no intermetallic compound formation was observed; there was no shifting or suppression of the anodic peaks, probably because of the low concentrations of heavy metals determined and the short deposition times used.

REFERENCES

1 F. Vydra, K. Stulik and E. Julakova, Electrochemical Stripping Analysis, Horwood, Chichester, 1977.
2 P. Beran, J. Dolezal and D. Mrazek, J. Electroanal. Chem., 6 (1963) 381.
3 J. Dolezal, P. Povondra and Z. Sulcek, Decomposition Techniques in Inorganic Analysis, Iliffe, London, 1969.
4 F. Von Strum and M. Z. Russel, Anal. Chem., 186 (1962) 63.
5 H. K. Ficker and L. Meites, Anal. Chim. Acta, 26 (1962) 172.
6 M. S. Shuman and G. P. Woodward, Anal. Chem., 48 (1976) 1979.

Analytica Chimica Acta, 199 (1987) 185—189
Elsevier Science Publishers B.V., Amsterdam — Printed in The Netherlands

Short Communication

DETERMINATION OF TRACES OF PALLADIUM BY ADSORPTIVE STRIPPING VOLTAMMETRY OF THE DIMETHYLGLYOXIME COMPLEX

JOSEPH WANG* and KURIAN VARUGHESE[a]

Department of Chemistry, New Mexico State University, Las Cruces, NM 88003 (U.S.A.)

(Received 12th February 1987)

Summary. Preconcentration is achieved by adsorption of a palladium-dimethylglyoxime complex on a hanging mercury drop electrode. Optimal conditions are a stirred acetate buffer solution (pH 5.15) containing 2×10^{-4} M dimethylglyoxime and an accumulation potential of −0.20 V. The height of the stripping peak in a negative-going linear scan is linearly dependent on palladium concentration and preconcentration time (over the ranges 0—16 $\mu g\ l^{-1}$ and 0—300 s, respectively). For a 10-min preconcentration time, the detection limit is 20 ng l^{-1} (2.1×10^{-10} M). Possible interferences by other trace metals are investigated. Palladium added to seawater samples was easily quantified.

Rapid methods for the determination of palladium in precious-metal plating baths, nuclear fuels, geological materials or natural waters are of interest. Recent procedures for traces of palladium include conventional and pulse polarography [1, 2] and liquid chromatography with ultraviolet detection of palladium-dithiocarbamate complexes [3]. Stripping voltammetry seems not to have been attempted.

In this communication, a sensitive adsorptive-stripping voltammetric procedure is described for traces of palladium(II), based on accumulation of its dimethylglyoxime (DMG) complex at the hanging mercury drop electrode. Under suitable conditions, palladium(II) forms a very stable DMG complex [4]. The selective gravimetric determination of palladium(II) with DMG under acidic conditions is well known. The adsorptive stripping voltammetry of nickel and cobalt as their DMG complexes, from weakly alkaline media, has been widely used [5—8]. It was therefore expected that analogous measurements of palladium(II) could be done from slightly acidic solution. It is shown below that the response resulting from the reduction of the adsorbed Pd-DMG complex allows palladium(II) to be determined down to the 10^{-10} M level.

[a]On leave from the Education Department, Government of Madhya Pradesh, Bhopal, India.

0003-2670/87/$03.50

Experimental

Apparatus and reagents. A PAR 264 voltammetric analyzer was used with a PAR 303 static mercury drop electrode, as described before [9, 10]. All solutions were prepared with double-distilled water. A 1000 mg l^{-1} palladium stock solution (atomic absorption standard; Aldrich) was diluted as required for standard additions. A 0.1 M stock solution of dimethylglyoxime (Aldrich) in aqueous ethanol (95% v/v) was prepared weekly. Supporting electrolyte was acetate buffer (pH 5.15). Seawater was unfiltered surface water collected at San Diego, CA, and stored frozen.

Procedure. The supporting electrolyte solution (10 ml), containing 2×10^{-4} M dimethylglyoxime, was pipetted into the cell, and purged with nitrogen for 8 min. The preconcentration potential (usually −0.20 V) was applied to a fresh mercury drop while the solution was stirred. Following the preconcentration period, the stirring was stopped, and after 15 s the voltammogram was recorded by applying a negative-going linear scan; the scan was terminated at −1.0 V. After background stripping voltammograms had been obtained, aliquots of the palladium standards were introduced. The adsorptive stripping cycle was repeated with a new mercury drop.

Results and discussion

Repetitive cyclic voltammograms for 50 $\mu g\ l^{-1}$ palladium in acetate buffer (pH 5.15) solution containing 2×10^{-4} M DMG were used to evaluate the interfacial and redox behaviors. In the absence of prior accumulation, only a small peak from the reduction of the Pd-DMG complex was observed at −0.73 V; no peaks were observed on scanning to positive potentials. When the same experiment was repeated after a 120-s stirring period at −0.2 V, a substantially (25-fold) larger cathodic peak associated with the reduction of the adsorbed complex was observed at −0.74 V in the first negative-going scan. The smaller but stable peaks observed in subsequent scans indicated desorption of the product from the surface. With the 50 $\mu g\ l^{-1}$ palladium solution, full surface coverage was achieved after stirring for 300 s. The maximum charge, obtained by integrating the reduction current, was found to be 1.44 μC (i.e., a surface coverage of 4.98×10^{-10} mol cm^{-2}). A plot of log (peak current, nA) against log (scan rate, V s^{-1}) for the surface-adsorbed complex over the range 5—200 mV s^{-1} was linear with a slope of 1.19 and correlation coefficient of 0.989.

Spontaneous adsorption of the Pd-DMG complex can be used as an effective preconcentration step prior to voltammetry. Figure 1 shows linear-scan voltammograms for 5 $\mu g\ l^{-1}$ (5.3×10^{-8} M) palladium after different preconcentration times; well-defined peaks were observed following preconcentration for $\geq$90 s and the plots of peak current vs. preconcentration time were linear with slopes of 29.28 for 5 $\mu g\ l^{-1}$ Pd and 60.24 nA min^{-1} for 10 $\mu g\ l^{-1}$ Pd (Fig. 1, inset).

Figure 2 shows the dependence of the Pd-DMG reduction current on various experimental conditions. The peak increased rapidly with the DMG

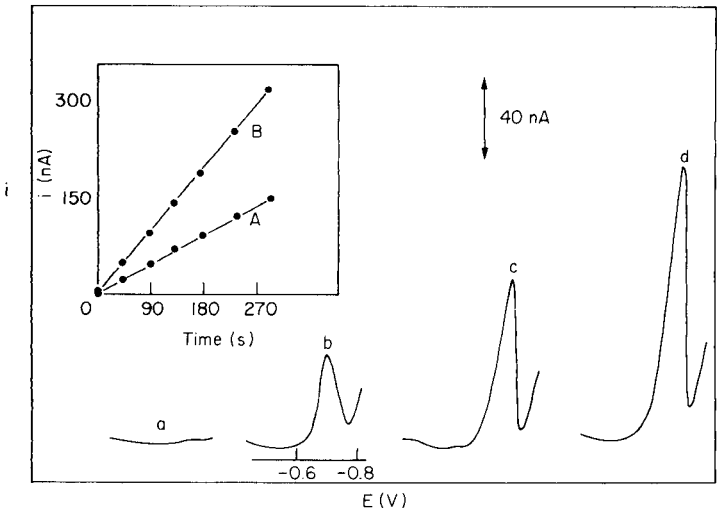

Fig. 1. Linear-scan voltammograms for 5 $\mu g\ l^{-1}$ palladium after different preconcentration periods: (a) 0; (b) 90; (c) 180; (d) 300 s. Preconcentration at −0.20 V; pH 5.15; 2×10^{-4} M DMG; 50 mV s^{-1}. The inset shows the resulting current/time plots at different concentrations: (A) 5; (B) 10 $\mu g\ l^{-1}$ palladium.

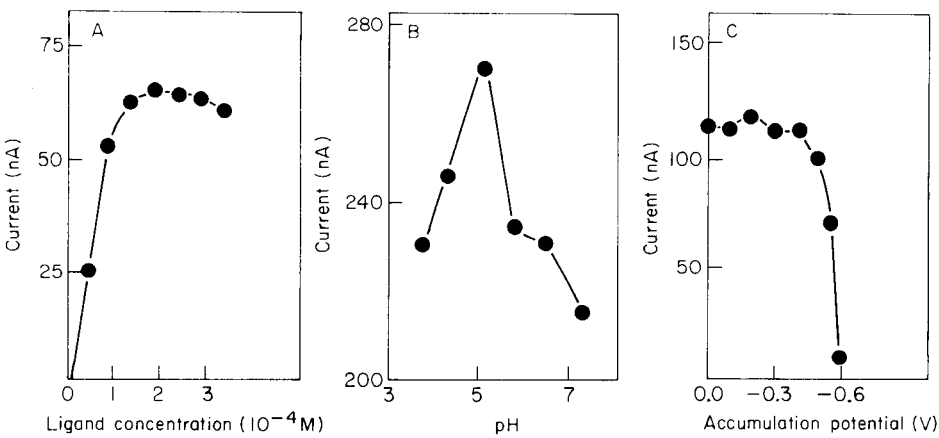

Fig. 2. Effect of DMG concentration (A), pH (B), and preconcentration potential (C) on the stripping peak current. Palladium concentration: (A, B) 10; (C) 20 $\mu g\ l^{-1}$. Preconcentration time, 120 s; preconcentration potential, −0.2 (A) and −0.3 (B) V. Other conditions as in Fig. 1.

concentration, up to about 2×10^{-4} M, and then started to level off (curve A). Increasing the solution pH from 3.8 to 5.15 resulted in a rapid increase of the peak height; a sharp decrease in the response was observed at pH > 5.15 (curve B). The preconcentration potential had little effect on the peak current over the 0.0 to −0.4 V region, but more negative potentials led

to a substantial decrease in current (curve C). Optimal conditions included an acetate buffer (pH 5.15) containing 2×10^{-4} M DMG, and preconcentration at −0.20 V. The differential-pulse and linear-scan waveforms yielded similar signal-to-background characteristics. The latter was preferred because of its speed advantage.

Figure 3 shows the well-defined stripping voltammograms obtained for 4—16 $\mu g\ l^{-1}$ palladium solutions after a 90-s preconcentration time. Calibration plots for the 2—16 $\mu g\ l^{-1}$ range using different preconcentration times are also shown in Fig. 3 (inset). The Pd-DMG response is linear for this range [slopes are 1.4 (A), 5.6 (B), and 10.4 (C) nA l μg^{-1} with correlation coefficients of 0.993 (A) and 0.999 (B, C)]. The reproducibility was estimated from ten successive measurements of a 8 $\mu g\ l^{-1}$ palladium solution (120-s preconcentration); the mean peak current was 130.5 nA, with a range of 127.5 to 135 nA and a relative standard deviation of 1.7%.

The interfacial accumulation of the Pd-DMG chelate produces extremely low detection limits. The detectability was estimated from measurements of 1 $\mu g\ l^{-1}$ (1.06×10^{-8} M) palladium, after preconcentration for 10 min; the detection limit was 20 ng l^{-1} (2.1×10^{-10} M) based on a signal-to-noise ratio of 3, i.e., 200 pg in the 10 ml of solution used. The adsorptive stripping

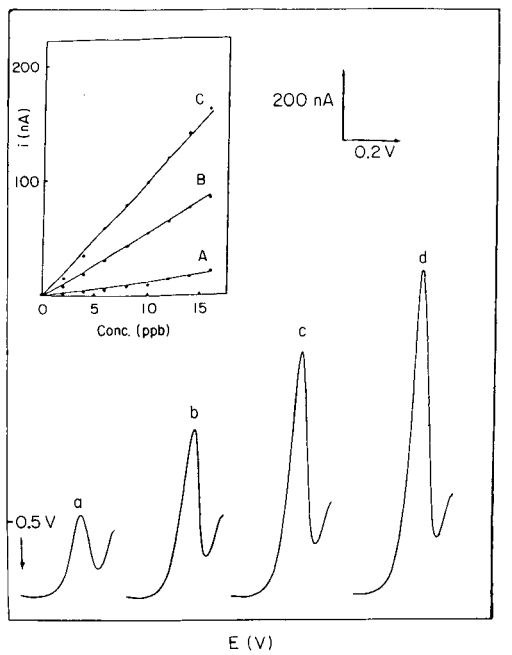

Fig. 3. Voltammograms obtained for solutions of increasing palladium concentration (4—16 $\mu g\ l^{-1}$). Preconcentration for 90 s at −0.2 V; other conditions as in Fig. 1. The inset shows the calibration plots after different preconcentration times: (A) 0; (B) 45; (C) 90 s.

procedure lowers the detection limit by four orders of magnitude compared to previous voltammetric schemes for palladium [2], and by one order of magnitude compared to graphite-furnace atomic absorption measurements [11].

As few metal ions form complexes with DMG [4, 12], there are few interferences. Ions tested at the 50 $\mu g\ l^{-1}$ level and found not to interfere in the determination of 10 $\mu g\ l^{-1}$ palladium were Ca(II), Cd(II), Co(II), Cu(II), Fe(III), Mn(II), Ni(II), Pb(II), and Ti(IV) (60-s preconcentration). The addition of nickel resulted in the appearance of a large Ni-DMG peak, ca. 120 mV negative to the Pd-DMG peak. The peak current for 10 $\mu g\ l^{-1}$ palladium was enhanced by 50 $\mu g\ l^{-1}$ Ag(I), Bi(III), Pt(II), or Zn(II) ions (ca. 52, 29, 61 and 13%, respectively). The formation of stable DMG complexes of Pt(II) and Bi(III) is well known [4, 12]; the silver and zinc interferences may be attributed to possible hydrogen catalytic processes, recently observed in the presence of DMG [13]. A separation step would be required for samples rich in these metals, e.g., precious metal plating-bath solutions "rich" in platinum.

Untreated coastal seawater, spiked with palladium, was used to demonstrate the selectivity of the method (8 ml of seawater plus 2 ml acetate buffer, 60-s preconcentration). Well-defined peaks (E_p = −0.74 V), similar to those found in pure solutions, were observed for 4−24 $\mu g\ l^{-1}$ palladium. The voltammogram for the original sample indicated the absence of interference around the Pd-DMG peak, with a single Ni-DMG peak appearing at ca. −0.86 V. Hence, simultaneous measurements of palladium and nickel were possible. The absence of palladium response in the original sample is expected from the short preconcentration time and the level of palladium in seawater. The calibration plot, resulting from the palladium additions, was linear with a slope of 6.5 nA l μg^{-1} (correlation coefficient, 0.999).

This work was supported in part by the National Institutes of Health under Grant No. GM 30913-03 and by the NM Water Resources Research Institute.

REFERENCES

1 R. Sreenivasulu, V. S. Rao and K. H. Reddy, Analyst, 110 (1985) 411.
2 T. C. Childers, P. Moncuse, J. J. Reiss and S. K. Vohra, Am. Lab., 16 (1984) 37.
3 B. J. Mueller and R. Lovett, Anal. Chem., 57 (1985) 2693.
4 R. P. Baldwin, J. K. Christensen and L. Kryger, Anal. Chem., 58 (1986) 1790.
5 B. Pihlar, R. Valenta and H. W. Nürnberg, Z. Anal. Chem., 307 (1981) 337.
6 S. B. Adeloju, A. M. Bond and M. H. Briggs, Anal. Chim. Acta, 164 (1984) 181.
7 A. Meyer and R. Neeb, Z. Anal. Chem., 315 (1983) 118.
8 L. Vos, Z. Komy, G. Reggers, E. Roekens and R. Van Grieken, Anal. Chim. Acta, 184 (1986) 271.
9 J. Wang, D. B. Luo, P. A. M. Farias and J. S. Mahmoud, Anal. Chem., 57 (1985) 158.
10 J. Wang, P. A. M. Farias and J. S. Mahmoud, Anal. Chim. Acta, 171 (1985) 215.
11 J. Fazakas, Anal. Lett., 15 (1982) 245.
12 J. Stary, The Solvent Extraction of Metal Chelates, Pergamon, Oxford, 1964.
13 B. Pihlar, P. Valenta and H. W. Nürnberg, J. Electroanal. Chem., 214 (1986) 157.

Analytica Chimica Acta, 199 (1987) 191—196
Elsevier Science Publishers, B.V., Amsterdam — Printed in The Netherlands

Short Communication

SANDWICH TECHNIQUES IN FLOW INJECTION ANALYSIS
Part 1. Continuous recalibration techniques for process control

J. ALONSO, J. BARTROLÍ*, M. DEL VALLE, M. ESCALADA and R. BARBER

Divisió Química Analítica, Departament de Química, Universitat Autónoma de Barcelona, Bellaterra, Barcelona (Spain)

(Received 2nd December 1986)

Summary. Flow injection methodology based on sample insertion between two different standard solutions used as carrier streams is described. This approach provides a simple system for continuous recalibration in process control; spectrophotometric and ion-selective electrode procedures are outlined.

The use of flow-injection techniques for on-line process control offers broad possibilities [1] but very little has been published in this field. Most effort has been put into the development of laboratory analyzers, many of which are now commercially available [2]. However, the requirements for a process control analyzer are different from those of the corresponding laboratory instruments [3]. On-line process analyzers have to work with little or no operator attention (if possible in a totally automatic manner), without the need for maintenance over long periods of time, with long-term operating stability and often in an aggressive environment. As continuous monitoring devices, flow-injection techniques may compare favorably with other types of analyzers because a trained operator can obtain valuable information about the correct functioning of flow system, e.g., about baseline drift. An important feature, in which it has an advantage over automated process titrator, is the high sampling frequency.

In order to provide quantitative measurements, the process (flow-injection) analyzer has to be recalibrated periodically. This implies the use of selection valves for the periodic intercalation of standards, increasing the complexity of the design and decreasing its ruggedness. The use of electronic calibration [4] requires the injection of one standard only but the hydrodynamically limited precision of gradient techniques in flow-injection analysis (FIA) [5] restricts its applicability. In this communication, a simple approach that allows continuous recalibration of the flow system is presented.

Sandwich operation for continuous recalibration

The principle of sandwich operation modifies substantially the original characteristics of flow-injection systems, but the basic theory is retained.

0003-2670/87/$03.50

Unlike the conventional flow-injection techniques (Fig. 1a), the sample plug in the "sandwich" method is inserted between two different carrier solutions (Fig. 1b). By means of the new injection procedure, three different zones are introduced into the carrier stream and so two different interfaces are formed between the sample and the carrier solutions.

When this approach is used for continuous recalibration, the sample is sandwiched between two different standard solutions. A typical example of the transient signal obtained is shown in Fig. 2. Before the injection, the output signal from the detector corresponds to the first standard (C) and defines the baseline. When the valve is switched, the second standard solution propels the sample contained in the loop towards the detector. The sample solution and the second standard solution define two plateaux corresponding to the respective steady-state signals. The switching back of the valve to the load position permits a constant check of the baseline drift. These plateaux should be as short as possible to allow for large sample throughputs.

The first step (A; Fig. 2) can be controlled by careful choice of the sample volume and the flow rate. The second step (B) depends entirely on the lapse of time before the valve is switched back to the load position. When the sample concentration lies within the range of concentrations defined by the standard solutions, an intermediate step appears.

Generally, process monitors have to work within a fixed range of analyte concentrations. This range can be covered by appropriate choice of standard solutions; the corresponding signals act as upper and lower limits for the proper process operation. When the sample step lies outside these limits, an alarm signal could be activated automatically.

When the detector response is linear within the working range, a simple interpolation between the two standards will yield accurate data, with adequate precision for process monitoring.

Experimental

Diagrams of the flow-injection systems used are shown in Fig. 3. Gilson Minipuls 2 peristaltic pumps were used. For potentiometric measurements,

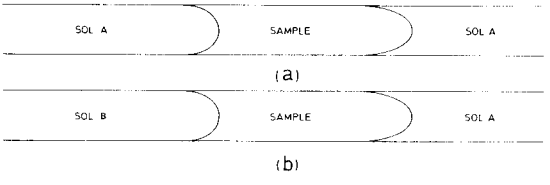

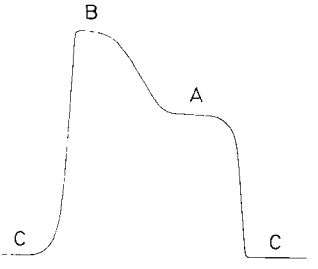

Fig. 1. Sample plug in the conventional technique (a); and in the sandwich technique (b).

Fig. 2. Recorder output obtained with the technique (see text).

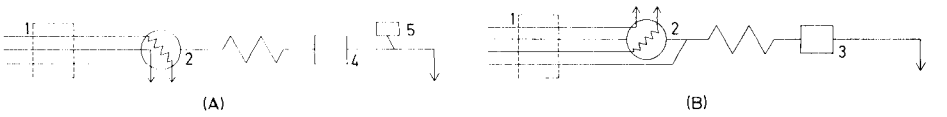

Fig. 3. Flow diagrams: (A) system for determination without additional reagent; (B) system for determination with additional reagent. (1) Pump; (2) injection device; (3) photometric detector; (4) flow-through electrode; (5) reference electrode.

the detector was constructed as previously described [6]; in the present experiments a tubular flow-through nitrate electrode [7] was used. The photometric measurements were made with a Tecator 5006 photometer fitted with an 8-μl Hellma flow-through cell.

The most important part of these systems is the injection device proposed for the continuous recalibration technique. It consists of an eight-port rotary valve to which an external sample loop is attached (Fig. 4). The injection valve used was locally constructed, but commercially available valves can also be used.

All the reagents used were of analytical grade or equivalent.

Results and discussion

Photometric determinations. A chemical reaction is usually necessary to produce a species suitable for measurement. Therefore, the carrier stream must be merged with appropriate reagents. The well-established iron(II)/1,10-phenanthroline reaction was chosen to test the procedure. The buffered 1,10-phenanthroline reagent was added by the auxiliary channel (Fig. 3B)

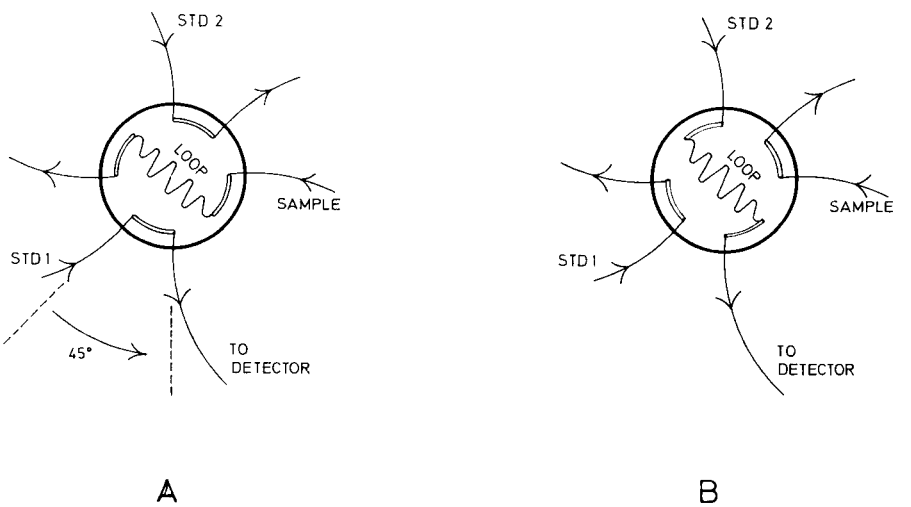

Fig. 4. Injection device: (A) load position; (B) inject position.

and adequate mixing and color development proceeded in a reaction coil fitted between the T-connector and the detector. The first standard solution reacts continuously with the reagent and the baseline signal is obtained. When the valve is switched to the inject position, steady-state signals of the sample and second standard appear.

Dispersion phenomena can provoke the appearance of a shoulder instead of the plateau corresponding to the sample steady-state signal (Fig. 5). To avoid this problem large sample volumes (500—1000 μl) are needed. Obviously, the sample throughput then decreases. A careful choice of the flow rate and reaction coil length minimizes this effect (Fig. 6).

In an optimized system, sample injection rates better than 45 h^{-1} are possible. A drawback of photometric detection is its limited linear working range.

Potentiometric determinations. Potentiometric detectors based on ion-selective electrodes are particularly suitable for process monitoring, owing to the wide range of concentrations that can be determined without loss of sensitivity, the low instrumental cost and the fact that there is no interference from colored or turbid samples [8]. Despite these advantages, there are often problems, especially with PVC electrodes based on liquid ion-exchangers, of poor long-term reproducibility so that frequent calibration is needed to provide accurate results. In cases where neither the standard potential, nor the Nernstian slope are known, the bracketing method is the procedure recommended for calibration [8—10].

In this method, the sample concentration is obtained from the equation

$$C_x = \exp\left[(E_x - E_1)\log C_2 + (E_2 - E_x)\log C_1/(E_2 - E_1)\right]$$

where E_1 and E_2 are the potentials measured with standards of concentrations C_1 and C_2 and E_x is the potential measured for the sample. The accessory equipment necessary to perform such two-point calibrations regularly is

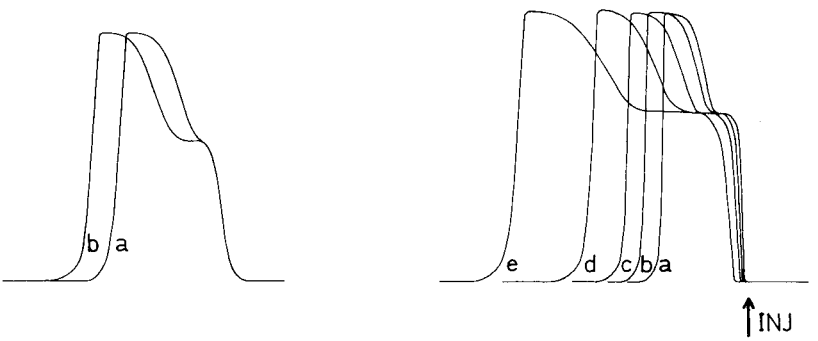

Fig. 5. Influence of sample volume on first step width: (a) 300 μl; (b) 1000 μl.

Fig. 6. Influence of flow rate on sample throughput: (a) 1.0; (b) 0.82; (c) 0.65; (d) 0.48; (e) 0.30 ml min^{-1}.

complicated for reliable applications in process control. With the proposed method, this two-point calibration can be done along with every sample determination. The performance of this technique was evaluated by using a flow-through tubular nitrate electrode, which was inserted into the flow system outlined in Fig. 3A. The use of a single channel and the short response time of these tubular electrodes enable the steady-state potential to be reached in a few seconds, thus improving the sampling rate. In this case, 60 samples/h can be injected and simultaneously with each sample injection a two-point standard calibration is made. The detector outputs are similar to those obtained with photometric detectors.

The standard concentrations used can be as different as is needed, within the Nernstian response range, to allow a high working range and to minimize errors. However, if the sample concentration lies exactly halfway between the two calibrating standards, the relative standard deviation is at a minimum [9] so that bracketing standards are desirable. If the sample matrix is known, it is advisable to prepare the standards in the same or similar matrix. If the ionic strength of the sample varies during the process, or if it is not sufficiently high to maintain reasonable electrical conductivity in the flow system, the main channel must be merged with another solution for adjustment of ionic strength before it passes through the detector.

Another benefit of the proposed technique is the permanent conditioning of the membrane, because the first standard solution is in contact with the membrane all the time except for sample injections. The membrane lifetime is increased in this way.

Conclusions

The continuous recalibration technique proposed here seems to be ideal for the construction of simple, reliable and cheap automatic monitors for process control. The sandwich techniques are still in the early stages of development. Simultaneous determinations done by changing the two standard solutions by two different reagent solutions will be reported soon. Further studies of the applications of this technique in multiparametric or kinetic flow injection analysis are presently under way.

Partial support of this research by CIRIT (Generalitat de Catalunya) is greatly appreciated. M. d. V. was supported by a Research Studentship from FPI program (Ministerio de Educación y Ciencia).

REFERENCES

1 W. E. van der Linden, Anal. Chim. Acta, 179 (1986) 91.
2 M. Valcárcel and M. D. Luque de Castro, Flow Injection Analysis: Principles and Applications, Ellis Horwood, Chichester, 1987.
3 P. J. Elving, E. Grushka and I. M. Kolthoff (Eds.), Treatise on Analytical Chemistry, 2nd Edn., Part I, Vol. 4, Wiley, New York, 1984, Chap. 6.
4 J. Růžička and E. H. Hansen, Anal. Chim. Acta, 145 (1983) 1.

5 M. Gisin, C. Thommen and K. F. Mansfield, Anal. Chim. Acta, 179 (1986) 149.
6 J. Alonso, S. Alegret, J. Bartrolí, J. L. F. C. Lima, A. A. S. C. Machado and J. M. Paulís, Quim. Anal., (1987) in press.
7 S. Alegret, J. Alonso, J. Bartrolí, J. M. Paulís, J. L. F. C. Lima and A. A. S. C. Machado, Anal. Chim. Acta, 164 (1984) 147.
8 D. Midgley and K. Torrance, Potentiometric Water Analysis, Wiley, Chichester, 1978.
9 G. Svehla, in W. Franklin Smyth (Ed.), Electroanalysis in Hygiene, Environmental, Clinical and Pharmaceutical Chemistry, Analytical Chemistry Symposia Series, Vol. 2, Elsevier, Amsterdam, 1980, p. 21.
10 T. S. Ma and S. S. M. Hassan, Organic Analysis using Ion Selective Electrodes, Academic, London, 1982.

Analytica Chimica Acta, 199 (1987) 197—202
Elsevier Science Publishers B.V., Amsterdam — Printed in The Netherlands

Short Communication

CORRELATION STEAM/SOLID CHROMATOGRAPHY OF TRACE ORGANIC COMPOUNDS IN WATER

M. KOEL, M. KALJURAND and E. KÜLLIK*
Institute of Chemistry, Academy of Sciences of the Estonian SSR, Tallinn (U.S.S.R.)
(Received 23rd February 1987)

Summary. Correlation steam/solid chromatography is used for direct determinations of traces of organic compounds in water. Because of suppression of detector noise, correlation chromatography is a practical alternative to single injections or sample concentration at low $\mu g\ l^{-1}$ levels.

The determination of organic compounds in water is a fundamental problem, particularly in environmental pollution studies. Gas chromatography seems to be the most suitable method because of its separation power and sensitivity, but direct injection of water into a gas chromatograph causes difficulties because large quantities of water in the system affect the baseline and remove the liquid stationary phase from the coated solid support. It has been reported previously that adsorption or gas/solid chromatography with steam as carrier enables sharp peaks to be obtained rapidly for many organic compounds in water [1]. Steam/solid chromatography [1] is possibly one of the most useful techniques for evaluating water quality in water-treatment processes. Direct injections of large samples of water are possible without the usual preconcentration or extraction procedures and steam does not significantly degrade the response of a flame ionization detector [2]. Moreover, steam decreases the sorption of compounds on the sorbent and reduces their retention times [3]. Steam/solid chromatography enables various compounds in water to be determined at concentrations $\geqslant 30\ \mu g\ l^{-1}$ without complicated pre-treatment [4, 5], but this is not low enough for the requirements of government regulations, which demand ca. $1\ \mu g\ l^{-1}$.

Process control or environmental control needs technology which is simple to automate. In-stream sampling is widely used in this kind of analysis. Sampling from the stream is done by introducing the sample during a time interval, Δt, into the chromatographic column. Chromatographic separation and sensitivity are enhanced by the elution of solutes as well-separated narrow bands. The length of the band eluted to the detector is a function of the length of the band at the start of the chromatographic process and of the efficiency of the column: the larger the interval Δt, the larger the amount of substance injected into the column, and the longer the length of the solute

0003-2670/87/$03.50

band in the column. However, increasing this interval to infinity does not increase the signal or the signal-to-noise ratio to infinity but to some constant value, while the resolution in the chromatogram is disastrously decreased. These two effects limit the measurement of flow streams with low sample concentrations.

To consider this problem in more detail, the injection of a sample during an interval Δt produces a concentration distribution at the end of the column according to the function

$$y(t) = \int_{-\Delta t/2}^{\Delta t/2} h(t - \tau)\mathrm{d}\tau \tag{1}$$

Here $y(t)$ is detector output signal and $h(t)$ a chromatogram for an injection of an infinitely narrow concentration pulse; $y(t)$ has a maximum y_m at $t = 0$ and if the chromatographic peak has the Gaussian form, then

$$y_m = A \int_{-\Delta t/2}^{\Delta t/2} \exp(-\tau^2/2\sigma^2)\,\mathrm{d}\tau = (2\pi)^{1/2}\sigma A \,\mathrm{erf}(\Delta t/2\, 2^{1/2}\sigma) \tag{2}$$

where $\mathrm{erf}(x)$ is the error integral [6], A is the area of the peak and σ is the band variance.

The error integral can be approximated to small argument values $\mathrm{erf}(x) = (2/\pi^{1/2})(x - x^3/3)$. This gives

$$y_m = A\,\Delta t\,[1 - (1/24)(\Delta t/\sigma)^2]$$

Then the condition $\Delta t/\sigma \leqslant 0.5$ determines the linear region of this sampling method within 1% precision: $y_m \to (2\pi)^{1/2}\sigma A$ if $\Delta t \to \infty$, and $y_m \leqslant 0.99\,(2\pi)^{1/2}\sigma A$ if $\Delta t \geqslant 6\sigma$. This condition establishes the largest Δt value that increases the signal-to-noise ratio. It is obvious that a very large value should not be used because it would not increase significantly the signal-to-noise ratio.

Of course, a long solute band severely affects the resolution of the chromatogram. A gas-sampling valve with short transit time provides the solute band as a plug. For this, the total second moment, σ_T^2, of the peak (or simply the width) is determined by the additivity rule of the variances [7]:

$$\sigma_T^2 = \sigma^2 + (\Delta t)^2/12$$

The second term $(\Delta t)^2/12$ is the increase in the chromatographic peak width caused by the finite length of the injection time. If the increase in peak width is not very large, then the relative increase in peak width can be described by

$$(\sigma_T^2 - \sigma^2)/\sigma^2 = 2(\sigma_T - \sigma)/\sigma = (1/12)(\Delta t/\sigma)^2 \tag{3}$$

The resolution R can be defined by

$$R = (1/2)(\Delta t_R/\sigma)$$

where Δt_R is the difference in retention times between two neighbouring peaks on the chromatogram. The relative decrease in resolution by varying $\Delta\sigma = \sigma_T - \sigma$ is $\Delta R/R = \Delta\sigma/\sigma$ and, by using Eqn. 3, the relative decrease in resolution can be described as a function of the sampling time:

$$\Delta R/R = (1/24)\,(\Delta t/\sigma)^2 \qquad (4)$$

This equation describes the shortest sampling time Δt, that is necessary to maintain acceptable resolution in the chromatogram. But, as follows from Eqn. 2, Δt also governs the amplitude of the peak and thus the signal-to-noise ratio on the chromatogram; thus, the two requirements for Δt cannot be satisfied simultaneously.

To maintain the required resolution on the chromatogram and an increased signal-to-noise ratio, correlation chromatography [8] can be used. Because of its noise suppression properties, the correlation technique enables operation with very short Δt values to maintain the necessary resolution and signal-to-noise ratio; i.e., the correlation technique can be used to increase the resolution at a constant signal-to-noise ratio which decreases in the common chromatographic mode, as is indicated by Eqns. 2 and 4. Usually in correlation chromatography, the sampling time Δt is equal to the digitization interval of the detector signal for later computer treatment; from the sampling theorem, it follows that $\Delta t \leqslant 0.5\sigma$ is a good value for the digitization interval and also for the injection time [9]. The increase in peak width is then 1%, as follows from Eqn. 3, and the decrease in resolution is similarly small. However, evaluating the numerical values for the error integral in Eqn. 2 indicates that the peak amplitude is 5 times less than the maximum attainable value for $\Delta t \to \infty$. Thus the use of a pseudo-random binary sequence (PRBS) input with $n = 127$ elements gives a correlogram which has no worse resolution and a signal-to-noise ratio better than that obtained with a single injection and $\Delta t \to \infty$.

Experimental

The Perkin-Elmer 900 gas chromatograph used was equipped with a flame ionization detector (FID), water feeder and sample feeder and special system for sample injection. The idea was taken from Deans' work [10] and it has an advantage over conventional samplers in having no moving parts in the sample path. The sample size is selected remotely through a timer, permitting an easy change of sample size. The apparatus outlined in Fig. 1 is homemade. Steam was generated at the column temperature maintained by means of the oven. The whole attachment is very simple and does not require complicated modifications of the chromatograph.

Glass columns (1 m or 2 m, 2 mm i.d.) were packed with large-porosity silica gel (Spherosil and Porasil) with different surface areas. The detector temperature was approximately 240°C during all measurements, in order to prevent any condensation. The injection valve temperature was the same as the oven temperature.

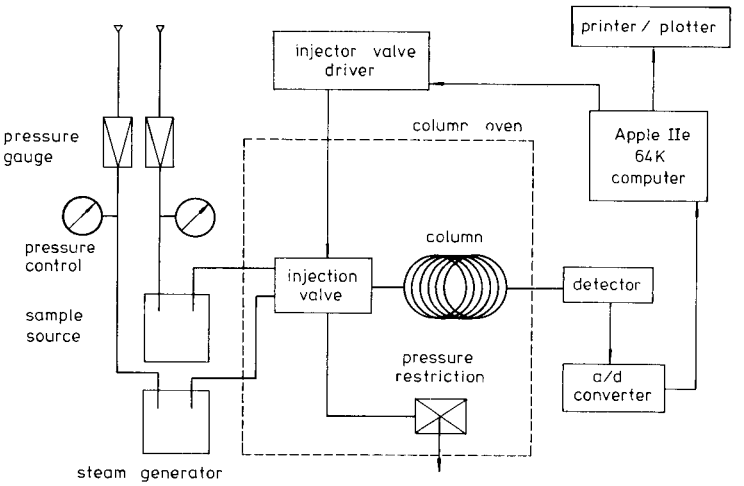

Fig. 1. Experimental set-up for correlation steam/solid chromatography.

The column was used at three constant temperatures (130, 140 or 150°C). The carrier flow rate was controlled by a constant water feed-rate which corresponded to 40—95 ml min^{-1} at 130—150°C. The same temperature was maintained for the sample feed. The volume of the injected sample was governed by the opening time of the valve at constant flow rate.

To control the switching and to record the data, an Apple-IIe computer was used. In a correlation experiment, decorrelation and print-out were done on-line by the same computer. With the Apple-IIe computer, it is possible to use PBRS with up to 2047 elements that theoretically gives a 23-fold increase in the signal-to-noise ratio. Decorrelation was done by using a fast Hadamard transform [11] and all the software was written in this laboratory.

In the experiments concerned with Fig. 4, a PBRS with 511 elements was used with a clock period of 1.3 s. In this case, the experiment lasted 22.1 min.

Results

Figure 2 shows a chromatogram illustrating the separating power of this type of chromatographic system. Separation is fast and peaks are symmetrical at quite a low temperature. The surface area of the packing material has a great influence on the retention time of solutes and must be taken into account when the length of the chromatographic experiment is selected.

Figure 3 shows that increasing the opening time of the injection switch (sampling interval) about 5-fold (for single injection) does not give a proportional increase in the signal. The injection of large sample volumes to detect trace components can lead to broadened peaks, which has adverse effects on separation. Some data related to Fig. 3 are given in Table 1.

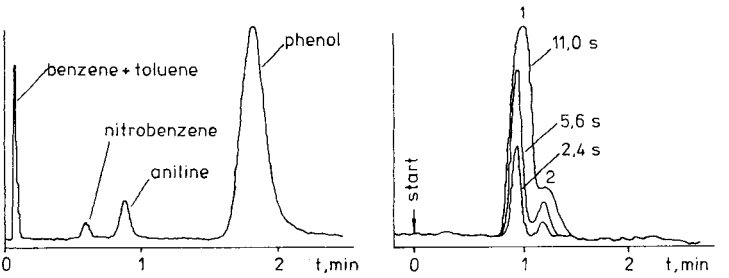

Fig. 2. Chromatogram of traces of organic material in water (concentrations at mg l^{-1} level). Packed glass column (1 m × 2 mm i.d.) with Porasil E (80—100 mesh). Column temperature 130°C.

Fig. 3. Influence of the opening time of the injection valve on resolution of nitrobenzene (peak 1) and nitrotoluene (peak 2).

Figure 4 demonstrates the enhancement of the signal-to-noise ratio in correlation chromatography and the better resolution compared with a single long injection.

The detection limit for this system (steam/solid chromatography with a conventional FID) based on the correlation technique makes it possible to detect traces in water at concentration levels of about 1 μg l^{-1} for alcohols and 0.10 mg l^{-1} for phenol.

Correlation chromatography seems to be well suited for environmental applications, because large amounts of sample are available. The instrument is relatively simple to build, taking advantage of the sophisticated data-processing capabilities of modern personal computers.

TABLE 1

The relationship between the sampler opening time and peak parameters (height and width at half height) for peak 1 (Fig. 3)

Run	Δt (s)	y_m (rel. units)	$w_{1/2}$ (s)
1	2.4	26	5
2	5.6	48	7
3	11.0	61	13

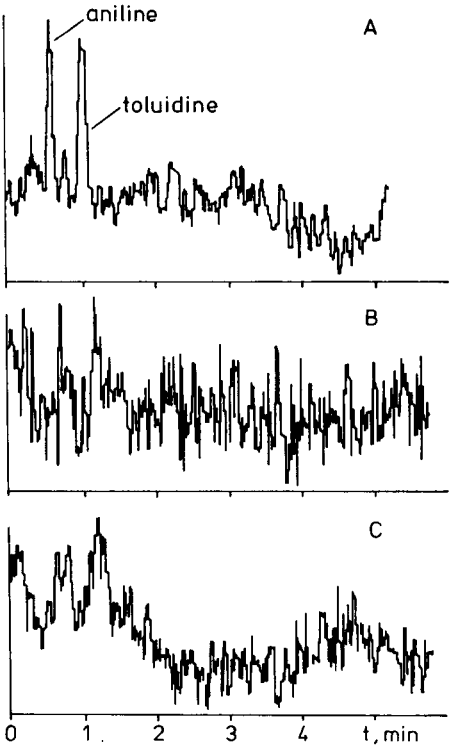

Fig. 4. Effect of using the correlation technique: (A) correlogram with corresponding opening time of 1.3 s; (B) single injection of the same sample with a valve opening time of 2.9 s; (C) as B with a valve opening time of 11 s. Concentrations of aniline and toluidine are 60 $\mu g\ l^{-1}$.

REFERENCES

1 A. Nonaka, Anal. Chem., 44 (1972) 271.
2 J. Teply and M. Dressler, J. Chromatogr., 191 (1980) 221.
3 B. L. Karger and A. Hartkopf, Anal. Chem., 40 (1968) 215.
4 K. Urano, K. Ogura and H. Wada, Water Res., 15 (1981) 225.
5 K. Urano, H. Maeda, K. Ogura and H. Wada, Water Res., 16 (1982) 323.
6 G. A. Korn and T. M. Korn, Mathematical Handbook for Scientists and Engineers. McGraw-Hill, New York, 1968.
7 J. C. Sternberg, in J. C. Giddings and R. A. Keller (Eds.), Advances in Chromatography, Vol. 2. M. Dekker, New York, 1966, p. 205.
8 See, e.g., H. C. Smit, Trends Anal. Chem., 2 (1983) 1.
9 P. C. Kelly and G. Horlik, Anal. Chem., 45 (1973) 518.
10 D. R. Deans, J. Chromatogr., 289 (1984) 43.
11 M. Kaljurand and E. Kullik, Chromatographia, 11 (1978) 328.

Analytica Chimica Acta, 199 (1987) 203—208
Elsevier Science Publishers B.V., Amsterdam — Printed in The Netherlands

Short Communication

DETERMINATION OF PARAQUAT BY FLOW-INJECTION SPECTROPHOTOMETRY

E. CHICO GUIJARRO, P. YÁÑEZ-SEDEÑO and L. M. POLO DIÉZ*

Department of Analytical Chemistry, Faculty of Chemistry, Complutense University of Madrid, 28040 Madrid (Spain)

(Received 13th October 1986)

Summary. The flow-injection determination of Paraquat (1,1′-dimethyl-4,4′-bipyridinium) is based on its reduction with sodium dithionite in alkaline medium and detection at 605 nm. Linear calibration plots are obtained for 0.1—1.0, 1.0—10 and 5.0—30.0 mg l^{-1} Paraquat, the lower limit being 40 times less than that of the usual spectrophotometric method. The method is applied to determine Paraquat in spiked potable water and potatoes after preconcentration by column ion-exchange. The determination of Paraquat in different herbicide samples yielded results in good agreement with those obtained by polarographic and manual spectrophotometric methods.

Paraquat (1,1′-dimethyl-4,4′-bipyridinium) is an extensively used herbicide. Several methods for its determination have been described, including techniques such as spectrophotometry [1—6], differential pulse polarography [7—9], gas chromatography [10—12] and high-performance liquid chromatography [13—16]. The spectrophotometric method most often used is based on the reduction of Paraquat to a blue radical by sodium dithionite in alkaline medium [3]. This method involves measurement of absorbance after 15 min and use of a blank prepared from a 4.0 mg l^{-1} Paraquat solution, which sets the lower limit of calibration graphs. Moreover, the radical is quite unstable under the experimental conditions because of its fast oxidation by atmospheric oxygen, which produces fading in solutions and causes handling problems, mainly in filling spectrophotometric cells. These inconveniences can be minimized by determining Paraquat in a flow-injection system, thus providing a rapid routine procedure.

Experimental

Apparatus. A Tecator model FIAstar 5020 flow-injection analyzer equipped with an injection valve, two peristaltic pumps with four channels (40 rpm) and a spectrophotometric detector was used in conjunction with a FIAstar 5022 recorder.

Polarographic measurements were made by the reference method using a Metrohm E-506 Polarecord equipped with a polarographic stand E-505. Electrodes and electrochemical cells are the same as described previously [9].

0003-2670/87/$03.50

For the spectrophotometric reference measurements, a double-beam digital Pye-Unicam 8-200 spectrophotometer was used with 1-cm glass cells.

Reagents. An aqueous 100 mg l^{-1} Paraquat stock solution was prepared from 1,1′-dimethyl-4,4′-bipyridylium dichloride (EGA Chemie). Less concentrated solutions were prepared by suitable dilution. A 1% (w/v) solution of sodium dithionite (Merck) in 0.1 M sodium hydroxide was prepared hourly. The cation-exchange resin Dowex 50W-X8 was used in the hydrogen form. All other chemicals used were of analytical grade.

The analyzed samples were commercial Paraquat and Diquat herbicides from ICI (Gramoxone Extra and Gramoxone Reglone mixtures). Potable water and potatoes spiked with Paraquat were also tested.

Calibration graphs. The flow system is shown in Fig. 1. Paraquat solution (120 µl), in the 1.0—10.0 mg l^{-1} range, was directly injected into the carrier stream (distilled water, or 30% (w/v) NaCl solution when preconcentration was by cation-exchange) and the peak height was measured at 605 nm.

Paraquat determination in commercial herbicides. In the absence of Diquat, the sample was diluted to obtain the appropriate concentration level. The sample solution was injected directly into the carrier stream (distilled water) and the above calibration graph was used to determine Paraquat. In the presence of Diquat, samples which contained less than 0.80 mg of Diquat dibromide were added together with 2 ml of 2 M sodium hydroxide to a test tube with a screw cap and diluted to 10 ml with distilled water; then the tube was sealed and left for at least 6 h. The precipitate was removed by centrifugation, and aliquots of the supernatant solution were injected into the carrier stream (distilled water). The above calibration graph for Paraquat determination was used.

Paraquat determination in potable water and potatoes. To determine Paraquat in potable water, 250 ml of sample was treated with 0.25 g of disodium-EDTA and adjusted to pH 9 with sodium hydroxide.

For potatoes, a representative sample was pulped in a blender and 250 g was weighed and transferred to a 1-l round-bottomed flask. Next 75 ml of 9 M sulphuric acid was added and refluxed for 30—60 min. After refluxing, the flask was removed and the condensers washed with water. The contents of the flask were filtered through a sintered glass filter (no. 4) and the filtrate transferred to a 1-l beaker. Finally 70 ml of 50% (w/v) sodium hydroxide and 3 g of disodium-EDTA were added and the pH was adjusted to 9 with sodium hydroxide.

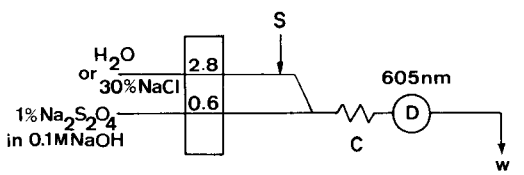

Fig. 1. Flow diagram for the spectrophotometric determination of Paraquat: S, sample injection, 120 µl; C, reaction coil, 12 cm long, 0.5 mm i.d.; flow rates in ml min^{-1}.

To preconcentrate the Paraquat by column cation-exchange, a glass-wool plug was placed at the bottom of a 30 × 1.2-cm column and 3 ml of cation-exchange resin in water was introduced followed by another glass-wool plug. Saturated sodium chloride solution (25 ml) was passed through the column, followed by 50 ml of water. Next, the Paraquat sample was run through the column (3 ml min^{-1}) and the resin was washed successively with 25 ml of water, 25 ml of 2 M hydrochloric acid and 25 ml of sodium chloride solution (1:10 water/saturated NaCl). All these effluents were rejected. Paraquat was then eluted with saturated sodium chloride solution (0.67 ml min^{-1}), exactly 50 ml of the effluent being collected. It is advisable to keep the resin in contact with the saturated sodium chloride solution for at least one night before eluting.

In both cases, the eluted Paraquat solution was injected into the 30% (w/v) NaCl carrier solution. The calibration graph was prepared by using this carrier as indicated above.

Results and discussion

Optimization of the flow system. The sample (120 μl) was injected directly into the carrier stream, which was distilled water or a 30% (w/v) sodium chloride solution, and reacted with the 1% (w/v) sodium dithionite reagent (Fig. 1). The effects of changed chemical conditions and manifold parameters were studied over the ranges shown in Table 1, in which the optimum values found for each variable are also listed.

Analytical characteristics. The calibration graphs for Paraquat were prepared under the optimum conditions listed in Table 1. For aqueous herbicide samples, with distilled water as the carrier stream, linear plots were obtained for three concentration ranges: 5.0—30.0, 1.0—10.0, and 0.1—1.0 mg l^{-1} Paraquat. The signal obtained from 5 mg l^{-1} Paraquat was 418 mV, equivalent to 0.167 absorbance. Typical plots are shown in Fig. 2.

The effect of Diquat (1,1′-ethylene-2,2′-bipyridinium) on the Paraquat determination was tested. Interference is caused by the formation of a green radical which also absorbs at 605 nm under the experimental conditions used. However, Diquat can be removed previously by precipitation with sodium hydroxide [4, 5] as indicated above.

The interference of high salt concentrations in solutions taken as eluents

TABLE 1

Results of the optimization studies

Variable	Range studied	Optimum value	Variable	Range studied	Optimum value
Flow rates (ml min^{-1})			Sample volume	40—220	120
Carrier stream	0.6—3.0	2.8	(μl)		
Reagent stream	0.4—2.8	0.6	$Na_2S_2O_4$ (%, w/v)	0.1—2.0	1.0
Coil length (cm)	52—112	64	NaOH (M)	0.02—2.0	0.10

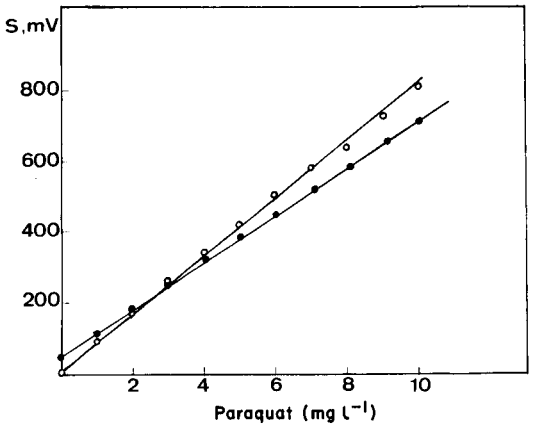

Fig. 2. Calibration graphs for Paraquat: (○) aqueous samples with water as carrier; (●) eluted samples with 30% NaCl as carrier.

for the cation-exchange procedure was also tested. Saturated ammonium chloride solution, which is the eluent most often recommended in the literature [17], provides good recoveries in spectrophotometric determinations of the herbicide at wavelengths near 396 nm. However, this eluent is unsuitable for the flow-injection procedure because it produces acid conditions quite different from the optimum necessary for the reduction reaction, thus decreasing the signal. This effect was avoided by using sodium chloride as eluent, but the recorded signals were increased by the refraction effects of the sample when water was used as carrier. To avoid this, the refractive indexes of the carrier and sample must be as close as possible. Good results were obtained by using a 30% (w/v) sodium chloride solution as the carrier when eluted samples were tested.

The interference of calcium(II) and magnesium(II) ions, which are usually present in water and potato samples, was also tested. Slight increments in the signals were observed for concentration levels between 25 and 400 mg l^{-1} in both species, probably because of precipitation reactions with the alkaline dithionite reagent. This interference can be avoided by treating the sample with EDTA at pH 9, before introduction to the column. In contrast, interferences from the different materials usually present in aqueous herbicide formulations, such as common surfactants, were found to be negligible after the sample solutions had been diluted to give suitable Paraquat concentration.

Determination of Paraquat in commercial herbicides, potable water and potatoes. In the case of commercial herbicides, the accuracy of the method was established by determining Paraquat in commercial herbicides containing Paraquat and Diquat in the usual ratios. Results obtained were statistically compared with those from polarographic [9] and manual spectrophotometric [3] methods using the Student *t*-test (Table 2). The *F* values

TABLE 2

Determination of Paraquat in commercial herbicides

Paraquat present[a] (% w/v)	Diquat present[a] (% w/v)	Paraquat found[b] (% w/v)				
		Flow injection	Polarography	t_{exp}	Manual spectrophotometry	t_{exp}
20	—	22.9 ± 0.3	22.6 ± 0.3	1.58	22.8 ± 0.6	0.34
20	—	22.0 ± 0.7	21.2 ± 0.5	2.07	22.3 ± 0.3	1.63
20	—	23.2 ± 0.2	22.8 ± 0.5	1.66	23.4 ± 0.3	1.26
8	12	8.1 ± 0.2	7.9 ± 0.2	1.58	8.3 ± 0.3	1.26
10	10	10.3 ± 0.3	9.8 ± 0.4	2.25	9.7 ± 0.7	1.75
12	8	11.8 ± 0.3	11.9 ± 0.2	0.63	12.1 ± 0.2	1.90

[a]Nominal values. [b]Mean of 5 determinations with standard deviation and t_{exp} from the Student t-test: $t_{4,0.95} = 2.31$.

showed no significant differences at the 0.05 significance level and the t values also showed no significant differences between means at the 95% confidence level, testifying to the reliability of the proposed method.

In the case of potable water and potato, recovery experiments were done by analyzing spiked potable water and potato samples to which the cation-exchange method was applied. The results obtained (Table 3) were common for this kind of study and showed that major losses of Paraquat occur at the extraction step, particularly for potato samples. The mean recoveries of Paraquat from these samples are lower than expected when saturated ammonium chloride is used as eluent. However, reproducibility is satisfactory and it is not necessary to correct the absorbance of the sample for background absorption by means of equations [1].

It can be concluded that the flow-injection technique allows Paraquat to be determined at concentrations up to forty times less than the lower concentration limit possible with the usual spectrophotometric method. The flow-injection method also provides economy of reagent and sample and higher sample throughput (80 h^{-1}).

The financial support of the Spanish C.A.I.C.y.T., project 2251/83, is gratefully acknowledged.

TABLE 3

Recoveries of Paraquat by applying the ion-exchange method

Sample	Size of sample	Paraquat added (mg l^{-1})	Recovery (%)	R.s.d. (%)
Standard solution	250 ml	0.2—1.0	64—70	2.1
Potable water	250 ml	0.5	65—69	2.8
Potatoes	250 g	0.2—0.4	54—57	3.1

REFERENCES

1 A. Calderbank and S. H. Yuen, Analyst, 90 (1965) 99.
2 A. A. Carlstrom, J. Assoc. Off Anal. Chem., 51 (1968) 1306; 54 (1971) 718; 55 (1972) 857.
3 S. H. Yuen, J. E. Baggness and D. Myles, Analyst, 92 (1967) 375.
4 M. Ganesan, S. Natesan and V. Ranganathan, Analyst, 104 (1979) 258.
5 P. Yáñez-Sedeño and L. M. Polo Díez; Talanta, 33 (1986) 745.
6 D. R. Jarvie, A. F. Fell and M. J. Stewart, Clin. Chim. Acta, 117 (1981) 153.
7 G. Franke, W. Pietrulla and K. Preussuer, Fresenius' Z. Anal. Chem., 298 (1979) 38.
8 J. Polak and J. Volke, Chem. Listy, 77 (1983) 1190.
9 P. Yáñez-Sedeño, J. M. Pingarrón Carrazón and L. M. Polo Díez, Mikrochim. Acta, Part III, (1985) 279.
10 A. J. Cannard and W. J. Criddle, Analyst, 100 (1975) 848.
11 S. U. Kahu, Bull. Environ. Contam. Toxicol., 14 (1975) 745; Anal. Abstr., 30 (1979) 6G6.
12 G. H. Draffen, R. A. Clare, D. L. Davies, G. Hawkasworth, S. Murray and D. S. Davies, J. Chromatogr., 139 (1977) 311.
13 Y. Kawano, J. Audino and M. Edlund, J. Chromatogr., 115 (1975) 289.
14 Z. J. Paschal, L. D. Needham, J. L. Rollen, M. Joyce and J. A. Lidle, J. Chromatogr., 177 (1979) 85.
15 R. Gill, S. C. Qua and A. C. Moffat, J. Chromatogr., 255 (1983) 483.
16 E. A. Queree, S. J. Dickson and S. M. Shaw, J. Anal. Toxicol., 9 (1985) 10.
17 P. F. Lott and J. W. Lott, J. Chromatogr. Sci., 16 (1978) 390.

Analytica Chimica Acta, 199 (1987) 209—214
Elsevier Science Publishers B.V., Amsterdam — Printed in The Netherlands

Short Communication

PRECONCENTRATION OF COPPER WITH THE ION-PAIR OF 1,10-PHENANTHROLINE AND TETRAPHENYLBORATE ON NAPHTHALENE

M. SATAKE* and G. KANO

Faculty of Engineering, Fukui University, Fukui 910 (Japan)

B. K. PURI

Department of Chemistry, Indian Institute of Technology, Hauz Khas, New Delhi-110016 (India)

S. USAMI

Department of Industrial Chemistry, Faculty of Engineering, Toyama University, Toyama 930 (Japan)

(Received 11th November 1986)

Summary. A solid ion-pair material produced from 1,10-phenanthroline and tetraphenylborate on naphthalene provides a simple, rapid and fairly selective means of preconcentrating copper from up to 1000 ml of aqueous samples (about 200-fold concentration is possible). Copper is quantitatively adsorbed in the pH range 1.6—10.4 at a flow rate of 3 ml min^{-1}. The solid mass (0.2 g) is dissolved from the column with 5 ml of dimethylformamide (DMF) and copper is measured by atomic absorption spectrometry at 324.7 nm. Linear calibration is obtained for 2—28 μg of copper in 5 ml of DMF solution. Replicate determination of 14 μg of copper gave a mean absorbance of 0.220 (n = 7) with a relative standard deviation of 1.5%. The sensitivity for 1% absorption was 0.093 $\mu g\ ml^{-1}$. After optimization, the method was applied to determine trace copper in standard reference materials, natural waters, beverages and hair.

Among the numerous preconcentration techniques used in trace-element determinations, liquid-liquid extraction is one of the most widely used, but it cannot be applied directly for extraction of metal ions which form complexes with the reagent only at a high temperature [1, 2]. This difficulty can be overcome by using molten naphthalene as the medium [3, 4], but then thermally unstable metal chelates cannot be utilized. Solid-liquid separation after adsorption of metal chelates on microcrystalline naphthalene is rapid and economical and can be applied to many types of metal complexes; it is especially useful for complexes which have poor solubility in non-aqueous organic solvents [5—7]. The only difficulty is in the filtration of small amounts of naphthalene.

In the method described below, copper is selectively preconcentrated from a moderate volume of the aqueous phase by using 1,10-phenanthroline/tetraphenylborate/naphthalene as the adsorbent. The adsorbed metal in the column is not removed by washing with water but can be dissolved along with naphthalene in a solvent such as dimethylformamide (DMF) for subsequent direct determination by atomic absorption spectrophotometry (a.a.s.).

0003-2670/87/$03.50

Somewhat similar methods have been developed in which adsorbents such as thiol cotton [8], silanized glass beads [9], Amberlite XAD-4 resin [10], cellulose [11] and metal oxides or hydroxides [12] have been applied. The proposed method is more economical (only 0.2 g of the adsorbent is used), faster (the solid mass is dissolved in a small volume of the solvent without elution) and sensitive (200-fold concentration is achieved easily). The method is applied for the determination of copper in complex materials like standard alloys, human hairs, wine, beer, whisky and waters.

Experimental

Apparatus. A Perkin-Elmer model 403 atomic absorption spectrometer and a Toa-Dempa HM-5A pH meter were used. The hollow-cathode lamp for copper was from Hamamatsu Photonics (Japan).

Reagents. Copper chloride stock solution was prepared in water and standardized against EDTA in the conventional manner. A pH 4.5 buffer solution was prepared by mixing 1 M acetic acid and 1 M ammonium acetate solution in a suitable ratio.

Naphthalene, 1,10-phenanthroline (Phen), sodium tetraphenylborate (TPB), DMF and all other reagents were of analytical-reagent grade. Twice-distilled water was used.

Preparation of 1,10-phenanthroline/tetraphenylborate/naphthalene mixture. A 20% (w/v) solution of naphthalene in acetone (100 ml) was transferred to 700 ml of 0.1 M hydrochloric acid containing 4.1 g of 1,10-phenanthroline. This solution was stirred magnetically at 40°C for a few minutes. Then 100 ml of an aqueous 6% (w/v) solution of TPB was added slowly. This solution was stirred for 3—4 h for complete coprecipitation of the naphthalene/Phen/TPB mixture. It was filtered through paper by suction, washed with water, dried in an oven at 40°C for several hours and then stored in a brown bottle which should be kept in a desiccator.

Glass tubes (7-mm internal diameter, 150 mm long) were loaded with 0.2 g of this mixture, held in position with quartz-wool wads.

General procedure. A portion of copper solution (2–28 μg of copper) was mixed with 1.0 ml of 1% (w/v) L-ascorbic acid solution, to reduce copper(II) to copper(I), and 1.0 ml of acetate buffer pH 4.5. The solution was diluted to 20—25 ml with distilled water. The column loaded with naphthalene/Phen/TPB was conditioned to pH 4.5 by passing 10—15 ml of the pH 4.5 buffer at a flow rate of 3 ml min^{-1} and then the sample solution was passed, with aspiration if necessary. The packing was washed with water and the metal complex along with the naphthalene was dissolved by passing 5 ml of DMF. This solution was aspirated into an air/acetylene flame and the absorbance was measured at 324.7 nm against the reagent blank.

The operating conditions were as follows: slit setting 4; current 8 mA; burner height 11 mm; acetylene pressure 0.5 kg cm^{-2} and air pressure 2.1 kg cm^{-2}.

Results and discussion

Adsorption characteristics of Phen/TPB. In acidic solution, 1,10-Phenanthroline is a singly charged cation [13, 14] and is capable of forming an ion-pair with the TPB anion. The ion-pair was easily coprecipitated with microcrystalline naphthalene. The extent of adsorption of the Phen/TPB ion-pair on naphthalene was enhanced by digesting the mixture on a hot plate and drying it at 40°C.

The adsorption of copper ions on naphthalene/Phen/TPB reached a maximum as the pH was increased from zero to 1.6 and then remained constant up to pH 10.4. The addition of 1.0–3.0 ml of the acetate buffer (pH 4.5) caused no significant variation in the adsorption of copper; the use of 1.5 ml of pH 4.5 buffer is recommended. The flow rate was varied from 0.5 to 20 ml min^{-1}; over this range, the adsorption was not affected. A flow rate of 3 ml min^{-1} is recommended for convenience.

The adsorption capacity of the loaded naphthalene was evaluated by a batch method. For this experiment, a solution containing 500 μg of copper, 1.0 ml of the buffer (pH 4.5) and 0.2 g of the loaded naphthalene mixture was diluted to 30 ml in a 100-ml separatory funnel and shaken well for 30 min. The maximum amount of copper adsorbed was found to be 750 $\mu g\ g^{-1}$ of the adsorbent. The adsorption capacity for copper depended greatly on the mole ratio of 1,10-phenanthroline to TPB. Experimentally, it was shown that the adsorption capacity was maximal when this mole ratio was 1:1, as expected.

Effects of reducing agent, sample volume and solvent. Varying amounts of L-ascorbic acid were added to a sample solution containing 14 μg of copper. Copper(II) was completely reduced to copper(I) with 1 ml of a 0.001% (w/v) solution of L-ascorbic acid. In this work, 1 ml of a 1% solution was used for security.

The effect of the volume of the aqueous phase on the adsorption of copper on the column was studied by the general procedure. The adsorption remained constant and maximum provided that the volume of the aqueous phase did not exceed 1000 ml.

Various solvents were tested for the removal of the copper(I)/Phen/TPB/naphthalene from the loaded column. This material was found to be insoluble in many nonaqueous solvents but dissolved easily in water-miscible solvents like DMSO, DMF or acetonitrile. DMF was selected to dissolve the mixture because of the high absorbance obtained. Although 3 ml of DMF sufficed, 5 ml is recommended for reliability.

Linearity, sensitivity and precision. Under the optimum conditions described above, the calibration curve obtained was linear over the concentration range 2–28 μg of copper in 5 ml of DMF solution. Eight replicate determinations of 14 μg of copper gave a mean absorbance of 0.220 with a relative standard deviation of 1.5%. The sensitivity for 1% absorption was 0.093 $\mu g\ ml^{-1}$ (0.133 $\mu g\ ml^{-1}$ for direct measurement from the aqueous solution). The preconcentration factor was 200.

Effect of diverse ions. Sample solutions containing 14 μg of copper and various amounts of different metal ions were examined by the general procedure. The tolerance limits (error < 3%) are given in Table 1. Many of the salts can be tolerated even up to milligram levels. EDTA interfered at low levels, suggesting that the formation constant of the Cu/EDTA complex is higher than that of the Cu(I)/Phen/TPB complex [15, 16].

Determination of copper in standard alloys. A 0.1–0.5 g sample of the standard alloy was dissolved in 20–30 ml of hydrochloric acid (1 + 1) by heating on a water-bath and then 2–3 ml of 30% (v/v) hydrogen peroxide was added. After the excess of peroxide had been decomposed by heating, the solution was cooled, filtered and diluted to 100 ml in a standard flask. An aliquot of this solution was examined by the general procedure. The results are given in Table 2.

Determination of copper in natural waters, beverages and hair. The method was applied for the determination of copper in natural water samples. An aliquot (300–500 ml) of the water sample was adjusted to pH 1.0 with nitric acid, filtered to remove suspended material and then subjected to the general procedure. The results (Table 3) are in good agreement with those obtained by the standard DDTC/MIBK method after preconcentration of the sample in a vacuum evaporator.

The method was also applied to the determination of copper in a few samples of wines, whisky and beers after wet oxidation with concentrated nitric acid and concentrated perchloric acid. A 100-ml portion of each sample was evaporated to about 5 ml on a hot plate and digested with the acid mixture; the solution was diluted with water in a 100-ml standard flask. For the

TABLE 1

Effect of diverse species

Tolerance limit	Salt or ion
1 g[a]	NaI, $NaClO_4 \cdot H_2O$, KNO_3, NaCl, $CH_3COONa \cdot 3H_2O$, NH_4Cl, Na_2SO_4, KSCN, $K_2C_2O_4$, KH_2PO_4, sodium tartrate, sodium citrate
100 mg	KCN
50 μg	Disodium EDTA
100 mg[a]	Mg(II), Mn(II), Mn(VI), Ca(II), Pb(II), Cr(VI), Cd(II), Al(III), Zn(II), Co(II)
30 mg	Ni(II)
15 mg	W(VI)
10 mg[a]	Ru(III)
5 mg[a]	Ir(III)
1 mg[a]	V(V)
500 μg	Fe(III)
200 μg	Hg(II)
100 μg	Pd(II), Au(III)
40 μg	Pt(IV)

[a]Maximum tested.

TABLE 2

Analysis of alloys for copper

Sample	Composition (%)	Copper content (%)	
		Certified	Found[a]
N.B.S. SRM-94c Zinc alloy	Mn 0.014, Ni 0.006, Sn 0.006, Al 4.13, Cd 0.002, Fe 0.018, Pb 0.006, Mg 0.042	1.01	1.00 ± 0.01
N.B.S. SRM-171 Magnesium alloy	Mn 0.45, Si 0.0018, Ni 0.0009, Al 2.98, Pb 0.0033, Fe 0.0018, Zn 1.05	0.0112	0.0110 ± 0.0003
Sumitomo Aluminium, No. 2011-2	Si 0.12, Fe 0.29, Ti 0.014, Mn 0.032, Mg 0.027, Bi 0.60, Ni 0.010, Pb 0.60, Zn 0.034	5.14	5.11 ± 0.2

[a]Mean of 5 determinations.

TABLE 3

Determination of copper in natural waters, beverages and hair

Sample	Copper found[a] ($\mu g\ l^{-1}$)	
	Present method	DDTC/MIBK method
Hot spring water	15 ± 0.8	13 ± 1.0
River water	7 ± 1.1	9 ± 1.4
River water	1.7 ± 0.4	—
River water	0.9 ± 0.4	—
Lake water	11 ± 1.3	13 ± 1.5
Wine	292 ± 2	321 ± 2
Whisky	105 ± 2	92 ± 2
Beer	26 ± 1	23 ± 2
Beer	33 ± 3	29 ± 3
Human hair (male)[b]	13.5 ± 0.2	14.3 ± 0.2
Human hair (female)[b]	26.3 ± 0.3	27.7 ± 0.3

[a]Mean of 5 determinations. [b]Results are given in $\mu g\ g^{-1}$.

analysis of human hair, a 10-g sample was decomposed by heating with 30 ml of concentrated nitric acid and 3 ml of 60% perchloric acid in a Kjeldahl flask; the solution was cooled, filtered and diluted to 200 ml with water in a calibrated flask. An aliquot of this solution was taken through the general procedure. The results obtained for these samples are also shown in Table 3.

Conclusion

The proposed technique is not only convenient but rapid and sensitive. Only 0.2 g of the adsorbent is needed and all of the 3–5 ml of DMF can be used for the absorbance measurement. The preparation of the adsorbent is easier than that of other sorbents used for similar purposes [8–12].

REFERENCES

1 J. Brandstetr and J. Vrestal, Collect. Czech. Chem. Commun., 26 (1961) 392.
2 J. P. Tandon and R. C. Mehrotre, Fresenius' Z. Anal. Chem., 176 (1960) 87.
3 A. Wasey, R. K. Bansal, B. K. Puri and A. L. J. Rao, Talanta, 31 (1984) 205.
4 T. Nagahiro, K. Uesugi, M. Satake and B. K. Puri, Bull. Chem. Soc. Jpn., 58 (1985) 1115.
5 T. Nagahiro, M. Satake, J. L. Lin and B. K. Puri, Analyst, 109 (1984) 163.
6 B. K. Puri, C. L. Sethi and A. Kumar, Mikrochim. Acta, Part I, (1983) 361.
7 M. Satake, G. Kano, M. C. Mehra, M. Katyal and B. K. Puri, Ann. Chim., 76 (1986) 45.
8 Mu-Qing Yu and Gui-Qin Lin, Talanta, 30 (1983) 265.
9 S. Taguchi and K. Goto, Talanta, 27 (1980) 819.
10 Y. Sakai and N. Mori, Talanta, 33 (1986) 161.
11 P. Burha and P. G. Willmer, Talanta, 30 (1983) 381.
12 S. Music, M. Gessner and R. H. H. Wolf, Mikrochim. Acta, Part I, (1979) 95.
13 C. V. Banks and R. C. Bystoff, J. Am. Chem. Soc., 81 (1959) 6153.
14 G. Anderegg, Helv. Chim. Acta, 46 (1963) 2397.
15 S. Maekawa and K. Kato, Jpn. Analyst, 16 (1967) 482.
16 D. D. Perrin, Masking and Demasking of Chemical Reactions, Wiley-Interscience, New York, 1970.

Analytica Chimica Acta, 199 (1987) 215—220
Elsevier Science Publishers B.V., Amsterdam — Printed in The Netherlands

Short Communication

SPECTROFLUORIMETRIC DETERMINATION OF PROGUANIL IN BIOLOGICAL FLUIDS

O. R. IDOWU

Department of Chemistry, University of Ibadan, Ibadan (Nigeria)

(Received 28th November 1986)

Summary. A spectrofluorimetric method for proguanil in biological fluids is described based on the reaction of proguanil with 9-fluorenecarboxylic acid chloride and measurement of the resulting s-triazine derivative. The limits of detection for proguanil in methanol, water, plasma, urine and saliva are 1.5, 5.1, 7.6, 4.2 and 11.9 ng ml^{-1}, respectively. Preliminary results for proguanil levels in plasma and saliva following a single 100-mg oral dose are reported.

Proguanil (I; N^1-*p*-chlorophenyl-N^5-isopropyl biguanide), also sometimes referred to as chlorguanide, is an effective agent for the prophylaxis and suppression of malarial infections. Although the appearance of strains of malaria parasite resistant to proguanil has been noted in many areas where it is used, there are often conflicting reports on its effectiveness as a prophylactic in such areas [1—3]; it has been suggested as an alternative or a complement to chloroquine in areas where parasite resistance to chloroquine has been established [4, 5].

The effectiveness of many drugs in humans is known to be related to their pharmacokinetic parameters. The paucity of information on the pharmaco-

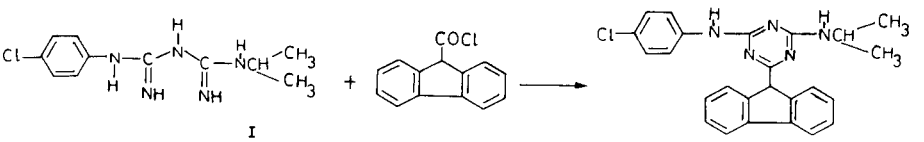

I II

kinetics of proguanil may have led to adoption of improper dosage regimens of the drug and hence the conflicting reports on its effectiveness. The only pharmacokinetic data on proguanil are those reported by Maegraith et al. [6] based on the determination of proguanil in blood by a colorimetric method of limited sensitivity and selectivity [7]. A more efficient application of proguanil in malarial chemotherapy requires a more extensive pharmacokinetic study of the drug, which requires a sensitive and selective method for the determination of the drug.

0003-2670/87/$03.50

Apart from the colorimetric method of Spinks and Tottey [7], only an indirect colorimetric method [8] and a high-performance liquid chromatographic method with an unfavorably high detection limit of 60 ng ml^{-1} [9] have been reported for the determination of proguanil in biological fluids. The present report describes a sensitive spectrofluorimetric method for proguanil based on its reaction with 9-fluorenecarboxylic acid chloride. Results are also presented for proguanil levels in plasma and saliva following a single 100-mg oral dose.

Experimental

Reagents and apparatus. Proguanil was obtained by crushing five tablets of Paludrine (ICI) and dissolving the powder in 10 ml of water. The solution was made alkaline with 2 ml of 2 M sodium hydroxide and extracted twice with 20 ml of dichloromethane, and the extract was dried over anhydrous sodium sulfate before evaporation of the solvent. Proguanil was obtained as a white powder with a melting point of 128—130°C (lit. 130—131°C [10]) and was stored in a desiccator. Quinine sulfate was recrystallized twice from hot water before use.

9-Fluorenecarboxylic acid chloride was obtained as a brown semi-solid after refluxing 700 mg of 9-fluorenecarboxylic acid (Aldrich) with 100 mg of phosphorus pentachloride for 2 h and removing the phosphoric acid generated during the reaction under reduced pressure. The acid chloride was stored and used as a solution in 50 ml of dichloromethane. Dichloromethane and methanol were of ACS grade (Fisher Scientific).

All fluorescence measurements were made on a Perkin-Elmer 204 spectrofluorimeter.

Reaction of 9-fluorenecarboxylic acid chloride with proguanil. Proguanil (100 mg) was dissolved in dichloromethane and treated with 150 mg of 9-fluorenecarboxylic acid chloride in 50 ml of dichloromethane. After refluxing for 30 min on a water bath, the solvent was evaporated and the residue shaken thoroughly with 1 ml of 2 M sodium hydroxide to remove the excess of acid chloride. The aqueous mixture was extracted with 50 ml of dichloromethane and the extract dried over anhydrous sodium sulfate before evaporation. The white solid obtained was recrystallized from methanol (m.p. 245°C; 15.5% N, 5.8% H; calculated for the s-triazine derivative (**II**, see above), 16.4% N, 5.15% H).

Calibration graphs for proguanil in methanol. A 100 μg ml^{-1} solution of proguanil in methanol was prepared and diluted serially to give a working solution of 100 ng ml^{-1} of the drug in methanol. Aliquots (0.1—1.0 ml) of the working solution corresponding to 10—100 ng of proguanil were placed in test tubes and the solvent was evaporated by keeping the tubes in a beaker of warm water (60°C) for a few minutes. The residues were each treated with 1 ml of the solution of 9-fluorenecarboxylic acid chloride. The mixtures were kept in a water bath (60°C) until the dichloromethane had evaporated, after which the residues were treated with 1 ml of 2 M sodium hydroxide

and the aqueous mixtures were extracted with 3 ml of dichloromethane by shaking on a vortex mixer for 1 min. After removal of the aqueous phases with a Pasteur pipette, the organic phases were dried over anhydrous sodium sulfate and transferred to another set of test tubes. The dichloromethane was evaporated and the residues redissolved in 4.0 ml of methanol. The fluorescence of the methanol solutions was measured at excitation and emission wavelengths of 310 and 370 nm, respectively. The procedure was repeated three times and average results were used.

Calibration graphs for proguanil in water, plasma, urine or saliva. Aliquots (0.1—1.0 ml) of the above working solution (10—100 ng of proguanil) were evaporated to dryness as described above. To each residue was added 1.0 ml of water (or drug-free plasma, urine or saliva) and the mixture was shaken on a vortex mixer for 30 s to give 10—100 ng ml^{-1} solutions of the drug in these media. The resulting solutions were made alkaline with 0.5 ml of 2 M sodium hydroxide and extracted with 5 ml of dichloromethane by shaking on a vortex mixer for 2 min. The mixtures were centrifuged at 2000 *g* for 10 min. Each organic phase was removed with a Pasteur pipette and 1 ml of the solution of 9-fluorenecarboxylic acid chloride was added to each. Subsequent evaporation of the solvent, removal of excess of reagent with sodium hydroxide, extraction of the product with dichloromethane and measurement of its fluorescence in methanol were as described in the preceding paragraph. The procedure was repeated six times for water and plasma, five times for urine and four times for saliva.

To correct for blank fluorescence and also to estimate the detection limit for proguanil in these media, six blank determinations were done with each type of fluid.

Determination of proguanil in plasma or saliva after ingestion of 100 mg proguanil hydrochloride. A single 100-mg oral dose of proguanil hydrochloride (Paludrine) was administered to each of two human volunteers after an overnight fast. Venous blood (10 ml) samples were taken before giving the drug and at 0.5, 1, 2, 4, 6, 24 and 48 h afterwards. The blood samples were collected into heparinized tubes and were immediately centrifuged to separate the plasmas, which was stored at −5°C until required. Unstimulated, mixed saliva samples (5—10 ml) were also collected at the same time as the blood samples.

The plasma and saliva samples (2.0 ml of each) were assayed in duplicate as described above within 4 days of collection.

Results and discussion

Determination of proguanil by reaction with 9-fluorenecarboxylic acid chloride. An easy route to the synthesis of 2,4-diamino-1,3,5-triazine derivatives is the condensation of biguanides with carboxylic acid derivatives including anhydrides and acid chlorides [11]. s-Triazine derivatives of the oral hypoglycaemic biguanides (phenformin, buformin and metformin) suitable for chromatographic analysis of these compounds, have been prepared by

their reaction with a variety of halogenated carboxylic acid anhydrides [12—14] and with *p*-nitrobenzoyl chloride [15, 16].

Proguanil was found to react readily with 9-fluorenecarboxylic acid chloride to give the s-triazine derivative 2-*p*-chloroanilino-4-isopropylamino-6-(9-fluorenyl)-1,3,5-triazine (II, see above). The yield of the reaction was found to be 95.9% by comparison of calibration graphs based on standard solutions of proguanil in methanol (Table 1) and calibration graphs based on standard solutions of the pure s-triazine derivative (regression equation: $y = 0.91x - 0.318$ where y is the fluorescence intensity and x is the concentration of the s-triazine derivative in ng ml^{-1}). A similar comparison of the calibration results for standard solutions of the s-triazine derivative and calibration results for standard solutions of quinine sulfate in 0.1 M sulfuric acid at its wavelength maxima gave a linear regression equation of $y = x + 0.825$, where y is as above and x is the concentration of quinine sulfate in ng ml^{-1}.

The high yield of the s-triazine derivative of proguanil (II) and its relatively intense fluorescence favors the spectrofluorimetric measurement of this derivative for the determination of proguanil after its extraction from water, plasma, urine or saliva. Linear calibration graphs were obtained when standard solutions of the drug in these fluids were treated as described. The results are shown in Table 1. A comparison of the regression equations for proguanil in these fluids and the regression equation for calibration in methanol shows the recovery of proguanil from water, plasma, urine and saliva to be 104.4 ± 4.7, 104.7 ± 5.5, 108.5 ± 6.1 and 94.4 ± 7.2%, respectively. Furthermore, there is no significant difference between the slopes of

TABLE 1

Calibration results for proguanil in methanol, water, plasma, urine and saliva

Proguanil taken (ng ml^{-1})	Fluorescence intensity[a]				
	Methanol	Water	Plasma	Urine	Saliva
10	14.8	6.8(40)	8.1(21.8)	—	—
20	26.3	22.7(16.3)	12.0(18.5)	3.1(18.6)	23.4(21.4)
40	37.9	37.8(15.3)	24.8(23.4)	22.5(14.1)	42.2(8.9)
60	59.1	53.8(10.8)	45.0(10.1)	38.0(16.0)	56.0(19.7)
80	78.4	72.4(14.2)	60.7(12.8)	49.3(2.6)	76.2(16.6)
100	93.4	94.3(1.2)	92.7(1.9)	83.6(1.2)	89.3(3.0)

[a]Mean (r.s.d., %) of 3 determinations for methanol, 6 determinations for water and plasma, 5 determinations for urine and 4 determinations for saliva. Regression equations are as follows: for methanol, $y = 0.879x$ (±0.054) + 6.31 (±1.51) where y is the fluorescence intensity and x (ng ml^{-1}) is the concentration of proguanil, standard error = 3.38, $r = 0.9932$; for water, $y = 0.918x$ (±0.064) + 0.89 (±3.98), standard error = 5.64, $r = 0.9828$; for plasma, $y = 0.920x$ (±0.081) — 6.64 (±1.73), standard error = 7.39, $r = 0.9746$; for urine $y = 0.954x$ (±0.094) — 17.70 (±6.39), standard error = 5.96, $r = 0.9785$; for saliva, $y = 0.830x$ (±0.12) + 7.62 (±8.05), standard error = 7.35, $r = 0.9564$.

TABLE 2

Concentration of proguanil in human plasma and saliva at various times after a single oral dose of 100 mg of proguanil hydrochloride

Time (h)	Concentration (ng ml^{-1})			
	Plasma		Saliva	
	Subject 1	Subject 2	Subject 1	Subject 2
0.5	2.6	12.3	<12	<12
1	7.0	48.9	19.9	21.2
2	6.6	17.4	15.0	38.9
4	32.7	14.1	16.3	38.3
6	27.1	22.3	25.9	37.3
24	24.4	—	28.0	30.4
48	19.7	14.1	22.6	33.4

the regression equations for water and plasma and the equations may be considered coincident. Aqueous standards of the drug may therefore be used for calibration when unknown plasma samples of the drug are to be assayed.

The 2σ limits of detection of the drug in methanol, water, plasma, urine and saliva were estimated as 1.5, 5.1, 7.6, 4.2 and 11.9 ng ml^{-1}, respectively.

Proguanil levels in plasma and saliva after ingestion of 100 mg of proguanil hydrochloride. Plasma and saliva samples collected at various times after ingestion of 100 mg of proguanil hydrochloride were assayed by the above method. The results are shown in Table 2. Proguanil could not be detected in saliva samples collected 0.5 h after drug administration. Thereafter, saliva levels of the drug were erratic in both subjects and did not correlate with the plasma levels of the drug.

Peak plasma levels of proguanil were attained within 4 h of dosage, in agreement with the report of Maegraith et al. [6]. The elimination half-lives of proguanil calculated from the data in Table 2 are 73.4 and 59.0 h for subjects 1 and 2, respectively. These values are in sharp contrast to the value of 15 h calculated by Ritschel et al. [17] on the basis of data reported by Maegraith et al. [6]. However, the sensitivity of the colorimetric method applied for proguanil [6] is limited to $\mu g\ ml^{-1}$ levels and the failure to determine blood levels of the drug beyond 24 h after drug administration may account for the relatively short half-life of 15 h calculated by Ritschel et al. from the data. The results of the present study suggest that proguanil may be more persistent in the body than had hitherto been assumed.

The author is grateful to Mrs. R. A. Adio of the Department of Pharmacology and Therapeutics, College of Medicine, University of Ibadan, for technical assistance during the in vivo studies.

REFERENCES

1 C. Covell, W. O. Nicol, P. G. Shute and M. Maryon, Trans. R. Soc. Trop. Med. Hyg., 42 (1949) 465.
2 W. Peters, Chemotherapy and Drug Resistance in Malaria, Academic, London, 1970.
3 L. J. Bruce-Chwatt, R. H. Black, C. J. Canfield, D. F. Clyde, W. Peters and W. H. Wernsdorfer, Chemotherapy of Malaria, W.H.O. Monograph series No. 27, Geneva, 1981.
4 V. V. Olsen, Lancet, 1 (1983) 649.
5 L. Rombo, P. Hedman, C. M. Kimahia, B. D. Ramji, A. Bjorkman and E. Bengtsson, Lancet, 1 (1983) 997.
6 B. G. Maegraith, M. M. Tottey, A. R. D. Adams, W. H. H. Andrews and J. D. King, Ann. Trop. Med. Parasitol., 40 (1946) 493.
7 A. Spinks and M. Tottey, Ann. Trop. Med. Parasitol., 39 (1945) 220.
8 J. C. Gage and F. L. Rose, Ann. Trop. Med. Parasitol., 40 (1946) 333.
9 R. R. Moody, A. B. Selkirk and R. B. Taylor, J. Chromatogr., 182 (1980) 359.
10 E. G. C. Clarke (Ed.), Isolation and Identification of Drugs, Pharmaceutical Press, London, 1969, p. 516.
11 E. J. Modest, in R. C. Elderfield (Ed.), Heterocyclic Compounds, Vol. 7, Wiley, New York, 1961, p. 663.
12 S. B. Matin, J. H. Karam and P. H. Forsham, Anal. Chem., 47 (1975) 545.
13 M. Mottale and C. J. Stewart, J. Chromatogr., 106 (1975) 263.
14 D. Alkalay, J. Volk and M. F. Bartlett, J. Pharm. Sci., 65 (1976) 525.
15 M. S. F. Ross, J. Chromatogr., 133 (1977) 408.
16 J. Brohon and M. Noel, J. Chromatogr., 146 (1978) 148.
17 W. A. Ritschel, G. V. Hammer and G. A. Thompson, Int. J. Clin. Pharmacol., 16 (1978) 395.

Analytica Chimica Acta, 199 (1987) 221—226
Elsevier Science Publishers B.V., Amsterdam — Printed in The Netherlands

Short Communication

CONTINUOUS-FLOW DETERMINATION OF MANGANESE IN NATURAL WATERS CONTAINING IRON

D. J. HYDES

Institute of Oceanographic Sciences, Brook Road, Wormley, Godalming, Surrey GU8 5UB (Great Britain)

(Received 17th December 1986)

Summary. A re-evaluation of the use of formaldoxime to determine manganese in natural waters at concentrations of 0—100 μM is reported. Addition of EDTA after formation of the manganese/formaldoxime complex removes interference from up to 100 μM iron. The extents of formation and destruction of the iron and manganese complexes with formaldoxime depend on the pH of the solution and on the time between reagent addition and measurement of absorbance.

The formaldoxime method is widely used for the determination of manganese in natural waters [1—3]. It has the advantages of being rapid, based on simple reagents, and having sufficient sensitivity for determinations in natural water in which dissolved manganese levels have been enhanced by anoxia. The drawback of the method is that iron, which is frequently present in anoxic waters, also forms a complex with formaldoxime with a similar molar absorptivity. Removal of the iron interference with EDTA was originally suggested by Goto et al. [4] and then applied in an automated method by Henricksen [1], but the mechanism was uncertain. In this communication, the removal of iron interference in the formaldoxime method is re-investigated in order to produce a method in which removal of the iron interference is reliable.

Experimental

Instrumentation. A Chemlab continuous-flow analyser was used for the development of the automated method; the manifolds are shown in Fig. 1. Manifold A was used for iron-free waters and manifold B for sediment pore water. A Pye SP500 spectrophotometer fitted with a 4-cm path length cuvette was used for measurements of the absorption spectra of the formaldoxime complexes of iron and manganese and measurements of the rate of colour development.

Reagents. Distilled water was used throughout. The formaldoxime solution (stock) was prepared by dissolving 4 g of hydroxylammonium chloride in 60 ml of water; 2 ml of 37% formaldehyde solution was added and the solution was diluted to 100 ml. This solution can be stored for several

0003-2670/87/$03.50

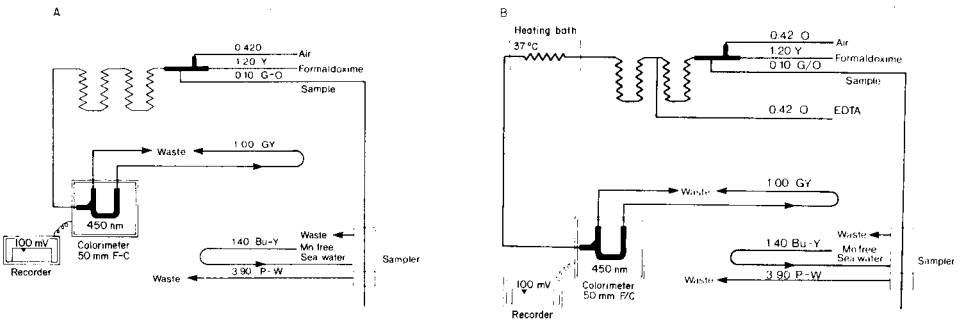

Fig. 1. Single (A) and two-reagent (B) manifolds for the continuous-flow determination of manganese. Flow rates are in ml min^{-1} O, orange; Y, yellow; G-O, green/orange; GY, grey; Bu-Y, blue/yellow; P-W, purple/white.

months. The working reagent was prepared by diluting 4.5 ml of stock formaldoxime solution in 200 ml of water; 9 ml of 10% (v/v) ammonia solution was added followed by 0.5 ml of Brij-35 solution (25% w/v) and the solution was diluted to 250 ml with water. For the EDTA solution, 10 g of ethylenediaminetetraacetic acid disodium salt, was dissolved in 100 ml of water. An aqueous 20% (w/v) solution of hydroxylammonium chloride was also prepared.

Results

Simple manifold. Manganese reacts rapidly with formaldoxime to give an orange-red solution. If a single reagent addition method is used [2], manganese can be determined by using the manifold shown in Fig. 1A. This manifold was used to evaluate the reproducibility of the method as well as its sensitivity to variations in the pH of the mixed reagent and dissolved iron concentration. The calibration was found to be linear up to a concentration of 60 μM. The precision (relative standard deviation, r.s.d.) for ten determinations on a solution containing 20 μM manganese was 1%, the standard deviation being 0.2 μM. Under the same conditions, a solution containing 100 μM iron produced an interference equivalent to 4.7 μM of manganese.

The effect of varying pH was tested by adjusting the pH of the formaldoxime solution with the hydroxylammonium chloride solution. The results

TABLE 1

Peak heights produced by solutions containing 80 μM Mn or 1 mM Fe reacting with formaldoxime solutions of different pH

pH	4.7	5.8	7.0	8.7	9.4	9.9
Mn peak[a]	—[b]	—[b]	—[b]	9.2	11.5	11.8
Fe peak[a]	1.9	2.2	3.0	4.8	5.6	6.0

[a]In cm. [b]Not detectable.

(Table 1) show that formation of the manganese complex is more sensitive to changes in pH than formation of the iron complex. Therefore, simply reducing the pH of a single mixed reagent cannot be used as a means of decreasing the iron interference. Addition of 4 ml of 10% (w/v) EDTA solution to the working formaldoxime solution (and then adjusting the pH back to 9.3 with ammonia solution) gave a mixture which allowed neither the manganese nor the iron formaldoxime complex to form.

Discrete sample measurements. The first step in deciding how best to remove the iron interference was to compare the absorption spectra of the formaldoxime complexes of iron and manganese. The spectra measured were similar to those reported by Goto et al. [4]. These measurements showed that formation of the iron complex was much slower than that of the manganese complex. At pH 9.9, formation of the iron complex was essentially complete only after 2.5 h and a 100 μM iron solution gave an absorbance of 0.17, whereas formation of the manganese complex was complete in <1 min and 100 μM manganese gave an absorbance of 0.405.

Experiments to distinguish if both hydroxylammonium chloride and EDTA were required to bring about the decrease in iron interference [1, 4] were initially conducted on discrete samples so that measurements could be made at different times after the start of the reaction. Tables 2 and 3 present

TABLE 2

Effect of decreasing the pH of the reaction mixture after formation of the manganese/formaldoxime complex at pH 9.9

pH[a]	Absorbance		pH[a]	Absorbance	
	After 5 min	After 100 min		After 5 min	After 100 min
9.9	0.318	0.332	6.7	0.260	0.223
9.4	0.318	0.332	6.5	0.242	0.136
9.0	0.321	0.323	6.3	0.227	0.050
7.7	0.289	0.286			

[a]After addition of increasing amounts of hydroxylammonium chloride.

TABLE 3

Effect of EDTA on the absorbances of the iron and manganese complexes of formaldoxime, added after complex formation at pH 9.9

pH	Mn absorbance		Fe absorbance	
	5 min	60 min	5 min	60 min
9.9	0.342	0.341	0.166	0.309
7.4	0.278	0.249	0.065	0.007
7.2	0.267	0.196	0.032	0.005
6.6	0.215	0.189	0.011	0.007
6.3	0.213	0.189	0.014	0.007

the results obtained by forming the iron and manganese complexes from 12 ml of working reagent solution and 1 ml of iron (1 mM) or manganese-spiked (80 μM) acidified seawater, and then after 2 min adding 4 ml of the hydroxylamine or EDTA solutions of various dilutions to give the final pH recorded in the tables. Initially, the effects of adding the hydroxylammonium solution after formation of the manganese complex were studied; the results of measurements taken 5 and 100 min after addition of the hydroxylammonium chloride are shown in Table 2. There was obviously considerable hysteresis in the kinetics of the formation and decomposition of the manganese complex but, once formed, it appeared to be stable at pH values above 7.7. Addition of EDTA solution had, at the same pH, a similar effect to the addition of hydroxylammonium chloride. This suggests that the decomposition of the manganese complex of formaldoxime is principally controlled by the pH of the solution. For the iron/formaldoxime complex, there was a significant difference in the effects of hydroxylamine and EDTA (Table 3). Additional hydroxylamine simply lowers the pH of the solution, so that its effects on the stability of the iron and manganese complexes were

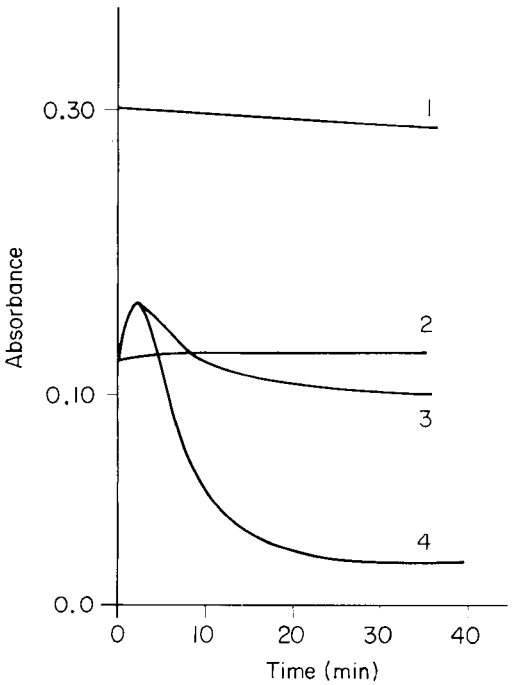

Fig. 2. Variation in the absorbance of solutions containing the iron or manganese complex with formaldoxime initially formed at pH 9.9, caused by addition of hydroxylammonium chloride or EDTA. Curves: (1) 100 μM manganese with EDTA added to give pH 7.7; (2) 1 mM iron with NH_2OH. HCl added to give pH 8.3; (3) as for (2) but final pH 7.0; (4) 1 mM iron with EDTA added to a final pH of 7.7.

similar in the alkaline range. The chelating ability of EDTA enhanced decomposition of the iron complex in the pH region where the manganese/formaldoxime complex was still stable.

The rate of decomposition of the iron and manganese complexes after the addition of either hydroxylamine or EDTA as a secondary reagent was examined. Typical results (Fig. 2) show that, below pH 8, the change in pH caused by the addition of the secondary reagent initially caused a rise in the amount of iron/formaldoxime complex formed. At 20°C, breakdown of the iron/formaldoxime complex by EDTA at pH 7.7 was effectively complete after 25 min. These measurements indicate that, for the addition of a second reagent to be successful, sufficient time has to be allowed after its addition for decomposition to occur. This was put into effect in building a continuous-flow manifold by running the reacting solution through a heating bath (37°C) after the addition of the second reagent.

Two-reagent manifold. The manifold shown in Fig. 1B was constructed. The 5% EDTA solution used gave a final pH of 7.7. When this manifold was used, interference from $\leqslant 100$ μM iron was undetectable and the interference from 1 mM iron was decreased to the equivalent of <5 μM manganese. The results of measurements made with and without EDTA addition and with and without a heating bath are given in Table 4. With a 5-cm cell in the spectrophotometer, the absorbance/concentration plot was linear up to 130 μM manganese. Operated with a full-scale deflection corresponding to 100 μM manganese (100-mV output, gain setting 3.0), the precision of ten replicate determinations of 20 μM manganese was 1.0%.

Discussion

Henricksen [1] and Goto et al. [4] suggested that for effective inhibition of the formation of the iron/formaldoxime complex, addition of both hydroxylamine and EDTA was necessary. The results presented here show that the reaction of formaldoxime with iron is slower than that with manganese. The extent to which both complexes are formed depends on the pH of the solution, and complex formation is favoured by higher pH values. Once the complex has formed, lowering the pH leads to the destruction of

TABLE 4

Comparison of the peak heights measured for the manganese and iron complexes, with and without the addition of EDTA and with and without heating

	Peak heights (cm)					
	100 μM Mn	100 μM Fe	1 mM Fe	100 μM Mn	100 μM Fe	1 mM Fe
	No heating			Heating at 37°C		
No EDTA	14.6	0.9	6.3	15.2	1.5	8.4
EDTA	10.1	0.2	1.8	8.6	—[a]	0.4

[a]Not detectable.

both complexes but at near neutral pH this is slow. In slightly alkaline solutions, addition of EDTA accelerates the reduction of the iron but not the manganese complex; the conditions in the mixture may be such that iron is oxidised to Fe(III) which forms a more stable complex with EDTA than do Mn(II) or Fe(II). The stability constants (pK_1) are 25, 14 and 14, respectively [5]. On the basis of these results, it appears likely that the earlier suggestion [1, 4] that both hydroxylamine and EDTA were necessary to remove the iron interference was based on a lack of awareness of the controlling influence of pH on the stability of the two complexes. Henricksen [1] reported that EDTA was ineffective for removing iron interference at low levels of iron. In this work, no evidence was found for the removal of iron interference being less effective at low iron concentrations.

REFERENCES

1 A. Henricksen, Analyst, 91 (1966) 647.
2 P. G. Brewer and D. W. Spencer, Limnol. Oceanogr., 16 (1971) 107.
3 J. J. Sawlan and J. W. Murray, Earth Planet. Sci. Lett., 64 (1983) 213.
4 K. Goto, T. Komatsu and T. Furukawa, Anal. Chim. Acta, 27 (1962) 331.
5 L. G. Sillen and A. E. Martell, Chemical Society Special Publication No. 25: Stability Constants, Suppl. No. 1, The Chemical Society, London, 1970.

Analytica Chimica Acta, 199 (1987) 227—232
Elsevier Science Publishers B.V., Amsterdam — Printed in The Netherlands

Short Communication

SPECTROFLUORIMETRIC DETERMINATION OF 1,4-THIENODIAZEPINES

FRANCISCO URREA SANCHEZ, JESUS RODRIGUEZ PROCOPIO and LUCAS HERNANDEZ HERNANDEZ*

Department of Analytical Chemistry, Autonoma University of Madrid, Canto Blanco, 28049 Madrid (Spain)

(Received 5th January 1987)

Summary. The fluorescence characteristics of four 1,4-thienodiazepines in aqueous and methanolic solutions and the effect of pH on fluorescence intensity are described. The pK_a values are calculated. Fluorimetric methods with limits of detection between 3 and 38 ng ml^{-1} were developed, and applied for determinations of one drug in tablets, and the others in serum after extraction with a Sep-Pak C_{18} cartridge.

Since the early 1960s, benzodiazepines have been used as minor tranquillizers, sleep inducers and muscle relaxants. Many analogous compounds which have certain structural modifications have been developed in order to increase, create or remove some of the pharmacological characteristics of benzodiazepines. For example, the 1,4-thienodiazepines (**I**—**IV**) have a thiophene ring instead of the benzene ring in the 1,4-benzodiazepines. 1,4-Thieno-

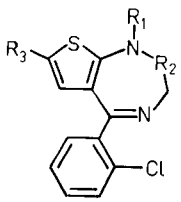

	R_1	R_2	R_3
I	CH_3	C=O	CH_2CH_3
II	H	C=O	Br
III	H	C=O	H
IV	H	C=S	Cl

diazepines have been determined by u.v. spectrophotometry [1] and polarography [2—4], but these methods suffer from poor sensitivity and selectivity in clinical analysis.

Of the methods utilized in pharmaceutical analysis, fluorescence techniques are amongst the most sensitive. A characteristic of 1,4-benzodiazepines is their low native fluorescence in aqueous solutions [5], but there is increased fluorescence in acidic [6—8] and methanolic media [8, 9]. This communication presents an examination of several 1,4-thienodiazepines by spectrofluorimetry in aqueous media. The influence of several acids and methanol is studied and methods are established for determinations of these compounds in pharmacological and clinical samples.

0003-2670/87/$03.50

Experimental

Apparatus and reagents. Fluorescence measurements were made with a Shimadzu RF-540 spectrofluorimeter equipped with a xenon source. Excitation and emission slits were set at 10 nm. A Metrohm E-510 pH meter equipped with a combined glass-Ag/AgCl electrode was also used.

Clotiazepam (compound I) was purchased from Esteve (Barcelona) and other compounds were obtained from Roche (Madrid). Aqueous solutions of drugs were prepared by successive dilutions of a 1×10^{-3} M stock solution, prepared by dilution in methanol and stored under refrigeration, protected from light. All other chemicals were analytical grade.

Determination of clotiazepam in tablets. Weigh exactly 30—35 mg of finely powdered tablets (Distensan) into a beaker. Add 20 ml of methanol, stir vigorously with a magnetic stirrer for 10 min, filter and dilute to 100 ml with methanol. Pipette 1 ml of this solution into a 50-ml graduated flask, dilute to the mark with methanol and measure its fluorescence intensity at 438 nm with excitation at 240 nm. Calibrate with methanol solutions of the drug.

Extraction procedure. Insert a Sep-Pak C_{18} cartridge (Waters) in the luer tip of a syringe and prewash with 20 ml of chloroform followed by 20 ml of water. Mix 1 ml of serum sample and 1 ml of 1.0 M phosphate buffer solution (pH 7) and inject the mixture with the syringe through the cartridge. Wash with 2 ml of water and 2 ml of 1:1 water/methanol. Elute the drug with 2 ml of chloroform. Dry the eluate at 70° C under a stream of nitrogen, dissolve the residue in 2 ml of the appropriate medium for each drug and measure the fluorescence intensity.

Results and discussion

Native fluorescence. The structures of the compounds studied are shown above. The fluorescence of these compounds was tested in aqueous solution at several pH values, adjusted with perchloric acid or sodium hydroxide. Of the four 1,4-thienodiazepines studied, all but IV fluoresced under these conditions. For compound I, two different spectra were observed as a function of pH, one in acidic media (pH < 4) and the other in neutral and alkaline media. However, compounds II and III had three different spectra, in acidic (pH < 4), neutral (pH 5—8) and alkaline media (pH > 10) (Fig. 1). These results are in agreement with earlier spectroscopic studies [1] and indicate that two and three species predominate in solution in the pH range 0—13. The species in acidic media arises from protonation of the 4-nitrogen and the species in alkaline media for compounds II and III involves deprotonation of the 1-nitrogen [1]. The absence of a hydrogen on the 1-nitrogen in compound I explains the absence of the latter species in alkaline medium.

The fluorescence behaviour of 1,4-thienodiazepines with changes in concentration of acid was studied for sulphuric, perchloric and hydrochloric acids. Compounds II and III gave a more intense fluorescence in all the acids studied than in neutral or alkaline media, that in perchloric acid having a

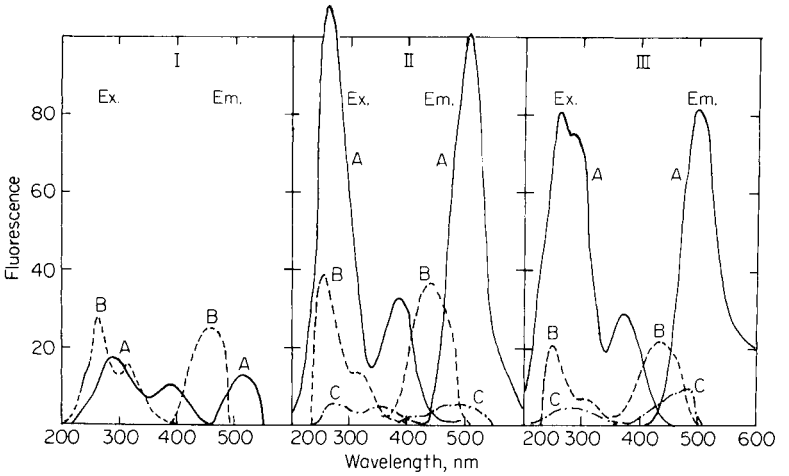

Fig. 1. Corrected excitation (Ex) and emission (Em) spectra of 20 μM solutions of I, II and III. Medium: (A) 1.0 M $HClO_4$; (B) water; (C) 1.0 M NaOH.

higher relative fluorescence intensity than in the other acids (Table 1). However, compound I had less intensity in acidic media than in neutral solution. Compound IV did not fluoresce in perchloric or sulphuric acid, but intense fluorescence was observed in hydrochloric acid (Fig. 2) as the hydrochloride was formed. The fluorescence of compounds II and III increased when the perchloric acid concentration increased up to 0.5 M and remained virtually constant at higher concentrations (Fig. 3). For compound IV a rapid increase of fluorescence was observed with increasing acid concentration up to about 5.0 M, with a slower increase at higher concentrations (Fig. 3). From the variation of intensity at the characteristic maxima for each species with pH variation, pK_a values for all drugs were calculated [10]. The values obtained are shown in Table 2. No evidence of excited state phototropism was observed because the pK_a values determined by fluorescence measurements corresponded to the pK_a values obtained by spectrophotometry [1].

Influence of methanol concentration. The presence of methanol in solution enhances the fluorescence of some benzodiazepines [8]. For this reason, the effect of methanol concentration on fluorescence intensity was studied. An increase in the methanol concentration decreased the fluorescence of compounds II and III in an acidic medium, whereas the fluorescence intensity of I and IV increased as the methanol concentration was raised to 100 and 20% (v/v), respectively.

Calibration graphs and limits of detection. The statistical characteristics of the calibration graphs for the fluorimetric determination of the various 1,4-thienodiazepines are shown in Table 3. The relative standard deviation (r.s.d.) was $<3\%$ for concentrations between 30 and 400 ng ml^{-1} for compounds II–IV and between 0.16 and 3.0 μg ml^{-1} for compound I. For all compounds,

TABLE 1

Fluorescence characteristics of 20 μM solutions of 1,4-thienodiazepines (wavelength of maximum excitation/wavelength of maximum emission/relative fluorescence intensity)

Compound	Acidic media			Neutral medium	Alkaline medium
	1.0 M $HClO_4$	1.0 M HCl	1.0 M H_2SO_4		1.0 M NaOH
I	288/515/12.8	265/502/16.8	271/509/16	255/458/28.8	—
II	277/507/102	265/501/90	279/505/82	255/440/36.8	259/480/8.0
III	259/493/82	265/501/56	259/491/63	251/440/22.4	258/483/8.8
IV	NF[a]	247/517/53.6	NF	NF	NF

[a]No fluorescence.

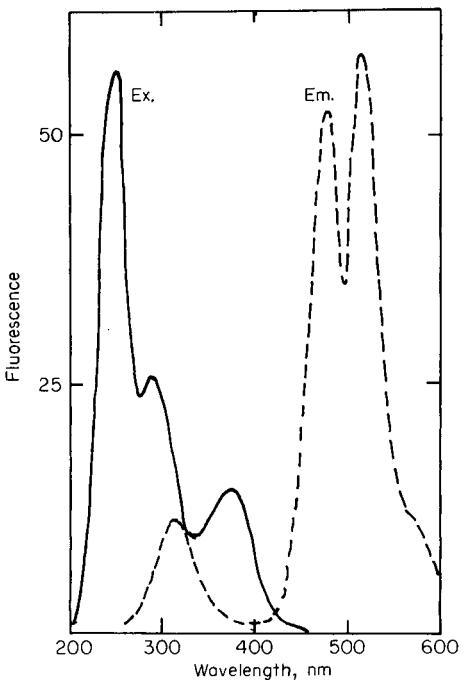

Fig. 2. Corrected excitation (Ex) and emission (Em) spectra of a 20 μM solution of compound IV in 1.0 M HCl.

the linearity of the calibration plots was excellent, as shown by the correlation coefficients (Table 3). The linear dynamic range covers two orders of magnitude. The method is an order of magnitude more sensitive for compounds II—IV than for compound I.

Analytical applications. Because of the differences in sensitivity, the method is suitable for the determination of compound I only in tablets but for the determination of compounds II—IV in body fluids. In a rapid method suitable for quality control of tablets of compound I (Clotiazepam), the

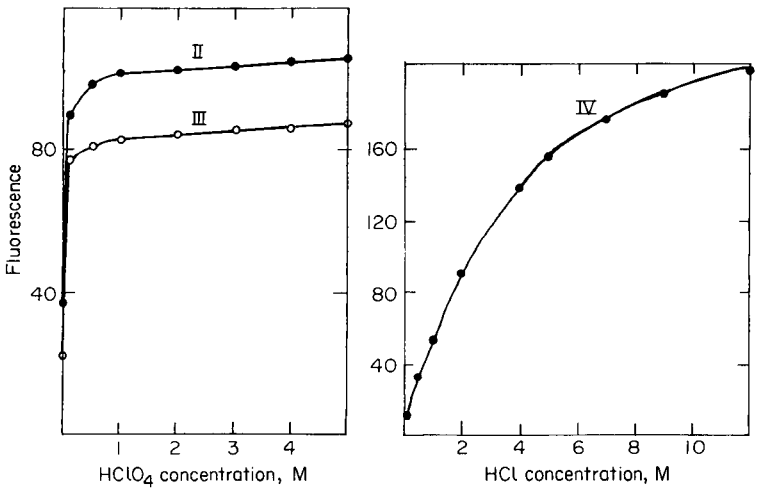

Fig. 3. Influence of acid concentration on relative fluorescence intensity of compounds II, III and IV.

TABLE 2

pK_a values for the 1,4-thienodiazepines

Compound	pK_a by fluorescence		pK_a by absorbance [1]	
	pK_{a1}	pK_{a2}	pK_{a1}	pK_{a2}
I	4.40 ± 0.15	—	4.25 ± 0.10	—
II	3.46 ± 0.10	8.03 ± 0.05	3.24 ± 0.06	8.61 ± 0.04
III	3.91 ± 0.08	9.11 ± 0.07	3.85 ± 0.05	9.70 ± 0.05
IV	2.87 ± 0.14	—	2.60 ± 0.05	6.52 ± 0.04

tablets were simply ground to a fine powder and the active constituent was dissolved in methanol for measurement of fluorescence intensity (see Experimental). The results of eight assays of tablets containing 10 mg of clotiazepam gave a mean value of 10.04 mg per tablet, with a standard deviation of 0.04 mg (r.s.d. 0.4%).

Compounds II—IV were quantitatively extracted from serum with Sep-Pak C_{18} cartridges. The recoveries obtained from five serum samples spiked with compounds II, III and IV were 99.3 ± 0.4, 99.0 ± 1.4 and 98.2 ± 0.5, respectively, for concentrations between 20 and 800 ng ml^{-1} of drug added to serum. The combination of Sep-Pak C_{18} cartridges and fluorimetry is clearly useful for the determination of 1,4-thienodiazepines in serum at such levels.

TABLE 3

Analytical parameters for the 1,4-thienodiazepines

Compound	Solvent	$\lambda_{ex}/\lambda_{em}$ (nm)	Upper limit of linearity ($\mu g\ ml^{-1}$)	Correlation coefficient ($n = 7$)	Limit of quantitation ($ng\ ml^{-1}$)	Limit detect (ng ml
I	Methanol	257/438	12.7	0.99994	130	38
II	1.0 M $HClO_4$	277/507	2.5	0.9998	17	5
III	1.0 M $HClO_4$	259/493	1.1	0.9992	62	18
IV	5 M HCl in 58% methanol	294/503	1.6	0.9998	10	3

The authors thank C.A.I.C.yT. for the economic support of this work (project no. 2077-83).

REFERENCES

1 M. A. Fernandez-Arciniega, J. Rosas, L. Hernandez and R. M. Alonso, Boll. Chim. Farm., 124 (1985) 19.
2 K. A. Kovar, D. Linden and E. Breitmaien, Arch. Pharm. (Paris), 316 (1984) 834.
3 F. I. Segun, A. Alubelen, K. Ulas and I. Fedai, Sci. Pharm., 52 (1984) 66.
4 R. Alonso Rojas and L. Hernandez Hernandez, Anal. Chim. Acta, 186 (1986) 295.
5 S. J. Mulé, J. Chromatogr., 55 (1971) 255.
6 D. D. Maness and G. I. Yakatan, J. Pharm. Sci., 64 (1975) 651.
7 S. R. Sim, J. Pharm. Sci., 67 (1978) 1413.
8 J. R. Procopio, P. Hernandez, M. T. Sevilla and L. Hernandez, An. Quim., 82 (1986) 317.
9 G. Caille, J. Brawn and J. A. Mockle, Can. J. Pharm. Sci., 5 (1970) 74.
10 A. Albert and E. P. Serjeant, The Determination of Ionization Constants, Chapman and Hall, London, 1974, p. 44.

Analytica Chimica Acta, 199 (1987) 233—236
Elsevier Science Publishers B.V., Amsterdam — Printed in The Netherlands

Short Communication

DETECTION OF NITROBENZENE AND RELATED AROMATICS BY REDUCTION AND INDOPHENOL FORMATION

KRISHNA K. VERMA* and DAYASHANKER GUPTA

Department of Chemistry, Rani Durgavati University, Jabalpur 482001 (India)

(Received 26th February 1987)

Summary. The detection of nitrobenzene is based on its partial reduction with zinc in slightly acidic medium to yield phenylhydroxylamine, acid-catalyzed rearrangement to form a mixture of 2- and 4-aminophenol, and formation of indophenol blue by 4-aminophenol on oxidative coupling with an alkaline phenol solution. The limit of detection is 0.1 μg ml^{-1} nitrobenzene in the test solution. A positive test is also given by 2- and 3-nitrotoluene but various other aromatics containing nitro groups do not interfere. The method was tested on wastewaters.

Nitroaromatic compounds are toxic and are regarded as potential health hazards [1, 2]. The methods commonly used for their detection include reduction and colour development with pentacyanoammineferrate(II) or 1-naphthylamine [3], formation of colours with acetone [4] or dimethylsulphoxide in the presence of sodium hydroxide [5] or sodium sulphite [6], and charge-transfer complex formation with *N*,*N*-diethylaniline [7—9]. Conversion of nitro compounds to *N*-aryl-*N*-benzoylhydroxylamine and treatment with vanadate [10] provides a sensitive but inselective method. The arylhydroxylamine formed by the reduction of nitroaromatics has been coupled sequentially with phenyldiazonium salt and diphenylamine to give a pink or violet solution [11]; aromatic amines and phenols interfere.

The spontaneous acid-catalyzed reaction, the Bamberger rearrangement [12, 13], of arylhydroxylamine, formed by reduction of nitroaromatics in weakly acidic medium, to yield aminophenols, and formation of highly coloured indophenol dyes [14, 15] on oxidative coupling with phenol are used to detect nitrobenzene, and 2- and 3-nitrotoluene in this study. The products of the rearrangement, 2- and 4-aminophenols, are separated by paper chromatography with a mobile phase that contains nickel(II), and visualized by spraying with 4-dimethylaminobenzaldehyde to yield coloured Schiff bases. 4-Aminophenol is responsible for the indophenol dye formation.

0003-2670/87/$03.50

Experimental

Reagents. An alkaline solution of phenol was prepared by dissolving 2 g of trisodium orthophosphate dodecahydrate, 2 g of sodium hydroxide and 6 g of phenol in water and diluting to 100 ml with water.

The mobile phase was a mixture of 2 g of sodium acetate, 0.1 ml of anhydrous acetic acid, 1 ml of methanol, 5 ml of 5% (w/v) nickel(II) acetate solution and 100 ml of water.

Procedure. In a micro test tube are placed 100 μl of the aqueous sample solution (ca. 0.001% w/v), 0.5 ml of 10% (v/v) acetic acid and 5 mg of zinc dust. The mixture is shaken for 2 min; the clear supernatant solution is transferred with a syringe, to another micro test tube, mixed with 0.5 ml of 2% (v/v) sulphuric acid and gently boiled for 1 min. A 10-μl portion of the cooled solution is spotted on Whatman No. 1 paper and sprayed with the alkaline solution of phenol. Formation of an intense indophenol blue colour is a positive test for nitrobenzene, and 2- and 3-nitrotoluene. If no blue colour appears within 2 min, the paper is sprayed with aqueous 0.5% (w/v) *N*-chlorosuccinimide solution; certain nitroaromatics then produce faint to intense blue colours (Table 1).

Results and discussion

Phenylhydroxylamine, which is formed by the reduction of nitrobenzene in weakly acidic medium, undergoes acid-catalyzed rearrangement to produce a mixture of 2- and 4-aminophenols. Other arylhydroxylamines behave similarly but the formation of aminophenol isomers depends on the vacant positions *ortho* and *para* to the hydroxylamino group. The aminophenols formed by nitrobenzene, and 2- and 3-nitrotoluene were separated by paper chromatography. The presence of nickel(II) in the mobile phase is essential for their separation (Table 2); 2-aminophenol forms a chelate with nickel(II) whereas 4-aminophenol does not [16]. Because only certain functional groups with particular orientations bind to specific metal ions, such secondary equilibria can be utilized to achieve selective separations [17].

4-Aminophenol is responsible for the formation of the indophenol blue dye on oxidative coupling with alkaline phenol (Table 2). Atmospheric oxygen serves as the oxidant to bring about reaction with 4-aminophenol or its derivatives obtained from nitrobenzene, and 2- or 3-nitrotoluene. The indophenol produced from nitrobenzene absorbed maximally at 620 nm in its visible spectrum, as does the authentic indophenol [15]. A large number of other nitroaromatics do not interfere with the test (Table 1), ostensibly because their 4-aminophenol derivatives are either sterically hindered or too reducing in character for coupling. Probably the latter type of nitroaromatic gives the indophenol blue coloration only after spraying with *N*-chlorosuccinimide. Other substances which do not vitiate the detection include acetone, acetaldehyde, formaldehyde, phenol, aniline, 1-naphthylamine, hydroxylamine and hydrazine. Arylhydroxylamines and 4-aminophenol interfere but their presence can be confirmed by using the proposed procedure

TABLE 1

Detection of nitroaromatics by their reduction, rearrangement and indophenol dye formation

Compound	Colour produced[a]		Limit of detection (μg)	Compound	Colour produced[a]		Limit of detection (μg)
	A	B			A	B	
Nitrobenzene	Blue	Blue	0.01	2-Nitrobenzoic acid	None	Blue	8
2-Nitrotoluene	Blue	Blue	0.01	3-Nitrobenzoic acid	None	Blue	4
3-Nitrotoluene	Blue	Blue	0.01	4-Nitrobenzoic acid	None	None	
4-Nitrotoluene	None	Blue	5	1,3-Dinitrobenzene	None	Blue	10
1-Iodo-2-nitrobenzene	None	Blue	1	3,5-Dinitrobenzoic acid	Reddish	Reddish	5
1-Nitronaphthalene	None	Blue	8	2-Chloro-5-nitrobenzaldehyde	None	Blue	5
2-Nitroaniline	None	Violet	10	Picric acid	None	None	
3-Nitroaniline	None	Violet	8	5-Nitrosalicylic acid	None	Blue	3
4-Nitroaniline	None	Blue	8	1-Chloro-2,4-dinitrobenzene	None	Blue	10
2-Nitrophenol	None	Blue	1	Phenylhydroxylamine[b]	Blue	Blue	0.01
3-Nitrophenol	None	None		*N*-Phenyl-*N*-benzoylhydroxylamine[c]	Blue	Blue	0.04
4-Nitrophenol	None	Blue	1				

[a]Colour after spraying with alkaline phenol solution (A) or alkaline phenol followed by *N*-chlorosuccinimide (B). [b]The test was made without the reduction step. [c]The substance was boiled with concentrated hydrochloric acid and tested as for phenylhydroxylamine.

TABLE 2

R_f values of aminophenols formed by reduction and rearrangement reaction of nitroaromatics, in paper chromatography with nickel(II) in the mobile phase[a]

Substance	R_f[b]		R_f[c]
	Lemon yellow spot	Dark yellow spot	Blue spot
Nitrobenzene	0.79	0.94	0.78
2-Nitrotoluene	0.77	0.91	0.77
3-Nitrotoluene	0.78	0.94	0.76
2-Aminophenol	—	0.92	—
4-Aminophenol	0.78	—	0.77

[a]The values reported are averages of five runs. [b]Spray reagent: 4-dimethylaminobenzaldehyde. [c]Spray reagent: alkaline phenol solution.

without the reduction step (when nitroaromatics do not interfere). Stirring the wastewater acidified with concentrated hydrochloric acid to effect rearrangement of arylhydroxylamines and salt formation with aminophenols, extracting the nitroaromatics with diethyl ether, evaporating the ether and testing for nitroaromatics in the residue circumvents interference by 4-aminophenol and arylhydroxylamines.

REFERENCES

1 F. A. Patty, Industrial Hygiene and Toxicology, Vol. II, 2nd edn., Interscience, New York, 1963, pp. 2072—2073.
2 I. M. Kolthoff, P. S. Elving and F. H. Stross, Treatise on Analytical Chemistry, Vol. 2, Part III, Wiley-Interscience, New York, 1971, p. 125.
3 F. Feigl and V. Anger, Spot Tests in Organic Analysis, Elsevier, Amsterdam, 1975, pp. 279, 650.
4 N. D. Cheronis, J. B. Entrikin and E. M. Hodnett, Semimicro Qualitative Organic Analysis. The Systematic Identification of Organic Compounds, Interscience, New York, 1965, p. 404.
5 S. A. Nabi, S. Haque and P. M. Qureshi, Talanta, 30 (1983) 989.
6 S. Qureshi, P. M. Qureshi and S. Haque, Talanta, 32 (1985) 51.
7 J. P. Sharma and R. D. Tiwari, Mikrochim. Acta, (1974) 323.
8 R. D. Tiwari, G. Srivastava and J. P. Misra, Analyst, 103 (1978) 651.
9 K. K. Verma and S. K. Dubey, Talanta, 28 (1981) 485.
10 J. Nair and V. K. Gupta, Int. J. Environ. Stud., 10 (1977) 124.
11 K. R. Paul and V. K. Gupta, Microchem. J., 30 (1984) 280.
12 G. T. Tisue, M. Grassmann and W. Lwowski, Tetrahedron, 24 (1968) 999.
13 R. T. Coutts and N. J. Pound, Can. J. Chem., 48 (1970) 1859.
14 C. T. H. Ellcock and A. G. Fogg, Analyst, 100 (1975) 16.
15 K. K. Verma and A. Jain, Analyst, 110 (1985) 997.
16 R. S. Charles and H. Freiser, J. Am. Chem. Soc., 74 (1952) 1385.
17 H. P. Walton, in J. Marinsky and Y. Marcus (Eds.), Ion-Exchange and Solvent Extractions, Vol. 4, M. Dekker, New York, 1973, p. 121.

Analytica Chimica Acta, 199 (1987) 237—240
Elsevier Science Publishers B.V., Amsterdam — Printed in The Netherlands

Short Communication

SPECTROPHOTOMETRIC DETERMINATION OF PERCHLORATE AFTER EXTRACTION OF ITS BRILLIANT GREEN ION-PAIR WITH MICROCRYSTALLINE BENZOPHENONE

D. THORBURN BURNS* and N. TUNGKANANURUK

Department of Analytical Chemistry, The Queen's University of Belfast, Belfast, BT9 5AG (Northern Ireland)

(Received 30th January 1987)

Summary. Perchlorate (0—30 μg) can be determined spectrophotometrically at 639 nm after its adsorptive extraction with Brilliant Green on microcrystalline benzophenone at pH 6.5 after dissolution of the solid phase in benzene. The effects of pH and diverse ions are reported. The system is applied to the determination of ≥0.003% (w/w) perchlorate in samples of potassium chlorate after prior destruction of chlorate.

Relatively few spectrophotometric and spectrofluorimetric methods have been reported for the determination of perchlorate ions [1, 2]. Most extractions utilise basic dyes [2—7] or onium [1, 8—10] salts in conventional liquid/liquid systems and so far no solid/liquid system has been reported [11] for anions other than phosphate, which has been extracted as 12-molybdiphosphate into molten benzophenone [12].

The present communication is an extension of earlier studies on the perchlorate ion [1, 4] and of Brilliant Green as an ion-pairing reagent [3, 4] including its use in solid/liquid extraction [13]. A novel adsorptive ion-pair extraction of Brilliant Green perchlorate by microcrystalline benzophenone is described. The solid benzophenone can subsequently be dissolved in benzene and the determinations completed spectrophotometrically at 639 nm. The system is applied to the determination of perchlorate in samples of analytical reagent-grade potassium chlorate.

Experimental

Equipment. Pye Unicam SP8—400 and SP6-550 ultraviolet-visible spectrophotometers were used for recording spectra and for routine measurements, respectively, with matched quartz 1-cm cells.

Reagents and solutions. Brilliant Green (Aldrich Chemical Co., dye content ca. 95%) was used as supplied. Elemental analysis gave 66.9% C, 7.0% H, 5.6% N (theor. for $C_{27}H_{34}N_2O_4S$: 67.2% C, 7.1% H, 5.8% N). A 0.05% (w/v) solution was prepared in absolute ethanol, and stored in a dark brown bottle. A stock 1000 μg ml^{-1} perchlorate solution was prepared by dissolving 0.1393 g of potassium perchlorate (analytical-reagent grade dried to constant weight

0003-2670/87/$03.50

at 105°C) in 100 ml of water. More dilute solutions were prepared as required. A pH 6.5 buffer was prepared by dissolving 6.8 g of potassium dihydrogen-orthophosphate and 5.0 g of ascorbic acid in water, adding 13.9 ml of 0.1 M sodium hydroxide solution and diluting to exactly 1 l in a volumetric flask. The benzophenone solution was 20% (w/v) in acetone. All other reagents were of analytical grade. Twice-distilled water was used throughout.

General procedure. Place a 1—6 ml aliquot of sample solution containing 5—30 μg of perchlorate in a stoppered Erlenmeyer flask. Add 10 ml of pH 6.5 buffer and 1.0 ml of Brilliant Green solution. Swirl to mix and allow to stand for 5 min. Add 2.00 ml of benzophenone solution and shake vigorously for 30 s. Filter the blue solid formed through a sintered glass filter (no. 2 porosity). Wash with water, drain or suck dry, dissolve the solid in benzene and dilute to volume in a 10-ml volumetric flask. Dry the solution by addition of 1 g of anhydrous sodium sulphate. Measure the absorbance at 639 nm against a reagent blank prepared in the same way.

Examination of the main experimental variables

Naphthalene, diphenyl, 1,4-dichlorobenzene and benzophenone were each examined for their adsorptive/extraction properties when used for micro-crystalline solid formation from acetone solutions. Benzophenone provided the highest apparent molar absorptivity (2.9×10^4 l mol^{-1} cm^{-1} at 639 nm), which was 3× that of diphenyl and naphthalene and 10× that of 1,4-dichloro-benzene. Each solid examined gave acceptably low blanks (0.04—0.06 absorbance when measured against water).

Solvents with a range of functional group types were examined for dis-solution of the ion-pair and the solid extractant. Benzene was chosen for routine use because the ion-pair gave the highest apparent molar absorptivity, greater than that in any other solvent examined. The solutions were stable in all solvents except dimethylformamide and dioxan.

The effect of pH was examined for 10 μg of perchlorate ion by careful addition of 1 M hydrochloric acid or 1 M ammonia prior to extraction. The absorbance was measured as above and was almost independent of pH in the range 5.0—7.0, decreasing rapidly outside these limits. In subsequent work, the aqueous phase was buffered at pH 6.5. The extraction was constant when 8.0—13.0 ml of buffer was used; 10 ml was used in subsequent work.

The effect of varying the amount of Brilliant Green solution was examined for 10 μg of perchlorate. The absorbance of the extract increased with increasing volume of reagent up to 1.0 ml, remained constant up to 1.3 ml and decreased slowly thereafter. The reagent blank increased slowly with in-creasing volume of reagent. Thus 1.0 ml was used for routine measurements. The extent of extraction was found to be unaffected by ionic strength, phase volume ratios up to 7.5:1 water/benzophenone in acetone, sequence of addition of reagents, shaking times or standing times. Dissolved extracts were stable in diffuse daylight for >2 h but faded slowly in direct day-light. The composition of the complex was established by Job's method of

continuous variations [14] and by the mole ratio method [15, 16] to be $[C_{27}H_{33}N_2]ClO_4$. Curvature of the Job's plot indicates that the ion-pair is appreciably dissociated in solution.

Results and discussion

A linear calibration graph was obtained for 0—30 μg of perchlorate in the final 10-ml solution in benzene. The relative standard deviation for the determination of 10 μg of perchlorate was 0.53% (10 results).

Possible interferences of various ions were checked for the determination of 10 μg of perchlorate. The results are summarised in Table 1. The ions which interfered significantly (i.e., >3% change in absorbance) were zinc, uranyl, cobalt(II), nickel, copper(II), iron(III), permanganate, molybdate, tungstate, iodide, iodate, periodate, bromate, chromate, sulphate, chlorate and nitrate. Under the conditions of the general procedure, there was no interference from 200 mg of chloride or from 2 mg of ammonium, sodium, calcium, magnesium, manganese(II), vanadyl, bromide, acetate, oxalate, carbonate, citrate, tartrate, or thiosulphate. As chlorate ion interferes, it must be removed or destroyed prior to the extraction of perchlorate. This is readily achieved by evaporation of samples with concentrated hydrochloric acid, which also removes other interfering ions [4, 8, 17] such as bromide, iodide and nitrate.

TABLE 1

Effect of diverse ions on the determination of 10 μg of perchlorate (ions causing a change in absorbance of <3% are regarded as non-interfering)

Ion[a]	Ion/ClO_4^- ratio (w/w)	Absorbance change (%)	Ion[a]	Ion/ClO_4^- ratio (w/w)	Absorbance change (%)
Zn^{2+}	200	−13	BrO_3^-	200	−10
	50	—		100	—
UO_2^{2+}	200	−13	IO_3^-	100	—
	100	—	CrO_4^{2-}	200	−17
Co^{2+}	100	−17		100	—
	50	—	IO_4^-	200	−40
Ni^{2+}	100	+41		40	−23
	50	—		10	—
Cu^{2+}	100	−70	SO_4^{2-}	200	−10
	50	−9		150	—
	20	—	MnO_4^-	10	—
Fe^{3+}	40	−30	WO_4^{2-}	5	—
	20	—	MoO_4^{2-}	125	—
I^-	200	+24	NO_3^-	25	—
	20	—	ClO_3^-	160	−35
				110	—
			Cl^-	20,000	—

[a]Cations added as chloride and anions added as sodium salts.

TABLE 2

Determination of perchlorate in potassium chlorate by direct calibration (method A) and standard addition procedures (method B)

Method	$KClO_4$ added (μg)	Total $KClO_4$ found[a] (μg)	$KClO_4$ in $KClO_3$ ($\mu g\ g^{-1}$)	
			Present method	Amiloride method
A	—	—	24.2 ± 0.2	24.8 ± 0.6
B	0	12.24 ± 0.12	24.5 ± 0.2	23.6 ± 1.2
B	10	22.74 ± 0.08	25.5 ± 0.2	25.4 ± 0.6
B	15	26.30 ± 0.06	22.6 ± 0.1	—
B	30	—	—	24.8 ± 0.6

[a]Mean values ±95% confidence limit for 5 replicates in present method, 4 replicates in Amiloride method.

Perchlorate was determined in potassium chlorate by placing 5.00 g of sample in an evaporating dish, adding 100 ml of concentrated hydrochloric acid, and evaporating to dryness, under an infrared lamp in the final stages to avoid sputtering. The solution was evaporated to dryness a further 3 times after successive additions of 20 ml of water, in order to remove all the acid. The residue was dissolved in distilled water and diluted to 100 ml in a volumetric flask; a 10-ml aliquot was transferred to a stoppered Erlenmeyer flask and the general procedure was applied. The results obtained for samples of reagent-grade potassium chlorate from the calibration plot and by standard additions are shown in Table 2, together with results obtained by the Amiloride method [1]. The procedures give similar accuracy but the present method is more precise and sensitive than earlier methods [1, 4, 10].

REFERENCES

1 D. T. Burns and P. Hanprasopwattana, Anal. Chim. Acta, 118 (1980) 185.
2 S. Jaya, T. P. Rao and T. V. Ramakrishna, Talanta, 30 (1983) 363.
3 A. G. Fogg, C. Burgess and D. T. Burns, Talanta, 18 (1971) 1175.
4 A. G. Fogg, C. Burgess and D. T. Burns, Analyst, 96 (1971) 854.
5 S. Uchikawa, Bull. Chem. Soc. Jpn., 40 (1967) 798.
6 I. Iwasaki, S. Utsumi and C. Kang, Bull. Chem. Soc. Jpn., 36 (1963) 325.
7 M. Tsubouchi, Anal. Chim. Acta, 54 (1971) 143.
8 A. G. Fogg, D. T. Burns and E. H. Yeowart, Mikrochim. Acta, (1970) 974.
9 S. Akiyama, K. Nakashima, S. Nakatsuji, M. Hamada and Y. Izaki, Bull. Chem. Soc. Jpn., 56 (1983) 947.
10 K. Nakashima, S. Tomiyoshi, S. Nakatsuji and S. Akiyama, Talanta, 33 (1986) 274.
11 D. T. Burns, J. M. Jones and N. Tungkananuruk, Trends Anal. Chem., 4(2) (1985) VI.
12 N. Ichinose, S. Yamada, N. Sakurai, T. Fujiyama and N. Masuda, Z. Anal. Chem., 293 (1978) 23.
13 D. T. Burns and N. Tungkananuruk, Anal. Chim. Acta, 189 (1986) 383.
14 P. Job, Ann. Chim. (Paris), 9 (1928) 113.
15 J. H. Yoe and A. L. Jones, Ind. Eng. Chem. Anal. Ed., 16 (1944) 111.
16 K. Momoki, J. Sekino, H. Sato and N. Yamaguchi, Anal. Chem., 41 (1969) 1286.
17 A. G. Briggs, W. Hayes, P. A. Howling and D. T. Burns, Mikrochim. Acta, (1970) 888.

Analytica Chimica Acta, 199 (1987) 241—244
Elsevier Science Publishers B.V., Amsterdam — Printed in The Netherlands

Short Communication

SPECTROPHOTOMETRIC DETERMINATION OF MANGANESE(VII) AFTER EXTRACTION WITH THE ETHYLENE-BIS(TRIPHENYLPHOSPHONIUM) CATION

D. THORBURN BURNS* and D. CHIMPALEE

Department of Analytical Chemistry, The Queen's University of Belfast, Belfast, BT9 5AG (Northern Ireland)

(Received 1st December 1986)

Summary. Manganese(VII) (0—120 μg) can be determined spectrophotometrically at 548 nm after extraction at pH 6 as its ethylene-bis(triphenylphosphonium) ion pair into chloroform. The system is applied to the determination of manganese in a range of steels.

The oxo anions are the least studied group of species which form liquid/liquid extractable ion-pairs with onium cations [1, 2]. Manganese(VII) (permanganate) has been determined in high-quality calcium carbonate [3] and in iron, steel and some non-ferrous metals [4] after extraction of tetraphenylarsonium permanganate. Extraction with the tetraphenylphosphonium cation has similarly been applied in the analysis of ferrous alloys [5]. The present communication reports the use of the ethylene-bis(triphenylphosphonium) cation as an ion-pairing extractant for permanganate, and the application of the system for the spectrophotometric determination of manganese in steels, after oxidation of manganese(II) to manganese(VII) by periodate.

Experimental

Apparatus. Pye Unicam SP 8-400 and SP 6-550 u.v.-visible spectrophotometers were used for recording absorption spectra and for routine measurements, respectively, with matched quartz 1-cm cells.

Reagents and solutions. Distilled water was used throughout. Ethylene-bis(triphenylphosphonium) bromide (Lancaster Synthesis) was used as supplied. Elemental analysis gave 63.8% C, 4.9% H ($C_{38}H_{34}P_2Br_2$ requires 64.1% C, 4.8% H). A 1.0% (w/v) stock solution was prepared in water. A stock 500 μg ml^{-1} manganese(VII) solution was prepared by dissolving 1.438 g of potassium permanganate (AnalaR, BDH) in 500 ml of water, boiling the solution gently for 1 h, cooling, filtering through a sintered glass (porosity G2) filter to remove any manganese(IV) oxide formed, and diluting exactly to 1 l. This solution was stored in a dark brown glass bottle. A stock 500 μg ml^{-1} manganese(II) solution was prepared by dissolving 1.438 g of potassium

0003-2670/87/$03.50

permanganate in water and carefully adding to it a saturated solution of sulphur dioxide until the permanganate solution just became colourless; the solution was diluted to exactly 1 l. More dilute solutions of manganese(VII) and of manganese(II) were prepared as required.

A pH 6 buffer was prepared by mixing 61.5 ml of 0.2 M disodium hydrogenphosphate with 438.5 ml of 0.2 M sodium dihydrogenphosphate and diluting to 1 l with water. A sulphuric/phosphoric acid solution was prepared by mixing 150 ml of concentrated sulphuric acid and 150 ml of 85% orthophosphoric acid, and carefully adding the mixture to 600 ml of water, cooling and diluting to exactly 1 l. The 5% (w/v) potassium periodate solution was prepared by dissolving 25 g of potassium periodate in a mixture of 300 ml of water and 100 ml of concentrated nitric acid, gently warming to complete dissolution, cooling and diluting to 500 ml. All other reagents were of analytical grade.

General procedure. Place an aliquot (3 ml) containing ca. 60 μg of manganese present as manganese(VII) in a 100-ml separating funnel. Add 3 ml of 0.5% (w/v) potassium periodate solution, 5 ml of 10% (w/v) ammonium fluoride solution (to complex any iron(III) and also bring the pH to ca. 6), 5 ml of pH 6.0 buffer and 5 ml of 1% (w/v) ethylene-bis(triphenylphosphonium) bromide solution. Extract twice with 4-ml portions of chloroform, collect the extracts in a 50-ml beaker and dry the solution by addition of 1 g of anhydrous sodium sulphate. Transfer to a 10-ml volumetric flask and make up to volume with chloroform. Cover the flask with aluminium foil to protect from daylight. Measure the absorbance within 30 min at 548 nm against a reagent blank prepared in the same manner.

Procedure for steel samples. For samples containing 0.2—2% manganese, dissolve accurately weighed 0.3 g samples in 35 ml of the sulphuric/phosphoric acid mixture in 250-ml conical flasks. Oxidize with concentrated nitric acid and boil to expel nitrous fumes. If any carbides remain, evaporate to fumes and cool. Add 50 ml of water and warm to dissolve soluble salts. Cool and, if necessary, filter into a 250-ml beaker. Dilute to 70 ml and add 10 ml of concentrated nitric acid. Boil for 2 min, add 10 ml of 5% (w/v) potassium periodate solution and boil for a further 4 min. Cool, transfer to a 100-ml volumetric flask and make up to volume with water [6].

Place a 3-ml aliquot of this solution in a 50-ml beaker, and add 5 ml of 10% (w/v) ammonium fluoride solution. Adjust the pH to 6.0 by careful addition of 2 M ammonia solution with stirring. Transfer to a 100-ml separating funnel, add 5 ml of pH 6 buffer and 5 ml of 1% (w/v) ethylene-bis(triphenylphosphonium) bromide solution, and continue as in the general procedure. Measure the absorbance of the extract immediately if the steel contains large amounts of chromium.

Prepare a calibration graph over the range 0—120 μg of manganese by using 0.3 g of high-purity iron with aliquots of standard manganese(II) solution and proceeding as for the steel samples.

Examination of the main experimental variables

Various solvents including alcohols, ketones, esters, ethers, and chlorinated and aromatic hydrocarbons were examined for extraction efficiency for 60 μg of manganese(VII), 5 ml of pH 6 buffer, 1 ml of 1% ion-pair reagent solution and 10 ml of water, extracted as in the general procedure. The absorbance of extracts was measured immediately against the pure solvent. Chloroform and dichloromethane were the most efficient solvents. The ion-pair was not extracted into carbon tetrachloride, benzene or toluene. The permanganate colour faded rapidly in the other solvents examined. Chloroform was chosen for further work because the colour faded least rapidly in this solvent; the colour was stable for 1 min but thereafter faded rapidly. The addition of potassium periodate to the aqueous manganese(VII) solutions prior to extraction produced extracts in which the colour was stable for 30 min. Thus periodate was used as the oxidant when examining steel samples.

The effect of pH was examined; absorbances were constant over the pH range 4—8. Below pH 4 a slight decrease in sensitivity was noted whilst above pH 8 the colour of extracts faded rapidly. In subsequent work, the aqueous phase was buffered at pH 6. The absorbance of extracts increased with increasing amounts of ion-pairing reagent up to a constant value. A convenient amount of reagent, in the plateau region, is specified in the general procedure. The extent of extraction was independent of phase-volume ratios up to 5:1 water/chloroform. The 548-nm permanganate peak was chosen in preference to the 528-nm peak because the absorbance of chromium is much less at the former wavelength [7]. The composition of the ion pair was established spectrophotometrically by Job's method of continuous variation [8] and the mole-ratio method [9] to be $[(C_6H_5)_3P(CH_2)_2P(C_6H_5)_3][MnO_4]_2$.

Results and discussion

A linear calibration graph was obtained over the range 0—120 μg of manganese(VII) at 548 nm (apparent molar absorptivity 2.38×10^3 l mol^{-1} cm^{-1}). For the determination of 60 μg of manganese, the relative standard deviation was 0.54% (7 results).

The possible interferences of a number of cations and anions on 60 μg of manganese(VII) were checked under the conditions of the general procedure. Iron(III), sulphate, chloride, hydrogenphosphate, nitrate, fluoride, tartrate, citrate and vanadate in a weight ratio of 800:1, molybdenum(VI), tungsten(VI), sodium, potassium, ammonium, nickel, calcium, chromium(III) and zirconium (500:1), and cobalt(II), aluminium, lead, tin(IV), magnesium, zinc, cadmium, niobium, antimony(III) and copper(II) (100:1) were without significant effect (i.e., less than ±2%). Chromium(VI) was the only ion which interfered significantly and is of interest in the analysis of steels. Chromium(VI) extracts at the same time as manganese(VII) and affects the stability of the extract, especially in sunlight. In ratios up to 30:1, there was no significant effect at 548 nm provided that the chloroform extract was protected

TABLE 1

Determination of manganese in certified steels

BSC steel no.	Manganese content (% w/w)		BSC steel no.	Manganese content (% w/w)	
	Certified[a]	Found[b]		Certified[a]	Found[b]
Unalloyed			219/3	0.74 (0.73—0.75)	0.749 ± 0.0
239/3	0.87 (0.86—0.88)	0.857 ± 0.008	256/1	1.02 (1.00—1.03)	1.00 ± 0.02
435/1	0.41 (0.40—0.42)	0.407 ± 0.006	408	0.64 (0.63—0.65)	0.635 ± 0.0
456	0.17 (0.17—0.18)	0.162 ± 0.008	410/1	0.22 (0.21—0.23)	0.203 ± 0.0
457	0.28 (0.27—0.29)	0.280 ± 0.014			
458	0.42 (0.42—0.43)	0.430 ± 0.018	*Highly alloyed*		
			483	0.29 (0.28—0.31)	0.282 ± 0.0
Low alloy			485	0.50 (0.49—0.53)	0.488 ± 0.0
214/2	1.61 (1.59—1.62)	1.61 ± 0.02			
218/3	0.64 (0.63—0.65)	0.636 ± 0.013			

[a]With certified range in parentheses. [b]Mean ± 95% confidence limits for 5 replicates.

from daylight and the absorbance was measured immediately after phase separation. Cyanide, EDTA, thiosulphate and reducing agents should be absent.

The results for the determination of manganese in British Chemical Standard Steels (Table 1) are in good agreement with certificate values. The interferences are significantly lower than those observed in aqueous-phase spectrophotometric determinations of manganese(VII) when large amounts of other coloured ions interfere significantly and have to be compensated by difference methods.

REFERENCES

1 A. J. Bowd, D. T. Burns and A. G. Fogg, Talanta, 16 (1969) 719.
2 D. T. Burns, Anal. Proc., 19 (1982) 355.
3 M. L. Richardson, Analyst, 87 (1962) 435.
4 H. Goto and Y. Kakita, Z. Anal. Chem., 254 (1971) 18.
5 Deputy Minister of the Romanian Ministry of Petroleum Industry and Chemistry, British Patent 1,094,778, date appl. 2.3.65. See Anal. Abstr., 15 (1968) No. 4681.
6 Analytical Panel, Methods of Chemical Analysis of Iron and Steel, British Steel Corporation, Sheffield, 1974, pp. 82—83.
7 W. J. Williams, Handbook of Anion Determination, Butterworths, London, 1979, p. 163.
8 P. Job, Ann. Chim. (Paris), 9 (1928) 113.
9 J. H. Yoe and A. L. Jones, Ind. Eng. Chem. Anal. Ed., 16 (1944) 111.

Analytica Chimica Acta, 199 (1987) 245—248
Elsevier Science Publishers B.V., Amsterdam — Printed in The Netherlands

Short Communication

DETERMINATION OF TRACES OF BORON IN SEMICONDUCTOR AMORPHOUS SILICON FILM BY FILAMENT-VAPORIZATION INDUCTIVELY-COUPLED PLASMA/ATOMIC EMISSION SPECTROMETRY

EIICHI KITAZUME*

College of Humanities and Social Sciences, Iwate University, Ueda, Morioka, Iwate 020 (Japan)

SACHIO ISHIOKA and EISUKE MITANI

Central Research Laboratory, Hitachi Ltd., Kokubunji, Tokyo (Japan)

(Received 5th January 1987)

Summary. Silicon is dissolved from the platinum substrate by nitric/hydrofluoric acids. The recovery of boron on direct analysis was poor, but was increased to >95% by the addition of 500—5000 $\mu g\ ml^{-1}$ phosphorus as phosphoric acid. The results compared well with the molar ratio of the gases ($B_2H_6/(Ar + H_2)$) used to form the film and the intensity ratio of $^{11}B^+$ and $^{30}Si^+$ obtained by secondary-ion mass spectrometry.

Amorphous silicon films formed by a discharge or reactive sputtering method are likely to be effective materials for solar batteries, photosensitive detectors and other semiconductor devices [1]. The characteristics of these devices are critically affected by the concentration of the dopant elements, so that semiconductor wafer-to-wafer differences must be determined with good accuracy and precision. However, each wafer contains only a few milligrams of amorphous silicon, thus microanalytical techniques for the determination of impurities are required. Secondary-ion mass spectrometry and electron-probe microanalysis have been used for the determination of impurities including dopant elements [2—4].

Boron is one of the most widely used doping donors. It can be determined sensitively by filament-vaporization inductively-coupled plasma/atomic emission spectrometry (i.c.p./a.e.s.) [5, 6]. This communication extends this technique to the determination of boron in amorphous silicon films.

Experimental

The apparatus for boron determination was as reported previously [5]. A secondary-ion mass spectrometer (Hitachi, Model IMA-2) was used for the determination of the intensity ratio of boron and silicon.

0003-2670/87/$03.50

Boron standard solutions were prepared by dissolving boric acid (Kanto Chemicals Corp.) in water. All other reagents mentioned below were of analytical-reagent grade.

A sample comprising an amorphous silicon film deposited on a platinum substrate (50 mm diameter) was weighed and placed in a 100-ml teflon beaker. The film (about 2 μm thick) was dissolved by 0.5 ml of etching solution (5.8 M nitric acid/11.2 M hydrofluoric acid). After the film had dissolved, the platinum substrate was removed from the solution, washed, dried and reweighed. The etching solution was transferred to a 1-ml teflon beaker and phosphoric acid (1 mg of phosphorus) was added. The solution was evaporated completely by heating at 110°C. After cooling, 200 μl of water was added. If the silicon film contained >10 μg g^{-1} boron, 2 ml of water was added. The residue was dissolved by ultrasonic mixing for 2 min. A 10-μl sample was deposited on the top of the platinum filament from a suitable pipette, and boron was determined under the conditions described previously [5].

Results and discussion

Boron released from the silicon film is present in solution as tetrafluoroboric acid, which is decomposed at 130°C. As this solution is preconcentrated on the filament by heating to >100°C, it was necessary to test if such treatment could cause any loss of boron. This was done by heating 10 μg of boron as boric acid in 0.5 ml of etching solution, in a platinum crucible at 110°C and determining boron by conventional i.c.p./a.e.s. after dissolving the residue in 5 ml of water. The recovery was less than 2%. As the emission intensity obtained from potassium tetrafluoroborate solutions was not affected in this way [5], addition of potassium salts to the boric acid was tried. For the determination of 10 μg of boron, addition of over 250 μg potassium showed >97% recovery at 110°C. The recovery of 0.1 μg of boron varied between 76 and 101%. This shows that the addition of a large quantity of potassium decreases the reproducibility and causes matrix effects [5].

Boron reacts with phosphorus to form stable boron phosphide [7]. Various amounts of phosphorus as phosphoric acid as well as perchloric acid were therefore added to 10 μg of boron and the solution was heated to fumes of perchloric acid. The results are shown in Fig. 1A. When the amount of phosphorus added was >300 μg, the recovery was >95%. As shown in Fig. 1B, for the determination of 0.1 μg ml^{-1} boron by the filament vaporization method, addition of >500 μg ml^{-1} phosphorus gave almost constant intensity, nearly the same as when potassium tetrafluoroborate was used as the boron standard. The emission intensities were not suppressed by an increase even to 5000 μg of phosphorus. Hence phosphoric acid was used as the additive for subsequent work.

The recovery and repeatability through the total procedure were investigated by using test mixtures. The results are shown in Table 1. Relative standard deviations were ca. 4% at the concentrations studied. A rectilinear calibration graph was obtained from 0.01 to >10 μg ml^{-1}. The graph was

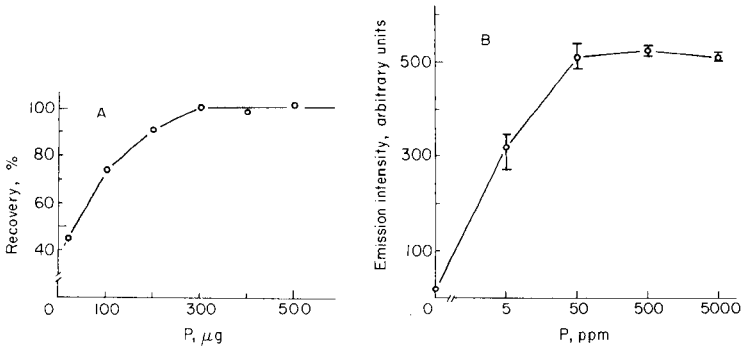

Fig. 1. Effect of phosphoric acid concentration on the recovery of boron: (A) 10 μg of boron as boric acid heated in a platinum crucible until fuming of perchloric acid; (B) determination of 0.1 μg B ml^{-1} by filament-vaporization i.c.p./a.e.s.

TABLE 1

Recovery of boron from synthetic mixtures[a]

B present (μg)	Si present (mg)	B found (μg)	Recovery (%)
0	0	0.007	—
0	0	0.007	—
0	10	0.013(0.013)	—
0	10	0.013(0.012)	—
0.1	10	0.096(0.099)	96(99)
0.1	10	0.093(0.098)	93(98)
0.1	10	0.104(0.101)	104(101)
0.2	10	0.194(0.200)	97(100)
0.2	10	0.194(0.200)	97(100)
0.2	10	0.190(0.196)	95(98)

[a]The values in parentheses were obtained by conventional i.c.p./a.e.s.

TABLE 2

Determination of boron in amorphous silicon films

Sample	10^6 $B_2H_6/(Ar + H_2)$ molar ratio	Boron found[a] (μg g^{-1})	10^6 $^{11}B^+/^{30}Si^+$ intensity ratio[b]
A	100	130	400
B	10	17	10
C	5	8	5
D	2	1	3

[a]By proposed method. [b]By secondary-ion mass spectrometry.

slightly more reproducible in the presence of 500 compared to 5000 $\mu g\ ml^{-1}$ of phosphorus, samples were analysed with addition of the lesser amount of phosphorus.

The proposed technique was applied to the determination of boron in amorphous silicon films formed by a glow-discharge sputtering method in an atmosphere of argon, hydrogen and diborane. The results are shown in Table 2, which also shows the intensity ratio of $^{11}B^+$ and $^{30}Si^+$ obtained by secondary-ion mass spectrometry. These results show fair correspondence between the results for boron and the molar ratio of $B_2H_6/(Ar + H_2)$.

The author is grateful to Dr. Atsushi Mizuike and Dr. Hiroshi Kawaguchi for their helpful suggestions, to Dr. Seiki Harada and Dr. Fumio Nagata for their encouragement, and to Dr. Kanji Tsujii, Mr. Hisao Kojima, Dr. Kazuo Kuga and Mr. Masatoshi Nakazawa for valuable discussions.

REFERENCES

1 D. E. Carlson, Appl. Phys. Lett., 28 (1976) 671.
2 G. J. Scilla and G. P. Ceasar, Surf. Interface Anal., 4 (1982) 253.
3 W. Wach and K. Wittmaack, Phys. Rev. B, 27 (1983) 3528.
4 H. Aharoni and P. L. Swart, Vacuum, 33 (1983) 221.
5 E. Kitazume, Anal. Chem., 55 (1983) 802.
6 E. Kitazume, Anal. Chim. Acta, 187 (1986) 313.
7 L. Whekwska, Fresenius' Z. Anal. Chem., 163 (1958) 45.

Analytica Chimica Acta, 199 (1987) 249—252
Elsevier Science Publishers B.V., Amsterdam — Printed in The Netherlands

Short Communication

THE EFFECT OF THE ORDERED PHASE CuAu ON THE ACCURACY OF EMISSION ANALYSIS OF GOLD ALLOYS

R. DE MARCO and D. J. KEW

Royal Melbourne Institute of Technology, GPO Box 2476V, Melbourne 3001, Victoria (Australia)

J. V. SULLIVAN

CSIRO Division of Chemical Physics, PO Box 160, Clayton, Victoria 3168 (Australia)

(Received 4th February 1987)

Summary. The accuracy of emission determinations of gold, silver and copper in ordered Au/Ag/Cu alloys is compared with similar determinations when these alloys are disordered. The relative slope factors, K_{Cu} and K_{Ag}, depend on the concentration of copper present. The accuracy obtained in the analysis of the disordered alloys cannot be achieved for the ordered ones unless the standards used closely match the samples in composition. The ordered phase responsible for the effect is CuAu.

The precision and accuracy of emission spectrometric determinations of gold in some gold alloys have been discussed elsewhere [1, 2]. The results obtained for disordered alloys, where there was little or no CuAu present, showed that one standard was sufficient for determining gold in the concentration range 80—100% (w/w) [1]. When alloys which had been ordered [2] were analyzed, an inter-element effect was observed and two standards were required for maximum accuracy (0.03% w/w). One standard was required for the range 80—90%; the other for the range 90—100%.

Experimental

Emission determinations of gold, silver and copper in five alloys containing gold and copper in the ranges 59—75% and 31—15%, respectively, were conducted. The alloys contained 10.00 ± 0.05% (w/w) silver. The alloys were prepared by using the methods already described [2]. The optical system, excitation source and the measuring system have also been described in previous work [1, 2]. The analytical lines used were the resonance lines, viz, Au I 242.795 nm, Cu I 327.396 nm and Ag I 338.289 nm. Internal standardization was used to calculate the concentrations of the constituents in the alloys.

Two sample cathodes were made for each alloy. One set of five was heated in a hydrogen atmosphere for several hours at 450°C to ensure disordering of the CuAu phase; the other set was heated in a hydrogen atmosphere for

0003-2670/87/$03.50

10 h at 280°C to produce some ordering. Hydrogen was used to prevent oxidation of the samples. The gold in each alloy was determined by fire assay, the silver by gravimetric means and the copper by difference. The values so determined were compared with those obtained by emission spectrometry.

Results and discussion

The ranges of concentration were chosen to give alloys in which the ratio of copper to gold varied around 1:3.1, the stoichiometric proportion of the compound CuAu. The alloy containing 68% gold and 22% copper, when ordered, should consist almost entirely of the CuAu phase and could be expected to sputter differently from the other ordered alloys.

The relative slope factors of copper, K_{Cu}, and silver, K_{Ag}, were evaluated in the samples and these were constant for the disordered alloys. However, the K_{Cu} values for the ordered alloys decreased with increasing copper concentration, in a non-linear fashion. The values of K for gold, silver and copper are given in Table 1. The constancy of the K values for each element in the disordered samples indicates that only one standard is required for analysis. The variability of the K_{Cu} values for ordered alloys suggests that the presence of the compound (CuAu) can seriously affect the accuracy of emission determinations. The standard used was the disordered alloy containing 70.99% Au, 18.95% Cu and 10.05% Ag.

Figure 1 shows the curves of concentration of gold and copper (marked Au and Cu, respectively) determined by emission spectrometry versus concentration of the gold and of copper determined by the chemical means. The curves for disordered alloys are linear with a slope of unity indicating that the emission determinations are as accurate as the chemical ones. The curves for the ordered alloys show the inaccuracy which can result when the CuAu compound is present. The emission results obtained for disordered and ordered alloys were identical (within experimental error) only for the alloy containing 68% Au and 22% Cu.

The effects observed with copper and gold in ordered alloys indicate that the sputtering efficiency of the alloy changes with composition and that,

TABLE 1

Relative slope factors for gold, silver and copper in some ordered (a) and disordered (b) alloys

Concentration (% w/w)			K_{Au}		K_{Ag}		K_{Cu}	
Au	Ag	Cu	a	b	a	b	a	b
58.98	10.17	30.85	1.00	1.00	6.66	7.21	2.60	2.79
63.00	10.10	26.90	1.00	1.00	7.30	7.24	2.78	2.80
67.90	10.11	22.00	1.00	1.00	7.24	7.23	2.81	2.81
70.99	10.10	18.91	1.00	1.00	7.30	7.20	2.92	2.80
75.01	10.05	14.94	1.00	1.00	7.72	7.22	3.17	2.79

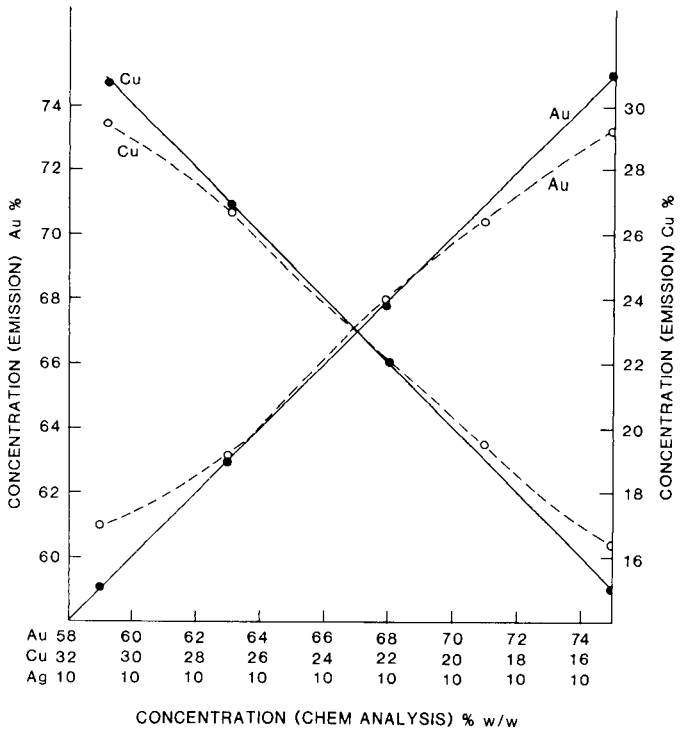

Fig. 1. Curves of concentration of gold and copper determined by emission spectrometry versus concentration of the gold and of the copper determined by chemical means. (——) Disordered alloys; (— — —) ordered alloys.

for maximum accuracy, standards closely matching the samples are required. As the curves show, the standard used in the analysis of the disordered alloys is applicable only to the ordered alloy containing 68% gold and 22% copper.

Naganuma et al. [3] have discussed selective sputtering of a θ-phase containing the compound, Al_2Cu, in aluminium alloys and have attributed it to distortion of the electric field around this phase. This leads to preferential ion bombardment of the θ-phase.

If a similar effect occurs with the CuAu phase in ordered gold alloys, samples having an actual concentration ratio of Cu to Au less than 1:3.1 will give an apparent higher copper content and lower gold content. But samples having an actual concentration ratio of Cu to Au greater than 1:3.1 will give an apparent lower copper content and higher gold content. The sample containing an actual concentration ratio of Cu to Au of 1:3.1 will give apparent concentrations of gold and copper identical to the actual concentrations, because the composition of the preferentially sputtered CuAu phase is similar to the actual composition of the alloy. In such a case, the internal standardization procedure corrects for the differences in sputtering efficiency between the ordered and disordered phases.

The results shown in Fig. 1 confirm this trend, suggesting preferential sputtering of the CuAu phase as a possible explanation for the sputtering efficiency of ordered alloys varying with composition.

Conclusion

The presence of the ordered phase, CuAu, in Au/Ag/Cu alloys leads to variation in sputtering yield depending on the amount of CuAu present. This variation affects the accuracy of emission analyses unless the standards used are similar in composition to the samples. If care is taken to ensure that the alloys are disordered, then, analyses over a wide range of concentration can be made with high accuracy using one standard.

REFERENCES

1 R. De Marco, D. Kew, D. Owen and J. V. Sullivan, Proc. 10th Int. Precious Met. Inst. Conf., Lake Tahoe, NV, June 8—12, 1986.
2 R. De Marco, D. J. Kew, C. Chadjilazarou, D. W. Owen and J. V. Sullivan, Anal. Chim. Acta, 194 (1987) 189.
3 K. Naganuma, M. Kubota and J. Kashima, Anal. Chim. Acta, 98 (1978) 77.

Analytica Chimica Acta, 199 (1987) 253—257
Elsevier Science Publishers B.V., Amsterdam — Printed in The Netherlands

Short Communication

ECHELLE-SPECTROMETER/IMAGE-DISSECTOR SYSTEM FOR ELEMENTAL QUANTITATION BY CONTINUOUS-SOURCE ATOMIC ABSORPTION SPECTROMETRY

RONALD MASTERS, CHUNMING HSIECH and HARRY L. PARDUE*
Department of Chemistry, Purdue University, West Lafayette, IN 47907 (U.S.A.)
(Received 18th February 1987)

Summary. The performance of an echelle-spectrometer/image-dissector system is evaluated for elemental quantitation by continuous-source atomic absorption spectrometry. Flame and graphite-furnace atomizers were used, as well as two different spectrometer configurations. Quantitative results obtained with the flame atomizer and a low-resolution spectrometer configuration are discussed briefly; results obtained with the graphite-furnace atomizer and a higher-resolution configuration are presented in detail. Absorption sensitivities for calcium (422.7 nm), chromium (425.4 and 357.9 nm), copper (324.8 nm), and manganese (403.1 and 279.5 nm) were all within a factor of 4—6 of comparable line-source absorption sensitivities, and calibration curves were linear up to absorbances of about 0.1. Further development of the system for simultaneous multi-element quantitation is discussed.

Although atomic absorption and atomic emission spectroscopy offer complementary capabilities, line-source atomic absorption suffers from the limitation that it is not easily adaptable for simultaneous multi-element quantitation. The two commonest approaches to simultaneous multi-element quantitation by atomic absorption spectrometry (a.a.s.) have involved the use of multi-element hollow-cathode lamps and continuous sources; the former is limited to a few (2—5) elements and the latter has not proven very practical to date.

One of the most promising approaches to continuous-source atomic absorption has involved an echelle grating spectrometer with multiple slits and detectors for monitoring spectral lines of interest [1]. Although this approach appears to offer significant advantages relative to earlier systems, it has the limitation that only preselected lines can be monitored. An approach that can overcome this limitation involves the use of the echelle spectrometer with an imaging detector [2—4].

This communication describes the results of a study of the use of an echelle-spectrometer/image-dissector combination for continuous-source a.a.s. Although the study does not provide a practical approach to multi-element quantitation, it does identify the nature of the problems associated with multi-element quantitation when this system is applied, how these

0003-2670/87/$03.50

problems can be solved, and the quality of the results that can be expected. These results are used to suggest the next step in the development of a versatile system for multi-element quantitation by continuous-source a.a.s.

Experimental

Instrumentation. The instrumental system consists of a continuous-source, atomizer, echelle spectrometer, and image dissector interfaced to a computer. Much of the system, including the image-dissector camera, interface and computer, has already been described [2, 3], so only the details unique to this sutdy are included below.

Echelle spectrometer. Two different configurations of the spectrometer were used. In one configuration, the dispersed spectrum is reduced by a factor of 3.9 as described earlier [3] so that the entire wavelength range from 200 to 800 nm is displayed on the addressable area of the photocathode of the image dissector. The resolution found experimentally with this system is about 0.04 nm at 400 nm. In the other configuration, the spectral reduction system is not used and the addressable region of the detector photocathode samples only a portion of the dispersed spectrum. The resolution of this system is improved to about 0.01 nm at 400 nm at the expense of the spectral range that can be monitored by the photocathode at one time. Although this configuration has limited practical utility for simultaneous multi-element quantitation, it provided substantially improved quantitative performance and served as the basis for an alternative design that should offer both good quantitative performance and practical multi-element quantitation.

Continuous source. Two different sources were evaluated. For studies of the low-resolution spectra, a 600-W tungsten/halogen lamp (GE DYS) in an air-cooled housing provided adequate intensity down to about 300 nm. For higher-resolution studies, the intensity of the tungsten/halogen lamp was not sufficient to provide adequate signal-to-noise ratios, so a 500-W xenon-arc lamp (Optical Radiation Corporation, Model EP102M) was used instead. This lamp provides adequate intensity down to about 270 nm.

Atomizer. Both flame and electrothermal atomizers were used. For flame atomization, the burner system was as previously described [3]. Acetylene and air flow rates and sample uptake were 1.2 and 6 l min^{-1} and 6.7 ml min^{-1}, respectively, for all elements, except calcium for which the air flow rate was 4.5 l min^{-1}. The observation height was 5 mm above the burner head.

Most data presented were obtained with a graphite-furnace atomizer (Perkin-Elmer HGA2100) with an argon flow rate of 60 ml min^{-1}. The atomization cycle was to dry the sample at 100°C for 30 s, to char the residue at 1000°C for 1 s, and to atomize at 2700°C for 10 s. Because all samples were standards in deionized water, the charring step was not necessary but was included as a convenient point at which to begin data acquisition.

Reagents. Solutions of the elements of interest were prepared by appropriate dilution of certified atomic absorption standards (Alfa Products, Denvers, MA 01923) with distilled, deionized water.

Results and discussion

Elements included in this study were those in Table 1 plus Na (589.0 nm), Al (396.2 nm), Fe (373.7 nm), and Ni (341.5 nm). Initial studies were done with the low-resolution spectrometer configuration. When this configuration was used with flame atomization, only sodium and calcium were detectable at concentrations below 50 $\mu g\ ml^{-1}$. With electrothermal atomization, all elements were detectable down to 1 $\mu g\ ml^{-1}$; but sensitivities were low relative to line-source a.a.s., detection limits were about the same as for line-source a.a.s. with flame atomization, and calibration curves were nonlinear throughout the concentration ranges examined (e.g., curve a in Fig. 1). Based on these results, it was concluded that the spectral resolution of the system was inadequate for practical applications of continuous-source a.a.s. and the spectrometer configuration was modified to obtain improved resolution. As noted in the experimental section, the modification involved removal of the reducing optics so that only a portion of the total spectrum was monitored by the addressable area of the photocathode. This had the effect of improving the spectral resolution about four-fold.

One effect of this change is illustrated in Fig. 1, where the responses for chromium with lower (curve a) and higher (curve b) resolution are shown. The 4-fold improvement in resolution results in a 40-fold improvement in sensitivity. This configuration was used to obtain the calibration data for single-component solutions of the elements listed in Table 1, which includes least-squares statistics for fits of absorbance, A, vs. mass (ng) as well as the linear range and so-called characteristic mass and the lower limit of linearity which is the lowest mass examined in each case. Intercepts and standard errors of the estimate (in absorbance) are easily transformed to equivalent masses with the aid of the characteristic masses which correspond to absorbance changes of 0.0044. Intercept values range from about +9 pg for copper

TABLE 1

Summary of results for elements quantified by continuous-source a.a.s. with electrothermal atomization

Element	Wavelength (nm)	Least-squares statistics[a]					
		Log-log plot	Linear plot		Characteristic mass (pg)[b]		Linear range (pg)
		Slope	Intercept	S.c.	This work	Comparison[c]	
Ca	422.7	0.94 ± 0.07	0.001 ± 0.002	0.002	26	—	100—300
Cr	425.4	0.95 ± 0.06	0.001 ± 0.002	0.003	116	—	500—2000
Cr	357.9	0.97 ± 0.07	0.002 ± 0.001	0.002	46	10	200—800
Cu	324.8	1.04 ± 0.05	0.0005 ± 0.002	0.005	81	22	500—2000
Mn	403.1	0.99 ± 0.03	0.001 ± 0.001	0.003	94	—	400—4000
Mn	279.5	0.96 ± 0.07	0.002 ± 0.002	0.003	27	5	100—400

[a]Uncertainties are quoted at ±1 s.d. Intercept and standard error (s.c.) of the estimate are given as absorbances. [b]Mass required to give absorbance change of 0.0044. [c]Taken from Ref. 1.

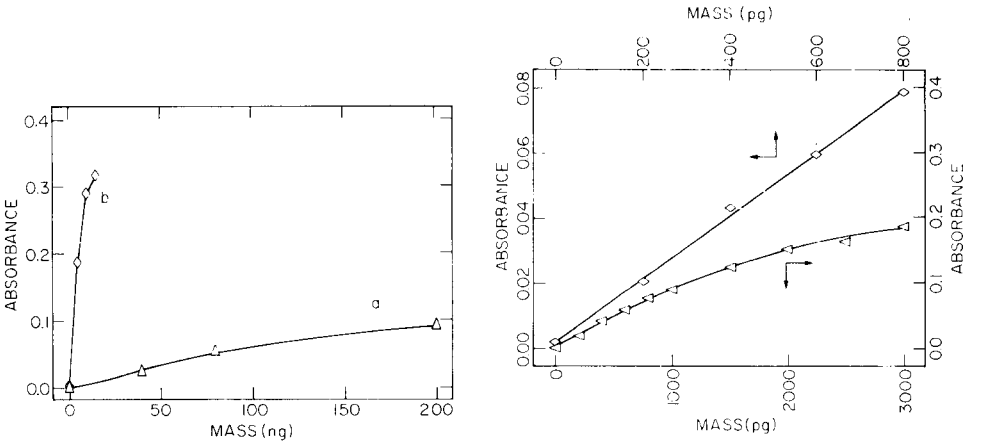

Fig. 1. Calibration curves for chromium (425.4 nm) with graphite-furnace atomization: (a) low-resolution configuration, Xe lamp; (b) high-resolution configuration, tungsten/halogen lamp.

Fig. 2. Calibration curves for chromium (357.9 nm) with high-resolution configuration and electrothermal atomizer.

at 324.8 nm to about 26 pg for chromium at 425.4 nm. Also, the noise level for absorbance measurements was about 0.004 so that detection limits at any desired level of confidence can be estimated as multiples of the characteristic masses. For comparison purposes, characteristic masses reported for the electrothermal atomizer with line-source detection [1] are included in the table. Values obtained in this study are all within a factor of six of those obtained with line-source a.a.s. It should be noted that the characteristic masses reported for line-source a.a.s. were obtained with atomizer conditions optimized for each element; the results of continuous-source a.a.s. reported here were obtained with a single set of atomizer conditions for all elements so that the results are more nearly representative of those that could be obtained for simultaneous multi-element quantitation.

Representative calibration curves for chromium are shown in Fig. 2. Curves for all the elements listed in Table 1 were nonlinear above absorbances of 0.1, a result of the fact that the spectrometer bandpass of 0.01 nm is somewhat larger than the absorbance line half-widths of 0.002 nm [5].

Because of the loss of spectral range, it was necessary to reposition the final focusing mirror of the spectrometer for each element line listed in Table 1. Thus, although this spectrometer configuration gives line-source a.a.s. results that compare favorably with those obtained by continuous-source a.a.s., it does not provide the capability of simultaneous multi-element quantitation. To achieve this capability and still retain the resolution needed for good results in continuous-source a.a.s., it will be necessary to make a significant change either in the size of the detector or in the size and shape of the

spectrum that is produced. The current detector has a 43-mm diameter photocathode which is one of the larger sizes currently available. Accordingly, our attention is currently focused on the development of a modified echelle spectrometer.

The equations that describe the spectrum produced by an echelle grating [6] suggest that if the visible spectrum is dispersed into the 120th to 480th order (instead of the 30th to 120th order as is the case with the current system), and if the blaze angle could be increased to 76° (instead of the 63°26′ angle of the current grating), a spectrum would be produced that is compatible in size with the dimensions of the imaging detector used. Such a system would provide twice the resolution (0.005 nm) of the current system and provide a continuous spectral range of about 200—450 nm, depending on the device used to disperse diffraction orders in the vertical dimension. This range would include most of the spectral lines of interest for quantitation by continuous-source a.a.s. Based on the preliminary results presented above, it is expected that a system that includes a grating similar to that described above would prove to be a versatile instrument for simultaneous multi-element quantitation by continuous-source a.a.s.; such a system is being developed currently and results will be reported later. The principal limitation of the system is expected to be the limited linear range, a characteristic that will require improved resolution, which in turn will require either a sacrifice of spectral range or detectors with larger areas.

REFERENCES

1 J. M. Harnly, T. C. O'Haver, B. Golden and W. R. Wolf, Anal. Chem., 51 (1979) 2007.
2 H. L. Felkel, Jr. and H. L. Pardue, Anal. Chem., 49 (1977) 1112.
3 H. L. Felkel, Jr. and H. L. Pardue, Clin. Chem., 24 (1978) 602.
4 H. L. Felkel, Jr. and H. L. Pardue, Anal. Chem., 50 (1978) 602.
5 G. D. Christian, Flame Spectroscopy. Instrumental Analysis, Allyn and Bacon, 1978, p. 263.
6 G. R. Harrison, J. Opt. Soc. Am., 39 (1949) 522.

Analytica Chimica Acta, 199 (1987) 259—263
Elsevier Science Publishers B.V., Amsterdam — Printed in The Netherlands

Short Communication

THE COPRECIPITATION OF AN ORGANOPHOSPHATE FRACTION FROM HARBOUR WATER FOR X-RAY FLUORESCENCE SPECTROMETRY

F. AHERN, J. M. ECKERT*, S. F. HAIN, K. E. A. LEGGETT and N. C. PAYNE

Department of Inorganic Chemistry, University of Sydney, Sydney, N.S.W. 2006 (Australia)

K. L. WILLIAMS

Department of Geology and Geophysics, University of Sydney, Sydney, N.S.W. 2006 (Australia)

(Received 3rd March 1987)

Summary. The film x-ray fluorescence spectrum of a cobalt pyrrolidinedithiocarbamate carrier complex, precipitated in harbour-water samples, contains a previously unreported peak at the wavelength of the first-order K_α line of phosphorus. The coprecipitated phosphorus is an organophosphate fraction of biological origin, constituting approximately 10% of the dissolved organophosphorus in the waters.

The precipitate formed by mixing cobalt(II) and pyrrolidinedithiocarbamate solutions has been used as a carrier in the preconcentration of a number of trace metals from sea and harbour waters. The determinations have been completed either by atomic absorption spectrometry (a.a.s.) after acid digestion of the precipitate [1—3] or by x-ray fluorescence (x.r.f.) spectrometry after collection of the precipitate as a film on a membrane filter [4—7].

It is shown here that the x.r.f. spectrum of the precipitate contains, in addition to the peaks which have been used for trace metal determinations, a peak at a wavelength of 0.616 nm, the position of the first-order K_α line of phosphorus. Evidence is presented that the peak is caused by an organophosphate fraction of biological origin. This appears to be the first example of the preconcentration of organophosphorus compounds from a natural water by selective coprecipitation.

Experimental

The reagents, x.r.f. spectrometer and filtration equipment were described previously [4].

Coprecipitation procedure. This was also as described previously [4], with one difference. Count rates of the carrier precipitate at the P K_α line were found to be unaffected by the pH at which the coprecipitation was done, in the pH range 4—8. In the present work, the pH of the water samples

0003-2670/87/$03.50

was adjusted with buffer to pH 8, the natural pH of sea water, instead of pH 4, as in previous applications of the cobalt pyrrolidinedithiocarbamate (Co-PDC) carrier system.

Preparation of film standards. A set of phosphorus film standards was prepared by delivering, from a micropipette, 2-μl volumes of standard orthophosphate solutions on to Co-PDC blank films (one 2-μl drop per filter) and allowing the added drops to evaporate to dryness.

Oxidative digestion. After addition of nitric acid (Merck Suprapur) to provide 5 ml l^{-1}, the water sample was irradiated with a 35-W U-tube immersion lamp for 24 h, and then boiled gently on a hot plate for 4 h. Some samples were also subjected to peroxodisulphate oxidation [8].

X.r.f. spectrometry. The loaded filters were mounted with the sample side towards the x-ray beam and teflon sleeves 2 mm thick were fitted inside the sample holders to reduce background scattered from the holders. The following working conditions were used: chromium anode tube operated at 60 kV and 45 mA, fine collimator, germanium crystal, 2θ values of 141.0° (for peak) and 140.0° and 142.0° (for background), automatic pulse-height selection, flow and scintillation detectors in tandem and counting times of 100 s and 40 s for peak and background, respectively. These conditions yielded a linear net P K_α intensity of 175 cps/μg P for films bearing 0—1 μg of phosphorus.

Results and discussion

Assignment of the peak at 0.616 nm to the first-order P K_α line could not be confirmed by observation of weaker emissions in the phosphorus x.r.f. spectrum. These were indistinguishable from background. However, all possible alternative assignments, including harmonic overlaps such as that caused by the second-order Ca K_β emission, were investigated and discounted. For example, the peak in question was not observed in the film spectrum of a carrier precipitate formed in artificial sea water.

Studies on harbour water. Surface samples were collected at The Spit in Middle Harbour, Port Jackson, Sydney. The samples were filtered through 0.4-μm pore-size membrane filters within 4 h of collection and 100-ml aliquots of the filtrate were treated immediately to precipitate the Co-PDC carrier complex.

Table 1 shows the net x.r.f. count rates (at the P K_α line) of the carrier precipitates as films on membrane filters and the concentrations of coprecipitated phosphorus in the waters, obtained from the carrier count rates by reference to the phosphorus calibration data from films. Briefly, active (coprecipitated) phosphorus levels in the waters ranged from 0.5 to 2.3 μg l^{-1}, averaging 1.1 μg l^{-1}. The highest concentrations were in samples collected in January, February and December, the summer months. The lowest concentration was in the June (winter) sample.

Concerning the chemical nature of the coprecipitated phosphorus fraction, there are various possibilities [9]. Dissolved inorganic phosphorus in sea

TABLE 1

Coprecipitated phosphorus in harbour waters

Collected	pH	Salinity (‰)	Net count rate[a] (cps)	Coprecipitated phosphorus[b] ($\mu g\ l^{-1}$)
Jan. 1986	8.0	30.8	29.0	1.7
Feb.	8.0	33.1	40.2	2.3
March	7.8	32.3	17.4	1.0
June	8.1	32.8	8.5	0.5
Aug.	8.1	31.1	14.9	0.9
Oct.	8.2	32.4	12.9	0.7
Nov.	8.1	30.8	15.4	0.9
Dec.	8.1	31.9	22.2	1.3

[a]Mean of 4 determinations, relative standard deviations 5—15%; corrected for blanks of 4—6 cps. [b]Obtained from net count rate by taking the net cps/μg of phosphorus on the filter as 175; sample volume 100 ml.

water consists almost entirely of orthophosphate ions. In common with other nutrients, the highest concentrations of orthophosphate occur in deep ocean waters. The concentrations in surface waters are lower and more variable, with maximum values typically between 15 and 30 $\mu g\ l^{-1}$ phosphorus. Condensed phosphates are not a significant component of ocean water but occur in coastal and estuarine waters, as a result of pollution by detergents. Sea water also contains soluble organophosphates at levels which can match those of orthophosphate. This fraction probably consists of excretion and decomposition products of marine organisms, such as sugar phosphates, phospholipids and polynucleotides, but little is known about their chemical composition.

A range of phosphorus-containing compounds was tested, to see which, if any, would coprecipitate with the Co-PDC carrier system.

Studies on model compounds. Most of the species listed in Table 2 proved to be inactive. The carrier precipitate formed in a solution containing any one of these species at a concentration of 500 $\mu g\ l^{-1}$ phosphorus gave a zero net count rate for the P K_α line; and there was no significant increase in peak height upon standard addition of the species to harbour-water samples.

The species, all organophosphates, which were found to coprecipitate with the carrier complex are also listed in Table 2. The four synthetic organophosphates in this part of the table had low (<1%) coprecipitation efficiencies. The slight coprecipitation of these species and the failure of the other organophosphates in Table 2 to coprecipitate at all was not a consequence of hydrolysis to orthophosphate. This was established by measuring orthophosphate in the standard solutions by the ascorbic acid/molybdenum blue spectrophotometric method [8] both before and after the solutions were used in the coprecipitation tests. Less than 5% of the compounds hydrolysed during the course of the experiments.

TABLE 2

Behaviour of phosphorus species in coprecipitation tests with Co-PDC carrier[a]

Species not coprecipitated	
Orthophosphates	Dihydrogenphosphate, hydrogenphosphate
Condensed phosphates	Pyrophosphate, tripolyphosphate, hexametaphosphate
Synthetic organophosphates	Dibutylphosphate, trimethylphosphate, triethylphosphate
Biological organophosphates	Adenosine 5′-mono-, di- and tri-phosphate (AMP, ADP, ATP), adenylyl (3′,5′) adenosine (ApA), nicotinamide adenine dinucleotide (NAD), α-D-glucose-1-phosphate, D-fructose-1,6-diphosphate, ribonucleic acid (RNA) sodium salt.
Species coprecipitated	
	Tributyl phosphate, diphenylphosphate, dibenzylphosphate, bis-2-ethylhexylphosphate, deoxyribonucleic acid (DNA) sodium salt

[a]From solutions containing 500 $\mu g\ l^{-1}$ phosphorus.

The only model compound to exhibit a substantial coprecipitation efficiency (30% for 10 $\mu g\ l^{-1}$ phosphorus solutions in natural and artificial sea waters) was the DNA, a high-molecular-weight material ($M_r = 1.2 \times 10^6$) extracted from calf thymus as the sodium salt (Fluka). The observed carrier peaks (net count rates 10—40 cps) from the harbour waters were reproduced when solutions of this compound containing 2—8 $\mu g\ l^{-1}$ phosphorus were tested.

Effect of oxidative digestion. To test the conclusion that organophosphates are responsible for the peak in question, the harbour-water samples were analysed a second time by coprecipitation and x.r.f., after acidification and ultraviolet irradiation, a process which should convert organophosphorus to orthophosphate. With some samples, the x.r.f. peak was eliminated completely by this treatment. With other samples, however, the net count rate was only halved, indicating that organophosphates in natural waters may show unexpected resistance to oxidative digestion. Indeed, the peak heights were found to be largely unaffected by the widely-used peroxodisulphate digestion method.

Orthophosphate levels in the samples were also measured before and after the oxidative digestions, by the ascorbic acid/molybdenum blue method. This is the traditional approach to the determination of organophosphates which are then obtained by difference. The mean orthophosphate concentration in the harbour waters was 13 $\mu g\ l^{-1}$ phosphorus before irradiation and 23 $\mu g\ l^{-1}$ phosphorus afterwards. The difference, 10 $\mu g\ l^{-1}$, must to some extent underestimate the average concentration of dissolved organophosphates in the samples, because irradiation did not always completely remove the x.r.f. peak. It seems reasonable to conclude, however, that the coprecipitated phosphorus constituted approximately 10% of the dissolved organophosphorus in the waters.

Origin of coprecipitated phosphorus. The fact that the x.r.f. peak could be reproduced by using DNA solutions which contained environmentally realistic

levels of organophosphorus indicates, but does not prove, that the coprecipitated phosphorus is of biological origin. Certainly the coprecipitation process is highly selective because other naturally occurring organophosphates, including RNA, were found to be inactive.

Further evidence for the biological nature of the coprecipitated fraction comes from the seasonal dependence of the harbour-water results. Summer maxima and winter minima in the levels of organic phosphorus in marine waters, as observed here, are well-documented and have been attributed to the annual cycle of biological activity [9].

Finally, it should be noted that the usual method for the determination of dissolved organophosphates, involving orthophosphate measurement before and after oxidative digestion, is open to criticism on at least two grounds: there is no simple way of knowing if the organophosphates have decomposed completely in the digestion step and, being a "difference" method, the procedure cannot accurately measure low levels of organophosphates in the presence of high levels of orthophosphate. The method reported here could prove to be a useful alternative. The measured organophosphate fraction appears to be an indicator of biological activity and is obtained directly and without interference from orthophosphate ions.

We gratefully acknowledge support received from the Australian Research Grants Scheme, the help of Dr. Michael Hough of the University of Sydney's Department of Geology and Geophysics and the use of that Department's x.r.f. equipment.

REFERENCES

1 E. A. Boyle and J. M. Edmond, in T. R. P. Gibb (Ed.), Analytical Methods in Oceanography, Advances in Chemistry Series, No. 147, American Chemical Society, Washington, DC, 1975, p. 44.
2 E. A. Boyle and J. M. Edmond, Anal. Chim. Acta, 91 (1977) 189.
3 K. V. Krishnamurty and M. M. Reddy, Anal. Chem., 49 (1977) 222.
4 A. J. Pik, J. M. Eckert and K. L. Williams, Anal. Chim. Acta, 124 (1981) 351.
5 P. C. Cole, J. M. Eckert and K. L. Williams, Anal. Chim. Acta, 153 (1983) 61.
6 F. Ahern, J. M. Eckert, N. C. Payne and K. L. Williams, Anal. Chim. Acta, 175 (1985) 147.
7 T. Tisue, C. Seils and R. T. Keel, Anal. Chem., 57 (1985) 82.
8 Standard Methods for the Examination of Water and Wastewater, 15th edn., American Public Health Association, Washington, DC, 1980, Sect. 424, pp. 409—421.
9 C. P. Spencer, in J. P. Riley and G. Skirrow (Eds.), Chemical Oceanography, Vol. 2, 2nd edn., Academic, London, 1975, pp. 260—273.

Analytica Chimica Acta, 199 (1987) 265—270
Elsevier Science Publishers B.V., Amsterdam — Printed in The Netherlands

Short Communication

LONG-TERM STABILITY OF A GAS CHROMATOGRAPHY/MASS SPECTROMETRY SYSTEM IN QUANTITATIVE GAS ANALYSIS

HELGE EGSGAARD and ELFINN LARSEN*
Chemistry Department, Risø National Laboratory, DK-4000 Roskilde (Denmark)
(Received 2nd January 1987)

Summary. A gas chromatograph/quadrupole mass spectrometer (GC/MS) system was used to supervise a test programme for evaluating the potential of a natural gas storage plant. The dispersion characteristics of a large nitrogen reservoir located in a tight sandstone formation 1600 m below sea level between claystones, was investigated by injection and withdrawal of 350 000 m^3 nitrogen with argon as tracer gas. The GC/MS system was installed in a shed in an open field and operated under computer control continuously 24 h a day for three weeks; about 3000 analyses were done. The on-line results were in good agreement with those obtained from additional gas samples withdrawn every 4 h for independent quantitative gas analyses with a purpose-built mass spectrometer.

In 1984, Dansk Olie & Naturgas A/S conducted a test programme for evaluating the dispersion characteristics of a natural nitrogen reservoir with potential for natural gas storage [1]. The reservoir is located in South Jutland in Denmark in a tight sandstone formation between claystones approximately 1600 m below sea level. It contains large quantities of dry nitrogen with minor amounts of argon (0.03%), helium (0.2%) and methane (0.001%).

The test was based on the injection of nitrogen gas mixed with a tracer, argon, with the intended concentration of 0.7% by volume followed by a production period. During seven days, 350 000 m^3 (STP) nitrogen was injected into the reservoir at a constant rate, the first six days with the 0.7% argon tracer followed by a one-day injection of nitrogen only. Then a production period with constant rate equal to the injection rate continued until the concentration of argon approached the initial level of the reservoir. The entire experiment lasted three weeks.

During the whole experiment, the argon concentration had to be measured. In addition, the helium concentration was measured during the production period. Further, a gas sample was taken every four hours for independent laboratory testing; these samples were transported to the laboratory in cylinders under pressure and measured by mass spectrometry. The on-site measurements were done with a gas chromatograph/quadrupole mass spectrometer (GC/MS) installed in the open field in a shed located near the well. A gas line was established from the well to the computer-controlled inlet

0003-2670/87/$03.50

manifold of the GC/MS system. The gas analyses were done sequentially, three samples followed by a reference sample. In this communication the GC/MS measurements are reported. Close to 3000 samples were analysed. The results from the reference samples are presented and the on-site measurements are compared with the results from the 4-h samples.

Experimental

The GC/MS system was a Hewlett-Packard HP-5992B equipped with a turbo molecular pump (Balzers TPU-170). The chromatographic column was a 4-m stainless steel tube (2 mm i.d.) packed with molecular sieve 5A (50—60 mesh). The oven temperature was 100°C. Nitrogen was used as carrier gas at a flow rate of 12 ml min^{-1}. The connection between the column and the quadrupole was a glass restrictor allowing a flow rate of 0.7 ml min^{-1} into the ion source. The ionization was induced by electron impact (70 eV). The ions *m/z* 4 (helium), *m/z* 32 (oxygen) and *m/z* 40 (argon) were measured. The oxygen signal was used to check for possible leaks in the system.

A gas line was established from the well site to the computer-controlled inlet manifold of the GC/MS system, as shown in Fig. 1. The gas analyses were done sequentially, three samples followed by a reference sample with a total of 5—6 samples per hour. The results were recorded on-line and expressed relative to the reference samples measured immediately before and after the gas samples. Two reference samples were used: one with 0.7% argon in nitrogen and the other with about 0.7% argon and 0.1% helium in nitrogen. The linearity of the GC/MS system was checked by measuring standard gases with known concentrations of argon and helium in the range 0.05–1.0% Ar and 0.01—0.2% He.

Every four hours, gas samples were withdrawn near the well in a cylinder under pressure for independent testing in the laboratory. The magnetic mass spectrometer (type MAT CH-4) used was equipped with a thermostatted gas-inlet system with molecular flow into the ion source. Electron-impact ionization was done at 70 eV with a 20-μA trap current. Both Faraday collector and electron multiplier were used as detectors.

Results and discussion

Earlier experiments with the quadrupole instrument had shown that the background signal is sensitive to the total pressure in the ion source [2]. Consequently, a gas chromatographic separation of nitrogen was used before the mass spectrometric measurements of helium, oxygen and argon. A chromatogram of a gas sample from the production period is shown in Fig. 2. The GC/MS system integrated the argon peak satisfactorily and could evaluate the concentration of argon directly, after the reference sample had been measured. In the case of helium, the computer failed to integrate the small peaks; thus, the heights of the helium peaks were measured manually and the concentrations calculated.

With regard to the stability of the GC/MS system, the same reference

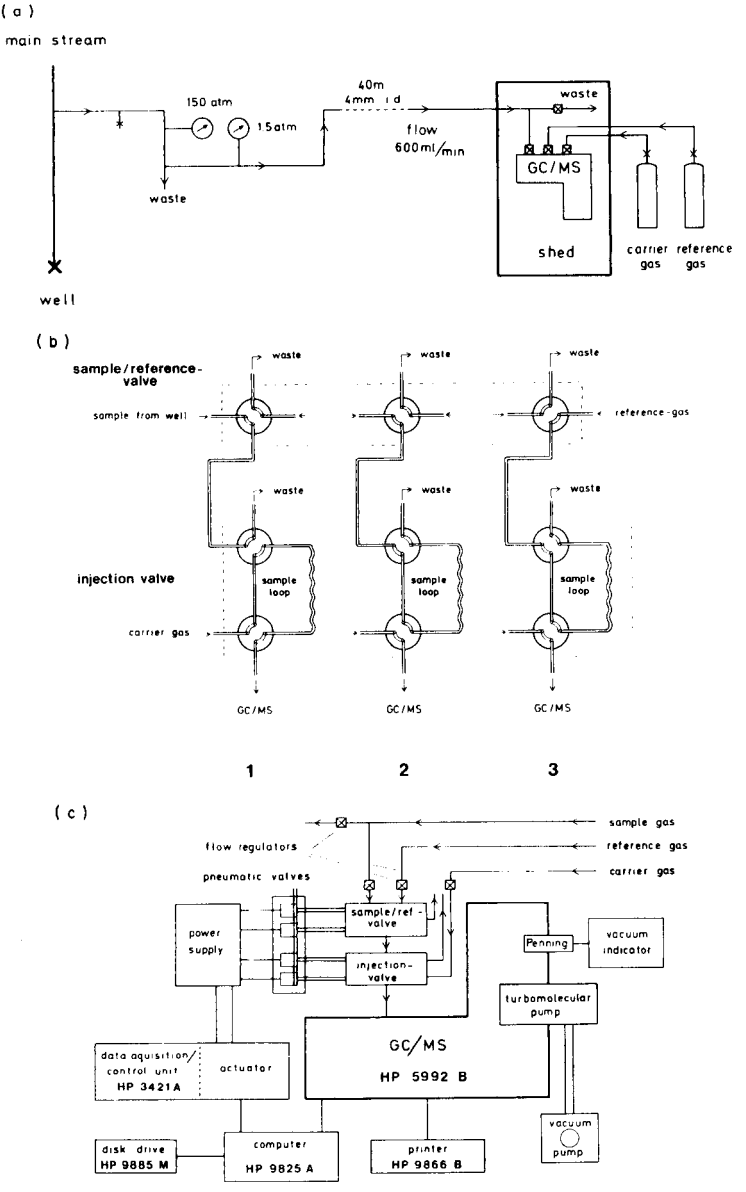

Fig. 1. The GC/MS system. (a) The gas flow from the well site to the GC/MS. (b) The gas inlet manifold shown in three positions: (1) the gas in the sample loop is injected; (2) the sample loop is flushed with gas from the well; (3) the sample loop is flushed with reference gas. (c) The connections to the computer.

sample containing 0.74% argon and 0.081% helium was measured about 650 times during two weeks in the production period from 27 September to 10 October. The results are shown in Fig. 3. The frequent standardization

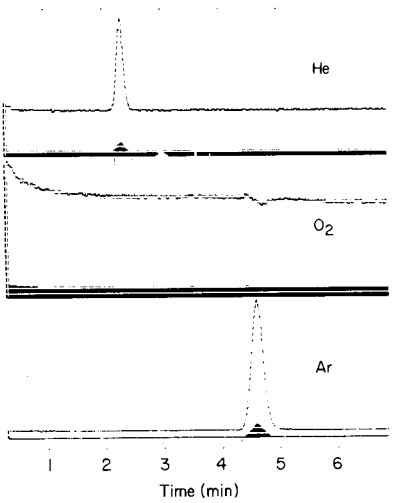

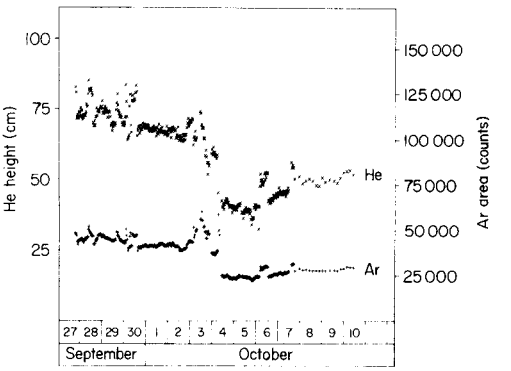

Fig. 2. A chromatogram of a gas sample from the production period. For helium, *m/z* 4.0 was measured (f.s.d. 26), for oxygen *m/z* 32.0 (f.s.d. 13) and for argon *m/z* 40.0 (f.s.d. 33).

Fig. 3. The absolute responses for argon (area) and helium (height) of the same reference gas sample during two weeks (approximately 650 injections).

against the reference gas was obviously necessary as the absolute sensitivity changed dramatically with time. The worst case occurred on 3 October; the supply of electricity failed and the vacuum was no longer maintained. The GC/MS system was out of operation for about four hours. However, from the results on the gas produced during the same period (Fig. 4) the four-hour interruption of the GC/MS data output can be recognized only by the gaps. The concentrations of argon and helium continuously decreased and increased, respectively, as would be expected. In the preceding two days, 1 and 2 October, the instrument was uninfluenced by external faults and worked very stably (Fig. 3); 66 measurements of the reference gas were obtained in this period. Results indicating the overall stability of the GC/MS system in those two days are shown in Table 1.

The relative error of the results of the gas samples was calculated from a linearity test with the GC/MS system. Measurements of argon were made at six different concentrations using the same reference sample (Table 2). Each day when gas analyses were run in the laboratory, two selected samples were measured, one with 0.39% argon and the other with 0.032% argon and 0.22% helium. Those results are also included in Table 2. For comparison, the relative standard deviations are given for helium, krypton and xenon at different concentrations. These results originate from measurements of fission gases with the same mass spectrometer during the last three years. Generally, in gas analysis, a relative standard error of between 0.1 and 0.2% is to be expected for a component at the concentration level of 10—20%.

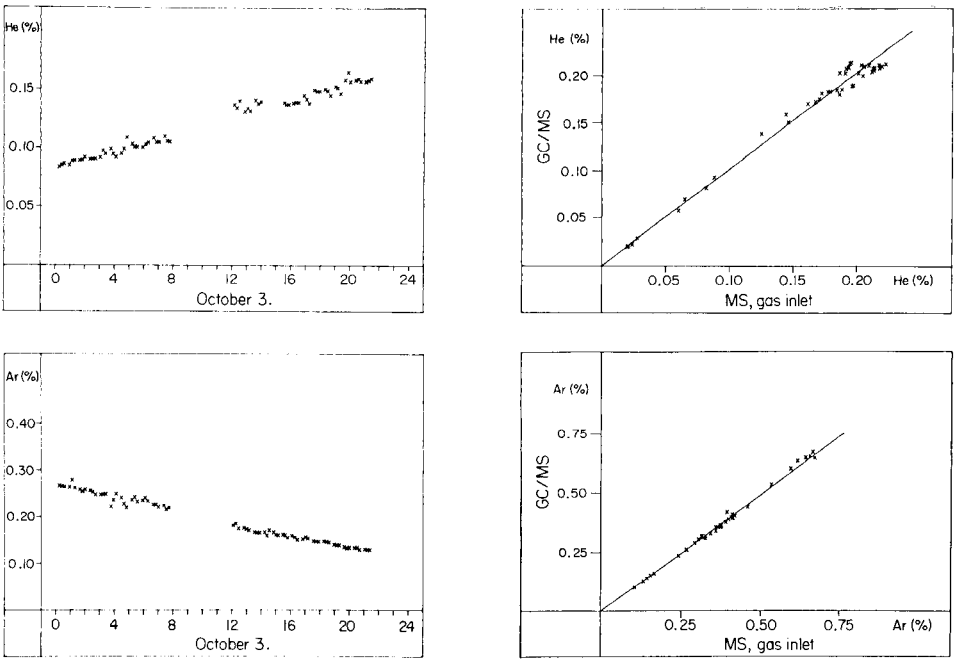

Fig. 4. The concentrations of the argon and helium in the produced gas measured on 3 October.

Fig. 5. The GC/MS result plotted against the MS result obtained in the laboratory at the equivalent 4-h interval.

TABLE 1

The relative standard deviations (n = 66) of the reference gas measured on-line on 1 and 2 October with the GC/MS system

Gas	Conc. (%)	Relative standard deviation (%)	
		Height	Area
Ar	0.735	2.8	2.8
He	0.081	2.5	

In Fig. 5, the results from the measurements with the GC/MS system are plotted against those from MS measurements in the laboratory at the equivalent times. No significant systematic deviations were observed. For helium, the slope of the plot is 1.024 (n = 40) and for argon, it is 0.986 (n = 30).

In conclusion, the computerized GC/MS system turned out to be very reliable for the on-site work. Its large analytical capacity was combined with high selectivity and accuracy. With the exception of the power-up period and

TABLE 2

The relative standard deviations of gas samples measured on the two mass spectrometric systems

System	Gas	n	n^a	Conc. (%)	Relative standard deviation[b] (%)
GC/MS	Ar		6	0.05—1.00	2.0
MS, gas inlet	Ar	8		0.032	3.7
	Ar	8		0.39	1.3
	He	8		0.22	4.7
	He		11	15—40	2.0
	Kr		11	1—5	1.4
	Kr		16	5—10	1.1
	Xe		11	10—30	2.2

[a]The number of series with at least two results. [b]All data refer to peak heights except for argon determined by GC/MS (area).

some closing calibration experiments, the gas analyses were done entirely under computer control with only brief inspections to check the supply of carrier gas, paper, etc. The instrument operated continuously 24 h per day during three weeks except for a few short-term interruptions caused by power failures. Close to 3000 analyses were done without the need for maintenance of the GC/MS system.

The authors thank Dansk Olie & Naturgas A/S, AGA A/S and N. Haunsø, Jydsk Technological Institute, for excellent cooperation during the test programme. We are indebted to Jytte Funck-Hansen and Dan Olvhøj for technical assistance.

REFERENCES

1 H. Øbro, paper presented at the 1986 Int. Gas Research Conf., Toronto, Canada, Sept. 1986.
2 E. Larsen, H. Egsgaard and N. Bjerre, J. Trace Microprobe Tech., 1 (1983) 387.

Analytica Chimica Acta, 199 (1987) 271—289
Elsevier Science Publishers, B.V., Amsterdam — Printed in The Netherlands

Book Reviews

D. Ammann, *Ion-Selective Microelectrodes, Principles, Design and Application.* Springer, Berlin, 1986 (ISBN 3-540-16222-4). xv + 346 pp. Price DM 158.

At present, ion-selective electrodes can be used for the direct potentiometric determination of at least thirty cations and anions and for the indirect determination of several gases and organic molecules. This text is directed particularly towards the use of neutral carrier-based liquid membrane microelectrodes for the determination of intracellular cation activities (hydrogen, lithium, sodium, potassium, magnesium and calcium). It is a comprehensive account of the subject, containing 153 Figures and 42 Tables, which clearly demonstrates the author's own interest in, and practical experience of, ion-selective electrodes.

The material is logically presented, with introductory chapters on the classification of ion-selective electrodes and the types of neutral carrier (natural and synthetic) that are available for membrane electrodes. This is followed by two chapters on the design and use of neutral carrier-based liquid membrane electrodes, which considers analytical criteria such as selectivity, detection limit, response time, stability and lifetime. The construction of liquid membrane microelectrodes is then discussed, with an electrode tip diameter of 0.045 μm being the smallest reported to date. The second half of the book covers general and specific aspects of the intracellular measurement of ions and compares the various analytical techniques available for the six cations listed above. The book also contains over 800 references (some as recent as 1985) and an assessment of the impact of neutral carrier microelectrodes.

This is an invaluable book for physiologists concerned with cellular activities and membrane transport processes and for analytical chemists interested in ion-selective electrodes. For the general reader it is an informative account of liquid membrane electrodes and their application to a particularly challenging area.

P. J. Worsfold

J. Cross (Ed.), *Nonionic Surfactants: Chemical Analysis (Surfactant Science Series, Vol. 19).* M. Dekker, New York, 1987 (ISBN 0-8247-7626-7). x + 417 pp. Price $99.25 ($82.75 in the U.S.A. and Canada).

Nonionic surfactants make up about 30% of all surfactants used and have a wide range of applications as emulsifiers, wetting agents, detergents and solubilizers. They are used in industries concerned with for example, leather, textile and metal processing, and the production of cosmetics, pharma-

ceuticals, toiletries and foodstuffs, as well as pesticide and herbicide formulations. Analytical chemists can meet these surfactants at various stages including manufacture, utilization and final disposal. This book is Volume 19 in the well-known Surfactant Science Series; the first volume appeared 20 years ago and was on nonionic surfactants. The use of this kind of surfactant has grown since then and during this time there have of course been considerable advances in analytical science. The appearance of this book, containing 11 chapters contributed by 10 authors, is therefore timely.

Following an introductory chapter the book is divided into two sections, the first dealing with specific methods of analysis of oxyalkylated surfactants. A chapter is devoted to methods involving the formation of complexes between the polyether chain and inorganic cations. Then trace analysis, including methods of preconcentrating solutions, is covered. A discussion of (as yet) little used potentiometric analysis, involving PVC barium ion-selective electrodes, follows. This section is concluded with a chapter on the determination of total oxyethylene content by fission into fragments.

The other main section covers the use of GLC, HPLC, thin-layer and paper chromatography (briefly), and IR and mass spectrometry. There is also a very good chapter on the broader use of NMR, not only covering analysis but also touching upon the investigation of molecular motion, micelle formation and structure, interactions between surfactant molecules in mixed micelles, and surfactant hydration. There is a concluding chapter on quality and process control.

The book is well-produced and although it claims not to be a laboratory manual it is full of useful practical information with ample references. It can be recommended to all those who have a practical interest in nonionic surfactants, industrial or academic.

R. Aveyard

G. Ertl and J. Küppers, *Low Energy Electrons and Surface Chemistry, 2nd edn.* VCH, Weinheim, 1985 (ISBN 3-527-26056-0). xii + 374 pp. Price DM 168.

Surface chemistry deals with the chemical and physical properties of the outermost atomic layers of (usually a solid) material and their reactive behaviour towards other systems. In order to characterize the surface with reference to its properties, information has to be gained about elemental composition, distribution of elements and compounds, geometric and electronic structure — often additionally in a time-resolved mode. A large number of experimental techniques based on the interaction of photons, electrons, ions and neutral particles is available to be used in this elaborate task of surface characterization. Low energy electrons, as treated in this monograph, provide the basis for a number of important analytical techniques which yield a large amount of information about surface chemistry.

Ertl and Küppers first discuss some basic concepts concerning vacuum requirements, interaction of electrons with matter and electron energy analyzers. The major part of the monograph is devoted to a presentation of the techniques: Auger electron spectrometry, X-ray photoelectron spectroscopy (XPS), UV photoelectron spectroscopy, electron spectroscopy with noble gas ions and metastable atoms, appearance potential spectroscopy, inverse photoemission, electron energy loss spectroscopy, low energy electron diffraction, X-ray absorption fine structure analysis, electron excited vibrational spectroscopy and electron and photon stimulated desorption. For each the basic process of signal generation is described in detail, methods of qualitative and quantitative analysis are discussed and illustrative results are presented.

Each chapter is written in a very clear style and concentrates on those aspects which are important for gaining meaningful chemical or physical information about a surface. The great experience of the authors in surface chemical studies, particularly with the aid of electron spectroscopies thus forms the basis of a really good and useful book. The usefulness for the practitioner is increased by an appendix of 22 pages which contains Tables of physical constants, crystal structures, XPS-lines, XPS relative sensitivity factors, kinetic energies of Auger electrons, relative Auger intensities and characteristic group frequencies. The monograph is highly recommended for those who have to deal with surface chemistry and physics. It serves not only as a clearly written introductory text for techniques involving low energy electrons (either as a reagent or signal) but also contains a wealth of information for more advanced scientists.

Manfred Grasserbauer

J. Schölmerich, R. Andreesen, A. Kapp, M. Ernst and W. G. Woods (Eds.), *Bioluminescence and Chemiluminescence: New Perspectives.* Wiley, Chichester, 1987 (ISBN 0-471-91470-3). xv + 600 pp. Price £55.00.

This is a collection, in camera-ready form, of 130 papers presented at the Fourth International Symposium on Bioluminescence and Chemiluminescence held in Freiburg in September 1986. The subjects covered are grouped into four sections: cell-dependent chemiluminescence, immunoassays, biotechnological aspects, and other applications. Most analytical interest will lie in the immunoassay section, where progress is extremely rapid, and in the wide range of applications, which again show how rapidly the analytical potential of chemi- and bioluminescence is being developed. Most procedures are based on luminol or peroxyoxalate chemiluminescence and luciferin bioluminescence, but several novel systems are also described. The great analytical interest in this type of luminescence lies in its great sensitivity, selectivity and the relatively simple instrumentation required, and these aspects are demonstrated very clearly in a large number of the papers. The book concludes with an author and brief subject index.

The appearance of the collection of papers so soon after the conference is to be applauded. Generally, the standard of production is good, although there is evidence of hurried proof reading in the supporting material such as the Table of Contents and the Preface.

R. P. Philp, *Methods in Geochemistry and Geophysics, 23: Fossil Fuel Biomarkers, Applications and Spectra.* Elsevier, Amsterdam, 1985 (ISBN 0-444-42471-7). xi + 294 pp. Price $63.00.

Organic geochemists employ biological markers ("biomarkers"), isolated from the soluble extracts of sedimentary organic matter, principally as a means of defining depositional environment or level of thermal maturity. Although many compound classes, including fatty acids, alcohols and porphyrins have been used for these purposes, hydrocarbons have had the widest application. Some of these, notably the n-alkanes and the acyclic isoprenoid alkanes, have been employed by petroleum geochemists in "source-input studies" for many years, but more recently a large number of biomarkers in other hydrocarbon classes, with much greater potential in depositional and maturity studies, has been discovered.

The successful development of high-resolution capillary gas chromatographs, combined with fast-scanning mass spectrometers, linked to computerised data systems, has been the principal agency in discovering biomarkers. The large volume of spectral data on these compounds disseminated in the literature persuaded R. P. Philp to collect between the covers of one book as many of the published spectra as could be found. Some of the compounds whose spectra are reported have been precisely identified through comparison with standards, but spectra for unidentified compounds are also included. Almost certainly many of these compounds will eventually be synthesized and unequivocally identified, but for immediate application in correlative petroleum exploration studies, precise identifications may hardly be urgent, since it is the "spectral fingerprints" that are important.

The book is therefore largely a collection of mass spectra, but there are two preliminary chapters. The first is a survey of methods of analysing for biomarkers, the second a brief essay principally discussing the different classes of biomarkers and their use in hydrocarbon exploration. Most of this second chapter is devoted to the hopanoids and steroids.

The great merit of this book is that it contains spectra for many compounds that are generally unavailable in commercial mass spectral libraries. It is also the first collection of hydrocarbon biomarker spectra for organic geochemists. As such it is most helpful and is certainly heavily used by research students and staff alike. Dr. Philp should, however, proceed as expeditiously as possible to produce a second edition in which the errors present in this first edition are removed. Improvements in three specific areas would also be desirable. First, some expansion of the chapter on bio-

marker classes would be a benefit to readers. Second, although the spectral index is perfectly adequate, the general index is not, being almost an apology for what an index should be. Third, perhaps the most irritating feature of the book is the omission of mass numbers on the major and/or diagnostic ions on the spectra presented. If these criticisms seem carping, they should be seen in the context of a wish to improve a publication that is a most useful addition to organic geochemical literature and one which has already proved valuable to research workers in the field.

Duncan G. Murchison

L. Packer (Ed.), *Methods in Enzymology, Vol. 127.* Academic, Orlando, FL, 1986 (ISBN 0-12-182027-0). 830 pp. Price $89.50.

Volume 127 completes the triplet of volumes devoted to state-of-the-art techniques used in the study of biomembranes. Whereas the previous two volumes had been devoted to membranes of bacteria, this present volume expands the base and devotes itself to a study of transport, especially of protons and water, through membranes in general. Within this volume can be found an amazing array of disparate techniques, ranging from measurement of cell water viscosity to techniques for measuring the bacterial nucleation of ice in plant leaves. The range of analytical techniques and methods covered appears to run the whole gamut: from X-ray and neutron diffraction methods, to NMR, ESR, Raman methods and even calorimetry.

As with previous volumes, the strength of this one relies on the multitude of contributors, with some 58 individual chapters falling approximately equally between a section devoted to interactions between water, ions and biomolecules, and another to protons and membrane functions. Few chapters in themselves are a single contribution and many arise from laboratories with international expertise in particular techniques. The wealth of information is truly staggering and the volume will take its usual place in those laboratories devoted to research into the subject area.

The compliments which reviewers continue to give to individual books within the series "Methods in Enzymology" never seem to cease; it is with good and sufficient reason that this is so, as the editors go to considerable trouble to ensure that they assemble the strongest possible contributions from throughout the world. Such is the prestige of being asked to participate in such a volume that even the most overworked expert will always have time to write up his 'method' for inclusion in one of these volumes. Analytical biochemistry would not be the same without this excellent and erudite series.

Colin Ratledge

G. W. Neilson and J. S. Enderby, *Water and Aqueous Solutions — Proceedings of the 37th Symposium of the Colston Research Society.* Adam Hilger, Bristol, 1986 (ISBN 0-85274-576-1). xiii + 349 pp. Price £35.00.

The proceedings are reported in four broad sections: water, ionic solutions, water in biological systems, and water in the environment. Within each section the spread of contributions is impressive: as an example, that on water includes the properties of the water molecule, computer simulation of metastable water (with an intriguing conclusion on the hydrophobic effect), n.m.r. and i.r. studies of the liquid and studies of the solid phase. The section devoted to ionic solutions, similarly wide ranging, commences with an outstanding contribution by Friedman on electrolyte solution structure, followed by C_p measurements, i.r, neutron and X-ray diffraction studies of water in colloidal and pre-colloidal systems — which should be required reading for all colloid scientists. The contributions to the role of water in biological systems are stimulating investigations of the importance of water and collectively sound a very timely warning that the influence of water is not solely, or even very often, primarily through the hydrophobic effect. The concluding section on water in the environment includes a salutory review of the problems now facing the water industry in providing potable water and an examination of the agricultural potential of marginal and estuarine waters.

D. Eagland

H. U. Bergmeyer (Editor-in-Chief), *Methods of Enzymatic Analysis, Vol. XI: Antigens and Antibodies 2.* VCH, Weinheim, 1986 (ISBN 3-527-26052-8). xxv + 508 pp. Price DM 315.

This book is one of twelve volumes in the comprehensive third edition of Bergmeyer's excellent "Methods of Enzymatic Analysis" series. Volume X, Antigens and Antibodies 1, was reviewed in Analytica Chimica Acta 193 (1987) 405 and the comments made are equally valid for this volume. The applications considered fall into three areas: antigens and antibodies in chlamydial and bacterial diseases (17 applications), antigens and antibodies in fungal and parasitic diseases (13 applications) and plant viruses (5 applications). It is a tribute to the authors and the editors that a consistently high standard of presentation has been maintained throughout the series, which remains the primary reference source for enzymatic analysis.

S. T. Balke, *Quantitative Column Liquid Chromatography — A Survey of Chemometric Methods (Journal of Chromatography Library, Vol. 29.)* Elsevier, Amsterdam, 1984 (ISBN 0-444-42393-1). xiv + 300 pp. Price Dfl 165.00 ($63.50 in the U.S.A. and Canada).

In introducing his book, the author suggests that it is aimed at the experienced chromatographer, but the style and presentation are such that everyone, from novice to expert, should find value in this survey. The stated objective is to examine in a practical way the methods available for obtaining quantitative information from liquid chromatographic separations, in particular high-performance and size exclusion.

The introductory chapter is used to define the terms which will be encountered later in the book and to set the scene. The second chapter provides a concise review of chemometric techniques in LC, focusing mainly on regression analysis (linear and non-linear) with brief discussions of experimental design, factor analysis and pattern recognition. This review gives pointers to the literature rather than providing an insight into the techniques themselves but should whet the appetite sufficiently to encourage a deeper exploration of the subjects. Chapter 3 is the heart of the book and deals with aspects of achieving an acceptable separation but it is somewhat misleadingly entitled "Fractionation". This is followed by a discussion of the possibility of predicting a separation through use of selectivity and solubility parameters and hydrophobic fragmentation parameters. Multi-dimensional chromatography, a review of methods for optimising isocratic separations, and a description of the mathematics of gradient elution processes are also included.

Chapter 4 is concerned with detection, particularly how to obtain a precise and accurate assessment of solute concentration from the detector response, with most attention focused on single channel UV detectors. Size-exclusion separations (SEC) occupy a major part of this chapter with a useful description of the appropriate computational methods. Quantitative calibration is the subject of Chapter 5 and the differing needs of HPLC and SEC are both examined in useful detail, although some of the definitions offered at the start of the chapter will confuse many readers. Finally, in Chapter 6, resolution correction is described as a means for determining component concentrations but is restricted to resolution correction with time and does not consider the techniques now available for use with, for example, rapid scanning UV detectors. Geometric construction, curve fitting and deconvolution are discussed, with particular reference to SEC but, surprisingly, the simple procedure of differentiation escapes mention. There are two appendices, one an extensive description and Fortran listing of a program to fit a Gaussian shape to an experimental chromatogram, the second a short description of the calculation of isoeluotropic mobile phases in reversed-phase chromatography.

Is this book a useful addition to your bookshelves? I would suggest a qualified "yes" for the chromatographer specialising in SEC but it is not for those involved primarily with HPLC.

John C. Berridge

E. Hodgson (Ed.), *Reviews in Environmental Toxicology, Vol. 2.* Elsevier, Amsterdam, 1986 (ISBN 0-444-80767-5). xi + 353 pp. Price Dfl. 250.00.

This volume contains six articles. By far the longest (135 pp.) describes the effect of copper on freshwater ecosystems (F. L. Harrison). It provides a wealth of information on copper species and concentrations in fresh water and organisms, as well as on copper toxicity to such organisms. The discussion is supplemented by an enormous amount of tabulated data and 473 references. Analytical chemists will be interested in the review of volatile organic compounds in air (N. Schamp and H. Van Langenhove), which considers the sampling and analysis aspects in a concise and up-to-date manner, as well as the occurrence and reactivity of numerous compounds. The other articles deal with dermal and gastrointestinal absorption of environmental contaminants, laboratory model ecosystems for evaluation of environmental contaminants, effects of selenium on freshwater teleosts, and trichothecenes as environmental toxicants. The book concludes with an extensive subject index. As most of these studies rely heavily on analytical data, the essential involvement of good analytical practice in these, often difficult areas, should not be forgotten. The reviews, therefore, show not only the great diversity of one area of toxicity, but also the great breadth of analytical expertise required to sustain it.

Alan Townshend

M. F. C. Ladd and R. A. Palmer, *Structure Determination by X-ray Crystallography, 2nd edn.* Plenum, New York, 1985 (ISBN 0-306-41878-9). xxiii + 502 pp. Price $39.50.

The first edition of this book was well received, and this second edition has been expanded but otherwise follows the same plan as the original. It is aimed at final year undergraduates and at postgraduate students beginning research in the field.

The first two chapters introduce the basic ideas of crystal geometry and crystal symmetry. The discussion is detailed and thorough, and will not be easy reading for the average student, but, as in the other chapters, the reader is offered enormous help in the form of problems with worked solutions, of which the book contains nearly sixty. Indeed, the approach throughout is kept on a firmly practical plane by the use of illustrative examples. Chapters 3 and 4 present the ideas underlying the interpretation of diffraction directions and diffraction intensities, and the application of these ideas is then developed in two chapters on methods in structure analysis, which deal with Fourier and Patterson synthesis and include a substantial section on the methods used for large biological molecules. Direct methods are treated in an elementary and practical spirit, and the final chapter takes the reader through two complete structure determinations, one using heavy-atom Patterson, and the other direct methods. The authors even offer to provide

the original data so that students can carry through the procedures themselves. This book will certainly be very useful to anyone who wishes to learn how to do X-ray crystal-structure analysis.

A. B. Blake

C. Lu and A. W. Czanderna (Eds.), *Applications of Piezoelectric Quartz Crystal Microbalances.* Elsevier, Amsterdam, 1984 (ISBN 0-444-42277-3). xiii + 393 pp. Price Dfl. 260.00 ($100 in the U.S.A. and Canada).

This collection of articles describes the basics and a range of areas of application of piezoelectric crystal mass detectors ("balance" is a misnomer in this context). The initial chapter on theory and practice by Lu is followed by detailed descriptions of the use of the detectors for control of thin film deposition (Pulker and Decosterd), stress effects in quartz crystals (EerNisse), applications in surface science (Levenson) and plasma-assisted etching (Coburn). Of most interest to analytical chemists will be the chapters on analytical chemistry (Guilbault), covering the well-known applications to gas detection, on space system contamination (Glassford) describing interesting applications to outgassing of equipment destined for space, and on aerosol mass measurement (Ho). The book is produced in camera-ready copy on a single typewriter and has been assembled carefully by the editors. Although piezoelectric detectors are developing only slowly as analytical sensors, this book provides a firm base and describes areas of application which will be valuable to those who are contemplating studies in this area.

Alan Townshend

A. P. Rowland (Ed.), *Chemical Analysis in Environmental Research.* Institute of Terrestrial Ecology, Grange over Sands, Cumbria, Great Britain, 1987 (ISBN 0-904282-98-8). 104 pp. Price £7.00.

This is a collection of 18 papers presented at an I.T.E. symposium in November 1985. The subject matter ranges from aspects of acid rain research and pH measurement to aluminium speciation, from ICP atomic emission spectroscopy to chemical sensors, and from detailed procedures for determination of phosphorus in soils to reference materials. The presentation is clear, and the range of subjects chosen will provide something of interest to all involved in environmental analysis, at a modest price.

P. J. Lloyd (Ed.), *Particle Size Analysis 1985.* Wiley, Chichester, 1987 (ISBN 0-471-90832-0). ix + 669 pp. Price £55.00.

This publication contains the formal Proceedings of the Fifth Particle Size Analysis Conference held at the University of Bradford, U.K., during Septem-

ber 1985. These Proceedings include four plenary lectures and forty original papers grouped under the subject headings: presentation and manipulation of data, standardization and reference materials, sampling, microscopy and image analysis, particle shape and morphology, light scattering methods, sieving analysis, electrical sensing zone methods, surface area and porosimetry, photon-correlation spectroscopy and hydrodynamic chromatography, and in-situ particle size analysis. Brief discussion sections are included following each paper. Overviews are presented on trends in particle characterization, sedimentation methods, multi-sensor particle counting and field-flow fractionation. The remainder of the papers are aimed more at the specialist and cover, inter alia, some novel instrumental methods including techniques for the simultaneous determination of particle size and velocity, and the pore size distribution of membranes. Results obtained using different techniques are compared and the discussions of the practical and theoretical limitations of the various methods are interesting and informative. Despite a lack of clarity in some of the contributions, this book should prove useful to workers in the areas of powder, emulsion and aerosol technologies.

P. D. I. Fletcher

K. L. Ratzlaff, *Introduction to Computer-Assisted Experimentation.* Wiley, New York, 1987 (ISBN 0-471-86525-7). xv + 438 pp. Price £43.25.

The interfacing of analytical instrumentation to computers is now commonplace, using "off-the-shelf" commercial packages or "home-made" devices. It is therefore important that the user of computer interfaced instrumentation has some idea of the capabilities and limitations of the interface in order to maximize the analytical performance of the system. This book is a particularly good one for the analytical chemist who wishes to understand the basic principles of computers and interfacing and/or to design appropriate interfaces for a particular task. The material is clearly and logically presented in twelve chapters that take the reader from basic material on computer fundamentals, software and high level interfaces, through more detailed chapters on analog and digital electronics, to a discussion of transducers (e.g., temperature, light and electrochemical inputs), data communications and computational techniques (e.g. simplex optimization and linear least-squares curve fitting). The description of a current-to-voltage converter for the analog output of photomultiplier tubes is just one of several examples throughout the text of directly useful information for analytical chemists.

The book requires only a rudimentary knowledge of computers and electronics and is a very readable account of computer-assisted experimentation. It is therefore recommended reading at a reasonable price.

Paul J. Worsfold

H. U. Bergmeyer (Editor-in-Chief), *Methods of Enzymatic Analysis Vol. XII: Drugs and Pesticides, 3rd edn.* VCH, Weinheim. F.R.G., 1986 (ISBN 3-527-26052-8). xxiii + 498 pp. Price DM 315.00/$170.50.

This book is the final volume in the third edition of the "Methods of Enzymatic Analysis" series. It follows the logical and concise format of previous volumes in that for each drug or pesticide there is a general introduction, detailed instructions on the preparation of reagents and experimental procedures, and a method validation. There are three chapters, one on drugs monitored during therapy (17 applications), one on drugs of abuse and of toxicological relevance (15 applications) and one on pesticides (5 applications). Experimental procedures are based predominantly on enzyme-linked immunosorbent assays and enzyme-multiplied immunoassays, although interesting procedures are given for the determination of paracetamol and salicylic acid using enzymes obtained from drug degrading micro-organisms. The inhibition of cholinesterase is the preferred method for the determination of organophosphorus and carbamate pesticide residues.

The twelve volume series is recommended as a comprehensive reference source for enzymatic analysis.

M. Morari and T. J. McAvoy (Eds.), *Chemical Process Control-CPC III.* Elsevier, Amsterdam, 1986 (ISBN 0-444-99532-3). xi + 932 pp. Price $153.25/Dfl. 345.00.

This book, published in September 1986, contains the proceedings of the third international conference on Chemical Process Control held at Asilomar, California on January 12—17th, 1986. The delegates represented a cross-section of industrialists, public sector personnel and academics, but with a common interest in process engineering rather than process analysis. The camera-ready presentations, 24 in all, are therefore only of indirect interest to analytical chemists, but nonetheless underline the current advanced state of process engineering, considering topics such as artificial intelligence, computer modeling and expert systems.

There are eight sections representing the main themes of the conference, each containing a useful session summary. The sections are: control in the presence of model uncertainty, an industrial view of advanced process control, model predictive control, process operability, adaptive control, on-line identification and optimization, control of chemical reactors, and expert systems in process control. This is not, therefore, a book that will give the analytical chemist an overview of process analysis. It does, however, clearly demonstrate the potential for robust chemical on-line analysers to supplement the current developments in mathematical modeling by process engineers.

C. A. Poole, Jr. and H. A. Farach, *Theory of Magnetic Resonance, 2nd edn.* Wiley, New York, 1987 (ISBN 0-471-81530-6). xvi + 359 pp. Price £57.50.

The first edition of this book was widely regarded as an excellent introduction to the physical theory of magnetic resonance and this second edition can only enhance that reputation. The authors set out to develop this topic in a general but versatile fashion using a rigorous mathematical treatment based upon the formalism of the secular equation. This book is concerned with theory and contains little discussion of applications to chemistry, physics or biology.

A particular attraction of the method used is that it permits the initial development of a unified treatment of NMR and ESR using a generalized two-spin Hamiltonian. Specialization to the particular cases of NMR and ESR follows naturally and is easily extended to three-spin systems in both areas. Using direct product matrix expansion further extension is made to cases of higher spin interactions, quadrupolar nuclei, atomic spectra, and crystal field effects. In the second half of the book (mostly new to this edition) the discussion is extended to include time as a variable and covers line shapes, double resonance (in ESR and NMR), dynamic polarization, acoustic and optical magnetic resonance and spin labels. The application of Fourier transforms to NMR is discussed including the extension to two dimensions but the plethora of new methods for the extraction of information from the various dimensions of a spin system is not examined in detail.

This book is essential reading for teachers and research workers who are interested in the theory of magnetic resonance across the whole field. The authors elaborate this theory in a way which emphasises the underlying unity of a subject which often suffers from a severly fragmented treatment. However the reader must be familiar with simple quantum mechanics and matrix algebra. A very high standard of production is evident in the Figures and the mathematical formulae are singularly free from error (only one was noted by this reviewer). A useful index is included.

D. F. Ewing

A. T. Andrews, *Electrophoresis: Theory, Techniques and Biochemical and Clinical Applications, 2nd edn.* Oxford Science Publications, Monographs on Physical Chemistry, Clarendon Press, Oxford, 1986 (ISBN 0-19-854633-5 hard back or -854632-7 soft back). xv + 452 pp. Price £30.00 (hard back), £15.00 (soft back).

This is a substantial book which covers in some 450 pages the large majority of the electrophoretic techniques, and is a major update from the first edition while retaining most of the information from that volume. The book is arranged in thirteen chapters which critically evaluate the various methods of performing electrophoresis; the final chapter is concerned with clinical

applications. The format of the successful first edition is followed again, where the background theory is first dealt with, albeit briefly, followed by an experimental discussion and finally applications. Precise practical detail is frequently included in a different typeface for ease of discrimination.

Inevitably in a book dealing with the whole range of electrophoretic techniques some of the subjects are sparsely dealt with, for example, isotachophoresis, high voltage capillary zone electrophoresis and some aspects of preparative electrophoresis could be given more weight. The book is very well referenced with the relevant papers up to 1984. This book should be on all analytical chemists' bookshelves and at its relatively low price, is excellent value for money.

C. F. Simpson

D. Glick (Ed.), *Methods of Biochemical Analysis, Vol. 32.* Wiley, New York, 1987 (ISBN 0-471-82195-0). vii + 450 pp. Price £47.95.

This volume is part of an annual collection of review articles in the field of biochemical analysis, with an emphasis on methodology and instrumentation for chemical, physical, microbiological and animal assays. In this particular volume there are seven reviews covering the following subjects: activator proteins for lysosomal glycolipid hydrolysis, isolation and analysis of cell walls from plant material, electro-optical reflection methods for studying bioactive substances at electrode-solution interfaces, isoelectric focusing in immobilized pH gradients, assays for superoxide dismutase, the radiation inactivation method as a tool to study structure-function relationships in proteins, and immunoassays with electrochemical detection. The two reviews of most general interest to analytical chemists are those on electro-optical reflectance methods and immunoassays with electrochemical detection.

The book is well produced and includes a cumulative subject and author index for the series. The style of presentation and the length of the articles vary considerably, but each includes a comprehensive and up-to-date reference list.

R. M. A. Azzam and N. M. Bashara, *Ellipsometry and Polarized Light.* North Holland, Amsterdam, 1987 (ISBN 0-444-87016-4). xvii + 539 pp. Price Dfl. 75.00.

Ellipsometry is an optical technique for the characterization of, and observation of events at, an interface or film between two media based on the polarization transformation that occurs as a beam of polarized light is reflected from or transmitted at the interface or film. The technique is essentially non-perturbing and can be used for in-situ measurements which may be very sensitive. The bulk of the text concerns a detailed theoretical approach for which the reader requires a knowledge of matrix algebra and

complex variables. This is followed by a full discussion of the instrumentation and techniques of ellipsometry. The main applications are in physics and physical chemistry of surfaces and thin films, although some interesting applications in clinical chemistry are surveyed. These include a study of the interaction of blood with foreign surfaces, the antigen-antibody reactions in thin films, the immunoelectroadsorption test and the measure of cell surface materials. The production of such a specialized monograph in an affordable format is to be welcomed.

D. Thorburn Burns

Maureen Melvin, *Electrophoresis*, ACOL (Analytical Chemistry by Open Learning) series. Wiley, Chichester, 1987 (ISBN 0-471-91375-8). 130 pp. Price £9.95.

This book is one of a rapidly growing series of texts aimed at senior technicians and others who may not be able to take conventional educational courses. It is pleasant to see that biochemical analysis methods, whose teaching is so often in inverse proportion to their great importance, feature strongly in this series. Each book sets out to explain above all the principles of the analytical techniques, and in that respect (and at a fairly elementary level) this book succeeds. The effects of solute size and charge (of nucleic acids as well as proteins), and of buffer pH, ionic strength and composition are clearly outlined, and the stationary phases and simple staining methods used in conventional electrophoresis are also adequately covered. Up-to-date developments, such as pulsed power sources, blotting methods and nucleic acid sequencing are, perhaps understandably, not discussed. At intervals, self-assessment questions are included, with answers in an appendix. I have never been entirely convinced of the efficacy of this method of learning, but some of the questions are certainly both interesting and testing.

At the same time, the book has a number of drawbacks. From time to time, the author writes in the first person: a homely touch, but poor tactics when it is very hard to persuade students to write proper laboratory reports in the third person! Much more serious is the lack of any index (other books in the series suffer similarly) — is it seriously supposed that a student will simply read the book from cover to cover and never refer to it or revise from it again? Even allowing for the brevity of the book, the choice of topics is hard to understand. For example paper electrophoresis, radiochemical detection methods, and the uv spectral detection of proteins in gels are only rarely used in practice, but get quite extensive treatment. In contrast isoelectric focusing (immensely widely used) is treated with a brevity that simply obscures the major features of the method, and densitometry seems not to be mentioned.

Most serious of all in a student text are the errors, some of fact, and some of proof-reading. For example, the term antiserum is not defined, cellulose

acetate is not expensive by any reasonable criterion, and it does matter to a student that a particular heart condition is a myocardial infarction, not an infraction! Worst of all are the structures of the amino-acids given at the end of the book. The structures of proline, phenylalanine (which is misspelt), tryptophane (sic), tyrosine and histidine are all incomplete. And the calibration graph on page 121 seems to bear no relation at all to the data accompanying it! Overall I would recommend the author and publishers to bring out an updated and corrected reprint as soon as possible, because in principle (though not, at present, in practice) this book has a good deal to offer.

J. N. Miller

J. Weiss, *Handbuch der Ionenchromatographie.* VCH, Weinheim, F.R.G., 1985 (ISBN 3-527-26442-6). 288 pp. Price DM 118.00.

This book gives a rather complete overview of the theory of both general chromatographic processes and ion-exchange. This is very useful as many users of ion chromatography (IC) have no background in chromatography and tend to use IC more or less as a black-box technique. Newer developments such as ion-exclusion chromatography and ion-pair chromatography are dealt with in a very clear way. In the chapter on quantitative analysis, however, the author fails to explain why calibration graphs for conductivity detection cannot be linear. In the chapters on instrumentation and applications only the equipment of one particular firm is considered (Dionex), omitting many new developments from other companies. This very one-sided orientation tarnishes the chapter on "Related ion-chromatographic techniques". The merits of single column IC are dismissed too easily. In the same manner the advantages of ion exchange materials, other than those produced by Dionex, are treated in a very off-hand fashion. A little more emphasis on the weak points of IC would also give a more realistic picture of its possibilities.

This book offers a lot of information, especially on the theoretical basis of IC, but it certainly should not be regarded as the sole guide for the practical application of this technique.

J. Slanina

F. Oehme, *Ionenselektive Elektroden.* Hüthig, Heidelberg, 1986 (ISBN 3-7785-1232-3). x + 197 pp. Price DM 48.00.

The book is a small concise encyclopedia dealing with principles, construction and applications of ion-selective electrodes. The author prefers a broad treatment to a deep understanding of the principles. The practical aspects are described in full detail. The methodical aspects, however, are treated only briefly, and the theoretical aspects are omitted. The carefully selected 154 items and many cross-references are arranged in alphabetical order. They cover the principles and applications of solid state electrodes, glass electrodes,

liquid membrane electrodes, gas electrodes, enzyme electrodes and chemically sensitive field effect transistors.

The merits of the book are the clearly written text, the well designed Figures, the detailed information about the construction of the ion-sensitive electrodes and a good selection of references including patent literature. The treatment is in general well balanced, with some exceptions, e.g. Gran's method, which are not adequately treated. The book is well produced and referenced. It represents a timely review of the current progress of development in this modern area of potentiometry. It will therefore be valuable for analytical chemists working in the laboratory and in industrial control, as well as for designers of new ion-selective electrodes and sensors.

P. Valenta

S. Ahuja (Ed.), *Ultratrace Analysis of Pharmaceuticals and Other Compounds of Interest.* Wiley, New York, 1986 (ISBN 0-471-82673-1). xvi + 384 pp. Price £57.50.

The general topic of low level drug analysis commands enormous interest at the present time and the instinctive response to the book's title is to enquire how one differentiates between trace and ultratrace analysis. In the preface Dr. Ahuja defines trace analysis as that carried out at parts per million ($\mu g\ ml^{-1}$) level or microgram amounts, and ultratrace analysis as that conducted below such levels. The point is further emphasised in his introductory chapter. In many ways these definitions are a hindrance rather than a help when first approaching the book as they are not uniformly applied by all contributing authors. It is better to view the work as an overview of current methodology used to solve the most demanding problems faced by analysts concerned with the regulation, safety, clinical and forensic aspects of pharmaceutical compounds.

Chapters 2—6 deal with specific analytical techniques: derivatization in gas and liquid chromatography (GC and LC), GC using mass spectrometry (MS) with selected ion monitoring, LC and LC/MS, high-performance thin layer chromatography and elemental analysis. The remaining seven chapters deal with many different application areas including the determination of impurities and excipients in pharmaceutical products, the forensic examination of illicit materials, the analysis of drug residues in animal feeds and animal-derived foods, and the determination of drugs and metabolites in biological fluids for clinical and forensic purposes. These applied chapters provide a fascinating comparison of the many different philosophies adopted as the analytical needs change.

Overall the book is well produced with few typographical errors and a satisfactory index. Most analysts involved in the diverse fields of drug analysis will find something of relevance and much food for thought.

Richard Gill

E. Upor, M. Mohai and Gy. Novak, *Photometric Methods in Inorganic Trace Analysis (Wilson and Wilson's Comprehensive Analytical Chemistry, Vol. XX.)* Elsevier, Amsterdam, 1985 (ISBN 0-444-99588-9). 420 pp. Price Dfl. 270.00/ $103.75.

This is a revised English version of the original Hungarian book. The authors have drawn on their considerable experience of method development in the laboratories of the Mecsek Ore-Mining Enterprise where very often unusual, complex samples have to be analysed. The book opens with a brief discussion of the reasons for choosing a spectrophotometric method of analysis. This fails to address the question of whether atomic absorption and emission techniques have effectively replaced spectrophotometric methods for many trace elements, as is generally agreed within the analytical community. Thus the book gets off to a rather shaky start. The second chapter on "Planning, elaboration and control of analytical methods" contains a mixture of theory (the treatment of complex formation) and practical advice. The style and choice of words clearly show the non-English origins and that a non-analyst translator has been at work. Apparently the translation has not been edited. For example, readers will find "disturbing" being used instead of "interfering". The next chapter, in much the same format, discusses "Methods for separation of interferences, and concentration possibilities". Chapter 4 addresses the question of "Preparation of samples for analysis" and again contains much sensible advice on practical aspects such as collection and storage. Methods of sample attack are tabulated and extensive references provided for both acid attack and fusion methods. Most of them, though, are to the Eastern European literature. Finally in this first half of the book there is a sizeable chapter devoted to a discussion of sources of inaccuracy.

The next 200 pages are an alphabetical survey of methods for 44 "individual" elements ranging from alkali metals to zirconium. A standard format is used; a brief description of the analytical chemistry of the ions in question is followed by a Table of the properties of the various reagents that have been prepared. However, if one reagent has been universally adopted, details of others are not given. Some indication of variations in the method needed for different sample types are given and this is followed by a detailed description of the method the authors are most familiar with. Finally, a brief mention is made of another technique by which the species in question can be determined. Atomic spectrometry is rarely mentioned. The final 50 pages of the book are taken up with a Table giving details of reagents (common name, structural formula and chemical name and elements determined). At best, the book provides a compilation of useful chemical pretreatment methods and strategies for masking potential interferences together with ideas on preconcentration and matrix isolation. The book also provides a comprehensive guide to the Eastern European literature in this area. At worst, the book is the product of a parallel analytical world in which atomic absorption and plasma emission spectrometries have not been invented!

J. F. Tyson

Leonard C. Feldman and James W. Mayer, *Fundamentals of Surface and Thin Film Analysis.* North Holland, Amsterdam, 1986 (ISBN 0-444-00989-2). xviii + 352 pp. Price Dfl. 125.00.

Surface and thin film analysis is one of the most important and most rapidly progressing areas of modern analytical science. At the present state of the art a large number of techniques is available which can all be traced back to a limited number of basic physical phenomena. It is the concept of this monograph to present these fundamentals in a consistent and sound way in order to provide the basis for those many techniques.

The book starts out with a presentation of the concepts of surface and thin film analysis, a description of basic units and the Bohr atom. The second chapter deals with atomic collision processes forming the basis of ion scattering spectrometry. The third chapter discusses energy loss phenomena of light ions (e.g. He^+) in the MeV range, the basis of gaining depth distribution information in Rutherford back scattering. Chapter 4 is devoted to sputter depth profiling, forming the basis of secondary ion mass spectrometry and secondary neutral mass spectrometry. Chapter 5 is devoted to channelling effects of ions in a crystal and the structural information which can be derived in ion scattering experiments. Chapter 6 discusses the basics of electron/electron interactions, on which the electron spectroscopic techniques rely. Chapter 7 deals with diffraction phenomena of photons and electrons leading to low energy electron and X-ray diffraction and transmission high energy electron diffraction. Chapter 8 presents the phenomenon of photon absorption in solids and the major technique using this process, EXAFS. Chapter 9 is devoted to X-ray photoelectron spectroscopy and Chapter 10 to radiative transitions which are the basis of X-ray analysis with electron or particle beams. Chapter 11 consequently presents non-radiative transitions forming the basis of Auger electron spectrometry. Chapter 12 deals finally with nuclear reactions for activation analysis and prompt radiation analysis.

The whole structure of the book is very logical. The reader is taken from a physical process to (analytical) information to a technique, and from one process to another. Each chapter is clearly written and provides an excellent and thorough treatment of the fundamentals. A number of exercises are included in each chapter. The 33-page appendix provides many useful Tables (e.g. scattering cross sections, electron binding energies and isotopic abundances). In summary, this is an excellent monograph which can serve as an advanced textbook for anyone concerned with surface analysis. It is indispensable for those who do not want to confine themselves to one single technique, but who want to get a thorough understanding of all of the major processes of signal generation in surface analysis. In every respect this book is highly recommendable for chemists and physicists.

M. Grasserbauer

M. R. Smyth and J. G. Vos (Eds.), *Electrochemistry, Sensors and Analysis (Analytical Chemistry Symposia Series, Vol. 25.)* Elsevier, Amsterdam, 1986 (ISBN 0-444-42719-8). xvii + 419 pp. Price Dfl. 295.00.

This volume contains the proceedings of an international conference held in Dublin on June 10—12, 1986. It includes 48 presentations in camera-ready form and is divided into 5 sections covering analytical voltammetry, analytical potentiometry, bioelectrochemistry, modified electrodes, and sensors and electroanalytical methods in clinical and pharmaceutical chemistry. It is typical of conference proceedings in that the novelty of the work presented is variable and ranges from general overviews to highly specialized applications. The editors have done well to get this volume published within six months of the conference, but the inclusion of at least a brief index would have been beneficial. It is nonetheless a useful reference for workers in the field of electroanalytical chemistry.

Analytica Chimica Acta, 199 (1987) 291—294
Elsevier Science Publishers B.V., Amsterdam — Printed in The Netherlands

Software Reviews

G. Kateman, P. F. A. van der Wiel, T. A. H. M. Janse and B. G. M. Vandeginste, *CLEOPATRA — CHEMOMETRICS LIBRARY: An extendable set of programs as an aid in teaching, research and application.* Elsevier Scientific Software, Amsterdam. Basis Version, 1985 (ISBN 0-444-42413-X). Price Dfl. 2220; Extension I, 1986 (ISBN 0-444-42649-3). Dfl. 1010.

Computer	IBM-PC
Operating system	PC-DOS 2.0 and later
Language	PC-BASIC
Required peripherals	360K 5 1/4-in diskette drive
Minimum memory	128K RAM
Storage minimum	5 1/4-in diskette

CLEOPATRA is an excellent turn-key system for exposing science students to the principles and applications of a variety of chemometrics tools. It is an exciting garden of common and rare flowers that should excite even the most reluctant computer user into applying these tools to improve the quality of their work and extract the most information from their data.

CLEOPATRA provides easy access to the delights of Fourier filtering, simplex optimization, curve fitting, factorial design, Kalman filtering, correlation techniques, and sampling theory. The modules can be used for implementing a turn-key, self-paced laboratory experience by both the novice user and the novice instructor. CLEOPATRA also provides source codes for these methods that will be of value to anyone who wishes to design custom research applications. ESS has provided a complete tool kit that may be used by those scientists having a moderate ability with DOS and BASIC (BASICA and BASIC compiler/linker, or HP-BASIC).

CLEOPATRA is unique, providing access to a broad range of topics, complete with a modifiable source code. It requires only 128K RAM, one flexible disk, PC-DOS 2.0 or later, and CGA compatible graphics adapter. The programs perform well on systems with Hercules monochrome graphics adapters using one of the user supported CGA software simulators. The software is not copy-protected: the license agreement allows the user to copy the software up to a maximum of four copies.

Raymond Dessy

Peter C. Jurs, *Computer Software Applications in Chemistry*. Wiley, New York, 1986 (ISBN 0-471-84735-6). xiv + 253 pp. Price $33.75.

Computers have become accepted tools in most branches of chemistry. Nowadays there is hardly a chemical laboratory without easy access to a general purpose computer, and most modern instruments include a microcomputer or are designed for direct connection to a computer work station. For most standard applications, programs are available, and their performance is generally adequate. However, the user sees the system as a black box. In particular, he hardly ever knows about the limitations of the programs. There is often no safeguard against misusing the system for applications outside the range assumed by the programmer. If the user understands the principle of the program, he can in most cases identify such situations and will be able to interpret the results of his calculations with the necessary reservation.

This book provides a wide overview of computer software applications in chemistry. A short introduction starts at a quite elementary level, providing a beginner with the fundamentals required to make full profit of the following parts. The first section deals with numerical methods and includes chapters on curve fitting and linear regression, on numerical integration (including the numerical solution of differential equations), on Monte Carlo simulation and on simplex optimization. The second section is devoted to non-numerical methods, including chemical structure information handling, graph theory and substructure searching. Chapters on pattern recognition, spectroscopic library searching and artificial intelligence systems follow. The last section very briefly deals with the graphic display of data and molecules. In each chapter, the mathematical background is well explained. In many cases, sample programs in FORTRAN are given, which allow the reader to trace each step of the respective algorithm. Finally, references to recent applications and to more specialized papers and books are given.

The book is well written and makes an excellent introduction for the beginner. It also provides the specialist with a very useful up-to-date overview of the very dynamic field of chemical software applications.

J. T. Clerc

T. F. Hartley, *Computerized Quality Control: Programs for the Analytical Laboratory*. Ellis Horwood, Chichester, 1987 (ISBN 0-85312-964-9). 165 pp. Price £18.50.

This slim volume follows its predecessors in giving a practical view of a well-defined topic. It contains details of eleven BASIC programs in a format that should make it useful for beginners both in statistical methods and in writing computer programs. Those more experienced may also find something of interest here. The subjects chosen cover three areas of statistics in quality control: linear calibrations and curve fitting; quality control charts and data filing; and trend analysis by cusum and other techniques. Although

these topics are usually well covered in statistical texts, the practical computing approach taken in this monograph is refreshing.

The format of presenting an actual BASIC program with a detailed description of its workings and a discussion of the statistical background works well and provides the necessary explanation for understanding just what is intended. As the programs are recommended for implementation on the reader's own computer the worked examples provide test sets of data and expected results to ensure that the implementation has been made correctly. Unfortunately, there is no mention of the different numerical precisions of different computers or of implementations of BASIC; these frequently give different rounding error characteristics and, with some data sets, quite unexpected results.

The text is largely free from error but some typographical errors have crept into the program listings. Inexperienced programmers may not recognise these until they get syntax or bad statement errors when trying to run the program. In a similar way, the author lists the BASIC word REM as being used but it does not appear in any of the programs. Instead, the system dependent abbreviation " ' " is used and this may cause some difficulties. Overall the book can be recommended to anyone about to write a program in one of the areas covered; even if they do not use the actual program listing the background information will be valuable.

R. L. Tranter

W. H. Press, B. P. Flannery, S. A. Teukolsky and W. T. Vetterling, *Numerical Recipes: the Art of Scientific Computing.* Cambridge University Press, Cambridge, 1986 (ISBN 0-521-30811-9). xx + 818 pp. Price £25.00.

Numerical Recipes FORTRAN Diskette (ISBN 0-521-30958-1). Price £15.00 + VAT.

**Numerical Recipes Pascal Diskette* (ISBN 0-521-30955-7). Price £15.00 + VAT.

Numerical Recipes Example Book (FORTRAN) (ISBN 0-521-31330-9). viii + 180 pp. Price £15.00.

Numerical Recipes Example Book (Pascal) (ISBN 0-521-30956-5). x + 236 pp. Price £15.00.

**Numerical Recipes Example Diskette (FORTRAN)* (ISBN 0-521-30957-3). Price £15.00 + VAT.

**Numerical Recipes Example Diskette (Pascal)* (ISBN 0-521-30954-9). Price £15.00 + VAT.

Nowadays many research chemists have a personal computer readily at hand. When a problem arises which requires computation we have to decide whether to buy a ready-made package which may (or may not) do the required job, try to persuade someone else to write a program, or, as a last resort, write a suitable program ourselves. In order to write good programs we need to understand the mathematics involved, and be skilled at program writing, as well as understanding the chemistry. This book has been written to help us. In it the fundamental mathematics of many different techniques of numerical analysis are pithily presented, and for each a program (usually a procedure or function) is given. For instance if you need a program to sort a list of values there is a short account of sorting methods, a warning (do not use bubble sorting procedures!), together with two programs for efficient sorting (one short one suitable for less than 50 items, and a longer, more efficient one for larger lists). Each of some 200 programs is given in both FORTRAN (in the text) and in Pascal (in an appendix). The sections on maximization of functions, statistical description of data, and modelling of data are of particular interest to analytical chemists.

When using routines written by someone else it is desirable to check that they are being used in an appropriate way. The Recipes Example booklets contain supplementary programs to drive the procedures or functions correctly, and are complete working programs with known answers. If you get these working you are in a good position to start to modify them for your own problems.

The programs are not short and the diskettes (readable by IBM PC or compatible computers) are well worth the cost to avoid typing mistakes (those asterisked were not tried by the reviewer). If neither FORTRAN nor Pascal is suitable it is not difficult to transcribe the programs into another similar language, but some of them would be quite difficult to code in Microsoft BASIC, the most widely available language on microcomputers. This book and associated material should prove a boon to program writers. The time saved by using tested programs should far outweigh their cost.

J. R. Chipperfield

ANALYTICA CHIMICA ACTA, 199 (1987)

AUTHOR INDEX

Ahern, F.
—, Eckert, J. M., Hain, S. F., Leggett, K. E. A., Payne, N. C. and Williams, K. L. The coprecipitation of an organophosphate fraction from harbour water for X-ray fluorescence spectrometry 259
Alonso, J.
—, Bartrolí, J., del Valle, M., Escalada, M. and Barber, R. Sandwich techniques in flow injection analysis. Part 1. Continuous recalibration techniques for process control 191
Arruda, M. A. Z.
— and Zagatto, E. A. G. A simple stopped-flow method with continuous pumping for the spectrophotometric flow-injection determination of boron in plants 137

Barber, R., see Alonso, J. 191
Bartrolí, J., see Alonso, J. 191
Batina, N.
—, Ćosović, B. and Težak, Dj. Determination of surface-active compounds in precipitation studies by a.c. polarography 177
Berg, C. M. G., van den, see van den Berg, C. M. G. 59
Bergveld, P., see van der Schoot, B. H. 157
Burns, D. T.
— and Chimpalee, D. Spectrophotometric determination of manganese(VII) after extraction with the ethylene-bis(triphenylphosphonium) cation 241
Burns, D. T.
— and Tungkananuruk, N. Spectrophotometric determination of perchlorate after extraction of its Brilliant Green ion-pair with microcrystalline benzophenone 237

Cecconie, T., see Hojjatie, M. 49
Chico Guijarro, E.
—, Yáñez-Sedeño, P. and Polo Díez, L. M. Determination of paraquat by flow-injection spectrophotometry 203
Chimpalee, D., see Burns, D. T. 241
Ćosović, B., see Batina, N. 177

Del Valle, M., see Alonso, J. 191
De Marco, R.
—, Kew, D. J. and Sullivan, J. V. The effect of the ordered phase Cu Au on the accuracy of emission analysis of gold alloys 249
Dhaktode, S. S.
Simultaneous determination of lead, copper, cadmium and zinc in pure zirconium metal by differential-pulse anodic stripping voltammetry 181

Eckert, J. M., see Ahern, F. 259
Egsgaard, H.
— and Larsen, E. Long-term stability of a gas chromatography/mass spectrometry system in quantitative gas analysis 265
Escalada, M., see Alonso, J. 191

Freiser, H., see Hojjatie, M. 49
Fuji, T., see Yonehara, N. 129

Gupta, D., see Verma, K. K. 233

Hain, S. F., see Ahern, F. 259
Harrison, R. M., see Rapsomanikis, S. 41
Henrion, G., see Scholz, F. 167
Hernandez-Hernandez, L. H., see Sanchez, F. U. 227
Hojjatie, M.
—, Cecconie, T. and Freiser, H. The effect of substituents on the extraction behavior of hydroxamic acids 49
Hsiech, C., see Masters, R. 253
Hydes, D. J.
Continuous-flow determination of manganese in natural waters containing iron 221

Idowu, O. R.
Spectrofluorimetric determination of proguanil in biological fluids 215
Ishioka, S., see Kitazume, E. 245

Jurs, P. C., see Rohrbaugh, R. H. 99

Kaljurand, M., see Koel, M. 197
Kamada, M., see Yonehara, N. 129
Kano, G., see Satake, M. 209
Karube, I.
—, Wang, Y., Tamiya, E. and Kawarai, M.
Microbial electrode sensor for vitamin B_{12} 93
Karube, I., see Suzuki, H. 85
Kawarai, M., see Karube, I. 93
Kew, D. J., see de Marco, R. 249
Kitazume, E.
—, Ishioka, S. and Mitani, E.
Determination of traces of boron in semiconductor amorphous silicon film by filament-vaporization inductively-coupled plasma/atomic emission spectrometry 245
Koel, M.
—, Kaljurand, M. and Küllik, E.
Correlation steam/solid chromatography of trace organic compounds in water 197
Kopanica, M., see Tocksteinová, Z. 77
Kubota, M.
—, Reimer, R. A., Terajima, K., Yoshimura, Y. and Nishijima, A.
Inductively-coupled plasma/atomic emission spectrometry of sulfur with a vacuum scanning spectrometer and its application to the analysis of coal liquefaction catalysts 119
Küllik, E., see Koel, M. 197

Larsen, E., see Egsgaard, H. 265
Lázaro, F., see Ríos, A. 15
Leggett, K. E. A., see Ahern, F. 259
Lloyd, J. B. F.
Anodic response to oxygen of an electrochemical detector in high-performance liquid chromatography and flow-injection analysis 161
Loriguillo, A.
—, Silva, M. and Pérez-Bendito, D.
Versatile automatic stopped-flow system for routine analysis 29
Luque de Castro, M. D., see Ríos, A. 15

Marco, R., de, see de Marco, R. 249
Masters, R.
—, Hsiech, C. and Pardue, H. L.
Echelle-spectrometer/image-dissector system for elemental quantitation by continuous-source atomic absorption spectrometry 253
Mitani, E., see Kitazume, E. 245

Nakajima, K.
— and Takada, T.
The S_2 emission characteristics of several organic sulfur compounds obtained by molecular emission cavity analysis and pyrolysis 147
Newton, M. P.
— and van den Berg, C. M. G.
Determination of nickel, cobalt, copper and uranium in water by cathodic stripping chronopotentiometry with continuous flow 59
Nishijima, A., see Kubota, M. 119
Nitschke, L., see Scholz, F. 167

Pantel, S.
Stat methods in analytical chemistry. Kinetic techniques for catalyzed and uncatalyzed reactions 1
Pardue, H. L., see Masters, R. 253
Payne, N. C., see Ahern, F. 259
Pérez-Bendito, D., see Loriguillo, A. 29
Polo Díez, L. M., see Chico Guijarro, E. 203
Procopio, J. R., see Sanchez, F. U. 227
Puri, B. K., see Satake, M. 209

Rapsomanikis, S.
— and Harrison, R. M.
Optimization of single-column anion chromatography with indirect ultraviolet photometric and fluorimetric detection 41
Reimer, R. A., see Kubota, M. 119
Ríos, A.
—, Lázaro, F., Luque de Castro, M. D. and Valcárcel, M.
Multidetection flow-injection techniques for manipulation of sensitivity. Amplification and dilution methods 15
Rohrbaugh, R. H.
— and Jurs, P. C.
Descriptions of molecular shape applied in studies of structure/activity and structure/property relationships 99

Sakmoto, H., see Yonehara, N. 129
Sanchez, F. U.
—, Procopio, J. R. and Hernandez-Hernandez, L. H.

Spectrofluorimetric determination of 1,4-thienodiazepines 227
Satake, M.
—, Kano, G., Puri, B. K. and Usami, S.
Preconcentration of copper with the ion-pair of 1,10-phenanthroline and tetraphenylborate on naphthalene 209
Scholz, F.
—, Nitschke, L. and Henrion, G.
Determination of mercury traces by differential-pulse stripping volammetry after sorption of mercury vapour on a gold-plated electrode 167
Schoot, B. H., van der, see van der Schoot, B. H. 157
Silva, M., see Loriguillo, A. 29
Smith, B. W., see Tremblay, M. E. 111
Struys, J.
— and Wolfs, P. M.
Determination of cyanuric acid in swimming pool water by differential pulse polarography 173
Sullivan, J. V., see de Marco, R. 249
Suzuki, H.
—, Tamiya, E. and Karube, I.
An amperometric sensor for carbon dioxide based on immobilized bacteria utilizing carbon dioxide 85

Takada, T., see Nakajima, K. 147
Tamiya, E., see Karube, I. 93
Tamiya, E., see Suzuki, H. 85
Terajima, K., see Kubota, M. 119
Težak, Dj., see Batina, N. 177
Tocksteinová, Z.
— and Kopanica, M.
Determination of caprolactam by adsorptive voltammetry after separation by thin-layer chromatography 77
Tremblay, M. E.
—, Smith, B. W. and Winefordner, J. D.
Laser-excited ionic fluorescence spectrometry of rare-earth elements in the inductively-coupled plasma 111
Tungkananuruk, N., see Burns, D. T. 237

Usami, S., see Satake, M. 209

Valcárcel, M., see Ríos, A. 15
Valle, M., del, see del Valle, M. 191
Van den Berg, C. M. G., see Newton, M. P. 59
Van der Schoot, B. H.
— and Bergveld, P.
The pH-static enzyme sensor. An ISFET-based enzyme sensor, insensitive to the buffer capacity of the sample 157
Varughese, K., see Wang, J. 185
Verma, K. K.
— and Gupta, D.
Detection of nitrobenzene and related aromatics by reduction and indophenol formation 233

Wang, J.
— and Varughese, K.
Determination of traces of palladium by adsorptive stripping voltammetry of the dimethylglyoxime complex 185
Wang, Y., see Karube, I. 93
Williams, K. L., see Ahern, F. 259
Winefordner, J. D., see Tremblay, M. E. 111
Wolfs, P. M., see Struys, J. 173

Yáñez-Sedeño, P., see Chico Guijarro, E. 203
Yonehara, N.
—, Fuji, T., Sakmoto, H. and Kamada, M.
Differential determination of antimony (III) and antimony(V) by indirect spectrophotometry with chromium(VI) and diphenylcarbazide, after reduction of antimony(V) 129
Yoshimura, Y., see Kubota, M. 119

Zagatto, E. A. G., see Arruda, M. A. Z. 137

INFORMATION FOR AUTHORS

:tailed "Information for Authors" was published in Vol. 190, No. 2, pp. 375–378. A free reprint is available from the litors or from:
sevier Editorial Services Ltd., Mayfield House, 256 Banbury Road, Oxford OX2 7DH (Great Britain)

'pes of contribution. The journal welcomes original research papers, short communications and reviews. :views are written by invitation of the editors, who welcome suggestions for subjects. Short communications are ually complete descriptions of limited investigations, and should generally not exceed six printed pages. Preliminary mmunications of important urgent work can be printed within four months of submission, if the authors are epared to forgo proofs.

anuscripts. The preferred language of the journal is English, but French and German manuscripts are also ceptable. For authors whose first language is not English, French or German, linguistic improvement is provided as rt of the normal editorial processing. Authors should submit three copies of the manuscript in double-spaced typing one side of the paper only, with a margin of 4 cm, on pages of uniform size. If any variety of machine copying is ed (e.g. xerox), authors should ensure that all copies are easily legible and that the paper used can be written on th both ink and pencil. Authors are advised to retain at least one copy of the manuscript. Manuscripts should be eceded by a sheet of paper carrying (a) the title of the paper, (b) the name and full postal address of the person to hom proofs are to be sent, (c) the number of pages, tables and figures.

formation on the *submission of papers* is given on the inside front cover.

ummary. Research papers and reviews begin with a Summary (50–250 words) which should comprise a brief ctual account of the contents of the paper, with emphasis on new information. Short communications and eliminary communications require summaries, which should not exceed 50 words. Uncommon abbreviations, gon and reference numbers must not be used. The Summary should be suitable for use by abstracting services ithout rewriting. Papers in French or German require a Résumé or Zusammenfassung preceded by a Title and ummary in English; authors are encouraged to provide translations where necessary.

troduction. The first paragraphs of the paper should contain an account of the reasons for the work, any essential storical background (as briefly as possible and with key references only) and preliminary experimental work.

gures. Figures should be prepared in black waterproof drawing ink on drawing or tracing paper of the same size as at on which the manuscript is typed. One original (or sharp glossy print) and two photostat (or other) copies are quired. Attention should be given to line thickness, lettering (which should be kept to a minimum) and spacing on es of graphs, to ensure suitability for reduction during printing. Axes of a graph should be clearly labelled, along the es, and outside the graph itself.

l figures should be numbered with Arabic numerals, and require descriptive legends. Explanatory information should placed not in the figure, but in the legend, which should be typed on a separate sheet of paper. Simple straight-line aphs are not acceptable, because they can readily be described in the text by means of an equation or a sentence. aims of linearity should be supported by regression data that include slope, intercept, standard deviations of the ope and intercept, standard error, and the number of data points; correlation coefficients are optional.

notographs should be glossy prints and be as rich in contrast as possible; colour photographs cannot be accepted. In neral, line diagrams are more informative and less liable to dating than photographs of equipment, which are erefore not usually acceptable.

mputer outputs for reproduction as figures must be good quality on blank paper, and should preferably be bmitted as glossy prints.

omenclature, abbreviations and symbols. In general, the recommendations of the International Union of Pure d Applied Chemistry (IUPAC) should be followed, and attention should be given to the recommendations of the nalytical Chemistry Division in the journal *Pure and Applied Chemistry* (see also *IUPAC Compendium of Analytical omenclature*, 1978).

eferences. The references should be collected at the end of the paper, numbered in the order of their appearance in e text (*not* arranged alphabetically), and typed on a separate sheet.

the list of references, the following forms should be adopted.

urnals

W. Lund and M. Salberg, Anal. Chim. Acta, 76 (1975) 131.

M. McDaniel, A. D. Shendrikar, K. D. Reizneir and P. W. West, Anal. Chem., 48 (1976) 2240.

ie title of the journal must be abbreviated as in the Bibliographic Guide for Editors and Authors.

ooks

D. D. Perrin, Masking and Demasking of Chemical Reactions, Interscience-Wiley, New York, 1970, p. 188.

S. Hofmann, in G. Svehla (Ed.), Wilson and Wilson's Comprehensive Analytical Chemistry, Vol. 9, Elsevier, Amsterdam, 1979, p. 89.

les of papers are unnecessary. Citations of reports which are not widely available (e.g., reports from government search centres) should be avoided if possible. Authors' initials should not be used in the text, unless real confusion uld be caused by their omission. If the reference cited contains three or more names, only the first author's name llowed by et al. (e.g., McDaniel et al.) should be used in the text; but the reference list must contain the initials and mes of *all* authors.